



# **Dissertation summary**

Scientific and didactic achievements

**Anna Mackojć, M.Sc. Eng.**

Analytical approach to modelling, analysis and dynamics studies  
on parametrically induced payload pendulation  
in offshore lifting operations

Supervisor  
Robert Zalewski, Prof.Ph.D., D.Sc.

Co-supervisor  
Bogumił Chiliński, Ph.D.

Warsaw, 2023

# Contents

<b>1</b>	<b>Name and surname</b>	<b>3</b>
<b>2</b>	<b>Diplomas and degrees</b>	<b>3</b>
<b>3</b>	<b>Employment in research institutes</b>	<b>3</b>
<b>4</b>	<b>Indication of a scientific achievement</b>	<b>3</b>
4.1	The title of a doctoral dissertation . . . . .	3
4.2	A list of thematically related publications representing a scientific achievement	3
<b>5</b>	<b>Overview of a series of publications representing a scientific achievement</b>	<b>7</b>
5.1	Offshore industry and lifting operations . . . . .	7
5.2	Offshore industry market - assessment of offered solutions . . . . .	9
5.2.1	Complex motion compensation - solutions review . . . . .	9
5.2.2	Heave motion compensation - solutions review . . . . .	11
5.3	Industrial practice review . . . . .	12
5.4	Literature review . . . . .	16
5.5	Objectives of thesis and motivation . . . . .	19
5.6	Scientific research assumptions . . . . .	20
5.6.1	Wave modelling and RAOs processing methodology - determination of an environmental impact on marine structures . . . . .	21
5.6.2	Proposal of a novel approach to modelling dynamics in offshore lifting - development of an innovative model for operation planning to simulate lifted payload behaviour in payload-vessel system . . . . .	27
5.6.3	Numerical research on regular and irregular waves - a versatility of results processing methods . . . . .	29
5.6.4	Model of a coupled payload-vessel system for offshore lifts of light and heavyweight objects - determination of the scope of applicability and development of methods supporting planning in offshore lifting design process . . . . .	33
5.6.5	Derivation of an analytical closed form solution of the proposed model on a basis of perturbative methods from nonlinear theory of vibration. A possibility of qualitative description of the system dynamic features .	35
5.6.6	Analytical research on regular waves - comparative analyses and results convergence check in a wide range of lifting cable lengths. The approximated solution accuracy assessment and its potential use in operation planning . . . . .	38
5.6.7	Modelling methodology for a variety of dynamic systems based on created Python library . . . . .	43
5.7	Summary . . . . .	46
<b>6</b>	<b>Didactic and organisational achievements</b>	<b>47</b>
6.1	Didactic achievements . . . . .	47
6.2	Scientific supervision of students' thesis . . . . .	49
6.3	Reviewing publications for international journals . . . . .	49
6.4	Participation in research projects . . . . .	49
6.5	Participation in international scientific conferences . . . . .	50
6.6	Prizes and awards . . . . .	51
<b>7</b>	<b>Summary of scientific achievements</b>	<b>51</b>

## 1. Name and surname

Anna Justyna Mackojć

## 2. Diplomas and degrees

**3.02.2014** B.Sc. degree in mechanics in the field of internal combustion engines awarded at the Faculty of Automotive and Construction Machinery Engineering of the Warsaw University of Technology

**10.09.2015** M.Sc. degree in mechanics awarded at the Faculty of Automotive and Construction Machinery Engineering of the Warsaw University of Technology

## 3. Employment in research institutes

**20.02.2017** Assistant - Warsaw University of Technology, Faculty of Automotive and Construction Machinery Engineering, Institute of Machine Design Fundamentals, Narbutta 84, 02-254 Warsaw

A copy of the diploma confirming MSc. Eng. degree is included as Appendix 1.

## 4. Indication of a scientific achievement

### 4.1. The title of a doctoral dissertation

The title of a doctoral dissertation under Art. 13 sec. 2 of the Act of March 14, 2003 on academic degrees, academic title and on degrees and title in the field of art (Journal of Laws of 2017, item 1789) is:

**Analytical approach to modelling, analysis and dynamics studies on parametrically induced nonlinear payload pendulation in offshore lifting operations**

### 4.2. A list of thematically related publications representing a scientific achievement

- A1 Chiliński Bogumił, Mackojć Anna, *Analytical solution of parametrically induced payload nonlinear pendulation in offshore lifting*, Ocean Engineering, 2022, vol. 259, pp.111835. DOI:10.1016/j.oceaneng.2022.111835
- A2 Mackojć Anna, Chiliński Bogumił, Zalewski Robert, *Preliminary research of a symmetrical controllable granular damper prototype*, Bulletin of the Polish Academy of Sciences, Technical Sciences, 2022, vol. 70, no. 3, pp.1-9, Article number:e141002. DOI:10.24425/bpasts.2022.141002
- A3 Mackojć Anna, Chiliński Bogumił, *Preliminary modelling methodology of a coupled payload-vessel system for offshore lifts of light and heavyweight objects*, Bulletin of the Polish Academy of Sciences, Technical Sciences, 2021, vol. 70, pp.9. DOI:10.24425/bpasts.2021.139003

- A4 Chiliński Bogumił, Mackojć Anna, Zalewski Robert, *Proposal of the 3-DOF model as an approach to modelling offshore lifting dynamics*, Ocean Engineering, 2020, vol. 203, pp.107235. DOI:10.1016/j.oceaneng.2020.107235
- A5 Chiliński Bogumił, Mackojć Anna, *Proposal of the Coupled Thermomechanical Model of a Crank Mechanism*, In: Transdisciplinary Engineering for Complex Socio-technical Systems – Real-life Applications / Pokojński Jerzy [et al.] (eds.), 2020, vol. 12, IOS Press, ISBN 978-1-64368-110-8. DOI:10.3233/ATDE200098



## Abstract

The subject of research outlines a relevant maritime problem regarding offshore lifting operations. One of the challenges during offshore lifts is the need to deal with the surrounding environment, which under unfavourable conditions can significantly reduce the operating window or increase the risk of an operational failure, which at best may result in damage to the lifted payload, deck crane or ship structure. The worst case scenario is an accident involving the ship's crew assisting in the operation. Due to increasing exploitation of either renewable (offshore wind farms) or underwater hydrocarbon energy resources, the intensification of offshore activities becomes more and more obvious and vessel crane operations are the basis of offshore installations. To assist the industry, engineers have developed several technologies and operational practices, however, access to appropriate modelling methods and methodologies is still significantly limited. In order to support the industry in a better understanding of the complexity of problems undertaken and provide fit-to-purpose solutions, the author proposed a novel approach to modelling offshore lifting operations. The concept of the model and extensive studies on its dynamics on regular and irregular waves are published in the article *"Proposal of 3DoF model as an approach to modelling offshore lifting dynamics"* in Ocean Engineering (2020). Further research allowed to propose an extended model (payload-vessel) with 5 degrees of freedom, which enables the analysis of operations in a wide spectrum of payload masses (*"Preliminary modelling methodology of a coupled payload-vessel system for offshore lifts of light and heavyweight objects"*, Bulletin of Polish Academy of Science, Technical Sciences, 2021). One of the most important scientific achievements was a development of the analytical solution for the payload dynamic response under conditions of parametric excitation on regular waves. The analytical solution was obtained based on perturbative method of multiple time scales. This solution was confirmed with the solution resulting from the numerical integration of the equation of motion, and its convergence was assessed as very good. The proposed approach allows to determine the working conditions - regions of dynamic instability. Moreover, it enables a description of dynamics of the lifting process and the lifted object response in an analytical form due to explicit physical dependencies. Another benefit is seen in reducing the computationally expensive design process and in the possibility of an efficient recognition of a potentially problematic scenario at early conceptual stages in order to plan an optimal lifting operation. A detailed analysis is available in Ocean Engineering journal, in the article, *"Analytical solution of parametrically induced payload nonlinear pendulation in offshore lifting"* (2022).

## Streszczenie

Tematyka prowadzonych prac dotyczy istotnego zagadnienia jakim jest operacja podnoszenia prowadzona na morzu. Jednym z wyzwań napotykanych podczas operacji jest konieczność radzenia sobie z warunkami środowiskowymi, tj. stanem morza, który w niekorzystnych warunkach może znacznie zmniejszyć okno operacyjne lub zwiększyć ryzyko niepowodzenia operacji, co w najlepszym przypadku może zakończyć się uszkodzeniem ładunku, żurawia czy konstrukcji statku, a w najgorszym, wypadkiem z udziałem załogi okrętowej asystującej przy operacji. W związku z rosnącą eksploatacją zarówno odnawialnych (morskie farmy wiatrowe), jak i podwodnych węglowodorowych zasobów energetycznych, intensyfikacja działań offshore staje się coraz bardziej widoczna, a operacje z wykorzystaniem żurawia okrętowego są podstawą instalacji morskich. Aby wspomóc przemysł, inżynierowie opracowali kilka technologii i praktyk operacyjnych, jednak nadal dostęp do odpowiednich metodologii modelowania procesów jest znacząco ograniczony. Aby wesprzeć prowadzone prace w lepszym zrozumieniu złożoności podejmowanych problemów oraz zapewnieniu bardziej dopasowanych do celu rozwiązań, zaproponowano nowatorski model operacji podnoszenia na morzu. Koncepcję modelu oraz szerokie badania dynamiki na falach regularnych i nieregularnych opublikowano w artykule *“Proposal of 3DoF model as an approach to modelling offshore lifting dynamics”* w czasopiśmie Ocean Engineering (2020). Dalsze prace publikacyjne pozwoliły również na zaproponowanie rozszerzonego modelu (ładunek-statek) o 5-ciu stopniach swobody, który pozwala na analizę operacji w szerokim spektrum tonażu ładunku (*“Preliminary modelling methodology of a coupled payload-vessel system for offshore lifts of light and heavyweight objects”*, Bulletin of Polish Academy of Science, Technical Sciences, 2021). Jednym z ważniejszych osiągnięć naukowych było opracowanie rozwiązania analitycznego dynamicznej odpowiedzi ładunku w warunkach parametrycznego wzbudzenia falą regularną. Rozwiązanie analityczne zostało otrzymane przy użyciu jednej z metod perturbacyjnych - metody wielu skal czasowych. Rozwiązanie to zostało skonfrontowane z rozwiązaniem wynikającym z numerycznego całkowania równania ruchu, a jego zbieżność oceniona na bardzo dobrą. Zaproponowane podejście pozwala na określenie warunków pracy (obszarów niestabilności dynamicznej), opisanie dynamiki procesu podnoszenia oraz odpowiedzi obiektu w analitycznej formie ze względu na występowanie jawnych zależności fizycznych w opracowanym wzorze, skrócenie procesu obliczeniowego oraz umożliwia rozpoznanie ograniczeń na wczesnych etapach planowania operacji w celu jej optymalizacji. Szczegółowa analiza jest dostępna w artykule czasopisma Ocean Engineering, pt. *“Analytical solution of parametrically induced payload nonlinear pendulation in offshore lifting”* (2022).

## **5. Overview of a series of publications representing a scientific achievement**

### **5.1. Offshore industry and lifting operations**

An increasing exploitation of either renewable (offshore wind farms) or underwater hydrocarbon energy resources (conventional oil and gas, coal), triggers a constant and rapid development of the offshore industrial technologies. Moreover, an assurance of safety and reliability during offshore operations and also tight project budget requirements cause the engineering teams to be forced to solve problems in a reduced timeframe. In order to support the engineers in a faster and in-depth understanding of the complexity of issues undertaken, the proposal of a novel approach to offshore operations modelling and providing more accurate and fit-to-purpose solutions is to assist even the experienced personnel allowing for a more productive project management.

One of the challenges encountered during offshore operations is naturally a necessity of dealing with the surrounding environment - a sea state, which when being unfavourable might considerably reduce the operating window or increase the operational risk. Naturally, the offshore activities intensification is seen in lifting operations, which are the basis of marine installations. In order to assist the industry, several technologies and operational practices have been developed however there is still limited access to a proper process modelling methodologies. Significant limitations for the lifting process are related to dynamic properties of the vessel-payload system (sea-keeping properties) and the sea states. In operational sea conditions, the oscillatory motion of a crane tip (the combined horizontal and vertical linear movements) may induce a specific type of the excitation resulting in unpredictable vibrations of the suspended object. A movement appearing due to heaving motion itself stimulates a parametric excitation which, if the value of the excitation frequency is unfavourable, may lead to the instability called parametric resonance [13]. An occurrence of this phenomenon during offshore lifting is one of the hazardous factors when considering oscillating system dynamics. This raises a need for an appropriate determination of the mutual relationship between the dynamics of the payload in relation to the exciting vessel. To ensure safety during lifting operations it is crucial to eliminate possible risks at the planning stage, thus development of an effective methodology consisting of the analytical model determining the possible relations between the system combined excitation and the lifted payload dynamic response, enabling in-depth studies of the possible couplings may help to estimate the allowable working conditions for marine lifting operations. This constitutes the need for a design process providing sufficient results. Simple analytical models serve best for these purposes, especially for the preliminary stage of computations. A solution allowing for a reliable performance in difficult weather conditions might offer a meaningful improvement to the operational expenditure by downtime minimisation, which is one of the largest non-productive costs that the offshore industry is exposed to.

All of the aforementioned issues related to intensification of offshore lifting operations, such as planning, development of modern technologies whilst still a lack of solution allowing for a reliable performance in difficult weather and sea conditions, cost reduction, and before all,

ensuring the highest possible safety standards, make the subject a matter of interest. The key phase of the lifting that causes most of the problems is in air-handling. Therefore it still requires an assistance of a skilled personnel - the so-called lifting triangle. Hence, the number of people engaged for a single lift is at least three - the crane operator, slinger and banksman. However, in practice, the number of personnel to assist the operation is much higher as the average mass and size of the lifted payload requires an assistance of at least a few slingers. An assurance of safety and reliability during installations is crucial as statistically proven, the offshore environment does not offer great stability conditions - 22 % incidents are classified as crane or lifting incidents and 86 % are lifting injuries involving a contractor. Figure 1 depicts offshore incidental statistics regarding lifting incidents and related injuries over last 7 years. The statistics are collected by Bureau of Safety and Environmental Enforcement (BSEE), one of the biggest organisation managing offshore industry issues in the United States but also around the world. Similar statistics can be found in annual reports of Health and Safety Executive (HSE) [16] responsible for regulating health and safety matters in the other industrial potentate - the United Kingdom.

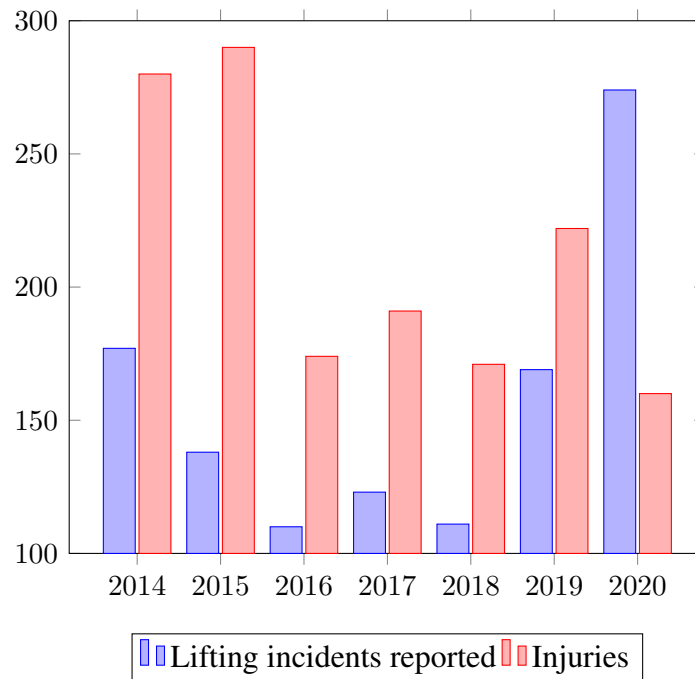


Figure 1: Offshore incident statistics by BSEE [40]

As can be seen the trend of unpredicted offshore events resulting in accidents is growing in recent years. Moreover, in the last two years, 12 fatalities were reported. Hence, a common practice when operating in difficult weather or high sea conditions is to limit or postpone in order to minimise the risk of any unfortunate event or incur costs when unexpected incident occurs (loss of control, collision, free fall, unintentional release). That prompts the research for solutions that would limit human participation.

In spite of ensuring the highest standards of human safety is one of the key aspects, there are other important reasons behind looking for new solutions. Overcoming the limitations of existing systems would increase the operational window of lifting capability resulting in mean-

ingful improvement of efficiency and productivity of marine operation significantly reducing costs. Moreover, in the era of developing wind farm energy many of the installations undertaken demand for high accuracy (eg. mating operations), therefore, an access to an appropriate dynamics modelling tool would allow to trigger a widespread research. It can be stated that a vital role when lifting offshore plays the first phase of handling the lifted load, where a special care must be exercised, whether for safety of people or the accuracy of the performed operation.

Generally, any lifting operation undertaken offshore consists of several phases depending on the operation characteristics. These might include but are not limited to:

- a) lift-off – an object is lifted off from its position,
- b) handling in air - an object is suspended in air or maneuvered to the desired position,
- c) splash zone crossing – an object immersing through a water surface,
- d) deep-water lowering – a payload lowering towards the seabed,
- e) seabed landing – an object installation onto the seafloor.

Dynamics of the lifted load in air is mainly driven by a ship motion with a minor (thanks to modern control filters) influence of the crane operation. Resulting payload motion problems are related to two prevailing phenomena - heave and pendulum. An appropriate understanding of the payload dynamics might considerably increase the operational efficiency and profitability. Several technologies and operational practices have been developed to assist with this, but it is believed that the boundaries can be still pushed further.

## **5.2. Offshore industry market - assessment of offered solutions**

Despite the struggle of the aforementioned problems, still the best possible operational efficiency must be maintained, therefore offshore industry market offers a small group of assisting solutions. The proposed industrial systems can be systematised accordingly to their functionalities. One of the proposals consist of solutions that compensate for a complex motion, while others are limited to one-directional compensation resulting from vessel heaving. Unfortunately, each of the equipment that might be encountered on the market has some operational limitations, however the biggest disadvantage of the offered solutions is an extremely high renting cost. This arises the need of a development of a simple and effective modelling tool offering an improvement and benefits in the whole operational process starting from planning, organising and finally undertaking lifting operation.

### **5.2.1. Complex motion compensation - solutions review**

One of the leading complex motion compensating solutions is the Barge Master Platform (BM-T700). The platform can be installed on any vessel to serve as a motion compensation working base. The producer claims any equipment necessary for offshore operations can be placed on the platform to eliminate the effect of vessel motions, making possible to operate the machinery with the same precision as onshore.

The principle of the platform operation is based on a hydraulic solution. The Barge Master measures vessel motions and actively compensates roll, pitch and heave by means of three hydraulic cylinders (Fig. 2a). The surge, sway and yaw of the vessel can be constrained by using a dynamic positioning or a traditional anchor system (Fig. 2b). The controller measures

the motions of the vessel using motion reference units. The cylinders are controlled by means of velocity feed-forward and position feedback. Redundancy is applied to the critical components assuring safe motion compensated offshore lifting. The BM-T700 platform compensates waves up to significant wave height of 2.5 m and wave periods from 4 s to 18 s [53].

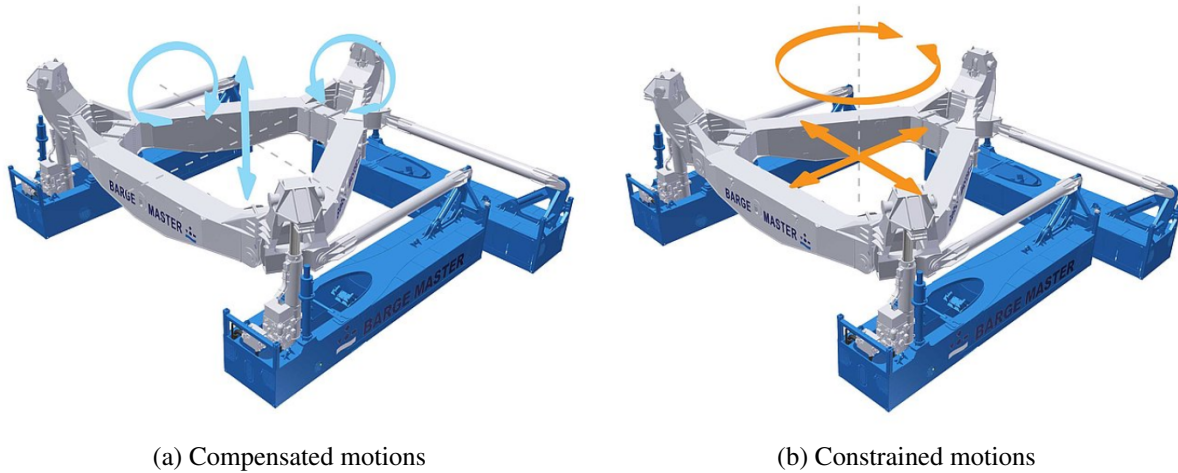


Figure 2: Barge Master - motion compensation platform [53]

However, it is worth to notice that the BM-T700 platform and foundations consist of containerised units, which take up to 10 days to assemble, hence additional operational time due to long-term installation has to be taken into account during planning total operational time. Additionally, the device requires a precious deck space to be taken or its costly modifications as the platform unit footprint dimensions are as follows: unit foundation 18.3x15.1 m, control room and HPU (hydraulic power unit) 12x2.5 m, platform working area 12x12 m. It should also be remembered that the total weight of the ship will change, as the platform and the equipment whose movement is to be compensated will be installed on it. The total added weight is 333 t, where 270 t is for the platform and foundation combined, leaving 63 t for control room and HPU. It has to be considered that this extra mass may influence the dynamics of the ship. A separate unit will also require dedicated software, the operation of which may be complex and requiring an additional training of employees or the employment of an experienced external operator. This creates further costs making the total device renting and service horrendously expensive.

Another device to assist with offshore lifting is the 3D Motion Compensator (3DMC). The MACGREGOR system is a flexible device, which is designed to enhance the load-handling precision of the crane, even in challenging sea states. The 3DMC can be fitted to the knuckle jib of a broad spectrum of new or existing MACGREGOR offshore cranes. It compensates for the roll, pitch and heave motions of the vessel to minimise any movement of the load, in relation to a fixed point in space [55].

The 3DMC has been designed for easy installation and active control utilising the existing hydraulic power unit and control system of the crane. The 3DMC interface is designed so that the unit can be swiftly refitted to a crane with the relevant fittings.



Figure 3: MACGREGOR - 3D motion compensator [55]

However, based on the design of the compensator presented in Fig. 3, it can be concluded that its installation requires interference in the construction of the crane what might not be always possible or even allowed. Besides, when the installation is done and the device is in use, the access difficulties may cause the maintenance and inspection issues, similarly to the previous device, generating additional costs.

### 5.2.2. Heave motion compensation - solutions review

Another type of market solutions to compensate for a vessel motion are heave compensators. In this broad group of solutions are included shock absorbers and drill string compensators, which are unsophisticated forms of this compensating systems. However, it is possible to specify a narrower group of solutions called 'passive' that operate on the basis of advanced hydraulic or mechanical systems.

A typical passive heave compensator (PHC) consists of a hydraulic cylinder and a gas accumulator (Fig. 4). When the piston rod extends, the total gas volume will be reduced and then the compressed gas (nitrogen) increases the pressure acting upon the piston. The combination of both forms a mechanism, in which the volume of the attached gas accumulators sets the stiffness of the system. In order to ensure relatively low stiffness (soft spring solution), the compression ratio is low.

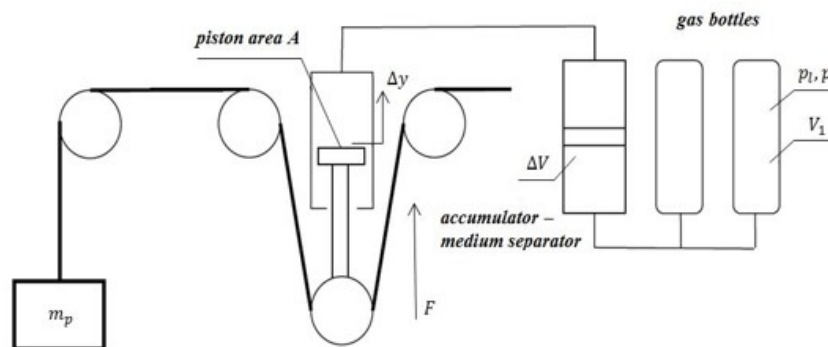


Figure 4: Passive heave compensator

The purpose of PHC is to keep a payload hanged from the crane on a moving vessel, motionless with regard to the seabed or another vessel. It is designed to store the energy from the external excitation (waves) influencing the system and dissipate it. The relative motion of the PHC device allows to hold the suspended load within allowable limits. Passive heave compensation systems do not require a power supply for their operation.

The most famous supplier of passive solutions is the Cranemaster (Fig. 5). The device is a spring-damper system based on gas pressure and hydraulic fluid. The system is self-contained - no external connections of hoses or wires are required. The working load range declared by the manufacturer is 0.5 t to 1600 t and the stroke range within 0.5 m to 5.0 m. It needs to be highlighted that the device compensates for heave exclusively.

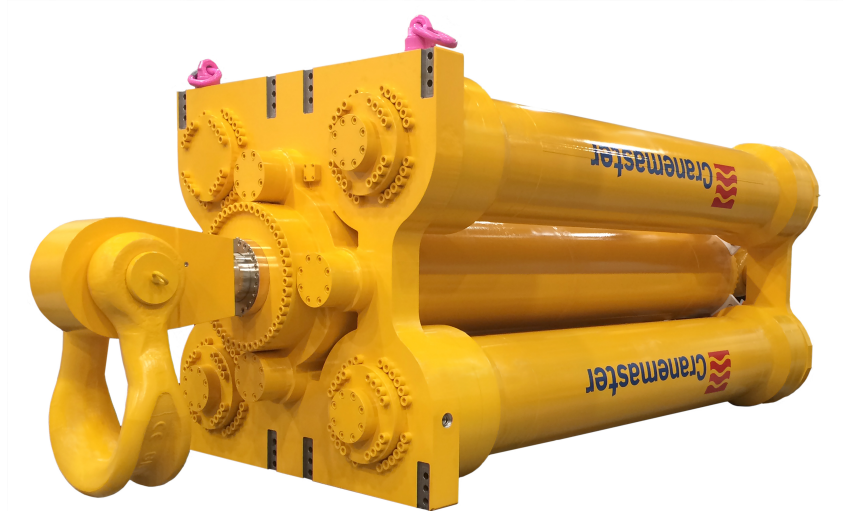


Figure 5: Cranemaster - passive heave compensator [54]

Active heave compensator (AHC) differs from PHC solution by utilising a control system that actively compensates for any movement at a specific point, using external power. In order to execute, industrial offshore cranes use a Motion Reference Unit (MRU) or a detection of pre-set measurement position to detect the current vessel displacements and rotations. Then, a control system, which is usually computer based, calculates the response of active elements (electric or hydraulic). The efficiency of the AHC device is naturally limited by power, motor speed and torque, by measurement accuracy and delay, or by computing algorithms. Choice of a control method, as using preset values or delayed signals, may affect performance and result in large residual motions, especially with unusual waves.

### 5.3. Industrial practice review

Any lifting operation undertaken offshore, which is always risky as subjected to unforeseen complexities that introduce the hazard factor, requires a careful planning. In order to assist with this, the industrial practice offers several modelling tools presented in standards or sold as an expensive engineering software.

When looking through the standards, one can find few very simplified proposals of modelling lifting operations. The most popular and commonly used are the regulations issued by DNV



(Det Norske Veritas) [10]. DNV is an independent expert in assurance and risk management accredited internationally, headquartered in Norway. The company operates currently in more than 100 countries and provides services for several industries including maritime, oil and gas, renewable energy, electrification, food and beverage, and healthcare.

The models that might be encountered in DNV standards are good enough for simple considerations but do not allow to fully understand a dynamic behaviour of the analysed object. Static models whose dynamic behaviour is obtained by introducing a dynamic amplification factor is the most popular one. As per *DNV Standard for Certification No. 2.22 Lifting Appliance* [49], the loads due to floating vessel motions acting on the crane tip, and hence on the lifted object, should be taken into consideration by multiplying the working load by a dynamic amplification factor (DAF),  $\psi$ . As stipulated in the regulation, the dynamic amplification factor can be obtained by [A4]:

$$\psi = 1 + V_R \sqrt{\frac{k}{W \cdot g}}, \quad (1)$$

where:

$k$  - geometric stiffness coefficient referred to hook position, defined as a force at hook to produce unit deflection at hook,

$g$  - gravitational acceleration,

$W$  - working load,

$V_R$  - relative velocity between the payload and hook at the time of pick-up.

The load on a crane wire during offshore lifting is equal to the dynamic load, which is the working load multiplied by dynamic amplification factor [A4]:

$$F_D = W \cdot \psi = W \cdot \left( 1 + V_R \sqrt{\frac{k}{W \cdot g}} \right), \quad (2)$$

Reduction in the dynamic load performed by limitation of relative velocity will lead to a reduction of the operating window. Either a limitation in working load may bring similar benefit however it will also lower the productivity of offshore operations. A decrease of the dynamic load imposed on the lifted payload and ultimately on the crane can be made by changes in the system stiffness characteristics - application of a spring with an adaptive stiffness or adjusting the length of a cable during lifting [A4].

Another popular model proposed by DNV standards is a model of 2 degrees of freedom, which represents a simplification of the dynamic system of a PHC, for which the excitation is created by kinematic function applied as a vertical displacement to a crane tip. A simplified dynamic system of a PHC according to *DNV RP-N103 Modelling and analysis of marine operations* [44] might be modelled by the following system:

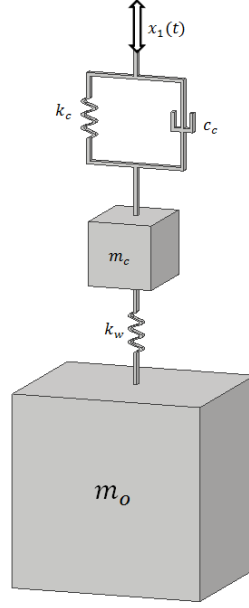


Figure 6: A simplified 2 DOFs passive compensator model [A4]

where:

$x_1(t) = x_A \sin(\omega t)$  - vertical displacement at the crane tip created by a kinematic excitation,

$x_A$  - amplitude of the exciting function,

$m_c$  - mass of heave compensator,

$m_o$  - mass of lifted payload,

$k_c$  - stiffness of heave compensator,

$k_w$  - wire stiffness,

$c_c$  - viscous damping of heave compensator.

The equations of motion for the simplified model is presented in the following:

$$\begin{bmatrix} m_c & 0 \\ 0 & m_o \end{bmatrix} \begin{bmatrix} \ddot{x}_c \\ \ddot{x}_0 \end{bmatrix} + \begin{bmatrix} c_c & 0 \\ 0 & 0 \end{bmatrix} \begin{bmatrix} \dot{x}_c \\ \dot{x}_0 \end{bmatrix} + \begin{bmatrix} k_c + k_w & -k_w \\ -k_w & k_w \end{bmatrix} \begin{bmatrix} x_c \\ x_0 \end{bmatrix} = \begin{bmatrix} c_c \dot{x}_1 + k_c x_1 \\ 0 \end{bmatrix} \quad (3)$$

It is worth noting that the proposed model does not consider a pendulatory motion of the lifted payload. Moreover, the vertical excitation introduces a vessel heaving only, ignoring its other possible motions. Although the model is sufficient to simulate the behaviour under water, however it will poorly reflect the actual behaviour of the object during in air-lifting, which is crucial for the lifting process.

On a contrary to overly simplified models, the industrial market software leaders offer numerical solutions, which in a lot of cases are either too complex or too expensive. Two leading software suppliers are Orcina [32] and DNV.

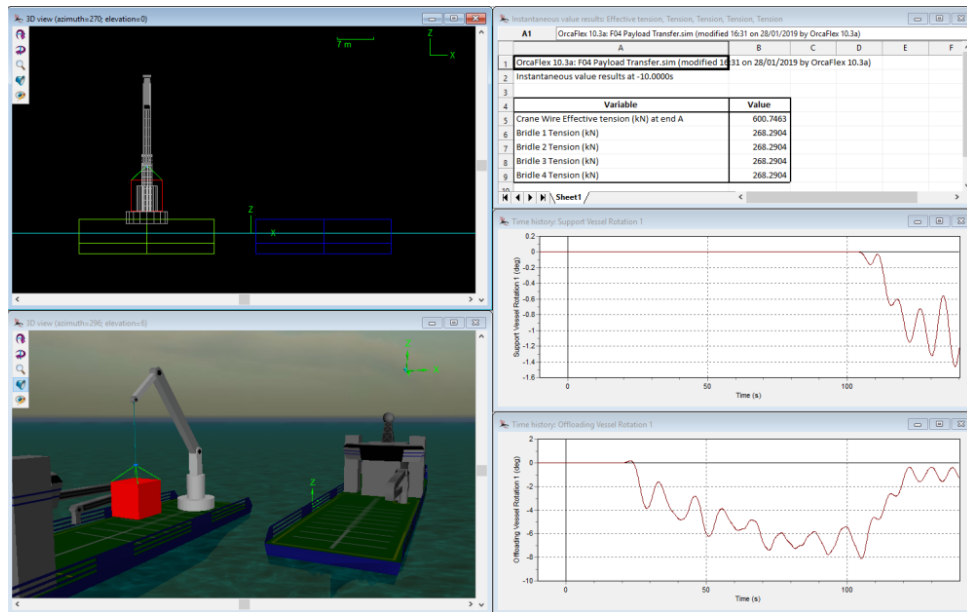


Figure 7: OrcaFlex user interface - preview [32]

OrcaFlex is a commercial software provided by Orcina for a dynamic analysis of offshore marine systems. It is particularly popular for its breadth of technical capability and user friendliness. OrcaFlex is a GUI based software providing GUI data input and results. The software enables modelling of a wide range of marine objects (lines, vessels, buoys, winches, links, constraints) and offers many options to apply environmental loads (sea, seabed, wind, waves, current). It provides a possibility to perform time domain, modal and fatigue analysis. However, all of the procedures utilise numerical integrating schemes that do not provide possibilities of an explicit analysis of physics of the modelled phenomena. Moreover, the rental cost of the package is £ 1500 per month or £ 25 000 for annual subscription. Similar functionalities are offered by Sesam package delivered by DNV. Sesam for marine systems includes the modules Sima, Simo and Rilex. Sima is the graphical front end for running Simo and Rilex simulations of marine operations. The scope of features provided is, among others, lifting and installation of subsea equipment, offshore wind turbine installation, offshore crane operations, subsea installation (eg. subsea templates), transportation (towing).

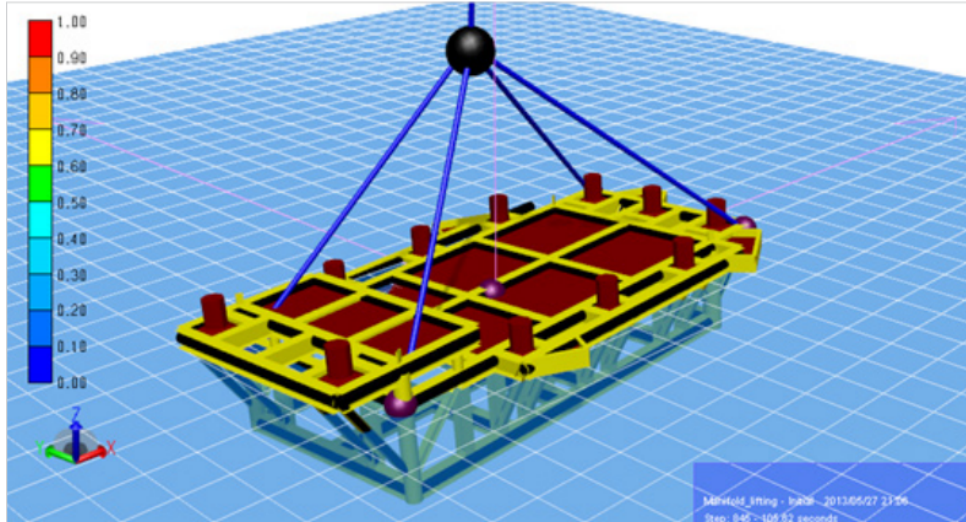


Figure 8: Sesam Sima result representation - 3D visualization [11]

There is no doubt that the both are to assist and support actual operations through familiarisation and allow for evaluation of their feasibility, however the biggest disadvantage in relation to some utilisation purposes is the cost that often prevents a purchase by smaller companies. The cost of a monthly license in case of one-time needs becomes unprofitable. Buying and maintaining such software with technical support is a high capital investment. In such case, it is more efficient and cheaper to perform calculations by internal means, especially when the analysis does not require highly advanced computational resources. Besides many of benefits, another disadvantage is a necessity to study an extensive documentation in order to be able to efficiently operate the software. Even experienced users report many problems with the post-processing of results related to software limitations.

In conclusion, it is understood despite utilisation of more sophisticated models and commercial software packages in the industry, offshore lifting planning is still a time-consuming process and requires more resource in order to execute particularly when simulating models of multi-degrees of freedom. Thus a simplicity and flexibility of the methodology to be proposed could give an advantage over presented solutions. Additionally, the proposed methodology is to provide a processing versatility allowing for a utilisation of various processing methods - time-domain, spectral and phase plane analysis. As one can notice an evident lack of a non-complex but comprehensive and effective solution, it is suggested that creation of a balanced, easily accessible tool placed between the overly simplified and highly complex alternatives will bring an advantage to lifting process operation planning.

#### 5.4. Literature review

Many publications examining the problem of offshore lifting operations can be found in a worldwide literature, however, in the vast majority they address either numerical analyses regarding coupled models with a particular focus on the lowering process or discuss proposals of deficient models neglecting relevant aspects of excitation-related phenomena that might occur during lifting operations. This leaves a scientific and also industrial gap to consider an equally important part of an offshore lift operation, which is in-air handling. This is the phase that

carries the greatest risk of resonance vibrations occurrence (either parametric or main), and thus the payload uncontrolled motion of large amplitudes that might be a threat for human health and life or cause damage to equipment. Moreover, due to a wide range of weights of structures installed, it is essential to study the mutual dynamics between the lifted weight and the lifting vessel and determine the limit of applicability of simplified models, which are widely proposed within literature.

As there are records reporting heavy lifts focusing only on a lowering phase, where the payload pendulation is naturally suppressed by the water, it seems to be essential to propose a modelling methodology of a coupled payload-vessel system allowing for a reliable assessment of the entire system dynamics when handling in air. The proposed model should enable analyses in a whole spectrum of lifted objects whether these are light or heavyweights. Some considerations addressing the problem of heavy lifts with a particular focus on lowering phase can be found in [31], [65], [20] and [21].

Energy recovery solutions based on rotational pendulum motions were very popular in the first decade of the 20th century. A lot of publications can be found regarding the concept of extracting energy from sea waves using pendulum dynamics [60], [61], [63], [19].

Considering the recovered energy applications, it seems to be relevant to investigate the pendulum dynamics carefully in terms of effects of the various and combined excitations - horizontal and vertical. Some of the studies do not consider a simultaneous action and compensation for heave, which seems to be a weakness, especially in case of large system displacement. However, an extensive group of publications are the studies discussing methods of compensation for heave and pendulum separately. The proposals of models and methods to compensate vessel heaving exclusively can be followed based on studies presenting very simple mathematical pendulums [24], shock absorbers [27], passive heave compensators (fully hydraulic or integrated with mechanical systems) [2], [44], through more advanced active compensation controlled with PLC [59] or engaging PID controllers that allow the changes of system stiffness characteristics [57]. A popular way of compensation encountered is also a choice of the right winch drive function. Such an approach was shown in [41], [12] and [58].

Most of the discussed papers present a simplified approach to modelling dynamics of real object, neglecting either its pendulatory motion or horizontal excitation. It seems to be too much of a simplification, especially when analysing dangerous scenarios looking for resonant states.

Scientific research regarding control or compensations of a pendulum motion can also be found although they are much rarer. The reason may be that the pendulum swing motion attenuation is more difficult to achieve than a compensation for heave. The current state-of-the-art provides the examples of active compensation using mechanical filters [3] or computer based controllers enabling position tracking and control [51], [38], [47], however the weakness might be seen in a lack of heave considerations. Other proposals include interference to the design of a deck crane [34], [35].

The mentioned articles do not consider a simultaneous action and compensation for heave, which seems to be a weakness of current approaches. Despite operational measures were introduced in order to reduce the uncontrolled pendulation risk under certain weather conditions

what became industry standard, the operational windows could be maximised should another reliable solution be found.

Regarding modelling of the payload itself, one can find a variety of propositions. The publications encountered present the models where the lifted load is simplified to either a single degree of freedom system described in three-dimensional space (spherical pendulum) or in two-dimensional planar motion (mathematical pendulum). The authors of [15], [64] investigated the dynamics of parametrically induced spherical pendulum vibrations and the investigation presented in [37] analyses a spherical pendulum damper dynamics and its stability under horizontal excitation. A wide study of a parametric pendula damping identification is provided in [26], [19] and [48]. Simple models of mathematical pendula might be found in [43], [52], [39], where the lifting model is presented as a single pendulum the excitation incorporated as an angular roll, ignoring the heave and the potential influence of the vessel. This methodology eliminates the ability to capture the parametric resonance. The dynamics for oscillatory and rotational motion of a parametric pendulum were studied by means of analytical methods and approximate analytical solutions were found in [62], [29] and [28]. Although the models are not discussed in the context of the lifted payload specifically, they are still a better representation as do not neglect an importance of the vertical excitation. When considering 2D motion, two degrees of freedom systems might be found and the problem is formulated based on a double pendulum systems. The research discuss the problems of both linear [8], [50], [14] and nonlinear vibrations [22].

On the other hand, one might encounter overly complex model proposals, where the study is based on a single, particular case preventing a reliable assessment of the whole phenomena. Such models can be found in [45], [25] and [1]. The authors of [45] propose a pendulation control by enormous number of lifting wires and hence multiple cranes or complex machinery involved.

A sufficiently accurate research model of the discussed phenomenon can be a mathematical pendulum (if all of the occurring phenomena included), which is an archetype for studying non-linear dynamics and complex phenomena, in various fields of science and engineering. Despite the fact that the first scientific interest in pendulum dynamics dates back centuries ago, it is still actively investigated. However, complex issues regarding the analysis of the motion of a pendulum the vibrations of which are induced parametrically are not particularly popular. In order to determine a nature of the phenomena, a model should be represented and described by its analytical solution. Some scientists proposed a method of harmonic balance in order to propose a closed form analytical solution [7], [36], [4]. Other research papers regarding dynamic behaviour of pendulum-like systems under nearly parametric excitation result in considerations of a model described in [18], [46] and [42]. The studies present the effects of an excitation in the form of a movement along an ellipse, perturbing the classical parametric pendulum.

Hardly any reports can be found regarding experimental research of parametrically driven pendulum. Experimental studies combined with analytical predictions based on multiple time scale method were developed by the authors of [33]. In works [23], [30] and [9] the authors verified experimentally the early theoretical predictions of periodic and chaotic behaviour of the pendulum-like system.

A more detailed analysis of the discussed articles can be found in the publications of mine listed in 4.2.

## **5.5. Objectives of thesis and motivation**

Despite the extensiveness of the analyses provided in scientific literature, a comprehensive approach, where the model and its investigating methodology allows for an intuitive analysis with regard to environmental factors is still not offered. Besides a purely mathematical modelling, the physical context and its interpretation in terms of lifted load dynamics has not been yet well-recognised. Analysing the available market solutions and disadvantages of the current modelling methodologies provided in scientific literature or engineering standards, it can be concluded that development of a new, properly balanced approach could be an effective solution allowing for a better performance that might benefit the whole operational process starting from very early stages of lifting planning through the control or compensation of the payload pendulatory motion. Amongst a variety of currently applied methods being either overly simplified or on a contrary, highly complex, the purpose of the dissertation is:

*'A development of a comprehensive payload-vessel analytical model for offshore lifting operation providing the possibility of a formulation of the solution on a basis of multiple-scale method in a closed analytical form that allows lifting process planning and modelling of the payload dynamic behaviour.'*

Moreover, the analytical formulation of the problem being usually numerically evaluated allows for a description of the lifting dynamics in a more interpretable form by exposing the influencing factors in the derived mathematical functions. The author's motivation is to provide a qualitative information as opposed to purely numerical investigation that might not be as precise as the utilisation of a closed form solution. Since the proposed analytical approach would allow for an in-depth study on mathematical dependencies related to physical effects occurring in the system, conducting the further research seems to be justified. What is more, one of the key elements of the study is a possibility to determine laws governing the phenomena related to lifted payload dynamics. The proposed model would incorporate the most relevant features of the models that might be already encountered in scientific field but also would introduce a significant advantage to the research methodology. The methodology is to provide a better understanding of the lifting system dynamics resulting in not only a quantitative but also qualitative information of the system dynamic behaviour.

Modelling methodology allowing for a determination of parameters constituting the vibrations of the object in terms of their selection in order to control or at least compensate the payload response might contribute the lifting operation increasing its safety. The opportunity for a better planning and understanding of offshore lifting unpredicted events may offer an avoidance of dangerous, high amplitude oscillations which, if uncontrolled or under unfavourable conditions, can turn into resonance phenomena leading to a huge problem of the operational instability of the system.

Industrially, the methodology offers an efficient recognition of a potentially problematic sce-

nario at early conceptual stages. It can constitute an additional step in a verification of numerical results or ultimately, in simpler cases, it can replace the numerical approaches completely. It can be stated that the methodology will address a better targeting at the design stage providing an interesting insights into control system design. It is also believed that the proposed algorithm might be preferable in terms of accessibility and computational efficiency on a contrary to commonly used integrating schemes.

The additional objective of the proposed modelling approach regarding a payload-vessel system is to determine the model uncoupling condition in a form of a threshold value related to the physical properties of the lifting object or the vessel in dependence on the lifting operation type. The distinction between the proposed lifting models with regards to modelling of environmental conditions was made and the classification based on the number of degrees of freedom, where 3 degrees of freedom model (3DoF) is related to payload dynamics only, whilst 5 degrees of freedom model (5DoF) describes the complete payload-vessel system dynamics. The qualitative contribution is seen in a fully payload-vessel system or decoupled (3DoF model) analysis taking into account hydrodynamic interaction and ship seakeeping properties based on the RAOs functions.

The modelling study may also enable a determination of operational conditions in order to access the stability regions. In terms of planning lifting operations, the presented methodology does not require a full analysis of the considered system dynamics. A determination of occurrences of undesirable resonance phenomena can be calculated based on the adapted to lifting case diagram creating the stable and unstable operational ranges with regard to length of the lifting set.

## **5.6. Scientific research assumptions**

The scientific contribution presented in the form of a series of publications allows to prove the assumed scientific objectives:

1. Wave modelling and RAOs processing methodology - determination of an environmental impact on marine structures.
2. Proposal of a novel approach to modelling dynamics in offshore lifting - development of an innovative model for operation planning to simulate lifted payload behaviour in payload-vessel system.
3. Numerical research on regular and irregular waves - a versatility of results processing methods.
4. Model of a coupled payload-vessel system for offshore lifts of light and heaveweight objects - determination of the scope of applicability and development of methods supporting planning in offshore lifting design process.
5. Derivation of an analytical closed form solution of the proposed model on a basis of perturbative methods from nonlinear theory of vibration. A possibility of qualitative description of the system dynamic features.



6. Analytical research on regular waves - comparative analyses and results convergence check in a wide range of lifting cable lengths. The approximated solution accuracy assessment and its potential use in operation planning.
7. Modelling methodology for a variety of dynamic systems based on created Python library.

### 5.6.1. Wave modelling and RAOs processing methodology - determination of an environmental impact on marine structures

In the article A4 one presented a brief overview of the developed methodology of a wave excitation modelling adopted for further research purposes. The article omits detailed considerations of the ship motions, on which the simplifications regarding the number of degrees of freedom of the payload-vessel model were based.

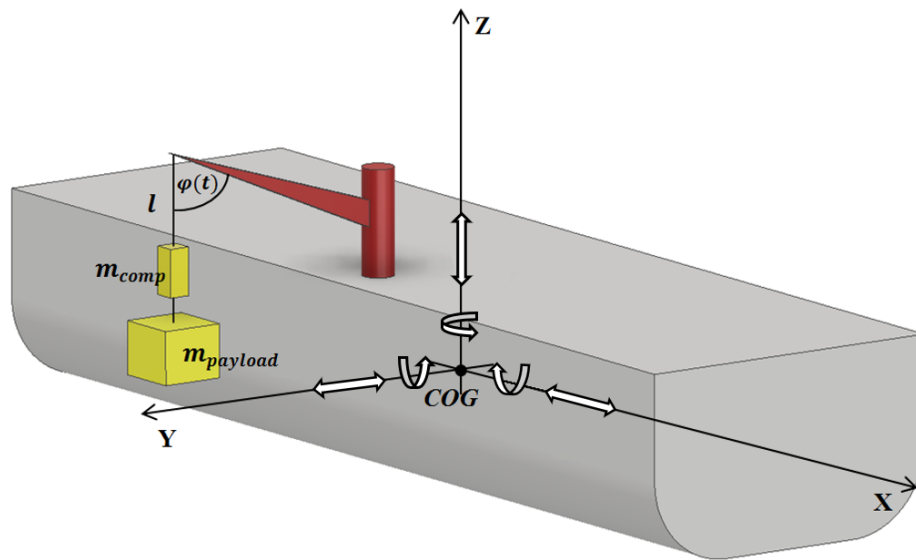


Figure 9: A 6DoFs vessel with the 3DoFs lifting system and its parameters [A4]

In order to verify the simplifying assumptions, one conducted an extensive numerical study taking into account 6 degrees of freedom vessel model related to its motions. A precise analytical description of ship motions requires a consideration of two types of motion on sea waves. The first type is of a linear character and is described by the following three movements: sway, surge and heave. The second one describes the three angular movements: roll, pitch and yaw, which are respectively transverse, longitudinal and vertical oscillations of the floating units. Floating objects are considered as continuous systems, which are subjected to complex motion characteristics being a composition of a rigid body motion and its vibration. In engineering practice, naval designs are stiff enough allowing to omit elastic properties of the vessel. In analytical considerations, it enables the application of a simple model of a rigid body described by 6 degrees of freedom. Such an approach allows the hydrodynamic forces to be represented as hydrodynamic added mass, fluid damping and restoring forces. Hence the considered vessel might be modelled by the following matrix equation:

$$(M_V + A(\omega)) \cdot \ddot{X}(\omega, \text{dir}) + C_V \cdot \dot{X}(\omega, \text{dir}) + K_V \cdot X(\omega, \text{dir}) = F(\omega, \text{dir}) \quad (4)$$

where:

$M_V$  - mass matrix of the vessel,

$A(\omega)$  - hydrodynamic added mass matrix,

$C_V$  - hydrodynamic damping matrix,

$K_V$  - vessel stiffness matrix,

$F(\omega, \text{dir})$  - hydrodynamic force vector,

$\omega$  - natural frequency,

$\text{dir}$  - wave direction,

$X(\omega, \text{dir})$  - vessel displacement vector.

Assuming the vessel hull has a longitudinal symmetry with respect to the  $OXZ$  plane, the matrix of generalised masses might be expressed as follows:

$$M_V = \begin{bmatrix} m_V & 0 & 0 & 0 & 0 & 0 \\ 0 & m_V & 0 & 0 & 0 & 0 \\ 0 & 0 & m_V & 0 & 0 & 0 \\ 0 & 0 & 0 & I_4 & 0 & -I_{46} \\ 0 & 0 & 0 & 0 & I_5 & 0 \\ 0 & 0 & 0 & -I_{64} & 0 & I_6 \end{bmatrix} \quad (5)$$

where:

$m_V$  - mass of the vessel,

$I_4 = r_{44}^2 m_V$  - moment of inertia of 4-th degree (with respect to  $x$  axis, determined by the radius of gyration),

$I_5 = r_{55}^2 m_V$  - moment of inertia of 5-th degree (with respect to  $y$  axis, determined by the radius of gyration),

$I_6 = r_{66}^2 m_V$  - moment of inertia of 6-th degree (with respect to  $z$  axis, determined by the radius of gyration),

$I_{46} = I_{64}$  - product of inertia.

It is worth noting that the inertia product  $I_{46}$  occurring in the matrix as a product of lateral rolling and yawing is generally of a negligible value and in numerical evaluation was further assumed to be equal 0.

The vessel mass term is modified with the implementation of a frequency dependent function, which is the hydrodynamic added mass  $A(\omega)$  and the final form of the vessel mass matrix

is given as  $M_V + A(\omega)$ . A hydrodynamic force due to the unit acceleration consists of 36 components. Assuming that  $A_{ij}$  is a component of the  $i$ -th direction caused by  $j$ -th direction acceleration, the added mass matrix can be expressed as follows:

$$A = \begin{bmatrix} A_{11} & A_{12} & A_{13} & A_{14} & A_{15} & A_{16} \\ A_{21} & A_{22} & A_{23} & A_{24} & A_{25} & A_{26} \\ A_{31} & A_{32} & A_{33} & A_{34} & A_{35} & A_{36} \\ A_{41} & A_{42} & A_{43} & A_{44} & A_{45} & A_{46} \\ A_{51} & A_{52} & A_{53} & A_{54} & A_{55} & A_{56} \\ A_{61} & A_{62} & A_{63} & A_{64} & A_{65} & A_{66} \end{bmatrix} \quad (6)$$

Assuming the symmetry of the vessel's body in  $OXZ$  plane, it can be concluded that vertical motion being a resultant due to heave and pitch does not induce a transversal force. Additionally considering a symmetry of the added mass matrix, it can be stated that  $A_{ij} = A_{ji}$  and the following dependencies might be obtained:

$$\begin{aligned} A_{32} &= A_{34} = A_{36} = A_{52} = A_{54} = A_{56} = 0 \\ A_{23} &= A_{43} = A_{63} = A_{25} = A_{45} = A_{66} = 0 \end{aligned} \quad (7)$$

Applying the same consideration to the longitudinal vessel motion, the following matrix elements might be omitted:

$$\begin{aligned} A_{12} &= A_{14} = A_{16} = 0 \\ A_{21} &= A_{41} = A_{61} = 0 \end{aligned} \quad (8)$$

Thus, the added mass matrix can be reduced to the following form:

$$A = \begin{bmatrix} A_{11} & 0 & A_{13} & 0 & A_{15} & 0 \\ 0 & A_{22} & 0 & A_{24} & 0 & A_{26} \\ A_{31} & 0 & A_{33} & 0 & A_{35} & 0 \\ 0 & A_{42} & 0 & A_{44} & 0 & A_{46} \\ A_{51} & 0 & A_{53} & 0 & A_{55} & 0 \\ 0 & A_{62} & 0 & A_{64} & 0 & A_{66} \end{bmatrix} \quad (9)$$

All of the components of the added mass matrix were determined based on strip theory with Lewis transformation and were considered in the vessel governing equations. The numerical values of the influencing elements presented in (10) are provided for reference for one exemplary frequency only:

$$A = \begin{bmatrix} 0.029 & 0 & 0 & 0 & 0.025 & 0 \\ 0 & 0.941 & 0 & 0.573 & 0 & 0.021 \\ 0 & 0 & 0.977 & 0 & 0.037 & 0 \\ 0 & 0.573 & 0 & 0.013 & 0 & 0.111 \\ 0.025 & 0 & 0.037 & 0 & 0.051 & 0 \\ 0 & 0.021 & 0 & 0.111 & 0 & 0.039 \end{bmatrix} \quad (10)$$

Hydrodynamic damping matrix of the vessel was obtained based on classic Rayleigh damping model being a viscous type of damping - proportional to the linear combination of mass and stiffness of the considered system. The damping model is then defined as follows:

$$C_V = \alpha M_V + \beta K_V \quad (11)$$

where:

$\alpha$  - mass proportional Rayleigh damping coefficient,

$\beta$  - stiffness proportional Rayleigh damping coefficient,

$M_V$  - vessel mass matrix,

$K_V$  - vessel stiffness matrix.

To determine the elements of the stiffness matrix, the hydrostatic stability of the vessel was analysed. The  $K_V$  is the considered vessel stiffness matrix:

$$K_V = \begin{bmatrix} 0 & 0 & 0 & 0 & 0 & 0 \\ 0 & 0 & 0 & 0 & 0 & 0 \\ 0 & 0 & \rho g A_w & 0 & -\rho g A_{wl} (CoF - CoB) & 0 \\ 0 & 0 & 0 & \rho g V G M_T & 0 & 0 \\ 0 & 0 & -A_w g \rho (CoF - CoB) & 0 & \rho g V G M_L & 0 \\ 0 & 0 & 0 & 0 & 0 & 0 \end{bmatrix} \quad (12)$$

where:

$g$  - acceleration of gravity,

$\rho$  - fluid density,

$V$  - submerged volume of the vessel,

$A_w$  - wetted area,

$CoB$  - centre of buoyancy,

$CoF$  - centre of floatation,

$GM_T$  - transverse metacentric,

$GM_L$  - longitudinal metacentric height.

Finally, the wave forces and moments were obtained as functions of wave frequency and direction. The hydrodynamic force vector for 6-directional excitation scenario might be then expressed as follows:

$$F(\omega, \text{dir}) = \begin{bmatrix} m_V \omega^2 A_1 \cos(\omega t + \varphi_1) \\ m_V \omega^2 A_2 \cos(\omega t + \varphi_2) \\ m_V \omega^2 A_3 \cos(\omega t + \varphi_3) \\ -m_V \omega^3 A_4 \sin(\omega t + \varphi_4) \cdot \frac{\omega}{g} \\ -m_V \omega^3 A_5 \sin(\omega t + \varphi_5) \cdot \frac{\omega}{g} \\ -m_V \omega^3 A_6 \sin(\omega t + \varphi_6) \cdot \frac{\omega}{g} \end{bmatrix} = \begin{bmatrix} F_1 \cos(\omega t + \varphi_1) \\ F_2 \cos(\omega t + \varphi_2) \\ F_3 \cos(\omega t + \varphi_3) \\ M_4 \sin(\omega t + \varphi_4) \cdot \frac{\omega}{g} \\ M_5 \sin(\omega t + \varphi_5) \cdot \frac{\omega}{g} \\ M_6 \sin(\omega t + \varphi_6) \cdot \frac{\omega}{g} \end{bmatrix} \quad (13)$$

where:

$F_j$  - amplitude of hydrodynamic forces given respectively for  $j = 1, 2, 3$  degree of freedom,

$\varphi_j$  - phase of hydrodynamic forces given respectively for  $j = 1, 2, 3, 4, 5, 6$  degree of freedom,

$M_j$  - amplitude of hydrodynamic moments given respectively for  $j = 4, 5, 6$  degree of freedom,

$\omega$  - frequency of excitation.

The system described by the relationship given in equation (4) is a composition of 6 second order differential equations what implies 6 linear independent eigenvectors and corresponding eigenvalues. An origin of the assumed coordinate frame is placed at the vessel Centre of Floation (CoF). Due to the fact that the centroid (CoG) of the vessel should not be assumed as the same point, that will cause the motion of CoG being a composition of the particular motions due to its eigenmodes. In practice, at least two or three natural frequencies will occur in the vessel response considered in frequency domain.

The system response can be determined by solving the governing equation (4) for the resulting motion defined as RAOs (Response Amplitude Operator), where  $X(\omega, \text{dir}) = RAO(\omega, \text{dir})$ . The solution vector is presented in equation (14):

$$RAO(\omega, \text{dir}) = F(\omega, \text{dir}) \cdot [-\omega^2 \cdot (M_V + A(\omega)) + i\omega \cdot C_V(\omega) + K_V]^{-1} \quad (14)$$

Considering the formula (14) it can be noticed that RAOs are effectively transfer functions used to determined the effect of sea state on ship motions. The solution can take many forms but most often represents a direction dependent displacement per meter wave versus the wave period. The RAOs amplitude is a representation of the motion amplitude per unit amplitude of a wave, whilst the RAOs phase lag represents the phase difference between the vessel motion and waves. The solution vector (14) will deliver separate RAO functions computed naturally

for each degree of freedom. The methodology of computing vessel motion response spectrum is presented schematically in Figure 10.

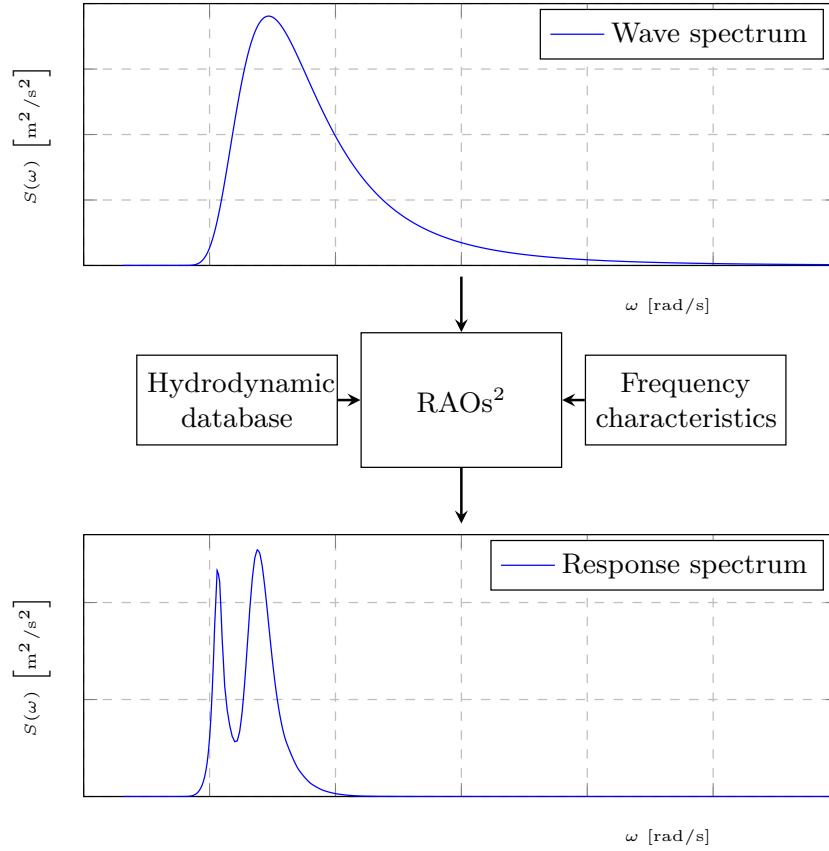


Figure 10: Methodology of computing motion response spectra of a floating unit at the specified remote point [A4]

Although the industrial practice offers alternatives to determine RAO functions these are expensive, time-consuming and available only for the existing units as the possibilities are based on empirical data collected during experimental investigation of the real floating object. Alternatively, RAOs can be obtained through a scaled model testing or with an application of one of the professional software discussed in section 5.3 but it still requires financial and computational resources. However, it is worth noticing that regardless the method used to determine the RAOs, a numerical set of data including the phase and direction information is obtained. Therefore, the methodology proposed in A4, which is about to finding the solution for the considered floating object omitting expensive hydrodynamic computations seems to be more advantageous.

In order to establish the excitation function being either a regular or irregular wave in case of offshore lifting operation modelling, the remote point spectrum or its specified point are used. Then the crane tip motions can be derived by applying basic geometrical properties and a complex signal adding method allowing for amplitude and phase information to be added and processed further into the harmonic (kinematic) excitation functions. An ability to adopt RAOs for computing an excitation enables the methodology to be economically viable within industrial or research environment. This significantly reduces the effort of modelling marine operations.

A more extensive information regarding signals adding and their transformations into harmonic functions can be found in paper A4.

#### **5.6.2. Proposal of a novel approach to modelling dynamics in offshore lifting - development of an innovative model for operation planning to simulate lifted payload behaviour in payload-vessel system**

The main objective of the research presented in article A4 was to propose a novel methodology for modelling offshore lifting operations by developing a model that would compensate the disadvantages of the encountered models and available solutions discussed in section 5. The presented 3DoF model incorporates vertical vibrations and pendulatory motion with an ability to process a bidirectional (elliptical) excitation. Additionally, the system includes a compensating element allowing for changes in its stiffness characteristics what enables a control of the model dynamic response. This approach, as proven within the article, allows to observe the interaction between various excitation directions and the payload dynamic response. The incorporation of bidirectional excitation results in ability to study the model parametric vibrations. Moreover, the advantage of the presented approach is seen in its versatility of the analysis that might be performed as it is based on analytical methods allowing a theoretical, numerical or combined analyses. A vessel motion is processed through RAO's methodology discussed in 5.6.1 resulting in a crane tip excitation in a form of kinematic functions providing a possibility to study responses to regular waving as well as systematic dynamic responses to irregular wave.

The presented method remains valid within the light lifts category as proven within the article A4. Heavy lifts require coupled analysis introducing additional complexity as broadly discussed in paper A3.

Taking into account the state-of-the-art, one proposed a balanced solution in the form of a three degrees of freedom dynamic model to study offshore lifting operation. The model consists of a crane tip equipped with a lifting cable with length dependent stiffness, mass and stiffness of the compensating element and also mass of the payload itself. In order to simplify analytical description of a complex model of ship motion, calculations regarding the excitation of the base movement transferred to the crane tip were based on assumptions of RAOs processing methodology. The proposed 3DoFs dynamic model is presented in Figure 11. The formulation of some simplifying assumptions allowed a derivation of the model governing equations. The equations of motion were derived based on the Lagrange's equations of second kind.

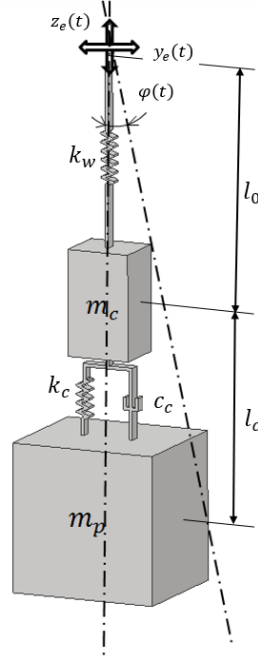


Figure 11: The proposed 3DoF dynamic model for offshore lifting analysis [A4]

where:

$y_e(t) = A_y \cos(\omega t + \Phi_y)$  - lateral displacement at crane tip obtained from RAOs (a regular wave excitation),

$z_e(t) = A_z \cos(\omega t + \Phi_z)$  - vertical displacement at crane tip obtained from RAOs (a regular wave excitation),

$A_y$  - amplitude of the lateral excitation,

$A_z$  - amplitude of the vertical excitation,

$\Phi_y$  - phase angle of the lateral motion,

$\Phi_z$  - phase angle of the vertical motion,

$m_p$  - mass of payload,

$m_c$  - mass of compensator,

$k_w$  - wire stiffness,

$k_c$  - stiffness of heave compensator,

$c_c$  - viscous damping of heave compensator,

$l_0$  - length of the lifting cable,

$l_c$  - length of the attached compensating element,

$g$  - standard acceleration of gravity  $9.81 \text{ m s}^{-2}$ .

A milestone in the proposed methodology was to confirm the correctness of a payload-vessel response assumption within the light lifts category. To ensure validity, one has conducted numerical analysis taking into account 6 degrees of freedom related to the vessel motion and



3 degrees of freedom describing the proposed model dynamics. The considerations concern one-dimensional forward propagating regular waves as a vessel excitation. According to the classification [44], the vessel motion characteristic is not altered until lifted objects weight is less than 2% of the vessel's displacement. This assumption allowed coupled dynamic analysis to be disregarded and utilise response amplitude operators and phases in order to obtain the excitation functions. The comparative analysis results have given satisfactory confirmation of the referenced assumption within the field of quantitative assessment. Further research being discussed in A3 allowed to define a more accurate boundary between the qualitative change of the dynamic response of the systems, and thus the change of the lifting category from light to heavy lift.

Simulation results of the proposed model's dynamics have been validated utilising the commercial package discussed in 5.3. The conditions from the analysed 3DoFs model were accurately replicated within the software-based model. The results extracted from the OrcaFlex were a sway angle of the system and vertical displacements for both of the masses. A created model enabled the implementation of the excitation in the kinematic form in two independent directions. The obtained results were considered as consistent and proving the validity of the proposed 3DoFs model. A more extensive study regarding lifting category and the model validation can be followed in A4, section 4.

### **5.6.3. Numerical research on regular and irregular waves - a versatility of results processing methods**

Numerical simulation studies presented in A4 were prepared in order to prove the comprehensiveness and versatility of the proposed lifting modelling methodology over existing solutions. An additional aspect increasing the value of the method was a development of the own modelling and simulation environment based on Python programming language. The environment was written utilising Python free libraries distributed under the GNU General Public License giving a possibility of a completely free use for private and commercial purposes. The advantage makes the methodology an interesting alternative to paid software packages.

Numerical simulations were performed for three independent models - the analysed 3DoF, Mathieu and one of the referenced models (a mathematical pendulum with moving support) in order to enable a comparative analysis revealing advantages of the proposed solution. Nevertheless, it should be highlighted that a direct dynamics analysis was not able to be conducted because of comparative models limitations. Exclusively, the results of pendulatory motion of each model were presented and discussed as the referenced models do not investigate linear displacements. The models were analysed for a variety of scenarios subjected to specific excitations applied as a regular or irregular wave resulting in crucial payload dynamic behaviour while considering operation planning.

The simulation sets were prepared so that to present the 3DoF model's stiffness/cable length manipulation allow a compensation of the amplitude of payload pendulation. One of the two analysed cases concerned an over-stiffened 3DoFs model (showing the same dynamics as the Mathieu model) whilst the other one when its adjusted stiffness allowed the compensation.

To emphasise crucial phenomena likely to occur under unfavourable conditions for the pay-

load sway response, the simulations were performed for some specified operational cable lengths determining an occurrence of a hazardous parametric or main resonance for high amplitude of heave excitation for 7 s wave period, which is a representation of a medium-slow wave. The vibration frequency was set equal to sub-harmonic critical frequency for the specific resonance to excite.

Numerical studies conducted regarded the proposed model sensitivity analysis by determination of heave excitation impact on the lifted object sway response proving a relevance of vertical excitation incorporation. Moreover, the compensation of parametric and main resonance vibrations for defined and random excitation parameters was assessed. The analyses were performed based on a fully nonlinear and linearised model. Some illustrative results are presented in Figures 12-15. The entire study can be traced in A4, section 5.2.

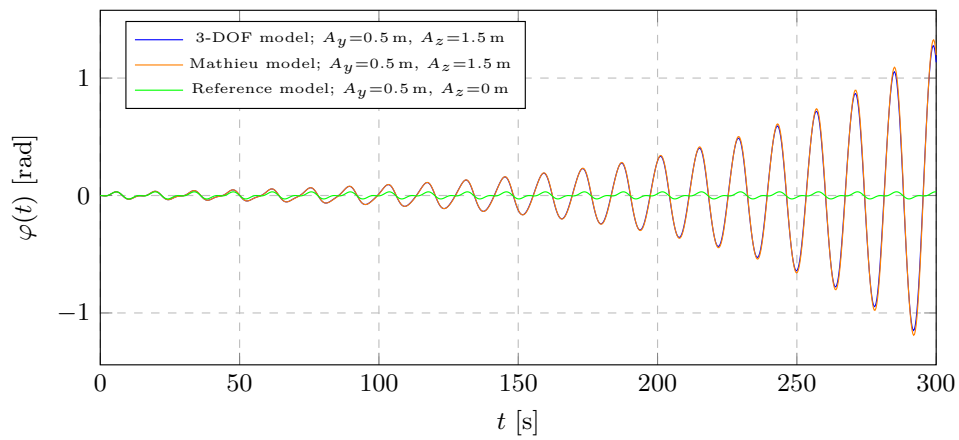


Figure 12: Sway angle response to high amplitude of heave excitation; parametric resonance case - stiffened 3DoF model [A4]

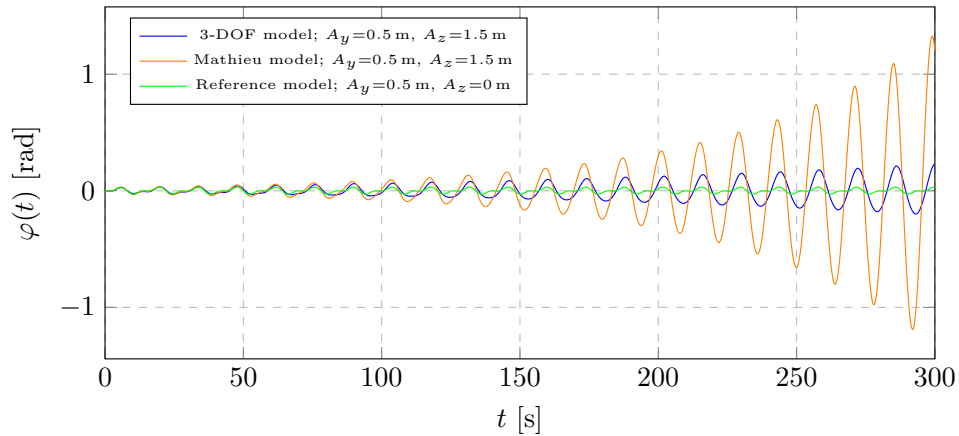


Figure 13: Sway angle response to high amplitude of heave excitation; parametric resonance case - reduced compensator stiffness [A4]

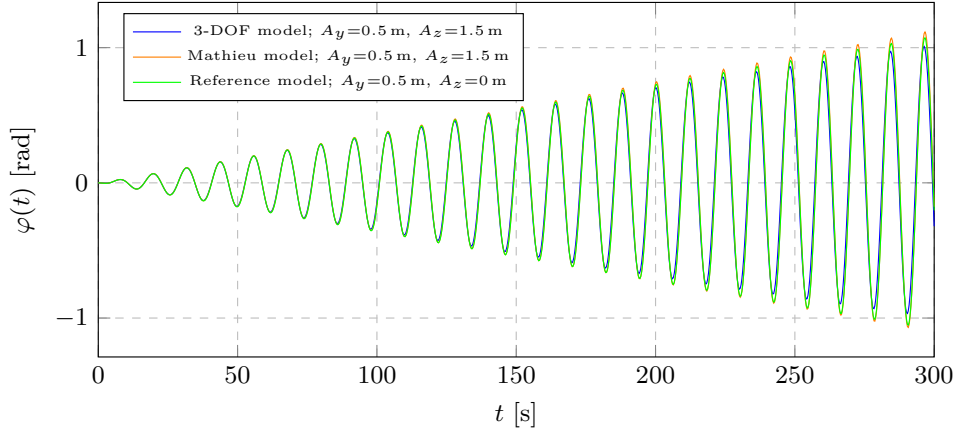


Figure 14: Sway angle response to high amplitude of heave excitation; main resonance case - stiffened 3DoF model [A4]

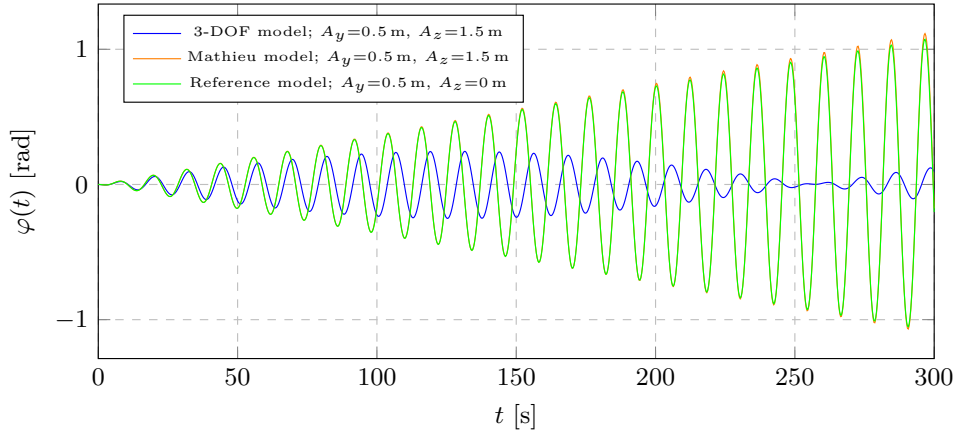


Figure 15: Sway angle response to high amplitude of heave excitation; main resonance case - reduced compensator stiffness [A4]

Additionally, the proposed methodology provides processing versatility as it allows for a utilisation of various processing methods - time-domain, spectral and phase plane analysis. Compatible solutions can be obtained and the lifted object dynamics can be assessed by analysing phase portraits presented in Figures 16, where the payload pendulation has a form of deformed unstable spirals and in Figure 17, where the resonance behaviour for the 3DoF model with a previously growing trajectory is replaced with a limited curve indicating stable dynamics.

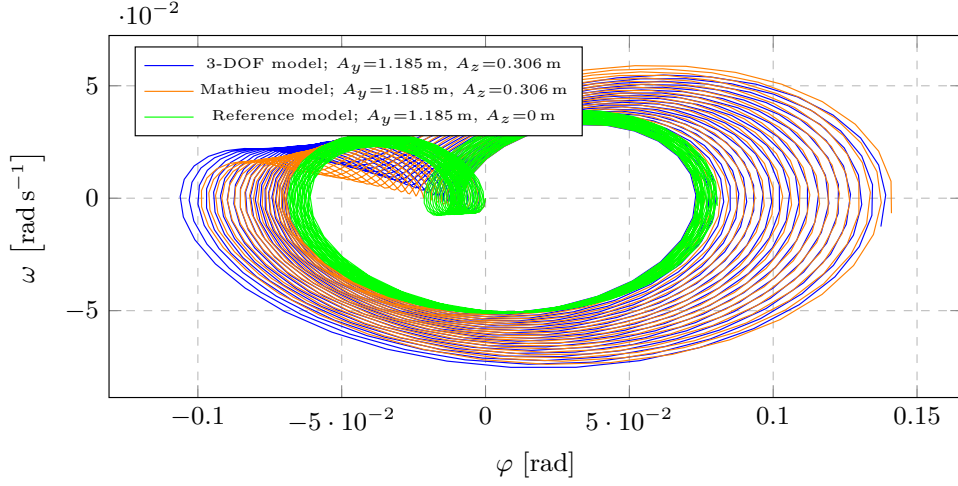


Figure 16: Phase portrait of sway angle response corresponding to the stiffened 3DoF model case [A4]

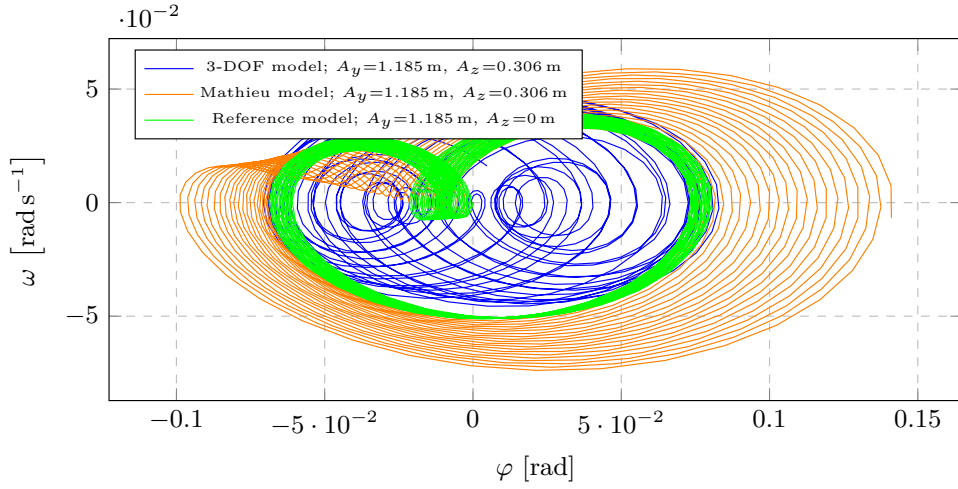


Figure 17: Phase portrait of sway angle response corresponding to reduced compensator stiffness case [A4]

Another interesting case study are simulations conducted for resonance beyond cable length for idealised regular wave scenario showing a behaviour of the nonlinear model. As can be seen in Figures 18 and 19, the nonlinear model exhibits features of self-limitation of the amplitudes of pendulation even for close values of resonant frequencies. This implies that the system should be stable however high displacements are still present allowing the possibility of a sudden change in the dynamics of the lifted object.

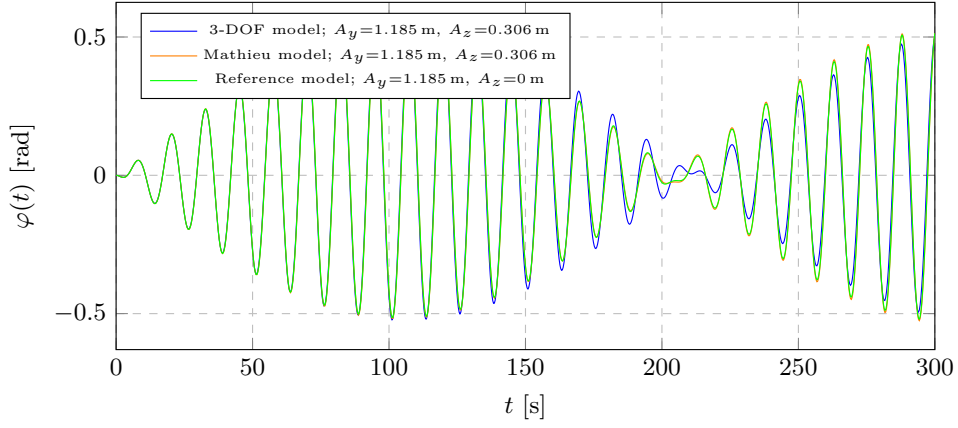


Figure 18: Sway angle response to induced excitation; non-resonant case - stiffened 3DoF model [A4]

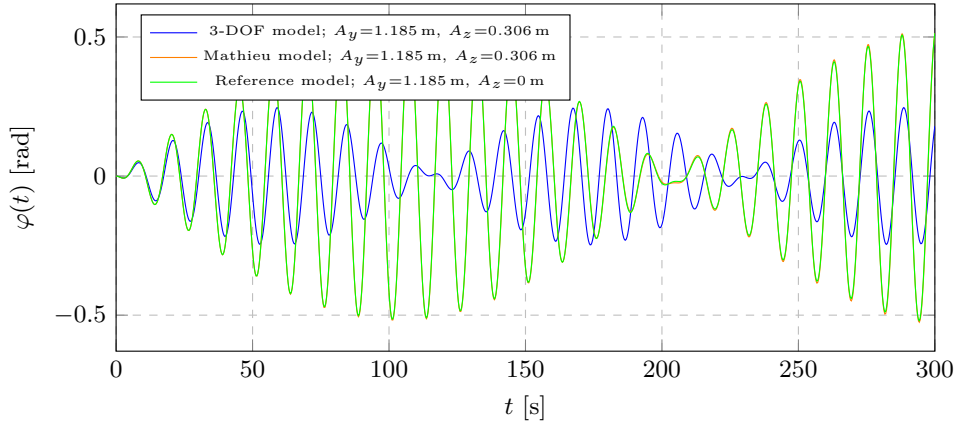


Figure 19: Sway angle response to induced excitation; non-resonant case - reduced compensator stiffness [A4]

Similar information can be obtained from the analysis incorporating irregular wave excitation derived based on JONSWAP spectra theory. The real sea-state excitation achieved from RAOs after inverse fast Fourier transform utilised to simulate an hour lifting operation process as well as simulations of linear and nonlinear model responses to irregular waving can be followed further in the discussed article. The 3DoF model response to the applied excitation confirmed the effectiveness of the proposed methodology.

#### 5.6.4. Model of a coupled payload-vessel system for offshore lifts of light and heavyweight objects - determination of the scope of applicability and development of methods supporting planning in offshore lifting design process

In order to provide a fully comprehensive procedure serving to model offshore lifting being able to represent a faithful payload dynamics when operating in air beyond the application of light lifts assumption, one proposed the methodology discussed within article A3. The proposed concept was created to achieve the best possible efficiency for the problems within both, light and heavy lifts category. The model allows the investigation of mutual relations between the

coupled payload-vessel degrees of freedom. The coupled model provides the results being convergent to the proposed 3DoF model in light lifts regime what makes the presented approach more widely applicable than the utilisation of the model representing the payload dynamics independently to a vessel. However, the choice between the models should be fitted to purpose and made depending on the scope of the analyses to be performed.

The analytical equations of motion for the coupled model were derived based on a total energy formulation presented in details in A3, section 3. Some selected results of numerical evaluation are depicted in Figures 20 and 21 in a form of time domain analysis (payload response) and frequency spectra (vessel heave). The following simulations depict a comparative analysis of the payload response results for a number of different payload masses for two different frequencies of excitation - medium slow waves in range of 7 s to 8 s.

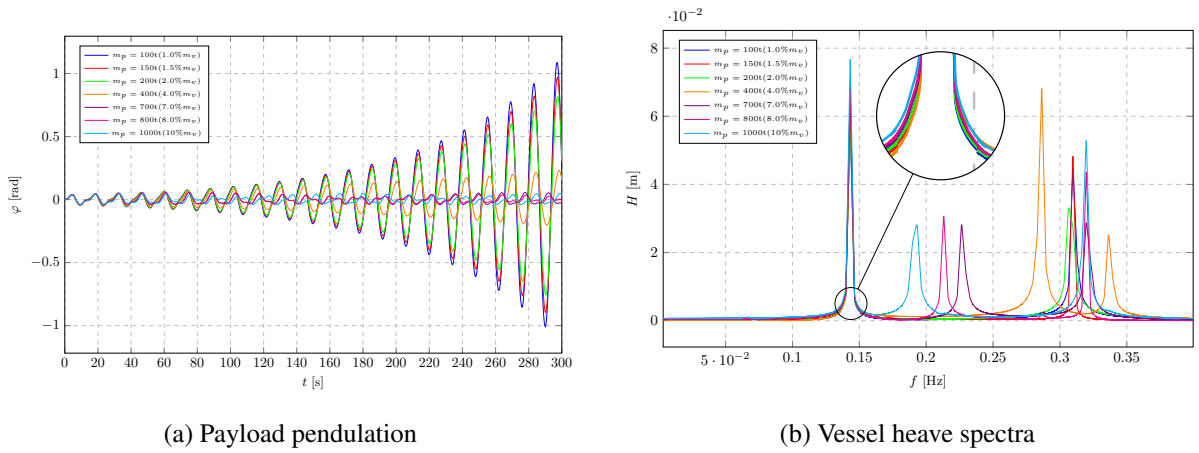


Figure 20: Comparative results for different payload weights ( $T = 7\text{s}$ ,  $l_0 = 48.7\text{m}$ ) [A3]

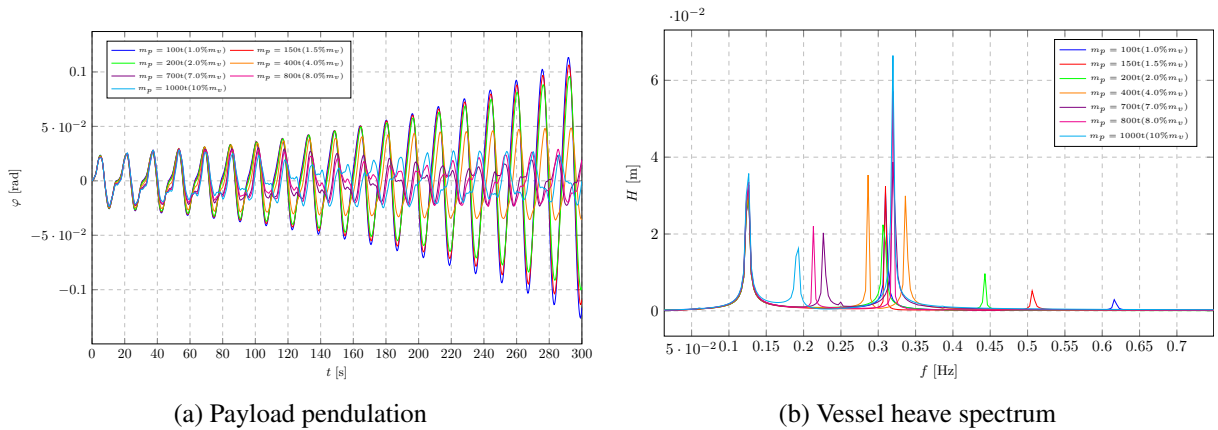


Figure 21: Comparative results for different payload weights ( $T = 8\text{s}$ ,  $l_0 = 63.6\text{m}$ ) [A3]

Payload mass to vessel displacement ratios were investigated for light and heavyweight objects lifts. The results of the investigation are depicted as waveforms confirming the same features of the considered system independently to the wave excitation. The payload response remains unchanged (negligible amplitudes changes) within light lift category in terms of quality of the phenomenon while after passing the threshold value of 3-4 %, the oscillations expose a

noticeably different character and amplitude values of payload dynamics. It confirms the coupled payload-vessel model gives a satisfactory confirmation of the referenced assumption given in A4 and strongly indicates the necessity to analyse coupled dynamics within heavy lifts category. An extensive analysis of many cases with direct comparative analyses is presented in A3, section 4.

#### **5.6.5. Derivation of an analytical closed form solution of the proposed model on a basis of perturbative methods from nonlinear theory of vibration. A possibility of qualitative description of the system dynamic features**

Despite the extensive literature studies, all of the research with regards to mathematical models serving to simulate offshore lifting operation are focused on a purely numerical evaluation of results. As the physical interpretation and qualitative information of the lifted load dynamic behaviour has not been yet still recognised, in order to assist with process of planning offshore lifting, one developed a nonlinear model and its purely analytical investigating methodology allowing an intuitive analysis regarding environmental factors. The analytical approach presented in the article A1 provides an explicit mathematical function determining the payload dynamic behaviour. That allows the analysis of parameters constituting the vibrations of the object in terms of their selection in order to compensate the payload response. The payload oscillations may be controlled throughout a proper planning being based on familiarisation of simulated and analysed problematic scenarios causing potentially dangerous resonance phenomena. Better targeting at the design stage might provide interesting insights into control system design. Moreover, having the analytical model and its closed form solution, aids the analysis process by supporting the numerical processing requirement constituting an additional step in a verification of numerical results or in some cases replacing the numerical approaches completely.

The governing equations were derived based on kinetic and potential energies of the considered subsystems and presented as a unique form of vectors being a representation of the ordered types of mathematical terms indicating the nature of occurring phenomena and assigning a proper physical context. Each vector represents a different type of either nonlinearity or external excitation. Analysing the particular vectors, they can be attributed to some physical phenomena due to the occurrence of explicit dependencies. This may allow a better understanding of the governing laws in terms of contributors disturbing stability of the lifted objects. A detailed analysis of the particular components of the governing equations can be found in A1, section 3.

The system eigenvalues and eigenmodes were determined based on the process of diagonalization of the system separated linear part  $M^{-1} \cdot K$  (15) of the equations of motion. Assuming some dependencies regarding the model's masses and stiffnesses relation, the eigenvalue and eigenmode matrix can be expressed as follows:

$$M^{-1}K = \begin{bmatrix} \frac{S_0 g}{I_0} & 0 & 0 \\ 0 & \frac{k_c}{m_p} & -\frac{k_c}{m_p} \\ 0 & -\frac{k_c}{m_c} & \frac{k_c + k_w}{m_c} \end{bmatrix} \quad (15)$$

$$\mathbf{\Omega}^2 = \begin{bmatrix} \frac{S_0 g}{I_0} & 0 & 0 \\ 0 & \frac{k_c \kappa}{2m_p \mu} - \frac{k_c \lambda}{2m_p \mu} + \frac{k_c}{2m_p} + \frac{k_c}{2m_p \mu} & 0 \\ 0 & 0 & \frac{k_c \kappa}{2m_p \mu} + \frac{k_c \lambda}{2m_p \mu} + \frac{k_c}{2m_p} + \frac{k_c}{2m_p \mu} \end{bmatrix} \quad (16)$$

$$\mathbf{P} = \begin{bmatrix} 1 & 0 & 0 \\ 0 & \frac{\kappa}{2} + \frac{\lambda}{2} - \frac{\mu}{2} + \frac{1}{2} & \frac{\kappa}{2} - \frac{\lambda}{2} - \frac{\mu}{2} + \frac{1}{2} \\ 0 & 1 & 1 \end{bmatrix} \quad (17)$$

where:

$$\kappa = \frac{k_w}{k_c}$$

$$\mu = \frac{m_c}{m_p}$$

$$\lambda = \sqrt{1 + \kappa^2 + \mu^2 + 2\kappa + 2\mu - 2\kappa\mu} ,$$

$I_0$  - second moment of area,

$S_0$  - first moment of area,

$M$  - inertia matrix of payload,

$K(t)$  - time-dependent stiffness matrix of payload.

Based on a transformation law  $Y = \mathbf{P}^{-1} \cdot X$ , one transformed the generalised coordinates into a modal form, hence the system of governing equations can be expressed in modal coordinates as per in equation (18):

$$\ddot{Y} + \mathbf{\Omega}^2 \cdot Y + \varepsilon \mathbf{P}^{-1} F_\varepsilon(\mathbf{P} \cdot Y, t) = 0 \quad (18)$$

where:

$Y$  - vector of modal coordinates.

The obtained form of linearly decoupled system allows the analysis of equations separately. For this type of problems, a perturbative methods from nonlinear theory of vibration can be used efficiently. A solution to be obtained is mainly composed of the elements, which come from the linear part of the ODE's. Additional small components (being proportional to small parameter) are caused by a cubic nonlinearity and parametric effects. A solution of the considered equations of motion (19) was derived based on a method of multiple scales of time:

$$\ddot{Y}(t) + \omega^2 Y(t) + \varepsilon \omega^2 Y^3(t) + F_e(Y(t), t) = 0 \quad (19)$$

The vector  $Y$  is determined as  $Y = [Y_\varphi \ Y_h \ Y_{h_c}]^T$ . The author assumed the following dependencies:  $Y_\varphi = Y_{00}$ ,  $Y_h = Y_{10}$  and  $Y_{h_c} = Y_{20}$ , where the first digit in the  $Y$  subscript



stands for the consecutive generalised coordinates and the second digit is a representation of the order of the equation considered.

In order to give a reliable insight on the dynamics of the parametrically induced (an elliptical crane tip motion resulting from the excitation of regular wave) payload pendulation, the considered 3DoF model has been simplified to the model close to Mathieu oscillator based on the model's similar behaviour presented in [5]. The payload pendulatory motion is determined by the generalised coordinate  $Y_0(t)$  and hence the equation on motion might be presented as follows:

$$\ddot{Y}_0(t) + \frac{\omega^2 (\delta\varepsilon + 1) Y_0(t)}{4} - \frac{\omega^2 (\delta\varepsilon + 1) Y_0(t)^3}{24} + A_z \omega^2 \varepsilon Y_0(t) \cos(\Phi_z + \omega t) - \frac{A_z \omega^2 \varepsilon Y_0(t)^3 \cos(\Phi_z + \omega t)}{6} - A_y \omega^2 \varepsilon \cos(\Phi_y + \omega t) = 0 \quad (20)$$

After applying the chosen analytical method, the zeroth-order approximate solution was obtained as the relation presented in (21):

$$Y_{00}(t) = \left( C_1 e^{-\frac{\omega t \varepsilon \sqrt{4A_z^2 - \delta^2}}{4}} + C_2 e^{\frac{\omega t \varepsilon \sqrt{4A_z^2 - \delta^2}}{4}} \right) \cos\left(\frac{\omega t}{2}\right) + \left( \frac{C_1 (2A_z \cos(\Phi_z) + \delta) e^{-\frac{\omega t \varepsilon \sqrt{4A_z^2 - \delta^2}}{4}}}{2A_z \sin(\Phi_z) - \sqrt{4A_z^2 - \delta^2}} + \frac{C_2 (2A_z \cos(\Phi_z) + \delta) e^{\frac{\omega t \varepsilon \sqrt{4A_z^2 - \delta^2}}{4}}}{2A_z \sin(\Phi_z) + \sqrt{4A_z^2 - \delta^2}} \right) \sin\left(\frac{\omega t}{2}\right) \quad (21)$$

where  $C_1$  and  $C_2$  are constants of integration.

First-order approximation of a particular solution for the excited vibrations given in the general form of  $Y_0(t_0, t_1) = Y_{00} + \varepsilon Y_{01}$ , takes the form presented in (23). The consecutive approximations can be obtained by repeating the procedure described in A1, section 4.

$$Y_0(t_0, t_1) = -\frac{4A_y \varepsilon \cos(\Phi_y + \omega t_0)}{3} - \frac{A_z \varepsilon C_1^3(t_1) \sin(\Phi_z + \frac{3\omega t_0}{2})}{32} + \frac{A_z \varepsilon C_1^3(t_1) \sin(\Phi_z + \frac{5\omega t_0}{2})}{288} - \frac{A_z \varepsilon C_1^2(t_1) C_2(t_1) \cos(\Phi_z + \frac{3\omega t_0}{2})}{32} + \frac{A_z \varepsilon C_1^2(t_1) C_2(t_1) \cos(\Phi_z + \frac{5\omega t_0}{2})}{96} - \frac{A_z \varepsilon C_1(t_1) C_2^2(t_1) \sin(\Phi_z + \frac{3\omega t_0}{2})}{32} - \frac{A_z \varepsilon C_1(t_1) C_2^2(t_1) \sin(\Phi_z + \frac{5\omega t_0}{2})}{96} + \frac{A_z \varepsilon C_1(t_1) \sin(\Phi_z + \frac{3\omega t_0}{2})}{4} - \frac{A_z \varepsilon C_2^3(t_1) \cos(\Phi_z + \frac{3\omega t_0}{2})}{32} - \frac{A_z \varepsilon C_2^3(t_1) \cos(\Phi_z + \frac{5\omega t_0}{2})}{288} + \frac{A_z \varepsilon C_2(t_1) \cos(\Phi_z + \frac{3\omega t_0}{2})}{4} + \frac{l_w \varepsilon C_1^3(t_1) \sin(\frac{3\omega t_0}{2})}{192} + \quad (22)$$

$$\begin{aligned}
& + \frac{l_w \varepsilon C_1^2(t_1) C_2(t_1) \cos\left(\frac{3\omega t_0}{2}\right)}{64} - \frac{l_w \varepsilon C_1(t_1) C_2^2(t_1) \sin\left(\frac{3\omega t_0}{2}\right)}{64} \\
& - \frac{l_w \varepsilon C_2^3(t_1) \cos\left(\frac{3\omega t_0}{2}\right)}{192} + \varepsilon C_1(t_1) \sin\left(\frac{\omega t_0}{2}\right) \\
& + \varepsilon C_2(t_1) \cos\left(\frac{\omega t_0}{2}\right) + C_1(t_1) \sin\left(\frac{\omega t_0}{2}\right) + C_2(t_1) \cos\left(\frac{\omega t_0}{2}\right)
\end{aligned} \tag{23}$$

The formulas for the constants  $C_1(t_1)$  and  $C_2(t_1)$  are given as presented in (24) and (25). A derivation of step-by-step solution with a utilisation of multiple time scale method can be followed in A1, section 4.

$$C_1(t_1) = C_1 e^{-\frac{\omega \sqrt{2A_z - \delta} \sqrt{2A_z + \delta} t_1}{4}} + C_2 e^{\frac{\omega \sqrt{2A_z - \delta} \sqrt{2A_z + \delta} t_1}{4}} \tag{24}$$

$$\begin{aligned}
C_2(t_1) = & - \frac{C_1 \cdot (2A_z \cos(\Phi_z) + \delta) e^{-\frac{\omega \sqrt{2A_z - \delta} \sqrt{2A_z + \delta} t_1}{4}}}{2A_z \sin(\Phi_z) + \sqrt{2A_z - \delta} \sqrt{2A_z + \delta}} + \\
& - \frac{C_2 \cdot (2A_z \cos(\Phi_z) + \delta) e^{\frac{\omega \sqrt{2A_z - \delta} \sqrt{2A_z + \delta} t_1}{4}}}{2A_z \sin(\Phi_z) - \sqrt{2A_z - \delta} \sqrt{2A_z + \delta}}
\end{aligned} \tag{25}$$

The presented methodology does not require a full analysis of the considered system dynamics in order to assess the stability regions (in terms of planning the system operation). The information provided by the conditions for a removal of the secular terms (the constants  $C_1(t_1)$  and  $C_2(t_1)$ ) is already sufficient for a determination of stable and unstable zones.

The presented analytical approach describes a method of finding the approximate solution for nonlinear dynamics of a payload forced pendulation allowing description of lifting dynamics in a more interpretable form by exposing the influence factors in the analysis formulas. As might be expected, the inaccuracy with regards to numerical results in the derived approximation will be less significant as more terms of the predicted solution are considered. Nevertheless taking into account the value of the small parameter recognised as  $\varepsilon = \frac{1}{l_w}$ , it can be stated that a much better results convergence will not be achieved in terms of quantitative results with consecutive approximations.

#### **5.6.6. Analytical research on regular waves - comparative analyses and results convergence check in a wide range of lifting cable lengths. The approximated solution accuracy assessment and its potential use in operation planning**

In order to deliver a satisfactory confirmation of the proposed analytical method, one presented an extensive research regarding a comparative study between the results obtained from a direct integration of the nonlinear governing equation and the analytically derived payload response first approximation. The base movement (vessel excitation) was introduced as a one directional regular wave resulting in elliptical crane tip motion. The proposed methodology was validated for two scenarios - payload oscillations outside the resonant region and on the resonance curve.

The analysis conducted covers time and spectral domain for three types of excitation - vertical (heave) only and two exciting ellipses diversified by a ratio of the semi-axes resulting in lateral and vertical exciting amplitudes. It is worth noting that the presented two sets differ from the first one by adding a lateral excitation  $A_y$  that will affect the results achieved. A direct comparisons for payload sway response in time domain were studied for two specific cable lengths - one being out of resonant zone (35 m), the other one causing parametric resonance vibrations (48.7 m), both for  $T = 7$ s wave period. An interesting dynamic properties are also provided to observe based on comparative analysis of results in spectral domain.

Some representative results, revealing the most relevant features of the proposed analytical solution are presented in Figures 22 - 24. An in-depth study can be followed in A1, section 5.

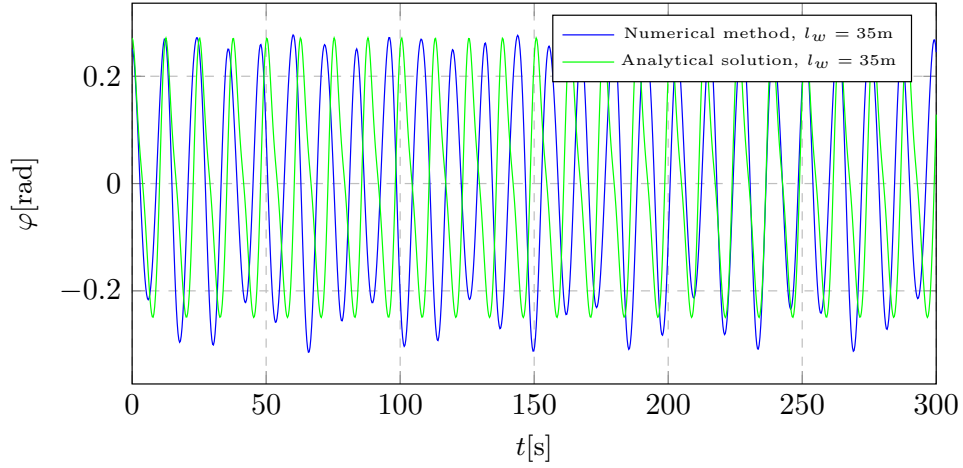


Figure 22: Payload pendulation comparative results for a numerical and analytical solution (elliptical excitation at the pivot point for  $A_y = 0.5$ m,  $A_z = 1.5$ m, cable length = 35 m) [A1]

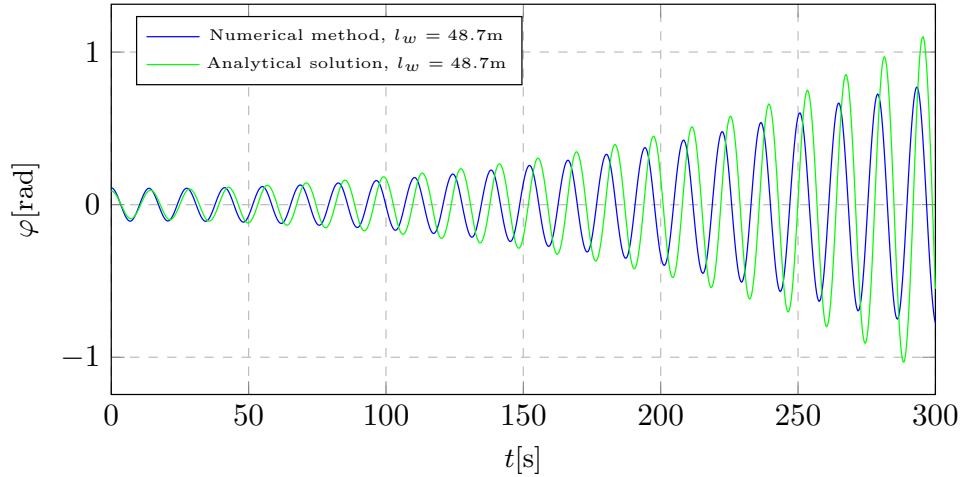


Figure 23: Payload pendulation comparative results for a numerical and analytical solution (elliptical excitation at pivot point for  $A_y = 0$ m,  $A_z = 1$ m, resonant cable length) [A1]

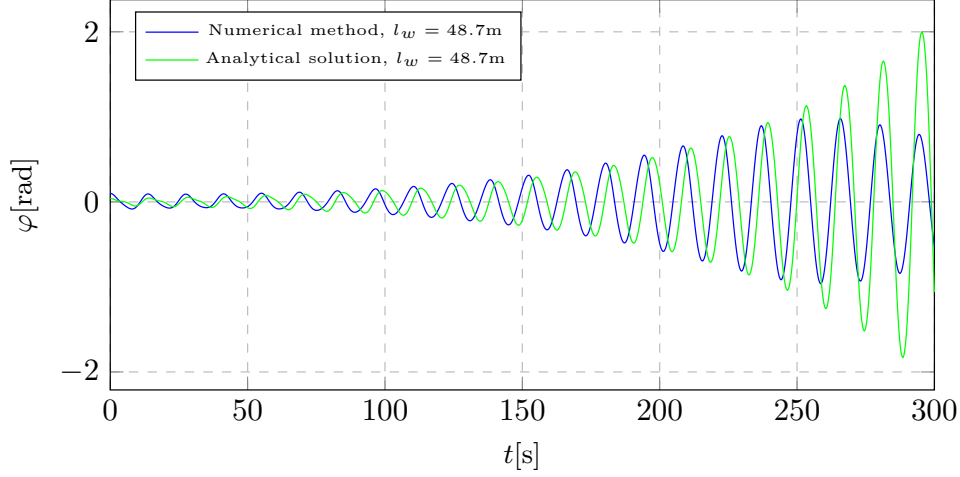


Figure 24: Payload pendulation comparative results for a numerical and analytical solution (elliptical excitation at pivot point for  $A_y = 0.5\text{m}$ ,  $A_z = 1.5\text{m}$ , resonant cable length)

As can be observed, the non-resonant vibrations (Fig. 22) show almost ideal correspondence in terms of amplitudes values. Greater discrepancies can be seen in resonant states. The factors amplifying the phenomenon are the higher values of excitation amplitudes clearly visible in Figure 24, where the analytical solution achieves more conservative values while the numerical integration curve shows a self-limitation of the payload response amplitude. The behaviour is a feature of nonlinear systems or is the result of damping used in the numerical integration scheme. Nevertheless, the analytical approximation confirms the correctness of nonlinear numerical model mapping. A detailed analysis is provided in discussion of the results presented in the corresponding article.

The evidence on the approximated solution accuracy and its potential use in operation planning is presented in Figures 25 and 26 where one can study the results of the lifted object dynamic behaviour presented as a direct comparison of the solutions' amplitudes reached by the analysed model in a wide range of lifting cable lengths. The results cover a range of two resonant states and a wide span of cable lengths in out-of-resonance zone.

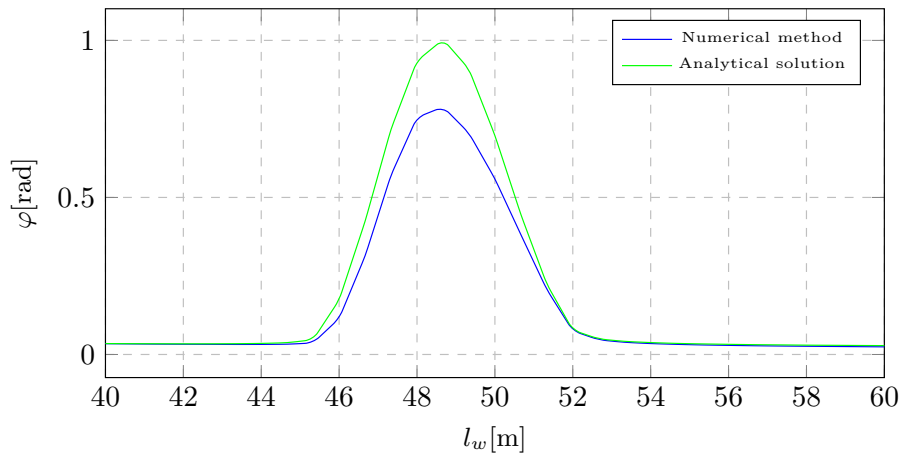


Figure 25: Results of a comparative analysis between the analytical and numerical solution,  $T = 7\text{s}$  [A1]

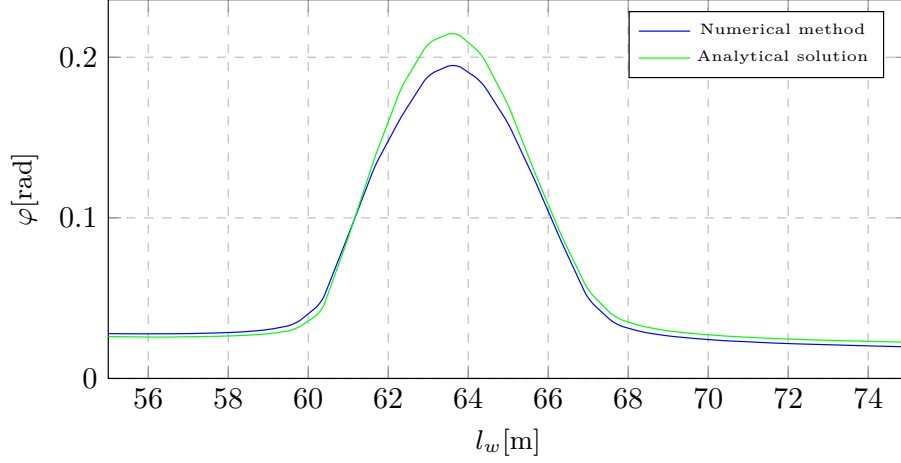


Figure 26: Results of a comparative analysis between the analytical and numerical solution,  $T = 8s$  [A1]

A characteristic feature for the proposed analytical solution is a more conservative dynamics. Slightly higher amplitudes values of the presented approach can be observed for each simulated scenario, however the discrepancies between the solutions are of a negligible nature. That constitutes the method to be beneficial in terms of payload dynamics stability assessment already at the lifting process design.

The presented algorithm is also preferable in terms of performing a significant number of simulations. The evaluation of a single result is faster (Table 1) due to the numeration of the already existing symbolic solution. The numeration process requires less time investment and computational resources in a contrary to commonly used numerical simulations utilising integrating schemes in which a new numerical evaluation is created during each simulation [6].

Table 1: Comparative results of computing times for the analysed algorithms [A1]

$l_w$ [m]	Computing time [s]	
	Numerical method	Analytical solution
40.0	0.843940	0.008568
44.0	0.879129	0.008747
48.0	0.826232	0.008472
52.0	0.894133	0.011800
56.0	0.897533	0.008663
60.0	1.082685	0.008101

Despite many advantages of the proposed algorithm, it needs to be emphasised that the determination process of analytical solution requires a good knowledge of nonlinear theory of vibration, which might not be accessible for an inexperienced user.

During further research, the solver accuracy was improved, which allowed to obtain analytical results entirely convergent to the results of the fully non-linear solution in terms of instability caused by parametric resonance. Additionally, the research area of the proposed analytical

method has been extended comparing to the case study analysed in article A1.

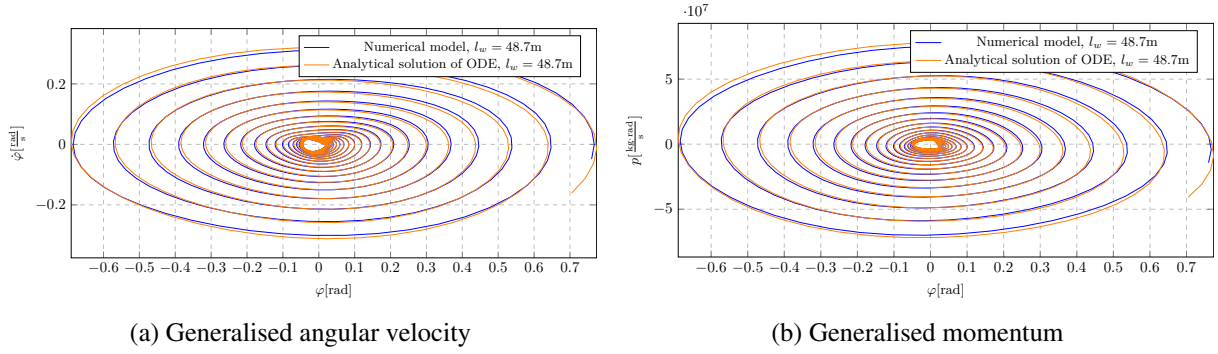


Figure 27: Phase portraits of analytical and numerical solution for parametric resonance case - comparative results

Besides studying the instability of the system caused by parametric excitation (Fig. 27), the study covers also another unstable state corresponding to main resonance vibrations (Fig. 28). This resonance can be observed for a half resonant frequency. Analysing the results presented in figure 28, it should be noted that the proposed method, due to the adopted assumptions (a limited description of the dynamics of the phenomenon including only third-order component of the Taylor series expansion, comparative research based on the first approximation of the analytical solution and the process of removing secular terms) does not provide fully qualitatively consistent results in the analysis of non-linear slowly-varying phenomena.

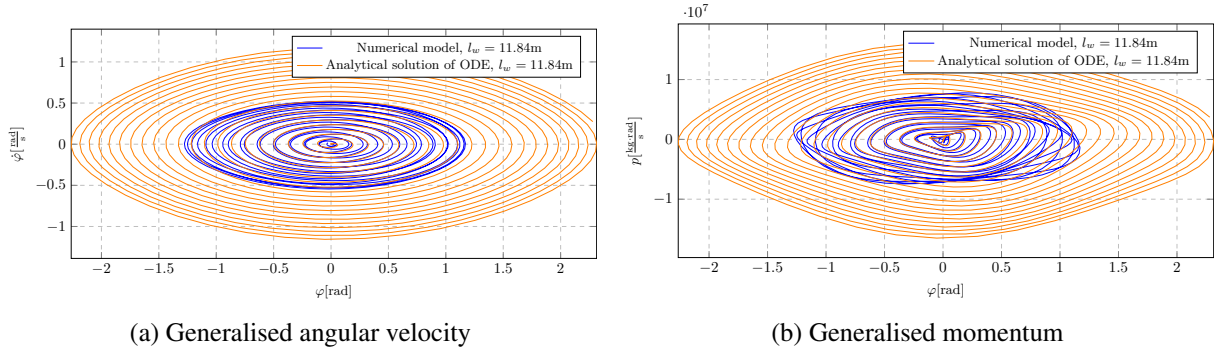


Figure 28: Phase portraits of analytical and numerical solution for main resonance case - comparative results

The analytical solution-based method reaches its full amplitude value of resonant vibrations already in the middle of the total simulation time, meaning that full information about the actual state of non-linear processes is partially false. Generally, nonlinear models tend to auto-limit resonance vibrations in opposite to characteristics for approximate (linearised) systems showing an infinite increase in amplitude values over time. However, in case of the presented methodology (approximate analytical solution), the unlimited increase in amplitude values is observed, which indicates the shortcomings of the proposed first approximation of the analytical solution in the field of system instability analysis in terms of main resonance vibrations assessment.

Table 2: Assessment of analytical solution accuracy

	Mean squared error
Parametric resonance accuracy $l_w = 48.7[m]$	0.001015
Main resonance accuracy $l_w = 11.84[m]$	1.748391

The solution errors for the two studied instabilities of the dynamics of the considered object are compared and presented in Table 2. As can be seen, the analytical solution within parametric resonance case study has an almost zero error value meaning the solution provides an accurate representation of the nonlinear numerical system response. However, the results evaluated for main resonant case are subjected to a greater MSE error, which confirms the aforementioned conclusions.

As can be observed, the improved analytical solution visualization takes place in the phase coordinate domain when the solution becomes a curve in the phase space ( $\dot{\varphi}\varphi$ ), parametrised by time. The technique allows for an interesting insight to oscillatory systems dynamic behaviour demonstrating their important properties of nonlinear vibrations, especially allowing to observe easily recognizable and well known unstable points of equilibrium.

As presented in the figures, depending on the selected phase coordinate, the provided results carry different information being diversified not only in quantity but also in their quality. The momentum-based phase-space analysis changes the commonly known portraits by reducing the importance of information about higher frequency components.

Table 3: Assessment of mean squared error between the phase-space coordinates

	MSE for MR case study $l_w = 11.84[m]$
Normalised variable	
Angular velocity $\dot{\varphi}$	0.486021
Momentum $p$	0.418727

Based on the results obtained (Tab. 3), it can be stated that the error between the solutions is lower for generalised momentum  $p$  than for the commonly used  $\dot{\varphi}$  coordinate what supports the claim regarding features of the variable that it allows to obtain qualitatively less complex solution by reducing the higher frequency component completely or at least its amplitude value.

The presented considerations (phase-space analysis) are the subject of another thematically related article being currently under review process.

### 5.6.7. Modelling methodology for a variety of dynamic systems based on created Python library

In articles A2 and A5, one proven the possibility of a utilisation of the developed methodology for modelling dynamic systems beyond the area of the previously discussed applications, i.e. modelling of marine objects.

In A2, one presented the problem of empirical investigation and mathematical modelling of a novel controllable damper using Vacuum Packed Particles. The study shows an alternative and innovative method of mechanical vibrations control by the proposed absorber made of granular material the macroscopic mechanical features of which can be controlled by the partial vacuum parameter. In order to represent the dynamic behaviour and changes to dissipative characteristics of the investigated device, one proposed an application of Bouc-Wen model with further parameters identification process. The verification of the model response was done based on experimental data and the results convergence confirmed as satisfactory. An extensive study including the tuned mathematical model and the experimental research is discussed in details in a comparative analysis presented in A2, however some selected simulation results are presented in Figures 29 and 30.

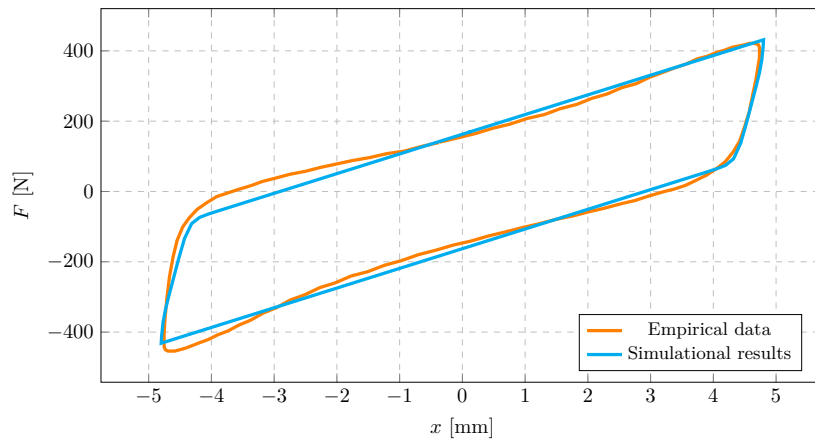


Figure 29: Experimental hysteresis loop for  $p = 0.04$  MPa; B-W model identified for the following parameters:  $a = 0.35$ ,  $A = 6$ ,  $\beta = 3$ ,  $\gamma = -2$ ,  $n = 4$  [A2]

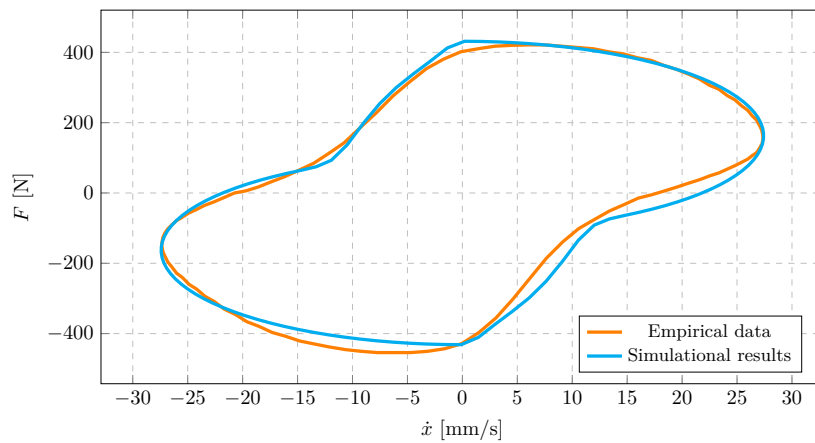


Figure 30: Experimental hysteresis loop for  $p = 0.04$  MPa; B-W model identified for the following parameters:  $a = 0.35$ ,  $A = 6$ ,  $\beta = 3$ ,  $\gamma = -2$ ,  $n = 4$  [A2]

In paper A5 one proposed a transdisciplinary approach to modelling engines' crank mechanism. An analytical coupled thermo-mechanical model of a crankshaft system enables the



examination of mutual relationships between thermodynamic and mechanical phenomena occurring in engines. The study covers analytical and numerical analysis exclusively in order to allow a faithful representation of the coupling and interactions between the state variables. A changeable stiffness of the fuel-air mixture and elastic properties of the system parts taken into consideration were found to be a cause for a different dynamics of the entire system. Numerical simulations proven an occurrence of thermo-mechanical effects in the global system response. Significant quantitative and qualitative changes are visible in Figures 31 and 32, where the phenomena of randomness and irregularity is confirmed and found to be compatible with empirical observations leading to conclusion that the proposed transdisciplinary approach offers a better representation of an irregular character of engines operation.

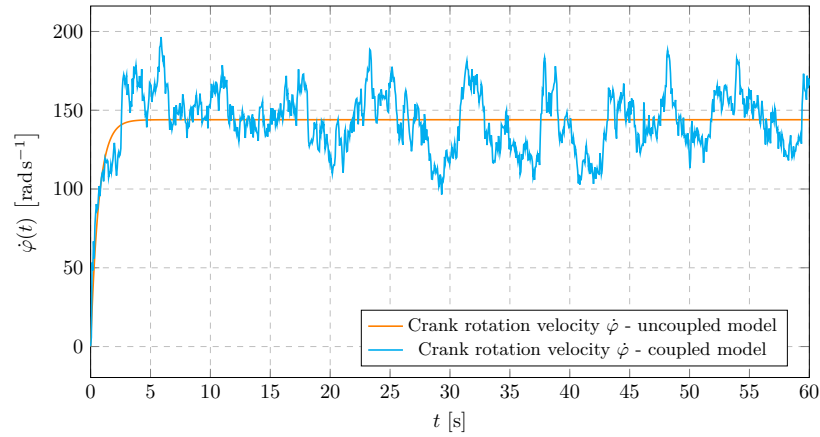


Figure 31: Crank angular velocity [A5]

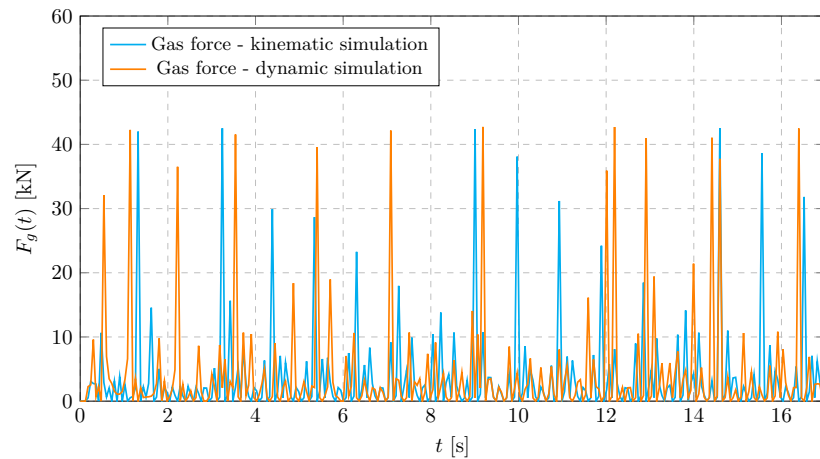


Figure 32: Gas force - comparative results [A5]

In both analyses, the same modelling methodology was used and the prepared Python-based software was utilised in order to perform analytical and numerical study. A development of the own modelling and simulation environment enables a comprehensiveness of research being simultaneously an interesting alternative to commercial software. This indicates the universality and versatility of the developed modelling methodology and the Python-based software.

## 5.7. Summary

The works carried out as part of the doctoral dissertation concern a problem of offshore lifting process. My scientific contribution is a development of comprehensive methods for analytical and numerical modelling of marine lifting operation. An innovative model with 3 degrees of freedom representing a dynamics of the lifted object was proposed, allowing incorporation of an elliptical (kinematic) excitation transferred from the ship's centre of mass to any remote vessel's point (deck crane tip considered) through utilisation of RAOs processing methodology. This part of the research concerns operations assumed to be in light lifts category (as proven for payload mass to vessel displacement ratio up to 3% – 3.5%), meaning the payload dynamics can be studied independently to the vessel.

Moreover, one demonstrated the approach being more widely applicable than analysis of the payload dynamics itself. The proposed concept eliminates RAOs as a method of vessel motion representation and can be applied either to light or heavy lifts category, where the uncoupled model cannot be utilised as high inaccuracy is observed for models neglecting coupling. This proposed model (having 5 degrees of freedom) is more universal and comprehensive what constitutes its main advantage.

The basis of the research were theoretical analyses, development of analytical and numerical lifted object and vessel's models utilising co-authorship software and what is more a determination of an analytical (qualitative) nonlinear solution of a considered nonlinear payload pendulation model based on multiple-scale method. The analytical approach provides an explicit function determining the payload dynamic behaviour, governing laws or physical effects responsible for operational instability of the system. Due to the closed form solution, the presented algorithm is also preferable in terms of performing a significant number of simulations. The result can be numerized once and re-used for further calculations constituting a unified model decreasing simultaneously computational time. It creates a considerable advantage over numerical methods.

To summarise, the completion of the doctoral dissertation enabled:

- development of an innovative model for operation planning to simulate lifted payload behaviour in payload-vessel system,
- incorporation of the axial oscillation simultaneously with pendulation including a compensating element with an ability to process an elliptical excitation,
- numerical research on regular and irregular waves for an hour compensated payload lifting simulation,
- development of a coupled payload-vessel model for offshore lifts of light and heavy-weight objects,
- determination of the scope of payload-vessel coupling law applicability,
- derivation of an analytical closed form solution of the proposed model on a basis of perturbative methods from nonlinear theory of vibration,
- possibility of qualitative description of the lifted object's dynamic features,

- proposal of methodology taking into account unstable dynamic states (parametric and main resonance) of the lifted object allowing for a more accurate offshore lifting process planing,
- better targeting at the design stage providing an interesting insights into control system design,
- acceleration of results' evaluation as the process of analytical solution numeration,
- development of modelling methodology for a variety of dynamic systems based on co-authored Python software libraries.

The presented achievements offer an efficient and comprehensive methodology serving for generalisation and perhaps standardisation of a potentially problematic scenarios at conceptual stages creating an advantage in lifting operation process planning. Furthermore, they can constitute an additional step in a verification of numerical results or in simpler cases, can replace the numerical approaches entirely.

## 6. Didactic and organisational achievements

### 6.1. Didactic achievements

#### Academic courses and work at the university

During my employment at Warsaw University of Technology, I conducted the following academic courses:

#### a) Polish language courses

<b>Mechanika Ogólna</b>	Tutorials for B.Sc. studies full-time courses, M.Sc. studies full-time and part-time courses
<b>Drgania Mechaniczne</b>	Tutorials for B.Sc. studies full-time courses, M.Sc. studies full-time and part-time courses
<b>Drgania Mechaniczne</b>	Lectures for M.Sc. studies part-time courses
<b>Podstawy Automatyki i Teorii Maszyn</b>	Lectures for B.Sc. studies part-time courses
<b>Podstawy Automatyki i Teorii Maszyn</b>	Projects for B.Sc. studies full-time courses
<b>Wytrzymałość Materiałów</b>	Tutorials for B.Sc. studies full-time courses

#### b) English language courses

<b>Theory of Machines and Automatic Control</b>	Projects for B.Sc. studies full-time courses
<b>Mechanical Vibrations</b>	Tutorials for B.Sc. studies full-time courses

#### Creation and development of academic courses programmes

I have developed or participated in development of the following courses:

1. Modelling of Machines and Vehicles (lectures, projects, laboratory classes)

2. Applied mathematics (lectures)
3. Advanced Modelling of Machines and Vehicles (projects)
4. Simple Finite Elements Method analysis in Ansys environment (lectures)

### **Co-authorship of scripts and other teaching aids**

In order to support the didactic process, I have developed a number of teaching aids for a group of mechanical subjects in the form of quizzes and tests on Moodle platform. The online courses were prepared for the following topics:

1. Mechanical Vibration - B.Sc. studies full-time course
  - 1.1 Harmonic synthesis
  - 1.2 Harmonic analysis.
  - 1.3 Undamped free vibration of single degree of freedom (SDoF) systems.
  - 1.4 Undamped excited vibration of single degree of freedom (SDoF) systems.
  - 1.5 Inertial excitation of SDoF systems.
  - 1.6 Logarithmic decrement.
  - 1.7 Damped free vibration of single degree of freedom (SDoF) systems.
  - 1.8 Damped excited vibration of single degree of freedom (SDoF) systems.
  - 1.9 Introduction to phase plane analysis.
  - 1.10 Dynamic system analysis on the phase plane.
  - 1.11 Affine transformations.
  - 1.12 Phase portrait in the neighbourhood of a critical point.
  - 1.13 Stability of phase portrait.
  - 1.14 Undamped free vibration of multi degree of freedom (MDoF) systems.
  - 1.15 Undamped excited vibration of multi degree of freedom systems.
  - 1.16 Damped free vibration of multi degree of freedom systems.
  - 1.17 Continuous systems - string.
  - 1.18 Continuous systems - rod.
  - 1.19 Continuous systems - beam.
  - 1.20 Continuous systems - separation of variable method.
  - 1.21 Nonlinear vibration - Galerkin method.
  - 1.22 Nonlinear vibration - free oscillations.
  - 1.23 Nonlinear vibration - excited oscillations.
2. Theoretical Mechanics - M.Sc. studies full-time course (in Polish)
  - 2.1 Drgania nieliniowe - metody wariacyjne (Nonlinear vibration - variational methods)

- 2.2 Drgania nieliniowe (Nonlinear vibration - orthogonalisation methods)
- 2.3 Wprowadzenie do teorii sprężystości (Introduction to the theory of elasticity)
- 2.4 Zginanie płyt kołowsymetrycznych (Bending of circularly symmetrical plates)
- 2.5 Drgania układów ciągłych (Continuous systems vibration)
- 2.6 Mechanika analityczna (Analytical mechanics)

## 6.2. Scientific supervision of students' thesis

I was a consultant and reviewer of several engineering and master's theses dealing with the study of dynamic systems' behaviour and structures that utilises smart materials.

## 6.3. Reviewing publications for international journals

I have reviewed the following articles for *Elsevier Ocean Engineering* journal:

1. Ren Z., Verma A., Ataei B., Halse K., Hildre H., *Model-free anti-swing control of complex-shaped payload with offshore floating cranes and a large number of lift wires*, Ocean Engineering, Volume 228, 2021, 108868, ISSN 0029-8018, <https://doi.org/10.1016/j.oceaneng.2021.108868>
2. Asadi M., Hassanzadeh R., *Assessment of Bach-type internal rotor on the performance of a hybrid wind turbine: Effects of attachment angle, tip speed ratio, and free-wind speed - rejected* (2022)

## 6.4. Participation in research projects

I participated in the following research projects:

- Grant awarded by the National Centre for Research and Development, entitled "Rapid-Chair - electric wheelchair drive." Grant number: POIR.01.01.01-00-0874/19 Operational Program Development 2014-2020. My duties included development of dynamic models of a wheelchair and electric drive, performing numerical simulations, conducting research and reporting on the work carried out. Project duration: from July 2020 to February 2021.
- Industrial grant of the Decommissioning Challenge Fund, awarded by the Scottish government in cooperation with Fathom Group Ltd. on the creation of the project entitled "Modular Recovery System" (MRS) for decommissioning infrastructure in the North Sea - <https://www.gov.scot/news/gbp-4-million-support-for-decommissioning/>. My duties included creating a structure model, numerical simulations, dynamics analysis and reporting. Project duration: from January to April 2020.

## Projects and external works for industry and international cooperation

In order to popularise science and improve my own professional qualifications in the industrial sector I have cooperated with Fathom Group Ltd. as a Dynamic Analysis Engineer ([www.fathom-group.co.uk](http://www.fathom-group.co.uk), Scotland). I participated as a contractor in the following research projects:

1. **Modular Recovery System** - Fathom's innovative Modular Recovery System developed to facilitate the recovery of subsea assets with a significantly reduced operational expenditure. The system removes the need for divers to be involved in recovery operations and therefore can significantly reduce the costs and risks associated with dive operations. The project gained backing from the Scottish Government as 1 of 10 successful projects in 2020s Decommissioning Challenge Fund Through market research, RD, concept development, front end engineering design (FEED) and detailed design, Fathom have developed this innovative system which challenges the existing recovery methods used in the decommissioning sector through high efficiency and safety [56].
2. **Remote Release Hooks** - were developed to meet a clients specific requirement during the construction of Aberdeen South Harbour. This equipment resolved issues around operational and diver safety by offering the construction client a method to release 40 tonne Accropodes safely and accurately. Fathom's design was commended by our client for its operational safety features ensuring that there was no way to unexpectedly release the payload whilst suspended. Fathom worked with our client to ensure the supplied products met all operational needs including the addition of bespoke tugger line attachments and swivel to assist in accurate placement. This turnkey project was delivered rapidly from concept to site in 3 weeks including design, fabrication, assembly, load test and full CE marking [17].

#### 6.5. Participation in international scientific conferences

1. 26th Polish – French Seminar in Mechanics, *Motion compensation systems for subsea and offshore installations motion control with ship-independent heave and pendulum motion compensator*, Warsaw, Faculty of Automotive and Construcion Machinery Engineering, 14-15.05.2018
2. 4th Common PhD-Candidates' Seminar TU Berlin - WUT, *Systemy kompensacji ruchu statków – kontrola trajektorii ładunku z wykorzystaniem „inteligentnego” kompensator ruchu wahadłowego*, Warsaw, Poland, 20.09.2018
3. 3rd Polish-German Ph.D. Seminar, *Ship motion compensation system – payload trajectory control with an adaptive heave and pendulum motion compensator*, Cottbus, Germany, 26-28.09.2018
4. Recent Advances on Nonlinear Mechanics, *Proposal of the 3-DOF model as an approach to modelling offshore lifting dynamics*, Łódź, Poland, 07-10.05.2019
5. 27th French-Polish Seminar of Mechanics, *A 3-DOF model as an approach to investigate parametric resonance phenomenon in offshore lifting operations*, Besancon, France, 04-08.06.2019
6. 4th Polish-German Ph.D. Seminar, *Modelling of irregular wave to study on payload dynamics in offshore lifting*, Forst, Germany, 26-28.09.2018

7. XXXth German – Polish Scientific Seminar, *Motion compensation systems for subsea and offshore installations – motion control with ship-independent heave and pendulum motion compensator*, Warsaw, Poland, 16-18.09.2019
8. 5th Polish-German Ph.D. Seminar, *Preliminary research on the 3-DOF analytical model for payload pendulation under nearly parametric excitation*, Warsaw, Poland, 22.09.2020
9. Applications of Physics in Mechanical and Material Engineering APMME, *Preliminary modelling methodology of a coupled payload-vessel system for offshore lifts of light and heavyweight objects*, Częstochowa, Poland, 19.02.2021
10. Applications of Physics in Mechanical and Material Engineering APMME, *Influence of the grains material on the dissipative properties of a novel Vacuum Packed Particles granular damper*, Częstochowa, Poland, 19.02.2021
11. 6th Polish-German Ph.D. Seminar, *Analytical modelling and solution of parametrically induced payload nonlinear pendulation in offshore lifting*, Warsaw, Poland, 28.09.2021
12. Applications of Physics in Mechanical and Material Engineering APMME, *An analytical solution of payload pendulation for offshore light lifting operations under regular wave excitation*, Częstochowa, Poland, 23.09.2022
13. Applications of Physics in Mechanical and Material Engineering APMME, *A proposal of a dynamic model of an adaptable tuned mass damper based on fluid transfer phenomenon*, Częstochowa, Poland, 23.09.2022

## 6.6. Prizes and awards

1. Rector's team award for scientific achievements in 2019-2020
2. Rector's team award for didactic achievements in 2020-2021
3. Dean's award for publication in 2020

## 7. Summary of scientific achievements

The doctoral dissertation consists of 5 selected publications, including 4 publications in peer-reviewed scientific journals distinguished in Journal Citation Reports® indexed in Thomson Reuters® Web of Science® and 1 peer-reviewed chapter in a monograph, the total Impact Factor of which is 11.744. I actively took part in 13 international and 9 national scientific conferences, I am a reviewer in scientific journals that are included to the JCR® journal database. During my research work I also participated in 2 external grants (national and international) and 2 internal research projects. Table 4 presents the quantitative scientific and research achievements. In order to evaluate the achievements, bibliographic indicators in the form of the number of citations and the Hirsch index from the three most popular databases were used: Thomson Reuters® Web of Science®, Scopus® and Google Scholar, as well as the Impact Factor and total points inherited from the list of publications of Polish Ministry of Education and Science.

Table 4: Summary of scientific achievements

Index description		Value
Number of citations of publications according to	Web of Science®	1
	Scopus®	8
	Google Scholar	9
Hirsch index according to	Web of Science®	1
	Scopus®	1
	Google Scholar	1
Number of articles in scientific journals featured in JCR®	-	4
Number of chapters in a monograph	-	1
Total Impact Factor	-	11.774
Total SNIP	-	6.444
Total MEiN score	-	500



# Appendix 1

1. A copy of the diploma confirming MSc. Eng. degree.

P O L I T E C H N I K A   W A R S Z A W S K A

Wydział Samochodów i Maszyn Roboczych



# DYPLOM

## UKOŃCZENIA STUDIÓW DRUGIEGO STOPNIA

Wydany w Rzeczypospolitej Polskiej

**Anna Justyna Mackojć**

urodzona 13 marca 1991 roku, Bydgoszcz

ukończyła studia stacjonarne drugiego stopnia na kierunku

**Mechanika i Budowa Maszyn**

specjalność - maszyny robocze

obszar kształcenia - nauki techniczne

profil kształcenia - ogólnoakademicki

z wynikiem bardzo dobrym

i uzyskała w dniu 10 września 2015 roku tytuł zawodowy

**magistra inżyniera**

*prof. dr hab. inż. Stanisław Radkowski*

(Dziekan Wydziału/Dyrektor Kolegium)

*prof. nzw. dr hab. inż. Krzysztof Lewenstein*  
*prorektor*

(Rektor Politechniki Warszawskiej)



*Anna Mackojć*  
(podpis absolwenta)

Numer dyplomu 72319

Warszawa, dnia 16 listopada 2015 roku

## Appendix 2

1. A copy of the article: Chiliński Bogumił, Mackojć Anna, Zalewski Robert, Proposal of the 3-DOF model as an approach to modelling offshore lifting dynamics, *Ocean Engineering*, 2020, vol. 203, pp.107235. DOI:10.1016/j.oceaneng.2020.107235
2. A copy of the article: Mackojć Anna, Chiliński Bogumił, Preliminary modelling methodology of a coupled payload-vessel system for offshore lifts of light and heavyweight objects, *Bulletin of the Polish Academy of Sciences, Technical Sciences*, 2021, vol. 70, pp.9. DOI:10.24425/bpasts.2021.139003
3. A copy of the article: Chiliński Bogumił, Mackojć Anna, Analytical solution of parametrically induced payload nonlinear pendulation in offshore lifting, *Ocean Engineering*, 2022, vol. 259, pp.111835. DOI:10.1016/j.oceaneng.2022.111835
4. A copy of the article: Mackojć Anna, Chiliński Bogumił, Zalewski Robert, Preliminary research of a symmetrical controllable granular damper prototype, *Bulletin of the Polish Academy of Sciences, Technical Sciences*, 2022, vol. 70, no. 3, pp.1-9, Article number:e141002. DOI:10.24425/bpasts.2022.141002
5. A copy of the article: Chiliński Bogumił, Mackojć Anna, Proposal of the Coupled Thermomechanical Model of a Crank Mechanism, In: *Transdisciplinary Engineering for Complex Socio-technical Systems – Real-life Applications / Pokojński Jerzy [et al.] (eds.)*, 2020, vol. 12, IOS Press, ISBN 978-1-64368-110-8. DOI:10.3233/ATDE200098



# Proposal of the 3-DOF model as an approach to modelling offshore lifting dynamics

Bogumil Chilinski<sup>a,\*</sup>, Anna Mackojc<sup>a,\*</sup>, Robert Zalewski<sup>a</sup>, Krzysztof Mackojc<sup>b</sup>

<sup>a</sup> Institute of Machine Design Fundamentals, Warsaw University of Technology, Poland

<sup>b</sup> Engineering Specialist, Fathom Group Ltd., 18 North Silver Street, Aberdeen, AB10 1JU, Scotland, United Kingdom of Great Britain and Northern Ireland

## ARTICLE INFO

### Keywords:

Pendulum motion compensation  
Regular and irregular wave excitation  
Offshore lifting modelling  
Offshore lifting operations  
Offshore dynamics  
Parametric resonance detecting capability

## ABSTRACT

This paper presents the challenges faced in modelling marine operations with a particular focus on lifting in air. Those challenges are looked at from a purely modelling perspective showing various approaches encountered in the literature. Paper further discusses the disadvantages of those models and proposes a 3-DOF solution that allows to observe all of the physical phenomena and their possible relation enabling efficient, in-depth studies of the operations in discussion.

The proposed model is presented in detail starting from a computation of excitation, through the numerical approach with a variety of interesting results. An advantage of the presented approach is seen in the analytical modelling what allows for a theoretical, numerical and combined analysis. The model allows for an implementation of a variety of excitation types providing an ability to study responses to regular and irregular wave. A phenomenon of a parametric resonance was discovered what allows for a reliable assessment of dynamic behaviour, emphasising another advantageous feature of the model in comparison to other approaches discussed.

Paper is concluded by a validation of the proposed methodology. It is also suggested that the model proposed is a good, computationally viable, easily accessible balance between overly simple and overly complex models.

## 1. Introduction

### 1.1. Overview

Increasing exploitation of underwater natural resources triggered rapid development of the offshore industry in the area of modern technologies over the course of last decades. One of the challenges in performing activities offshore is naturally the necessity to deal with the surrounding environment. The operational intensification with regards to lifting operations is therefore strongly related to the isolation of vibration between the floating object and a lifted payload. A solution allowing for reliable performance in difficult weather conditions offers meaningful improvement to the operational expenditure by minimising downtime — one of the largest non-productive costs that the offshore industry is exposed to. Several technologies and operational practices have been developed to assist with this, but it is believed that the boundaries can still be pushed further. A major limitation to trigger a widespread research is an access to an appropriate dynamic modelling tool.

Any lifting operation undertaken offshore consists of several phases depending on the operation characteristics. These might include but are not limited to:

- lift-off — an object is lifted off from its position,
- handling in air — an object is suspended in air or manoeuvred to the desired position,
- splash zone crossing — an object immersing through a water surface,
- deep-water lowering — a payload lowering towards the seabed,
- seabed landing — an object installation onto the seafloor.

Dynamics of the payload in air is mainly driven by the vessel motion with a minor (thanks to modern control filters) influence of the crane operation. Resulting payload motion problems are related to two prevailing phenomena — heave and pendulum. Appropriate understanding and control of the payload dynamics might considerably increase the operation efficiency and profitability.

\* Corresponding author.

E-mail addresses: [bogumil.chilinski@pw.edu.pl](mailto:bogumil.chilinski@pw.edu.pl) (B. Chilinski), [anna.mackojc@pw.edu.pl](mailto:anna.mackojc@pw.edu.pl) (A. Mackojc), [robert.zalewski@pw.edu.pl](mailto:robert.zalewski@pw.edu.pl) (R. Zalewski), [k.mackojc@fathom-group.co.uk](mailto:k.mackojc@fathom-group.co.uk) (K. Mackojc).

<https://doi.org/10.1016/j.oceaneng.2020.107235>

Received 13 February 2019; Received in revised form 25 December 2019; Accepted 8 March 2020  
0029-8018/© 2020 Elsevier Ltd. All rights reserved.



The purpose of this work is to propose a new, balanced approach between variety of currently applied methods being either overly simplified or on the contrary, highly complex. The authors present a model that incorporates the most important features of the models popular in the literature but also introduces a significant advantage to the research methodology. Two distinctive features of the proposed 3-DOF model are: allowing for a detection of system instability and controlling the dynamics by means of changing the system stiffness characteristic. The model also provides the ability to investigate the system heave excitation and heave response influence on the pendulum behaviour.

Amongst other aspects, the paper will discuss the computation of the kinematic excitation at the crane tip as a result of the ship motions. Proposed approach utilises RAO functions to achieve it as described further in this document. At this stage, all of the research will be carried out for lifting in air phase to signify the importance of the pendulum motion. Proposed modelling of the system will allow implementation of compensating stiffness (elastic element) as an adaptive parameter allowing for system stability analysis and evaluation of its performance. The analysis will be performed within the 'light lift' regime by satisfying the criteria stipulated in *DNV GL-RP-N103 Modelling and analysis of marine operations* (DNV GL, 2017) and only light lifts will be taken into account. This conclusion allows to disregard the payload influence on the vessel dynamic enabling greater efficiency in modelling the ship motions as discussed further in the text.

## 1.2. State of the art

Many proposals of offshore lifting modelling were found in the literature but most of them present methods of compensation for heave and pendulum separately.

The book (Albers, 2010) shows the hydraulic-based device as the simplest form of a passive heave compensator based on a hydraulic accumulator. The presented solution is modelled as a simplified second order linear dynamic model. The author also described an active control system, which utilises simple feed-forward mechanism. The same modelling approach was taken in DNV GL (2017), where a dynamic model of a two degree of freedom passive heave compensator is depicted as a simplified second order linear system moving only in the vertical direction.

The author Tong et al. (2013) presented a hydraulic arrangement integrated with a reeving system controlled with a PLC, where the compensation focuses on heave only. The system was modelled as a first order linear dynamic model taking into account the stiffness and damping of the compensator. Another paper (Kurowski et al., 2012) presents a mathematical model of an offshore pedestal crane, where the compensating element was referred to as a shock absorber and designed so that it works only under the tension load. According to the authors, it is characterised by a greater efficiency, simpler and more compact construction. The aforementioned shock absorber was modelled as a point mass connected to the boom by the means of a spring-damper system. The problem of compensation of vessel motions induced by waves is also described by Szczotka (2010). The author presents a different approach to control, where presented compensating system is based on a A-frame, mounted over the moonpool. The considerations concern an in-line cross beam mounted compensator. The main component responsible for the elimination of the load movement used a special actuator controlled by a digital PID that moved the pulleys and changed the length of the rope controlling the position of the payload. The most popular way of compensation is a choice of the right winch drive function. Such an approach was shown by Osiński and Wojciech (1998) and Fałat (2004). The selection of drives was made by the dynamic optimisation and several proposed solutions were described by Tomczyk (2009). All of the discussed papers present a simplified approach to modelling of axial motion of payload, uncoupling the pendulation. It seems to be too much of a simplification, especially in cases analysed for resonant states.

Scientific research regarding the subject of a pendulum motion compensation can also be found in literature although they are much rarer. The reason may be that the pendulum swing motion attenuation is more difficult to achieve than a compensation for heave — this makes the subject particularly worth of interest. Additionally, operational measures were introduced to reduce the pendulation risk often with avoiding operations in certain conditions specifically in regular, swell seas. Those measures became industry standard but despite general acceptance, weather windows could be maximised should another reliable solution be found. The article (Fragopoulos et al., 1999) examines the problems of controlling the load sway during offshore lifting operations. The kinematic model of a vessel and a crane with an anti-pendulation arm attached are presented. The whole system forms a double pendulum. The model consists of a control arm attached with one end to the crane tip and the other to the lifting cable. Linearised model engages Linear-quadratic-Gaussian control (LQG) and generalised predictive control methods. In the article of Balachandran et al. (1999) the authors proposed a concept of a mechanical filter to attenuate the pendulum oscillations. The idea is based on actively controlled pivot point around which the suspended load moves. Ship-roll-induced vibrations are considered only. Two active ship motion compensation methods of payload sway stabilisation during operations are discussed by Schaub (2008). A double-layer sliding manifold for offshore container crane (OCC) is presented in the paper of Sun et al. (2017) to enable the position tracking and sway control simultaneously. The model for the OCC consists of a ship-crane-trolley-payload system. The described model is characterised by the varying length of the wire and the sway angle of the lifted object. The authors underline its improved performance against a conventional controller. The weak point of the conducted analysis might be a lack of examination of a heave response of the studied model and its impact on the analysed pendulation angle. A similar model is proposed by the authors Ngo and Hong (2012), where it is considered as a three-dimensional system. The author Masoud (2000) and Masoud et al. (2004) shows a possibility of reducing sway motion by controlling the slew and luff angles of the boom. According to the paper, such control might be achieved with heavy equipment already being part of the crane so that rebuilding of existing cranes would require smaller effort. Additionally, parametric excitation studies were encountered. The article of Witz (1995) presents the research on time domain model demonstrating the effect of irregular waves on crane loads causing the parametric excitation. All of the mentioned articles do not consider simultaneous action and compensation for heave, which seems to be a weakness of current approaches, especially in the case of large system displacements.

## 2. Theoretical analysis

### 2.1. The dynamics of the lifted object

As per DNV GL Standard for Certification No. 2.22 Lifting Appliance (DNV GL, 2011), the vertical loads due to floating unit motions appearing at the crane tip – and hence on the lifting payload – should be taken into consideration by multiplying the working load by a dynamic amplification factor,  $\psi$ . The DAF was evaluated to cover all inertia forces and shock.

The dynamic amplification factor can be assessed by:

$$\psi = 1 + V_R \sqrt{\frac{k}{W \cdot g}}, \quad (1)$$

where:

$k$  - geometric stiffness coefficient referred to hook position, defined as a force at hook to produce unit deflection at hook [kN/m],

$g$  - standard acceleration of gravity 9.81 [m/s<sup>2</sup>],

$W$  - working load [kN/m],

$V_R$  - relative velocity [m/s] between the payload and hook at the time of pick-up.

Considering the above formula, the load on the crane wire during offshore lifting is then equal to the dynamic load, which is the working load multiplied by the DAF and is expressed as follows:

$$F_D = W \cdot \psi = W \cdot \left( 1 + V_R \sqrt{\frac{k}{W \cdot g}} \right), \quad (2)$$

Considering above, one might notice that the reduction in the dynamic load can be achieved by:

- (a) the reduction in relative velocity leading to a reduction of the operating window,
- (b) reduction in working load or,
- (c) adjustment in stiffness coefficient.

Reduction performed by (a) or (b) lowers the productivity of offshore operations. Alternatively, by applying a spring with adaptive stiffness into the model, an adjustment in the  $k$  value would be possible. That would directly lead to the decrease of the dynamic loads imposed on the lifted object and the crane.

## 2.2. Analysis of reference models

In the vast majority of offshore technical solutions the executive system is being hydraulically actuated. The principle of work of the hydraulic systems is based on a hydraulic cylinder connection with a piston type accumulator. The accumulator also has a function of separating the hydraulic part of the cylinder from the gas bottles filled with nitrogen. The combination of both forms a mechanism in which the volume of the attached gas accumulators sets the stiffness of the system.

A simplified dynamic system of a passive heave compensator, according to DNV GL-RP-N103 *Modelling and analysis of marine operations* (DNV GL, 2017) might be simplistically modelled by the following system:

where:

$x_1(t) = x_A \sin(\omega t)$  - vertical displacement at crane tip created by a kinematic excitation [m],

$m_c$  - mass of heave compensator [kg],

$m_o$  - mass of lifted object [kg],

$k_c$  - stiffness of heave compensator [N/m],

$k_w$  - wire stiffness [N/m],

$E$  - modulus of elasticity [Pa],

$A$  - nominal cross-sectional area of cable [m<sup>2</sup>],

$L$  - length of cable [m],

$c_c$  - viscous damping of heave compensator [N s/m].

The equations of motion for the simplified model might be then expressed as follows:

$$\begin{bmatrix} m_c & 0 \\ 0 & m_o \end{bmatrix} \begin{bmatrix} \ddot{x}_c \\ \ddot{x}_o \end{bmatrix} + \begin{bmatrix} c_c & 0 \\ 0 & 0 \end{bmatrix} \begin{bmatrix} \dot{x}_c \\ \dot{x}_o \end{bmatrix} + \begin{bmatrix} k_c + k_w & -k_w \\ -k_w & k_w \end{bmatrix} \begin{bmatrix} x_c \\ x_o \end{bmatrix} = \begin{bmatrix} c_c \dot{x}_1 + k_c x_1 \\ 0 \end{bmatrix} \quad (3)$$

Another popular and well-established case in literature for the modelling of suspended objects exposed to the influence of sea waves, is a model of a single or double pendulum. In literature sources, it is challenging to find any proposals of systems that could directly

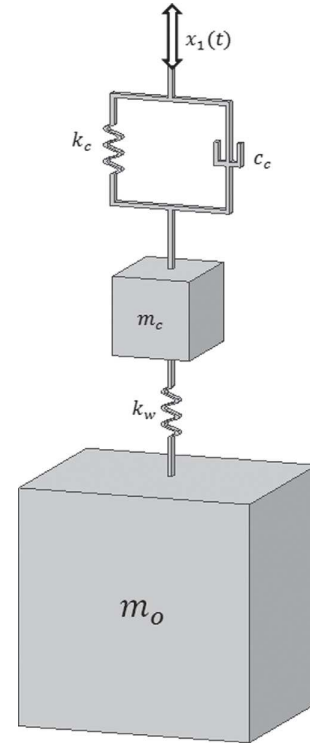


Fig. 1. A simplified 2-DOF passive compensator model as suggested in DNV GL (2017).

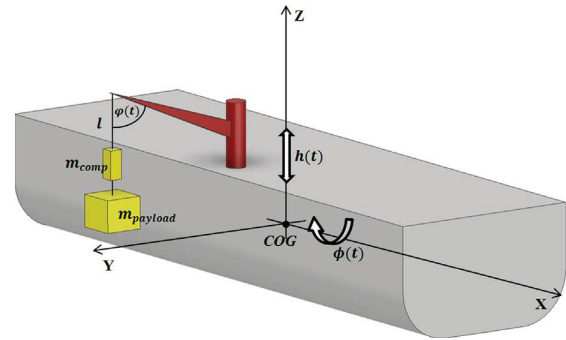


Fig. 2. A simplified model of an offshore lifting system and its parameters.

correspond to the model proposed by the authors of this study, which was intentionally designed to fit the operations performed by offshore column cranes. The authors Fragopoulos et al. (1999), Ngo and Hong (2012) and Sun et al. (2017) mentioned in 1.2, present systems that compensate ship motions analysed as double or single pendulum models, depending on the implemented compensating element.

## 3. Proposed model

Given the extensive simplifications in approaches mentioned above, it is suggested to consider a model combining the features of both. It is highlighted that the proposed model (shown on Figs. 2 and 4) considers planar motion only at this stage.

Precise analytical description of ships motion requires consideration of two types of motion on the sea waves. The first type has a linear character and is described by the following three movements: heave, sway and surge. The second one describes three angular movements

determined by yaw, roll and pitch, which are respectively vertical, transverse and longitudinal oscillations of the floating unit. Under the influence of waves, a floating vessel will produce a rocking motion affecting its buoyancy.

### 3.1. Excitation modelling

As mentioned, the investigations conducted were focused on light lifts, as per classification from DNV GL (2017). According to this code, objects that weigh less than 1%–2% of the vessel's displacement, estimated to be less than a few hundred tons, do not alter its motion characteristic. This assumption allowed coupled dynamic analyses to be disregarded and utilise response amplitude operators and phases (often referred to as RAOs) in order to obtain the excitation functions. RAOs are an output of diffraction–radiation analysis carried out on floating objects.

Floating units are considered to be continuous systems, which are subjected to a complex motion characteristics being a composition of a rigid body motion and its vibration. In most practical cases, naval designs are stiff enough to omit elastic properties of the entire vessel. In analytical considerations it allows to adopt the simple model of a rigid body, which is described by 6 degrees of freedom. Such an approach allows the hydrodynamic forces to be represented as a hydrodynamic added mass, fluid damping and restoring forces. Hence the considered case will be modelled by the following matrix equation:

$$(M_V + A(\omega)) \cdot \ddot{X}(\omega, \text{dir}) + C_V(\omega) \cdot \dot{X}(\omega, \text{dir}) + K_V \cdot X(\omega, \text{dir}) = F(\omega, \text{dir}) \quad (4)$$

The mass term is modified with the implementation of a frequency dependent function, which is the hydrodynamic added mass  $A(\omega)$  and the final form of the vessel mass matrix will be given as  $M_V + A(\omega)$ . The  $K_V$  is the considered vessel stiffness matrix related to its hydrostatic stability. A detailed description of the remaining symbols used is given as follows:

$M_V$  - mass matrix of the vessel,

$A(\omega)$  - hydrodynamic added mass,

$C_V$  - hydrodynamic damping matrix,

$K_V$  - vessel stiffness matrix,

$F(\omega, \text{dir})$  - hydrodynamic force vector,

$\omega$  - natural frequency,

$\text{dir}$  - wave direction.

The solution of the governing equation (4) for the resulting motion RAOs, where  $X(\omega, \text{dir}) = \text{RAO}(\omega, \text{dir})$  is given by the relation presented in (5) (see Fig. 3):

$$\text{RAO}(\omega, \text{dir}) = F(\omega, \text{dir}) \cdot [-\omega^2 \cdot (M_V + A(\omega)) + i\omega \cdot C_V(\omega) + K_V]^{-1} \quad (5)$$

System being described by the relationship given in (4) is composed of 6 second order differential equations what implies 6 linear independent eigenvectors and corresponding eigenvalues. An origin of the assumed coordinate frame is placed at the Centre of Floatation (CoF). In general, it cannot be assumed to be the same as a centroid (CoG) of the vessel. It causes that motion of CoG is a composition of the particular motions due to its eigenmodes. In practice, at least two or three natural frequencies will be visible at RAOs spectra.

RAOs can take different forms but are most often represented as a direction dependent displacement response per metre wave versus the wave period. The RAOs amplitude depicts a motion amplitude per unit amplitude of wave, the RAOs phase lag represents the phase difference between vessel motion and the waves. Separate RAOs are naturally computed for each degree of freedom.

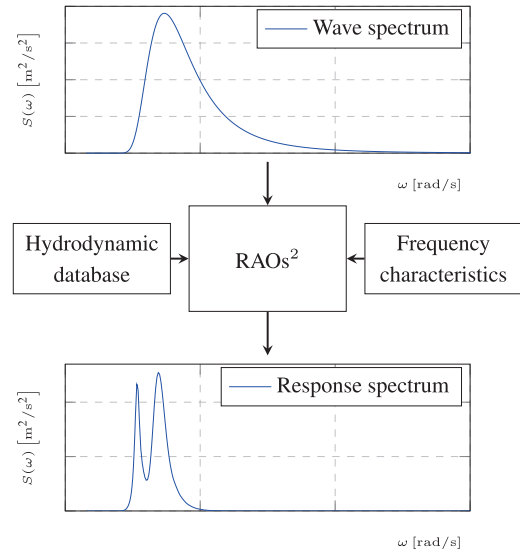


Fig. 3. Methodology of computing motion response spectra of a floating unit at the specified remote point.

RAOs functions can be obtained by the formula (4) or by an application of dedicated computational systems. Another possibility is to use the empirical data obtained during experimental investigation of the real object but this manner is expensive, time-consuming and available only for the existing units. Alternatively, the RAOs can be obtained through a scaled model testing.

Regardless the method used to obtain the RAOs, a numerical set of data including the phase and direction information is obtained. What needs to be emphasised, geometric properties and the method of establishing RAOs will to an extent have an influence over the results but will not affect the performance of the model proposed within this text. The remote point response spectrum or its specified point are used as an input for calculations of irregular and regular waving respectively and then to establish kinetic and potential energies (by computations of displacements and velocities of the system elements). That implies a different vessel would change only numerical values of the results but would not compromise the algorithm suitability and effectiveness. It is one of the most important advantages of the proposed model to eliminate the necessity to perform computationally expensive hydrodynamic computations.

Ability to adopt RAOs for computing the excitation enables the methodology to be economically viable within industrial/research environment. This significantly reduces the effort of modelling the marine operations.

The method (Fathom Group Ltd, 2018; Journée and Massie, 2001) used for derivation of the crane tip motions applied basic geometrical properties and a complex signal adding method allowing for both amplitude and phase information to be added correctly and processed further into the harmonic excitation functions. Excitation motions were calculated at the remote point representing a position of the crane tip. Small angle approximation was used based on the assumption of the limited operational pitch and roll angles. Translations due to rotation of the vessel were obtained using the complex map (6) and summed with the global translations.

$$\delta \vec{\omega} \times \vec{l}_{ct} = \begin{bmatrix} \vec{i} & \vec{j} & \vec{k} \\ A_y e^{i\phi_y} & A_r e^{i\phi_r} & A_p e^{i\phi_p} \\ z_{ct} & y_{ct} & x_{ct} \end{bmatrix} e^{i\omega t} \quad (6)$$

where:

$\vec{i}, \vec{j}, \vec{k}$  - unit vectors,

$A_n$  -  $n$  motion amplitude,

$\phi_n$  -  $n$  motion phase angle,

$n$  - motion characteristic subscript (y-yaw, p-pitch, r-roll),

$\vec{l}_{ct}$  - crane tip position vector (ship local coordinate system),

$\delta\vec{\omega}$  - infinitesimal rotation vector (components of  $\delta\vec{\omega}$  are individual rotations about their respective component axes).

### 3.2. Analytical analysis

To simplify the analytical description of a complex ship motion model, some assumptions were adopted at the preliminary stage of modelling and only the most important dependencies were used for the derivation of the equations of motion. The following assumptions were implemented in the model:

- the payload motion was considered in YZ plane, including three degrees of freedom – linear heave for the object and the compensator and the angular pendulum of the system,
- the payload was treated as a material point,
- the excitation for the base movement was calculated based on the assumptions described in 3.1 - this allowed the crane tip to be excited kinematically,
- the executive element of the compensator was modelled as a spring having stiffness within a specified range,
- as the considerations concern only lifting in air phase, the lifting cable was modelled as a massless element with a specified length and stiffness.

The purpose of introducing simplifying assumptions seems to be justified and allows a preliminary model to be obtained allowing for the study of the lifting dynamics using simple analytical methods. The work performed at this stage allowed for a development of a three degrees of freedom dynamic model of a crane tip equipped with a lifting cable with length dependent stiffness, mass and stiffness of the compensator and also mass of the payload. The model was prepared so that it allows for an adjustment of the compensator stiffness. The proposed 3-DOF dynamic model is presented in Fig. 4 and the system parameters explained in the description.

where:

$y_e(t) = A_y \cos(\omega t + \Phi_y)$  - lateral displacement at crane tip obtained from RAOs (a regular wave excitation) [m],

$z_e(t) = A_z \cos(\omega t + \Phi_z)$  - vertical displacement at crane tip obtained from RAOs (a regular wave excitation) [m],

$A_y$  - amplitude of the lateral excitation [m],

$A_z$  - amplitude of the vertical excitation [m],

$\Phi_y$  - phase angle of the lateral motion [rad],

$\Phi_z$  - phase angle of the vertical motion [rad],

$m_p$  - mass of payload [kg],

$l_0$  - length of the lifting cable [m],

$l_c$  - length of the attached compensating element [m].

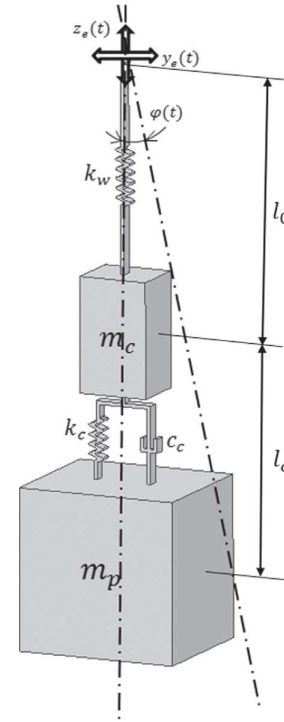


Fig. 4. The proposed 3-DOF dynamic model for offshore lifted objects.

The other parameters of the proposed model given in Fig. 4 are explained as referred in the symbols description for Fig. 1.

The equations of motions were derived from the Lagrange equations of a second kind, using the general formula given in (7):

$$\frac{d}{dt} \left( \frac{\partial L}{\partial \dot{q}_j} \right) - \frac{\partial L}{\partial q_j} + \frac{\partial D}{\partial \dot{q}_j} = Q_j \quad \text{for } j = 1, \dots, n \quad (7)$$

where:

$q_j, \dot{q}_j$  - vectors of generalised coordinates and their velocities,

$L = T - V$  - Lagrange function computed as a difference between kinetic and potential energy,

$D$  - Rayleigh dissipation function,

$Q_j$  - non-potential generalised force corresponding to the  $j$ th generalised coordinate,

$n$  - number of generalised coordinates.

The considered system can be described by the following equations:

$$M(t)\ddot{X} + G(t)\dot{X}^2 + C(t)\dot{X} + K(t)X = F(\dot{X}, X, t) \quad (8)$$

where the inertia, gyroscopic, damping and stiffness matrices are given respectively:

$$M(t) = \begin{bmatrix} m_p & 0 & 0 \\ 0 & m_p(a + 2x_e + 2l_0l_c) + m_c(b + 2x_cl_0) & 0 \\ 0 & 0 & m_c \end{bmatrix} \quad (9)$$

$$G(t) = \begin{bmatrix} 0 & -m_p c & 0 \\ 0 & 0 & 0 \\ 0 & -m_c d & 0 \end{bmatrix} \quad (10)$$



$$C(t) = \begin{bmatrix} c_c & 0 & 0 \\ 2m_p\dot{\varphi}c & 2(m_p\dot{x}c + m_c\dot{x}_c d) & 2m_c\dot{\varphi}d \\ 0 & 0 & 0 \end{bmatrix} \quad (11)$$

$$K(t) = \begin{bmatrix} k_c & 0 & -k_c \\ 0 & m_p f_1 & m_c f_2 \\ -k_c & 0 & k_c + k_w \end{bmatrix} \quad (12)$$

where:

$$a = (x^2 + l_0^2 + l_c^2)$$

$$b = (x^2 + l_0^2)$$

$$c = (x + l_0 + l_c)$$

$$d = (x_c + l_0)$$

$$e = (l_0 + l_c)$$

$$f_1 = (g \sin(\varphi) - 2\dot{x}\dot{\varphi}) - \frac{1}{2}\omega^2 g_1$$

$$f_2 = (g \sin(\varphi) - 2\dot{x}\dot{\varphi}) - \frac{1}{2}\omega^2 g_2$$

$$g_1 = A_y(\cos(\alpha_y) + \cos(\beta_y)) + A_z(\sin(\alpha_z) + \sin(\beta_z))$$

$$g_2 = A_y(\cos(\alpha_y) + \cos(\beta_y)) + A_z(\sin(\alpha_z) + \sin(\beta_z))$$

$$\alpha_y = (\omega t + \Phi_y + \varphi)$$

$$\beta_y = (-\omega t - \Phi_y + \varphi)$$

$$\alpha_z = (\omega t + \Phi_z + \varphi)$$

$$\beta_z = (-\omega t - \Phi_z + \varphi)$$

Non-linear and time-dependent terms vector  $F(\dot{X}, X, t)$  has a following form:

$$F(\dot{X}, X, t) = \begin{bmatrix} F_\varphi(\dot{X}, X, t) \\ F_x(\dot{X}, X, t) \\ F_{x_c}(\dot{X}, X, t) \end{bmatrix} \quad (13)$$

where:

$$F_\varphi(\dot{X}, X, t) = A_y h \omega^2 \cos(\omega t + \Phi_y) \cos(\varphi) \\ - A_z h \omega^2 \cos(\omega t + \Phi_z) \sin(\varphi) \\ + 2(l_0 + l_c)m_p \dot{\varphi} \dot{x} + 2l_0 m_c \dot{\varphi} \dot{x}_c - g h \sin(\varphi)$$

$$F_x(\dot{X}, X, t) = A_y m_p \omega^2 \cos(\omega t + \Phi_y) \sin(\varphi) \\ + (A_z \omega^2 \cos(\omega t + \Phi_z) + g)m_p \cos(\varphi)$$

$$F_{x_c}(\dot{X}, X, t) = A_y m_c \omega^2 \cos(\omega t + \Phi_y) \sin(\varphi) \\ + (A_z \omega^2 \cos(\omega t + \Phi_z) + g)m_c \cos(\varphi)$$

$$h = (l_0 m_c + l_0 m_p + l_c m_p)$$

All the  $\varphi$ ,  $x$  and  $x_c$  included in the equations are time dependencies and correspond to the following degrees of freedom of the considered model:

$\varphi$  - sway angle response,

$x$  - linear displacement of the payload,

$x_c$  - linear displacement of the attached compensating element.

The other symbols appearing in the matrices have been explained in the descriptions for the Figs. 1 and 4.

### 3.3. Numerical simulations environment

The dynamic model considered in the paper is described by three ordinary differential equations of a second order. In order to perform numerical simulations, the equations were transformed into the first order form. The obtained results provide basic information about the dynamic behaviour of the system. The SageMath environment ([sagemath.org](http://sagemath.org), 2019) was used to conduct the numerical simulations. SageMath (formerly SAGE from Software for Algebra and Geometry Experimentation) is a computer algebra system (CAS), which is a common platform of many advanced tools and programming libraries created to support complex mathematical calculations. The authors of the study decided to implement the whole simulation studies in SageMath as it seems to be convenient in its functionality allowing to perform either symbolic or numerical operations. The entire program was written in the scripting language Python. The utilised Python-based program consists of free libraries only and is distributed under the GNU GPL – this gives the possibility of a completely free use for private and commercial purposes. The presented advantages make the SageMath environment an interesting alternative to commercial software packages such as Mathematica or MATLAB.

The ordinary differential equations were solved using the lsoda from the FORTRAN library odepack. The utilised method switches automatically between the non-stiff Adams and the stiff BDF method. This procedure is characterised by a satisfactory speed and accuracy. Numerical simulations of the investigated systems were carried out and discussed. In the following section, the model itself is subjected to further investigation and verification activities.

### 4. Model validation

A building block of the proposed method was to introduce a vessel-payload decoupled response assumption. This was achieved by following the recommendation in DNV GL (2017) and restricting the method to be used within the light lifts regime. To ensure validity, the authors have conducted numerical analysis taking into account 6 degrees of freedom related to the vessel motion. These 6-DOFs provide the linear and angular vessel motions directly coupling the two considered systems. An initial model developed by the authors has given satisfactory confirmation of the referenced assumption. The following three cases were considered by the authors:

- comparative analysis of the 9-DOF model response (vessel-payload response) against the 3-DOF model (payload response) proposed in the article, in which the vessel excitation is based on RAO's processing methodology,
- comparative analysis of the payload and vessel response for two vessels of different seakeeping properties,
- comparative analysis of the payload and vessel response for a number of different payload masses.

The considerations concern one-dimensional forward propagating waves as a vessel excitation. The performed tests and results of some of the considered cases are reported for reference.

Fig. 5 presents the pendulation amplitude of the object suspended from the crane boom tip excited by the coupled vessel motions. For the considered forward propagating excitation wave (wave period  $T = 7$  s), the crane tip excitation amplitudes are of the following values: lateral tip displacement  $A_y = 0.5$  m, vertical tip displacement  $A_z = 1.5$  m, which correspond to the excitation amplitudes considered in the 3-DOF model payload response simulations presented in Fig. 15. Comparing the results obtained utilising the RAO's processing methodology it was observed that the payload response is identical, confirming the method's validity for the given mass relationship regime.

This validation of assumptions allowed time histories to be prepared of the RAO changes for a complex model of the vessel payload system (see Figs. 6 and 7).

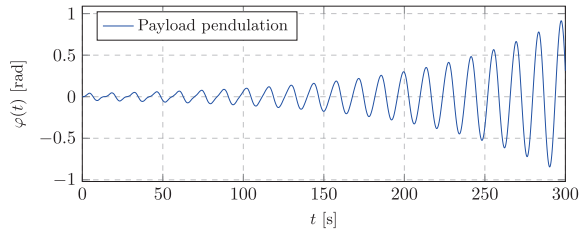


Fig. 5. Payload pendulation for 9-DOF model for crane tip excitation amplitudes  $A_y = 0.5$  m,  $A_z = 1.5$  m and wave period  $T = 7$  s.

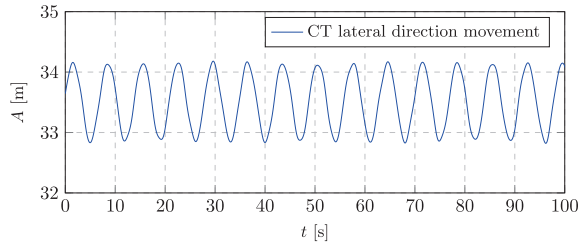


Fig. 6. Vessel crane tip in-plane lateral excitation amplitude.

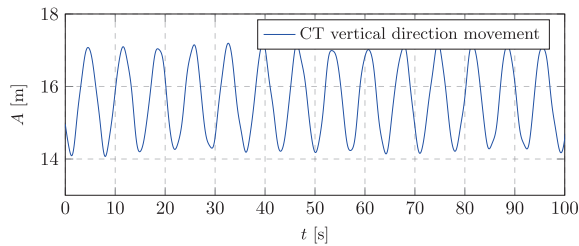


Fig. 7. Vessel crane tip in-plane vertical excitation amplitude.

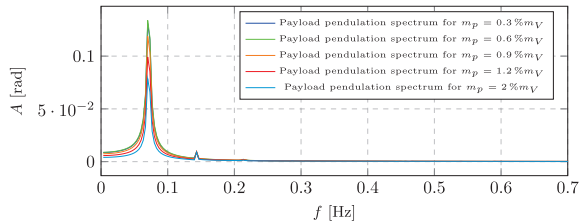


Fig. 8. Payload pendulation spectrum for 9-DOF model — comparative results for different payload weights.

The obtained results show a regular motion of the crane boom tip. The frequency, amplitude and phase shift are the same as computed with RAO's within the accuracy of numerical errors. It allows the conclusion that the vessel dynamic properties are transferred through the RAO's affecting payload dynamics. No additional effects were observed allowing for the claim of ship-lifted object coupling for the vessel-payload mass ratio regime in consideration. It confirms the authors' assumption and shows that the methodology based on RAO's can be successfully and efficiently used for uncoupled models.

Additionally, five subsequent masses up to 2% of total ship displacement (as adopted from reference mentioned) were considered. Results of the investigation are depicted in Figs. 8–10 as spectra obtained by utilisation of Fourier analysis in order to enable clearer presentation of the results.

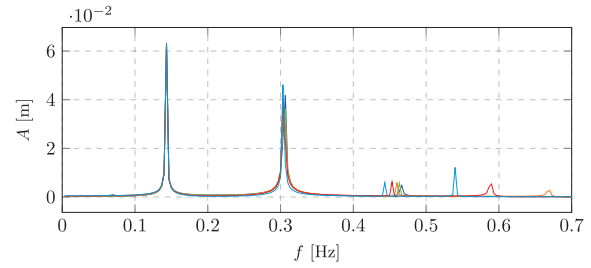


Fig. 9. Vessel heave spectrum for different payload weights (labels as per in payload pendulation spectrum).

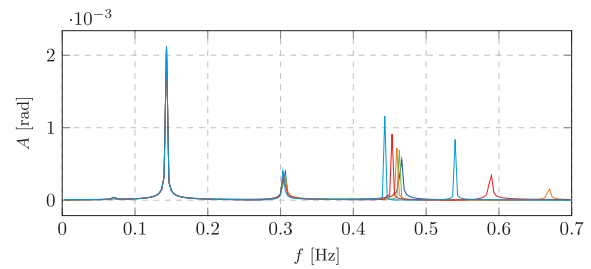


Fig. 10. Vessel pitch spectrum for different payload weights (labels as per in payload pendulation spectrum).

Based on the results provided, it might be stated that the frequency structure of payload vibrations is of a different character and is fully independent to vessel heave and pitch oscillations. In-depth analysis allows for an observation of low frequencies components being revealed in each spectrum but they are of zero amplitudes and are clearly negligible in a qualitative and quantitative evaluation of the results.

The obtained results revealed that there is no significant influence of payload weight on the system frequency structure for the considered mass regime. Critical harmonic components do not change their position even for limit value of lifted object mass. Amplitude of dynamic response is marginally lower for the heavier objects but it does not have a meaningful invalidating impact on the proposed methodology. Higher harmonic components are shifted relative to the reference position but the changes are small and outside of resonance range. Hence these elements can be omitted in the analysis. It was concluded that the assumed simplification is correct and allows the replacement of coupled analysis with the floating vessel RAO without raising significant modelling errors.

Payload mass to ship displacement ratios above 2% have also been checked. The expected discrepancy in quantitative measures was observed immediately past the threshold value while qualitative divergence between the two methods started to appear at 2.5%.

In order to validate the proposed mathematical model and hence simulation results, the authors of the study decided to involve also the world's leading commercial software package. OrcaFlex software is used for the dynamic analysis of offshore marine systems. The Orcaflex model was prepared so that the conditions from the discussed analytical model were accurately replicated. To examine specific parameters of the models appropriate tests were performed in both environments independently. The extracted results from the OrcaFlex model were a vertical displacement for both of the masses and the sway angle of the system. A created model enabled the implantation of the excitation in the kinematic form in two independent directions. The authors modelled the wire rope as several massless 2-node elements — this corresponds to the model used in the analytical model as per assumptions stipulated earlier in the text. The lifting wire was separated to 3 distinct segments:

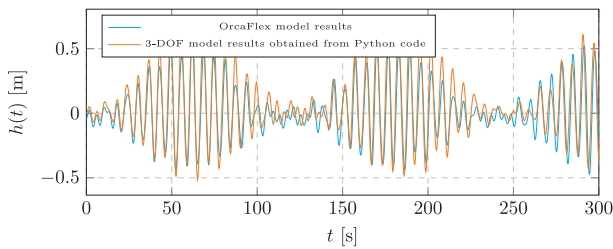


Fig. 11. OrcaFlex vs. Python — comparative simulation results for heave response.

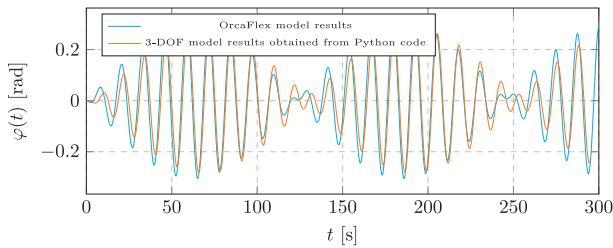


Fig. 12. OrcaFlex vs. Python — comparative simulation results for sway angle response.

- (a) winch — element allowing for the controlled length adjustment, modelled with the same properties as the lifting wire,
- (b) main lifting wire — element with a fixed length,
- (c) compensator length — element with a negligible stiffness allowing for the incorporation of the compensator element.

The compensator was represented as a link spanning through a length of the appropriate part of the lifting wire. This allowed close control of the stiffness parameter of the compensator and enabled post-processing of the desired results. Compensator mass was attached as a clump weight at the geometric centre of the element in its unstretched length. The object was represented as a lumped mass using the 6D buoy element. All geometric, environmental, elastic and rotational properties were neglected at this stage. The vessel was set to harmonic motions that only relate directly to the excitation derivation methodology described in 3.1.

The study on the OrcaFlex model allowed comparison of the results with previously performed simulations. The comparative results are depicted below.

Analysing the presented figures, it can be concluded that the obtained results correspond to the proposed mathematical model discussed in the previous section. The results show that the numerical output of the authors' dynamics equations and the software are consistent. However, in Figs. 11 and 12 some discrepancies between the obtained waveforms might be observed — this may be the result of utilisation of different integration methods. The OrcaFlex package (Orcina-Ltd, 2019) implements two complementary time domain dynamic integration schemes, which are an explicit and implicit. Both of them re-compute the system geometry at each time step so that the simulation takes into account all geometric non-linearities, including the spatial variation of contact and wave loads. While the integration scheme implemented by the authors solves a system of ordinary differential equations using lsoda from the FORTRAN library odepack described briefly in 3.3. Another reason for that inaccuracy might be the existence of a numerical damping in the integration scheme used in the commercial software for finite element models as they may contain false high frequency response. The generalised- $\alpha$  integration scheme utilised in OrcaFlex package is based on a controllable numerical damping, which removes artificial high frequency

response. A much more stable convergence is achieved when numerical damping is implemented into the integration scheme. The generalised- $\alpha$  integration scheme uses a built-in value of 0.4 that according to the software creators, was chosen to provide fast simulation run time without compromising its accuracy. Nevertheless, the obtained results might be considered as consistent since the important characteristics remains unchanged proving the validity of the proposed model.

## 5. Comparative analysis of the encountered models against the 3-DOF model

Based on the available literature models, the authors prepared reference models that allowed comparison of the proposed methodology to the existing ones. Considerations regarding literature models, as in the case of the analysed system, were reduced to the analysis of the dynamics of the in plane motion by the implementation of the simplifying assumptions described in 3.2.

For analysis purposes the authors proposed two comparative models. The first system was modelled on the basis of Ngo and Hong (2012) and Sun et al. (2017) as a single pendulum, where an excitation was incorporated as an angular roll, acting in the YZ model plane only. The lifted object was modelled as a point mass suspended at the end of pendulum. It is worth noting that the reference literature model does not take into account the stiffness characteristics of the system — neither the stiffness of the crane nor of the cable that are both crucial when considering lifting operations. The crane stiffness should be considered during a variety of lifting phases as it may lead to a change in the system's natural frequency. It is understood that with an increase in the cable length crane stiffness becomes less significant in the equivalent system stiffness.

The second proposed model to study dynamics of the oscillating motion system was the Mathieu model being a representation of the simplest model of parametric vibrations. Besides of vertical heave of the pendulum model moving support, the excitation was also given in a lateral direction by the roll angle, as in the reference literature model. Dimensionless form of the Mathieu model governing equation is presented in formula (14) as follows:

$$\ddot{\varphi}(\tau) + \omega_0^2 (1 + \epsilon \cos(\tau)) \cdot \varphi(\tau) = 0 \quad (14)$$

where:

$\tau$  - dimensionless time,

$\omega_0$  - natural frequency,

$\epsilon$  - modulation index.

Dynamics of payload sway motion for the simplified models of a mathematical pendulum with moving support was analysed for both cases and compared against the dynamics of the proposed 3-DOF model. A series of simulations were performed to study the behaviour of the models discussed.

### 5.1. Simulations data

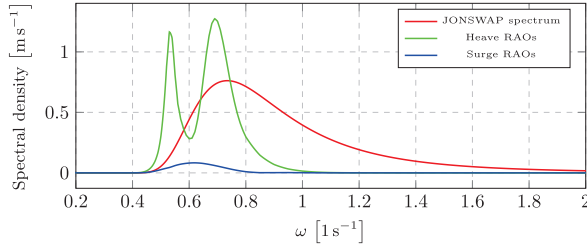
For a fully comprehensive study of the proposed 3-DOF model, two types of a wave excitation were applied - a regular and irregular wave. The parameters presented in Table 1 were used in simulations utilising the excitation of regular waving.

To enable more comprehensive model evaluation studies were also conducted in irregular waves derived based on JONSWAP spectra theory provided by DNV GL (2018) or DNV GL (2017) and calculated for the specified wave parameters (frequency and direction). Irregular random waves, reflecting a real sea state, can be represented as a summation of sinusoidal wave components with a random phases. Based on JONSWAP spectra, an empirical relationship between the distribution of the energy by frequency allows to obtain a reliable representation of a sea state.

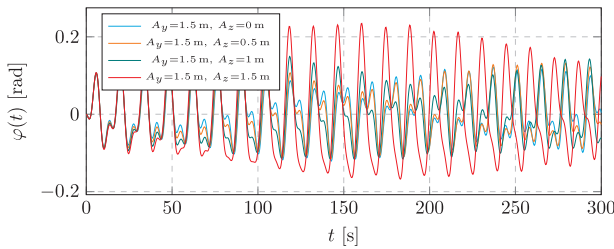
In Fig. 13, the RAOs utilised to establish the crane tip excitation are presented and the corresponding wave parameters depicted within the label.

**Table 1**  
Parameters used in simulations.

	Parameter	Corresponding value
Swaying motion	$s_y$	$1.185 \cos(0.52 t - 2.396)$ m
Heaving motion	$h_z$	$0.306 \cos(0.52 t + 0.315)$ m
Lifting set length	$l_0 + l_c$	48.7 m; 40 m
Payload mass	$m_p$	100 t
Compensator mass	$m_c$	10 t
Crane stiffness	$k_{cs}$	$5000 \text{ kN m}^{-1}$
Equivalent stiffness	$k_{eq}$	$3980 \text{ kN m}^{-1}$
Young modulus	$E$	92 GPa
Cable diameter	$d_w$	0.10 m



**Fig. 13.** RAOs obtained from JONSWAP spectrum utilised to establish the crane tip excitation.



**Fig. 14.** Sensitivity analysis of the proposed 3-DOF model for heave excitation.

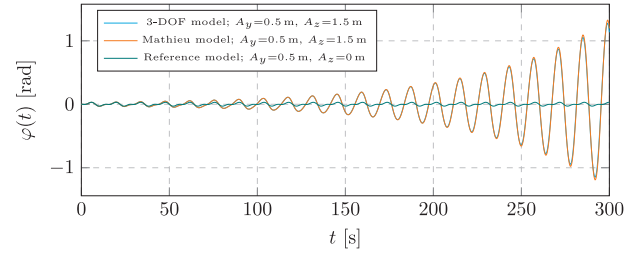
## 5.2. Results and discussion

Numerical simulations were performed for the three analysed models as described in the preceding sections. Nevertheless, it should be noted that the models proposed in the literature do not investigate the compensation for heave and swing motion simultaneously hence a direct comparison is somehow limited. Also the stiffness considerations seem to have a significant influence on the dynamics of the systems and simulation results.

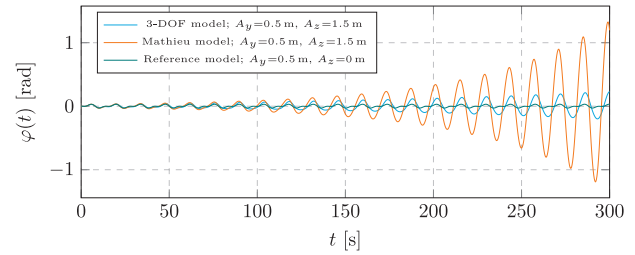
The results as shown in Figs. 14–25 are provided together for a comparison. As the reference models do not include the analysis of a vertical displacement of the payload, the comprehensive comparison cannot be fully accomplished, but the results for the pendulum angle of each model were depicted and are discussed below.

The comparison was carried out by adjusting the stiffness so that the simulation results of the 3-DOF model match the reference ones. For the sensitivity analysis of the proposed model, heave excitation was first set to 0 to allow for a direct comparison. In author's understanding it is one of the biggest issues with the reference models as heave motion is unavoidable in offshore operations. Further stages of the models comparison were performed by gradually increasing the heave excitation in the proposed model. Side-way excitation was kept the same — this shown how quickly the pendulum response deviates from the 'heaveless' model.

Fig. 14 shows influence of vertical amplitudes of tip oscillations on payload sway angle. Vibration frequency was set equal to subharmonic critical frequency of parametric resonance. Different values of heave



**Fig. 15.** Sway angle response to high amplitude of heave excitation; parametric resonance case — stiffened 3-DOF model.



**Fig. 16.** Sway angle response to high amplitude of heave excitation; parametric resonance case — reduced compensator stiffness.

$A_z$  and constant values of roll  $A_y$  magnitude were taken into account. As expected, higher heave excitation amplitudes led to an increase in the payload angular vibration amplitude. It also became apparent and proven how important it is to consider the heave excitation when studying and evaluating an amplitude of pendulation angle of lifted objects.

To emphasise the phenomenon and the payload sway response, the simulations were performed for a calculated parametric resonance cable length being within the operational range, for high amplitude of heave excitation, for 7 s wave period (medium-slow waves). Vibration frequency was set equal to subharmonic critical frequency of parametric resonance. For each of cases, the authors conducted two simulations enabling a direct comparison between the discussed models.

In each of the Figs. 15 and 16, three dynamic responses of the analysed systems obtained for the same magnitudes of excitation amplitudes are presented. Physical parameters of the models were set equal besides the stiffness of the compensating element in the proposed 3-DOF model. In Fig. 15 the compensator stiffness was set an order of magnitude higher than for the simulation results depicted in Fig. 16. Artificial stiffening of the 3-DOF model allowed to achieve the same simulation results as in the case of the Mathieu model, where the cable is assumed to be rigid. In Fig. 16, when the stiffness characteristics of the 3-DOF model was changed by means of a compensator stiffness value, it can be observed that manipulation of system stiffness characteristics, which is equivalent to changing the length of the cable, has a significant influence on the dynamic behaviour. The amplitudes of pendulation angle for the proposed model are then much smaller and even if the resonance is likely to occur, its raising rate is much slower and the reached amplitudes much smaller.

From Fig. 17 it can be stated that for all of the analysed models (when considering stiffened 3-DOF model), an occurrence of main resonance can be well-predicted. Analysis of Figs. 17 and 18 in comparison to 20 and 22, when simulations were run for idealised regular wave scenario generated using RAOs, allows to conclude that oscillations with natural frequency are important only for high values of vertical displacements. Moreover, it can be concluded that even small value of surge/sway can lead to a change of the resonance type. As depicted in Fig. 18, the model with reduced stiffness is limiting the amplitudes



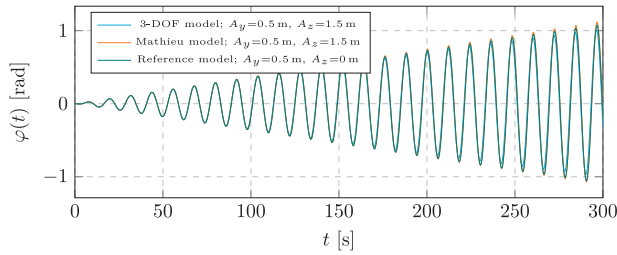


Fig. 17. Sway angle response to high amplitude of heave excitation; main resonance case — stiffened 3-DOF model.

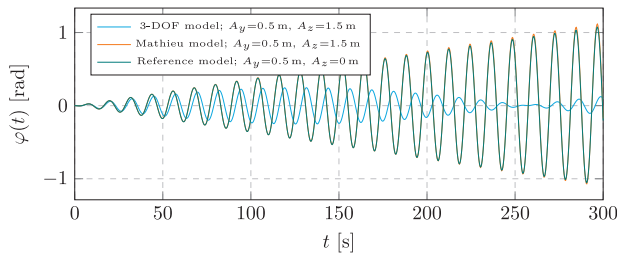


Fig. 18. Sway angle response to high amplitude of heave excitation; main resonance case — reduced compensator stiffness.

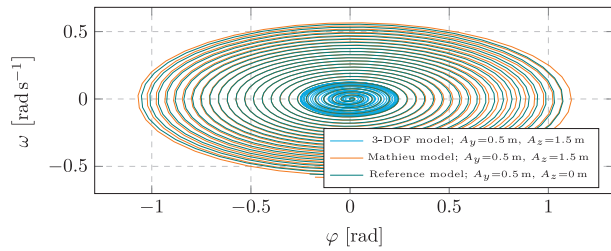


Fig. 19. Phase portrait of sway angle response to high amplitude of heave excitation corresponding to reduced compensator stiffness case.

of pendulation even for resonant frequencies. Results being compatible with Fig. 18 can be obtained from the analysis of phase portrait presented in Fig. 19. Resonance behaviour is visible as unstable spirals, which are tending to infinity. Stable vibrations are connected with the limited curve.

Figs. 20 and 22 present simulations performed for a resonant cable length for idealised regular wave scenario generated using RAOs. In comparison to Figs. 15 and 16, where the amplitude values of heave  $A_z$  and roll  $A_y$  were opposite and a little bit higher, it can be observed that parametric resonance is caused by heave of a crane tip. However, lateral displacement of the crane tip has an important role in the process of an amplitude increase. Phase portraits depicted in Figs. 21 and 23 show similar information. Resonance pendulation caused by vertical tip displacements has a form of deformed unstable spirals. Additional loop in the central position of portrait is connected with higher harmonics of the solution. It does not affect on the system stability. Regardless the method used to analyse, it can be stated that even for small values of its lateral amplitude, the resonant raising rate is higher. Parametric resonance is important in case of regular waves with period about 6–7 s. As in the previously discussed cases, the change in stiffness of the 3-DOF system through the rigidity of the compensator leads to a limitation of the sway amplitudes of the payload. It is especially visible at phase portrait shown in Fig. 23. Utilisation of the lower stiffness (enable of the compensator) leads to a significant change of trajectories.

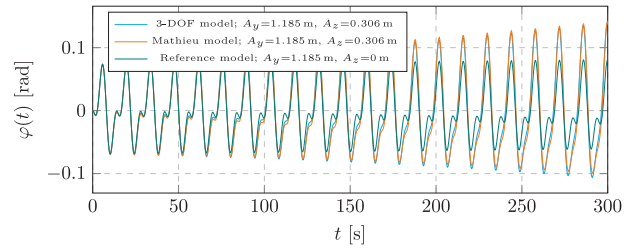


Fig. 20. Sway angle response to induced excitation — stiffened 3-DOF model.

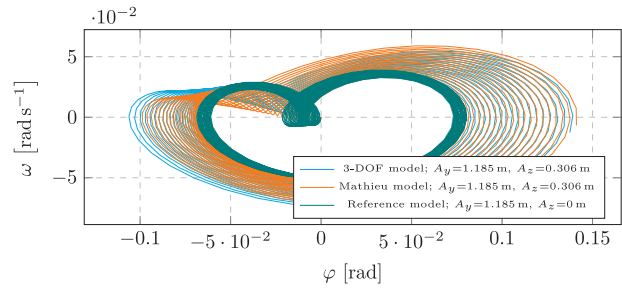


Fig. 21. Phase portrait of sway angle response corresponding to the stiffened 3-DOF model case.

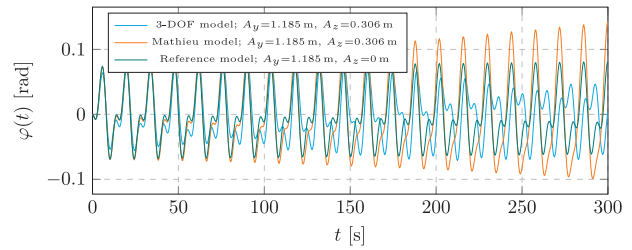


Fig. 22. Sway angle response to induced excitation — reduced compensator stiffness.

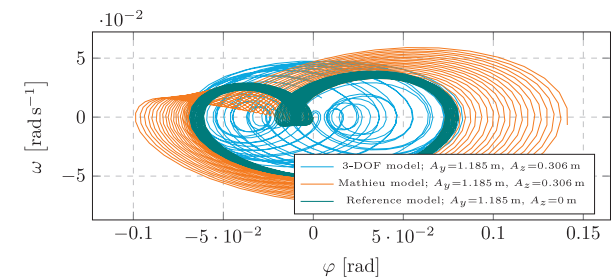


Fig. 23. Phase portrait of sway angle response corresponding to reduced compensator stiffness case.

Resonance behaviour with ‘growing’ trajectories is replaced with the limited curve, which means stable dynamics.

Because of significant simplifications adopted in the reference models (e.g. rigid cable, omitted influence of heave), simulations conducted for resonance beyond cable length for idealised regular wave scenario shown that the non-linear model is limiting the amplitudes of pendulation even for close values of resonant frequencies (Fig. 24). This implies that the system should be stable but high displacements are still present. In Fig. 25 it can be seen that by a change in stiffness of added compensator, the dynamic response of the proposed system is

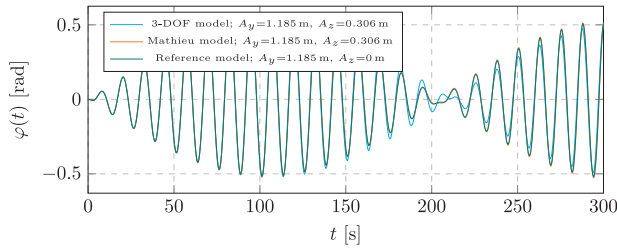


Fig. 24. Sway angle response to induced excitation; non-resonant case — stiffened 3-DOF model.

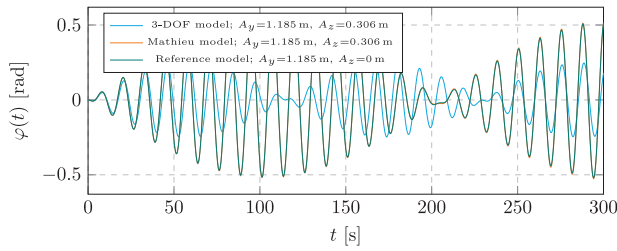


Fig. 25. Sway angle response to induced excitation; non-resonant case — reduced compensator stiffness.

characterised by the higher vibration frequency, but at the same time achieves only half of the amplitude of payload pendulation.

Analysis conducted on the basis of simulations carried out for each model leads towards relevant conclusions. A big disadvantage of the reference models is aforementioned in 2.2 disregarded stiffness of individual components of a system. The omission of the stiffness of the crane structure while assuming a lifting cable as a rigid rod, leads to changes in the dynamics of the system resulting in changes in its natural frequency. When considering a lifting in air phase, short cable length results in the high stiffness of the system. However along with the payload lowering, i.e. unwinding the lifting cable, continuous changes in the rigidity of the whole system occur, which certainly affect the dynamics of the analysed model.

Introducing into the 3-DOF model, an additional compensator spring, allowed to examine how changes in its stiffness affect the amplitudes of angle pendulation of the payload. The research led to interesting observations. It can be concluded that manipulations in the stiffness of the compensating element lead to a change in the total stiffness characteristics of the system, and thus the length between crane tip and payload. This in turn leads to a limitation of the amplitude of the payload sway angle. Changing the rigidity of the system, therefore, leads to a change and limitation of the angle of pendulation, which can be achieved for example through varying the cable length over time.

The ability to analyse the key vertical displacement of a hanging mass, due to heave motion is essential to conduct a fully comprehensive study of the dynamic behaviour of objects during lifting operations. All these weaknesses are compensated in the model proposed by the authors of this article.

As discussed, irregular wave studies were also conducted for comprehensiveness. Fig. 26 shows the proposed 'real sea state' excitation obtained from RAOs depicted in Fig. 13 after inverse fast Fourier transformation.

In order to assess the proposed model validity, the authors expanded the validation database and prepared a number of numerical simulations for irregular wave case. All of the obtained results are presented in Figs. 27–31.

As can be seen in Figs. 27 and 28, even a linear analysis allows to assess resonance occurrence regions reliably and possibly prevent

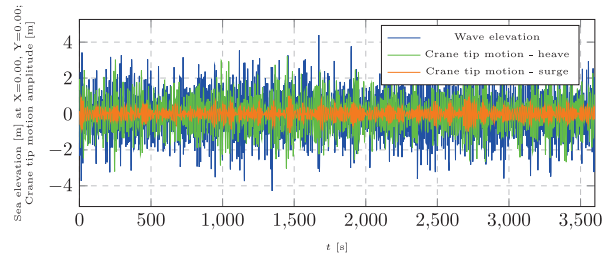


Fig. 26. Wave trains as a result of inverse fast Fourier transformation of RAOs spectral density functions.

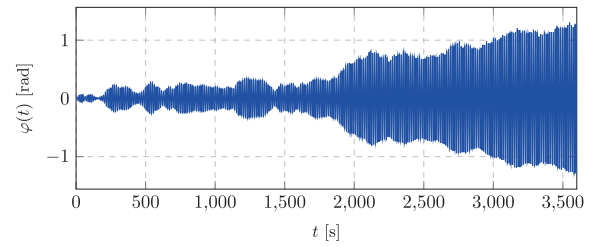


Fig. 27. Payload pendulation in irregular waves (linear analysis);  $l_w = 42$  m.

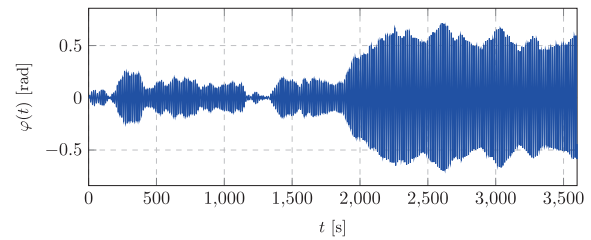


Fig. 28. Payload pendulation in irregular waves (nonlinear analysis);  $l_w = 42$  m.

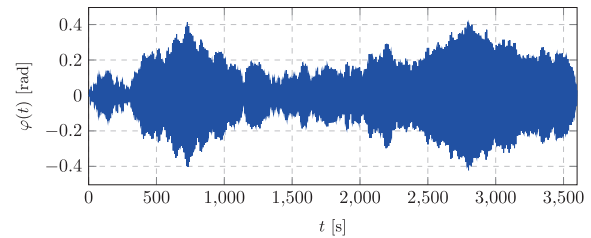


Fig. 29. Payload pendulation in irregular waves;  $l_w \approx 25$  m.

the system from hazardous operations for the specified lifting cable lengths. Naturally, the nonlinear model reflects the real behaviour of the system more truthfully despite limitation of amplitude values but as depicted in Fig. 28, the nonlinear model response also shows a dangerous behaviour of the system, excluding it from operation. Despite stable dynamics, the pendulation amplitudes are still very high.

Based on the results depicted in Fig. 29, operations carried out beyond resonant cable lengths ensure a significant decrease in amplitude value of payload pendulation and thereby again a stable system dynamic behaviour.

As can be observed in Fig. 30, oscillations around the resonant cable length can be a serious threat to operational safety. Payload angular vibrations within a resonance region are characterised by high amplitude values and even a slight change in lifting cable length (in the

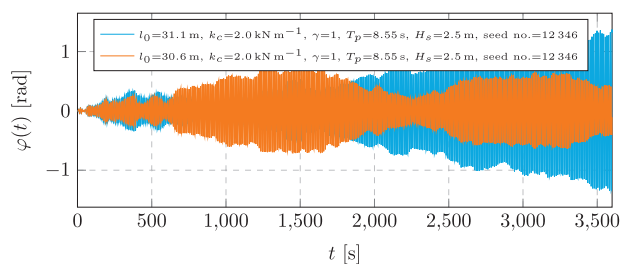


Fig. 30. The 3-DOF model angular response to irregular wave - a parametric resonant cable length region.

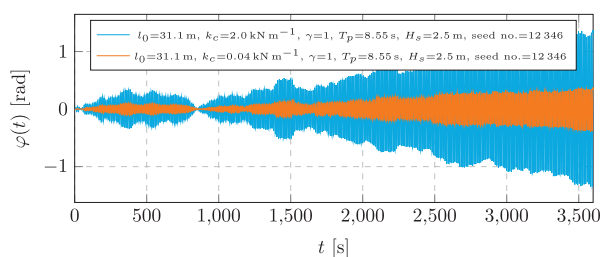


Fig. 31. The 3-DOF model angular response to irregular wave - a parametric resonance occurrence.

considered case - 0.5 m) may result in a sudden increase of amplitudes and reaching resonant vibrations.

Moreover, as shown in Fig. 31, the 3-DOF model response to the applied excitation confirms the effectiveness of the proposed methodology. Physical parameters of the model remained unchanged besides the stiffness of a compensating element. Artificial stiffening of the model allowed modelling dynamic behaviour as in the case of the Mathieu's model where the lifting cable is assumed to be rigid (as per the analysis conducted in case of the regular wave) resulting in ability to capture a parametric resonance. While manipulating the system stiffness characteristics by means of changing the compensating element stiffness value, a significant influence on its dynamic behaviour can be observed. The amplitudes of pendulation angle are attenuated and the resonance rising rate is slower, hence the behaviour of the lifted object might be controlled even throughout 1-hr operation. This manipulation could not be achieved utilising any of the reference models.

## 6. Conclusions

Concluding the paper, it is assumed that the target of introducing a simple but comprehensive model was achieved. Variety of models encountered in the literature were discussed and were all proven to be overly simplified. Proposed 3-DOF model incorporates the axial oscillation including a compensating element and pendulation with an ability to process a bidirectional excitation. This approach, as proven within this document, allowed to observe the interaction between various excitation directions that were proven to influence the response. Moreover, the presented approach is based on analytical methods what allows for a theoretical, numerical or combined analysis. Model utilises a computed crane tip excitation as a result of vessel motion. This is processed using well recognised RAO's processing methodology leading to further computational efficiencies. It is highlighted that RAO's set and the way it was derived cannot in anyway influence the efficiency of the model. The proposed model incorporates the algorithm processing the wave parameters, RAO data to obtain the excitation. The model allows for an implementation of a variety of excitation types. That provides an ability to study responses to regular wave as well as systematic dynamic responses to irregular wave. It needs to be highlighted that

the method remains valid within the light lifts category as classified in DNV GL (2017) and proven within this article. Heavy lifts require coupled analysis introducing additional complexity as briefly described within Section 4.

In contrast to the proposed 3-DOF model, the reference models discussed throughout the article do not provide such degree of freedom, which allows for an investigation of the models heave response what in fact omits following their axial oscillations. Only one of them — Mathieu model allows to apply vertical heave excitation, which is responsible for an occurrence of parametric vibrations. It proves how important it is to consider the heave excitation when studying and evaluating an amplitude of pendulation angle of lifted objects. Moreover, Mathieu model does not involve the lateral direction displacement of the supporting point (crane tip lateral excitation), which, as discovered during the studies, has a significant influence on the process of increasing the vibrations amplitude values. On the other hand, the model recommended by DNV is used only for axial vibrations investigation but does not incorporate the pendulum oscillations studies. In addition, it also does not include the lateral excitation. It should be noted that the models encountered in the literature do not allow to address the compensation for heave and swing motion simultaneously. All of these weaknesses are compensated in the model proposed. The suggested approach takes into account all of the significant phenomena that might be encountered. These are the axial vibrations, pendulation, coupling between these two, an influence of the compensating element and also the bidirectional (mutually perpendicular) excitation incorporation. It is concluded that the proposed model incorporates the most important features of the models popular in the literature and also introduces a significant advantage to the research methodology.

Additionally, the proposed model provides processing versatility as it allows for the utilisation of various processing methods — time-domain, spectral and phase plane analysis methods were applied in this paper. Compatible solutions were obtained but depends on cases different methods led to better effects.

It is worth highlighting that the mentioned advantages do not compromise the analysis efficiency as reliable and efficient tools are used to process the calculations. It was also proven that the proposed model converges well with the results obtained in the commercial software. Some discrepancies were observed but were generally found negligible as the most important system response parameters remained unchanged.

It is understood that more sophisticated models exist and that commercial software packages utilised in the industry allow for analysis of an infinite number of degrees of freedom. This however is a time-consuming process and requires more resource in order to execute. Thus a simplicity and flexibility of the proposed methodology give an advantage over the other solutions. It is suggested that the discussed model is a balanced, easily accessible tool between overly simplified ones and highly complex alternatives.

## Declaration of competing interest

The authors declare that they have no known competing financial interests or personal relationships that could have appeared to influence the work reported in this paper.

## CRediT authorship contribution statement

**Bogumil Chilinski:** Conceptualization, Methodology, Software, Validation, Formal analysis, Writing - original draft, Supervision. **Anna Mackojc:** Conceptualization, Methodology, Validation, Formal analysis, Investigation, Data curation, Writing - original draft, Writing - review & editing, Visualization, Project administration. **Robert Zalewski:** Supervision. **Krzysztof Mackojc:** Conceptualization, Validation, Writing - review & editing, Funding acquisition.

## References

- Albers, P., 2010. Motion Control in Offshore and Dredging, Vol. 11. Springer, Dordrecht Heidelberg London New York, pp. 208–227.
- Balachandran, B., Li, Y., Fang, C., 1999. A mechanical filter concept for control of nonlinear crane-load oscillations. *J. Sound Vib.* 228, 651–682.
- DET NORSKE VERITAS GL, 2011. Standard for Certification No. 2.22 Lifting Appliance Ch.2 Sec. 2–39.
- DNV GL, 2017. Recommended Practice N103 Modelling and Analysis of Marine Operations. DET NORSKE VERITAS GL, Sec. 9.2–9.3.
- DNV GL, 2017. Recommended Practice N103 Modelling and analysis of marine operations. DET NORSKE VERITAS GL, Sec. 2.2.3.
- DNV GL, 2018. Recommended Practice C205 Environmental Conditions and Environmental Loads Sec. 3.3.2.
- Fałat, P., 2004. Dynamic Analysis of a Sea Crane of an A-Frame Type (PhD Dissertation [in Polish]). University of Bielsko-Biała, Poland.
- Fathom Group Ltd, 2018. Engineering Procedure. FG-EP-OD-02-RAO PROCESSING PROCEDURE.
- Fragopoulos, D., Spathopoulos, M.P., Zheng, Y., 1999. A pendulation control system for offshore lifting operations. In: 14th World Congress of IFAC.
- Journée, J., Massie, W., 2001. Offshore Hydromechanics. Delft University of Technology.
- Kurowski, J., Maczyński, A., Szczotka, M., 2012. The influence of a shock absorber on dynamics of an offshore pedestal crane. *J. Theoret. Appl. Mech.* 953–966.
- Masoud, Z., 2000. A Control System for the Reduction of Cargo Pendulation of Ship-Mounted Cranes (Ph.D. Dissertation). Virginia Polytechnic Institute and State University, Blacksburg, Virginia.
- Masoud, Z., Nayfeh, A., Mook, D., 2004. Cargo pendulation reduction of ship-mounted cranes. *Nonlinear Dynam.* 35 (3), 299–311.
- Ngo, Q., Hong, K., 2012. Sliding-mode antisway control of an offshore container crane. *IEEE/ASME Trans. Mechatronics* 17, 201–209.
- Orcina-Ltd, 2019. OrcaFlex Help, <https://orcina.com/SoftwareProducts/OrcaFlex/Documentation/Help/>.
- Osiński, M., Wojciech, S., 1998. Application of nonlinear optimisation methods to input shaping of the hoist driver of an offshore crane. *Nonlinear Dynam.* 17, 369–386.
- sagemath.org, 2019. SageMath Help, <http://www.sagemath.org/>.
- Schaub, H., 2008. Rate-based ship-mounted crane payload pendulation control system. *Control Eng. Pract.* 16, 132–145.
- Sun, Y., Qiang, H., Xu, J., Dong, D., 2017. The non-linear dynamics and anti-sway tracking control for offshore container crane on a mobile harbor. *J. Mar. Sci. Technol.* 25, 656–665.
- Szczotka, M., 2010. Active heave compensation in offshore equipment with a neural network based control system. *Meas. Autom. Monit.* [in Polish] 56 (6), 593–596.
- Tomczyk, J., 2009. Review of Automation Cranes Methods, Vol. 4(6). Industrial Transport and Construction Machinery HMR-TRANS Ltd. [in Polish], pp. 22–30.
- Tong, M., Wang, Y., Qiu, H., 2013. Research on dynamic heave compensation on large floating crane in deep sea. In: Fifth Conference on Measuring Technology and Mechatronics Automation. pp. 898–901.
- Witz, J., 1995. Parametric excitation of crane loads in moderate sea states. *Ocean Eng.* 22(3), 411–420.



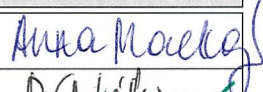

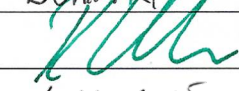
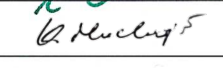
Warszawa, March 6, 2023

## AUTHORSHIP STATEMENT

As the authors of scientific article: Chiliński Bogumił, Mackojć Anna, Zalewski Robert, *Proposal of the 3-DOF model as an approach to modelling offshore lifting dynamics*, Ocean Engineering, 2020, vol. 203, pp.107235. DOI:10.1016/j.oceaneng.2020.107235 published in 2020,

we state

the participation and contribution to development and presentation of the work in the form of a scientific publication is as follows:

Name and surname, academic degree	Participation in work	Signature
Anna Mackojć, MSc.	50%	
Bogumił Chiliński, PhD.	35%	
Robert Zalewski, Prof. PhD. DSc.	10%	
Krzysztof Mackojć, MSc.	5%	

Warszawa, March 6, 2023

mgr inż. Anna Mackojć  
Politechnika Warszawska  
Wydział Samochodów i Maszyn Roboczych  
Instytut Podstaw Budowy Maszyn  
ul. Narbutta 84  
02-524 Warszawa

## AUTHORSHIP STATEMENT

I declare that in the work "Chiliński Bogumił, Mackojć Anna, Zalewski Robert, Mackojć Krzysztof, *Proposal of the 3-DOF model as an approach to modelling offshore lifting dynamics*, Ocean Engineering, 2020, vol. 203, pp.107235. DOI:10.1016/j.oceaneng.2020.107235" my participation in the article development consisted in developing the idea of the research, carrying out a comprehensive literature review, theoretical analysis of the presented problem, determining the analytical model and its numerical solution, developing research methodology, designing numerical simulation scenarios, preparing the analysed case studies, performing simulations, preparing the software tool, model validation, analysing and interpreting the results, formulating conclusions, writing (original draft), reviewing, editing and formatting the article text, preparing the final version before and after the review and the final editorial form of the article.

  
Signature

Warszawa, March 6, 2023

dr inż. Bogumił Chiliński  
Politechnika Warszawska  
Wydział Samochodów i Maszyn Roboczych  
Instytut Podstaw Budowy Maszyn  
ul. Narbutta 84  
02-524 Warszawa

## AUTHORSHIP STATEMENT

I declare that in the work "Chiliński Bogumił, Mackojć Anna, Zalewski Robert, Mackojć Krzysztof, *Proposal of the 3-DOF model as an approach to modelling offshore lifting dynamics*, Ocean Engineering, 2020, vol. 203, pp.107235. DOI:10.1016/j.oceaneng.2020.107235" my participation in the article development consisted in consultations of the scope and content, methodology verification and approval of the proposed approach to the problem being solved, participation in simulation research, interpretation of research results, preparing the software tool, participation in corrections in accordance with the reviewers' guidelines, writing (original draft), supervision.

  
Signature

Warszawa, March 07, 2023

prof. dr hab. inż. Robert Zalewski  
Politechnika Warszawska  
Wydział Samochodów i Maszyn Roboczych  
Instytut Podstaw Budowy Maszyn  
ul. Narbutta 84  
02-524 Warszawa

## **AUTHORSHIP STATEMENT**

I declare that in the work "Chiliński Bogumił, Mackojć Anna, Zalewski Robert, Mackojć Krzysztof, Proposal of the 3-DOF model as an approach to modelling offshore lifting dynamics, Ocean Engineering, 2020, vol. 203, pp.107235. DOI:10.1016/j.oceaneng.2020.107235" my participation in the article development was limited to a supervision of the conducted works, substantive verification of the article content, methodological verification of the correctness of the approach to the problem being solved.



Signature



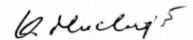
Warszawa, March 6, 2023

mgr inż. Krzysztof Mackojć  
Fathom Group Ltd.  
18 North Silver Street  
Aberdeen, AB10 1JU, Scotland  
United Kingdom of Great Britain and Northern Ireland

## **AUTHORSHIP STATEMENT**

I declare that in the work "Chiliński Bogumił, Mackojć Anna, Zalewski Robert, Mackojć Krzysztof, Proposal of the 3-DOF model as an approach to modelling offshore lifting dynamics, Ocean Engineering, 2020, vol. 203, pp.107235. DOI:10.1016/j.oceaneng.2020.107235" my participation in the article development was consisted in providing commercial software for dynamic analysis of offshore marine systems based on which verification of correctness of the model results was done. I conducted numerical model validation, assessment of usability of the model in the context of applicability for engineering purposes and reviewing process.

Signature



# Preliminary modelling methodology of a coupled payload-vessel system for offshore lifts of light and heavyweight objects

Anna MACKOJC<sup>✉\*</sup> and Bogumil CHILINSKI<sup>✉</sup>

Institute of Machine Design Fundamentals, Warsaw University of Technology, Poland

**Abstract.** This paper presents the concept of the modelling methodology of a payload-vessel system allowing for a comprehensive investigation of mutual interactions of the system dynamics for lifting in the air. The proposed model consists of six degrees of freedom (6-DoF) vessel and three degrees of freedom (3-DoF) lifting model that can replace the industrial practice based on a simplified approach adopted for light lifts. Utilising the response amplitude operators (RAOs) processing methodology provides the ability to incorporate the excitation functions at the vessel crane tip as a kinematic and analyse a wide spectrum of lifted object weights on a basis of regular wave excitation. The analytical model is presented in detail and its solution in a form of numerical simulation results are provided and discussed within the article. The proposed model exposes the disadvantages of the models encountered in engineering practice and literature and proposes a novel approach enabling efficient studies addressing a lack of access to reliable modelling tools in terms of coupled models for offshore lifting operations planning.

**Key words:** offshore lifting modelling; coupled payload-vessel model; payload pendulation.

## 1. INTRODUCTION

One of the challenges encountered during offshore operations is naturally a necessity of dealing with the surrounding environment. When considering operations of lifting in the air whilst at sea, the biggest accompanying factor to withstand is a sea state that when being unfavourable might considerably reduce the operating window or increase the risk. In order to assist the industry, several operational practices have been developed but there is still limited access to a proper, simple, dynamic modelling tool coupling the dynamics of both the lifted object and vessel. This raises a need for appropriate understanding of the mutual relationship between the behaviour of the payload and that of the vessel. That would allow the proposal of an effective methodology and lead to a reliable tool that might increase the operational efficiency and safety in terms of dynamic behaviour analysis and operation design and planning.

When discussing any lifting operation undertaken offshore, a distinction between two phases can be made. These include particularly handling the payload in the air and lowering it in water. Many publications addressing the problem of offshore lifting operations can be found, however, in the vast majority they address numerical analyses of heavy lifts concerning coupled models with a particular focus on the lowering process only. This leaves a scientific and industrial gap to consider an equally important part of an offshore lift operation – lifting in the air. This is the phase that carries the greatest risk of resonance vibrations occurrence, and thus the uncontrolled motion of large

amplitudes. Moreover, due to a wide range of weights of structures installed, it is essential to study the mutual dynamics between the lifted weight and the lifting vessel and determine the limit of the applicability of simplified models, which are widely proposed within the literature. The importance of setting such a limit is shown in the article [1], where the authors describe the methodology based on a specific case study of an installation of an offshore wind turbine monopile installation. This methodology, however, is not universal as it focuses on a very specific operation. The importance and complexity of offshore operations safety issue are also shown in [2], where the authors discuss and seek a method of control algorithm for a ship dynamic positioning with a neural network in order to reduce dependency on the determination of ship hydrodynamic coefficients.

The study [3] presents a numerical model of the coupled system of a monopile for an offshore wind turbine and a vessel. Numerical simulations are provided paying attention only to the lowering phase of the lifting operation. A similar focus might be found in [4] where the authors address the numerical analysis of the installation of a tripod foundation using a heavy lift vessel. In [5] and [6], the authors studied the dynamic behaviour of an offshore crane cable and its unstable states referred to as a parametric resonance vibration. The analysis was conducted for long cables only, used in subsea lowering operations. In the article [7], the authors present a dynamic model of a floating crane vessel with a hanging load. The model is defined as a linearized coupled double pendulum problem, as the pendulation of the suspended mass was limited by the assumption of small displacements. A similar simplification is presented in [8], where the authors propose a method for double pendulum cranes for minimisation of energy consumption when fulfilling the transportation tasks. Other simple models might

\*e-mail: [anna.mackojc@pw.edu.pl](mailto:anna.mackojc@pw.edu.pl)

Manuscript submitted 2021-04-07, revised 2021-06-24, initially accepted for publication 2021-08-19, published in February 2022.

be found in [9–11], where the lifting model is presented as a single pendulum, where excitation is incorporated as an angular roll, ignoring the heave and the potential influence of the vessel. This methodology eliminates the ability to capture the parametric resonance. In [12], the authors look for approximate analytical solutions for a model of the parametric pendulum. The system was modelled as a mathematical pendulum being excited by means of vertical harmonic force. The approximated solutions were found for oscillations and rotations of the pendulum. Although the model is not discussed in the context of the lifted payload specifically, the presented model is still a better representation as it does not neglect an importance of the vertical excitation. The authors of [13] investigate the dynamics of a parametrically induced spherical pendulum. They consider a moving support analysing the pendulum dynamics based on governing equations derived from the system energy formulation. The presented single degree of freedom model is analysed in the Cartesian coordinates, which may not be intuitive for interpretation purposes of a pendulum motion.

A little bit more complicated model is proposed in [14]. The authors model and study the dynamics of dual cranes carrying a distributed-mass beam and propose the control algorithm by predicting and incorporating the natural frequency of the system. On the other hand, one might encounter an overly complex model proposals, where the study is based on a single, particular case preventing a reliable assessment of the whole phenomena. Such models can be found in [15] and [16]. The authors of [15] propose a pendulation control by an enormous number of lifting wires and hence multiple cranes or complex machinery involved.

The article [17] describes a rapid development in the field of offshore renewable energy, particularly in the wind farms sector, where newly built turbines are to be installed mainly on the Baltic Sea area. That requires a huge effort to be put into the installation process of every single structure. This is related to the effective planning of maritime operations by a development of dynamic models allowing the simulation of behaviour and mutual relation of payload-vessel systems at sea during the installation. Moreover, as there are records reporting heavy lift operations focusing only on a lowering phase, where the payload pendulation is naturally suppressed by the water, the authors decided to propose a modelling methodology of a coupled payload-vessel system allowing for a reliable assessment of the lifted objects-vessel dynamic behaviour when handling in the air. The proposed model enables analyses in a whole spectrum of lifted objects whether these are light or heavyweights.

## 2. OBJECTIVES AND OVERVIEW

Lifting operations are a relevant part of many offshore activities. In order to complete operations successfully, the operators have to manage environmental phenomena sometimes leading to significant limitations. Critical cases occur in the lifting zone, where the payload-cable system behaves like a pendulum with a moving pivot point. This might cause the payload to be loaded by external forces, which lead to resonance phenomena. Depending on the type of vibrations, angular vibrations of

the payload due to parametric or forced resonance may be observed. These hazardous phenomena raise the necessity for the creation of simple and accessible tools allowing for their prediction.

The dynamics of heavy payloads cannot be considered independently to the vessel movement. DNV (DET NORSKE VERITAS) codes present a simplified approach for light lifts regime, where the mass of the payload is no greater than 2% of the floating unit displacement. For light lifts the crane boom can be treated as a stiff structure, hence the motion of the crane tip can be determined directly from the wave-induced rigid body motion of the vessel. The wave-induced translational motions (surge, sway and heave) of the crane tip are given from the vessel RAOs (response amplitude operators) for six degrees of freedom motion usually defined for the centre of gravity for the vessel [18–21]. The aim of this study is to propose a coupled model, which is sensitive to changes of the system parameters and allows for a comprehensive investigation of the system dynamics during the lifting in the air phase.

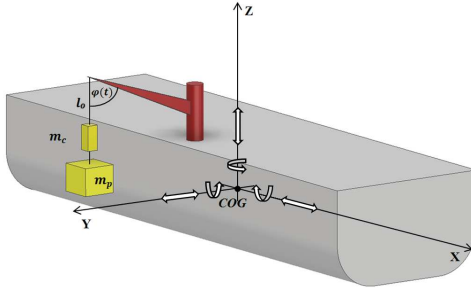
The study concerns 6 degrees of freedom related of the vessel, providing the linear and angular motions directly coupling the two considered systems. Floating units might be considered as continuous systems that when operating, are subjected to complex motions, which might be decomposed into a rigid body motion and its vibrations. In practice, the vessel elastic properties are omitted as the naval designs are stiff enough, which allows the adoption of a simple model of a rigid body in analytical considerations. Hence the hydrodynamic forces might be represented as hydrodynamic added mass, fluid damping and restoring forces. The vessel excitation is modelled as one-directional forward propagating waves. The lifting system is composed of a crane tip equipped with a lifting cable with length-dependent stiffness. The 3 degrees of freedom are related to the payload and compensator masses and also their pendulation as referred in [22]. The research outlines a novel approach produced in cooperation between the authors and Fathom Group Ltd.

The usefulness and further application of the proposed model shall be validated. The authors stated that ensuring convergence with the 3-DoF model for light lifts will be crucial from the point of view of the proposed model verification. For this purpose, a comparative analysis was initially proposed of the payload and vessel response for a number of different payload masses. According to the authors, this enables verification of the advantages of the coupled model that might be utilised in both, light and heavyweight objects regimes. Moreover, the proposed approach allows the user to analyse the impact of the vessel and payload properties on the system dynamics.

## 3. PROPOSED COUPLED MODEL FOR OFFSHORE LIFTS

The behaviour of 9-DoF model being composed of 6-DoF vessel and 3-DoF lifting system model must be considered. The vessel, as mentioned in Section 2, is modelled as a rigid body excited by forces caused by a hydrodynamic interaction with the hull. For the 3-DoF model, the description is similar to the modelling process of an elastic pendulum.

The following equations represent the total energy of the system under consideration presented in Fig. 1. It was possible to determine kinetic and potential energies of the subsystems in the analytical manner based on [22].



**Fig. 1.** A 6-DOF vessel with the 3-DOF lifting system and its parameters

The kinetic energy (1) was determined as a sum of the energy of all the system masses (payload and compensator). The  $T_p$  formula has the following representation:

$$T_p = \frac{m_c (\dot{y}_c^2 + \dot{z}_c^2)}{2} + \frac{m_p (\dot{y}_p^2 + \dot{z}_p^2)}{2}. \quad (1)$$

The potential energy of the system discussed results from the presence of a homogeneous gravitational field and the two springs representing respectively the cable stiffness  $k_w$  and the stiffness of the compensator  $k_c$ . The equation describing  $V_p$  is given in (2):

$$V_p = -gm_c z_c - gm_p z_p + \frac{k_c (-h_{ceq} + h_{eq} + h - h_c)^2}{2} + \frac{k_w (h_{ceq} + h_c)^2}{2}. \quad (2)$$

The kinetic energy  $T_v$  related to the vessel structure motion resulting from the wave excitation is provided by the relation presented in (3):

$$T_v = \frac{I_5 \left( -\frac{A_h \omega \sin(\phi_w) \ddot{\phi}_w}{g} - \frac{A_h \omega \cos(\phi_w) \dot{\phi}_w^2}{g} + \dot{\Phi} \right)^2}{2} + \frac{M_{vessel} (-A_h \sin(\phi_w) \dot{\phi}_w + \ddot{H})^2}{2}. \quad (3)$$

The potential energy of the vessel is expressed based on a hydrostatic stability of the structure and is given as presented in eqrefeq:Vvessel:

$$V_v = \frac{(-A_{wl} g \rho (-CoB + CoF) H + GM_L V g \rho \Phi) \Phi}{2} + \frac{(-A_{wl} g \rho (-CoB + CoF) \Phi + A_{wl} g \rho H) H}{2}, \quad (4)$$

where:

$(\phi, h, h_c)$  – payload generalized coordinates,  
 $t$  – independent variable (time),  
 $m_p$  – mass of payload,  
 $k_w$  – wire stiffness,  
 $l_0$  – length of the lifting cable,  
 $l_w$  – length of the lifting cable-payload system,  
 $R \sin \left( -\frac{A_h \omega \sin(\phi_w) \dot{\phi}_w}{g} + \alpha + \Phi \right)$  – lateral displacement at crane tip obtained from RAOs (a regular wave excitation),  
 $A_h \cos(\phi_w) + R \cos \left( -\frac{A_h \omega \sin(\phi_w) \dot{\phi}_w}{g} + \alpha + \Phi \right) + H$  – vertical displacement at crane tip obtained from RAOs (a regular wave excitation),  
 $m_c$  – mass of compensator,  
 $k_c$  – stiffness of heave compensator,  
 $l_c$  – length of the attached compensating element,  
 $g$  – acceleration of gravity,  
 $h_{eq}$  – equilibrium point of payload,  
 $h_{ceq}$  – equilibrium point of compensator,  
 $M_{vessel}$  – mass of vessel,  
 $I_5$  – moment of inertia of 5-th degree (with respect to y axis, determined by the radius of gyration),  
 $(H, \Phi)$  – vessel generalized coordinates,  
 $A_h \cos(\phi_w)$  – wave level,  
 $-\frac{A_h \omega \sin(\phi_w) \dot{\phi}_w}{g}$  – wave slope,  
 $\rho$  – fluid density,  
 $g$  – acceleration of gravity,  
 $A_{wl}$  – wetted area,  
 $V$  – submerged volume of the vessel,  
 $GM_L$  – longitudinal metacentric height,  
 $CoB$  – centre of buoyancy,  
 $CoF$  – centre of floatation.

In order to obtain governing equations, the methods of Lagrangian mechanics were adopted. Based on the obtained Lagrangian of the entire system, governing equations were found. Hence, the considered payload-vessel system might be modelled by the following matrix equations (5), (6):

$$(M_V + A) \cdot \ddot{X}(\omega, \text{dir}) + C_V \cdot \dot{X}(\omega, \text{dir}) + K_V \cdot X(\omega, \text{dir}) = F(\omega, \text{dir}), \quad (5)$$

$$M_P(t) \cdot \ddot{X} + G_P(t, \dot{X}) \cdot \dot{X} + C_P(t) \cdot \dot{X} + K_P(t) \cdot X = F(\dot{X}, X, t), \quad (6)$$

where:

$M_V$  – mass matrix of the vessel,  
 $A$  – hydrodynamic added mass matrix,  
 $C_V$  – hydrodynamic damping matrix,  
 $K_V$  – vessel stiffness matrix,  
 $F(\omega, \text{dir})$  – hydrodynamic force vector,  
 $\omega$  – natural frequency,  
 $\text{dir}$  – wave direction,  
 $M_P$  – inertia matrix of payload,  
 $G_P$  – payload gyroscopic matrix,  
 $C_P$  – damping matrix of payload,  
 $K_P$  – payload stiffness matrix.



The fundamental matrix obtained from the system of governing equations might be represented by relations of the system parameters. Their mutual relations and assumptions allowed to introduce some simplifications to the system Lagrangian. The dependencies used are as follows:

$$h_{eq} = l_0 v, \quad (7)$$

$$h_{ceq} = l_0 v, \quad (8)$$

$$k_c = \frac{m_p}{10}, \quad (9)$$

$$R = l_0, \quad (10)$$

$$l_c = \frac{l_0}{10}, \quad (11)$$

$$A_h = \gamma l_0, \quad (12)$$

$$\omega = \frac{\sqrt{g}\mu}{\sqrt{l_0}}. \quad (13)$$

$$\phi_w = \Phi_h + \omega t, \quad (14)$$

where:  $v, \mu, \gamma$  – simplifying proportionality factors.

A general form of the system fundamental matrix and its particular elements are given as:

$$A = \begin{bmatrix} A_{11} & A_{12} & A_{13} & 0 & A_{15} \\ A_{21} & A_{22} & A_{23} & A_{24} & A_{25} \\ A_{31} & A_{32} & A_{33} & A_{34} & A_{35} \\ 0 & A_{42} & A_{43} & A_{44} & A_{45} \\ A_{51} & A_{52} & A_{53} & A_{54} & A_{55} \end{bmatrix}. \quad (15)$$

Each of the elements of matrix  $A$  is presented in details as an individual equation:

$$\begin{aligned} A_{11} = & -\frac{11\Omega^2 l_0^2 m_p v^2}{10} - \frac{12\Omega^2 l_0^2 m_p v}{5} - \frac{131\Omega^2 l_0^2 m_p}{100} \\ & + \frac{11g\gamma^2 l_0 m_p \mu^6 v \cos(\gamma\mu^2 \sin(\phi_w)) \cos^2(\phi_w)}{10} \\ & + \frac{6g\gamma^2 l_0 m_p \mu^6 \cos(\gamma\mu^2 \sin(\phi_w)) \cos^2(\phi_w)}{5} \\ & - \frac{11g\gamma l_0 m_p \mu^4 v \sin(\gamma\mu^2 \sin(\phi_w)) \sin(\phi_w)}{10} \\ & - \frac{6g\gamma l_0 m_p \mu^4 \sin(\gamma\mu^2 \sin(\phi_w)) \sin(\phi_w)}{5} \\ & + \frac{11g\gamma l_0 m_p \mu^2 v \cos(\phi_w)}{10} + \frac{6g\gamma l_0 m_p \mu^2 \cos(\phi_w)}{5} \\ & + \frac{11gl_0 m_p v}{10} + \frac{6gl_0 m_p}{5}, \end{aligned} \quad (16)$$

$$\begin{aligned} A_{12} = & g\gamma^2 m_p \mu^6 \sin(\gamma\mu^2 \sin(\phi_w)) \cos^2(\phi_w) \\ & + g\gamma m_p \mu^4 \sin(\phi_w) \cos(\gamma\mu^2 \sin(\phi_w)), \end{aligned} \quad (17)$$

$$\begin{aligned} A_{13} = & \frac{g\gamma^2 m_p \mu^6 \sin(\gamma\mu^2 \sin(\phi_w)) \cos^2(\phi_w)}{10} \\ & + \frac{g\gamma m_p \mu^4 \sin(\phi_w) \cos(\gamma\mu^2 \sin(\phi_w))}{10}, \end{aligned} \quad (18)$$

$$\begin{aligned} A_{15} = & -\frac{11\Omega^2 l_0^2 m_p v \cos(\gamma\mu^2 \sin(\phi_w))}{10} \\ & - \frac{6\Omega^2 l_0^2 m_p \cos(\gamma\mu^2 \sin(\phi_w))}{5} \\ & - \frac{11g\gamma^2 l_0 m_p \mu^6 v \cos(\gamma\mu^2 \sin(\phi_w)) \cos^2(\phi_w)}{10} \\ & - \frac{6g\gamma^2 l_0 m_p \mu^6 \cos(\gamma\mu^2 \sin(\phi_w)) \cos^2(\phi_w)}{5} \\ & + \frac{11g\gamma l_0 m_p \mu^4 v \sin(\gamma\mu^2 \sin(\phi_w)) \sin(\phi_w)}{10} \\ & + \frac{6g\gamma l_0 m_p \mu^4 \sin(\gamma\mu^2 \sin(\phi_w)) \sin(\phi_w)}{5}, \end{aligned} \quad (19)$$

$$\begin{aligned} A_{21} = & g\gamma^2 m_p \mu^6 \sin(\gamma\mu^2 \sin(\phi_w)) \cos^2(\phi_w) \\ & + g\gamma m_p \mu^4 \sin(\phi_w) \cos(\gamma\mu^2 \sin(\phi_w)), \end{aligned} \quad (20)$$

$$A_{22} = -\Omega^2 m_p + k_c, \quad (21)$$

$$A_{23} = -k_c, \quad (22)$$

$$A_{24} = -\Omega^2 m_p, \quad (23)$$

$$\begin{aligned} A_{25} = & -\Omega^2 l_0 m_p \sin(\gamma\mu^2 \sin(\phi_w)) \\ & - g\gamma^2 m_p \mu^6 \sin(\gamma\mu^2 \sin(\phi_w)) \cos^2(\phi_w) \\ & - g\gamma m_p \mu^4 \sin(\phi_w) \cos(\gamma\mu^2 \sin(\phi_w)), \end{aligned} \quad (24)$$

$$\begin{aligned} A_{31} = & \frac{g\gamma^2 m_p \mu^6 \sin(\gamma\mu^2 \sin(\phi_w)) \cos^2(\phi_w)}{10} \\ & + \frac{g\gamma m_p \mu^4 \sin(\phi_w) \cos(\gamma\mu^2 \sin(\phi_w))}{10}, \end{aligned} \quad (25)$$

$$A_{32} = -k_c, \quad (26)$$

$$A_{33} = -\frac{\Omega^2 m_p}{10} + k_c + k_w, \quad (27)$$

$$A_{34} = -\frac{\Omega^2 m_p}{10}, \quad (28)$$

$$\begin{aligned} A_{35} = & -\frac{\Omega^2 l_0 m_p \sin(\gamma\mu^2 \sin(\phi_w))}{10} \\ & - \frac{g\gamma^2 m_p \mu^6 \sin(\gamma\mu^2 \sin(\phi_w)) \cos^2(\phi_w)}{10} \\ & - \frac{g\gamma m_p \mu^4 \sin(\phi_w) \cos(\gamma\mu^2 \sin(\phi_w))}{10}, \end{aligned} \quad (29)$$

$$A_{42} = -\Omega^2 m_p, \quad (30)$$

$$A_{43} = -\frac{\Omega^2 m_p}{10}, \quad (31)$$

$$A_{44} = A_{wl} g \rho - M_{vessel} \Omega^2 - \frac{11\Omega^2 m_p}{10}, \quad (32)$$

## Preliminary modelling methodology of a coupled system for offshore lifts

$$A_{45} = A_{wl}CoBg\rho - A_{wl}CoFg\rho - \frac{11\Omega^2 l_0 m_p \sin(\gamma\mu^2 \sin(\phi_w))}{10} - \frac{11g\gamma^2 m_p \mu^6 \sin(\gamma\mu^2 \sin(\phi_w)) \cos^2(\phi_w)}{10} - \frac{11g\gamma m_p \mu^4 \sin(\phi_w) \cos(\gamma\mu^2 \sin(\phi_w))}{10}, \quad (33)$$

$$A_{51} = -\frac{11\Omega^2 l_0^2 m_p v \cos(\gamma\mu^2 \sin(\phi_w))}{10} - \frac{6\Omega^2 l_0^2 m_p \cos(\gamma\mu^2 \sin(\phi_w))}{5}, \quad (34)$$

$$A_{52} = -\Omega^2 l_0 m_p \sin(\gamma\mu^2 \sin(\phi_w)), \quad (35)$$

$$A_{53} = -\frac{\Omega^2 l_0 m_p \sin(\gamma\mu^2 \sin(\phi_w))}{10}, \quad (36)$$

$$A_{54} = A_{wl}CoBg\rho - A_{wl}CoFg\rho - \frac{11\Omega^2 l_0 m_p \sin(\gamma\mu^2 \sin(\phi_w))}{10}, \quad (37)$$

$$A_{55} = GM_L V g\rho - I_5 \Omega^2 - \frac{11\Omega^2 l_0^2 m_p \sin^2(\gamma\mu^2 \sin(\phi_w))}{10} - \frac{11\Omega^2 l_0^2 m_p \cos^2(\gamma\mu^2 \sin(\phi_w))}{10} + \frac{11g\gamma l_0 m_p \mu^2 \cos(\gamma\mu^2 \sin(\phi_w)) \cos(\phi_w)}{10} + \frac{11gl_0 m_p \cos(\gamma\mu^2 \sin(\phi_w))}{10}. \quad (38)$$

Calculated formulas (5) and (6) (reduced to the first order) enable a series of numerical simulations of the payload-vessel system to be performed.

#### 4. NUMERICAL SIMULATIONS – COMPARATIVE ANALYSIS

As discussed, the authors conducted numerical analysis in order to give a satisfactory confirmation of the proposed methodology. The considerations concern one-dimensional forward propagating waves as vessel excitation. The following simulations depict a comparative analysis of the payload response results for a number of different payload masses.

The results of simulations for a payload pendulation and vessel heave motion for the subsequent masses up to 10% of a total ship displacement considered in the study are depicted in Figs. 2 and 3 in a form of time domain analysis (payload response) and frequency spectra (vessel heave) for convenience.

The masses examined in the regime of light lifts reveal similar behaviour (Fig. 2) – the higher the subsequent mass, the lower the amplitude of oscillations. The nature of the waveforms remained unchanged and only slight quantitative changes can be observed. This leads to the conclusion of uncoupled analysis for the referenced payload-vessel mass relation. The numerical simulations for the relation above the threshold value 2%, depict a qualitative change clearly observable in the

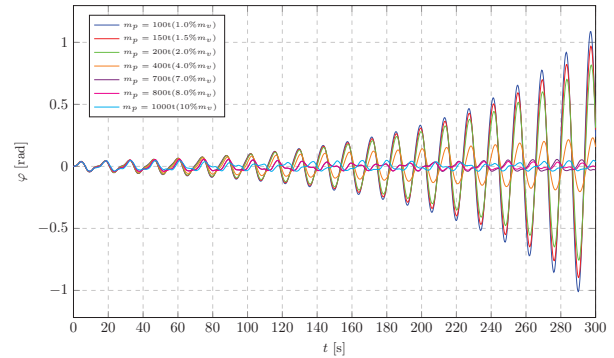


Fig. 2. Payload pendulation – comparative results for different payload weights ( $T = 7$  s,  $l_0 = 48.7$  m)

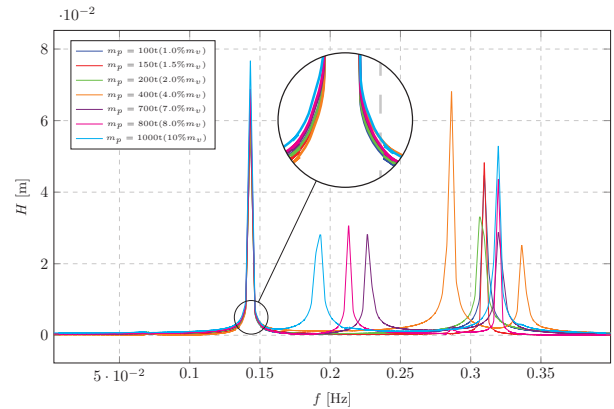


Fig. 3. Vessel heave spectra – comparative results for different payload weights ( $T = 7$  s,  $l_0 = 48.7$  m)

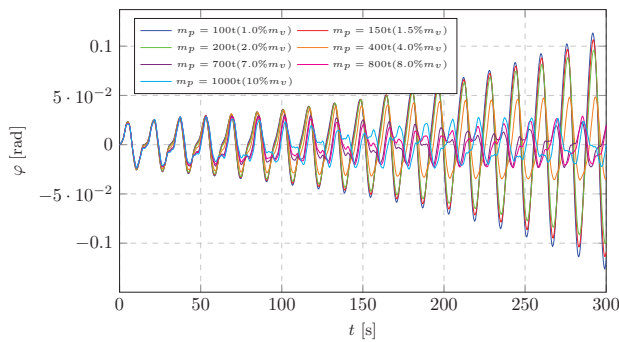
character of waveforms. The expected divergence in not only quantitative measures is captured immediately past the threshold value while qualitative discrepancy started to appear at around 3–4% of the vessel displacement. The results obtained from the proposed model are consistent with the results of the 3-DoF model proposed in [22] in light lifts regime.

Results for vessel heave (Fig. 3) reveal no significant influence of payload weight on the system frequency structure for the referenced light lifts. Critical harmonic components do not change their position even for the limit value of lifted object mass. The amplitude of dynamic response is marginally lower for the heavier objects (considered still in the light lifts regime) but it does not have a meaningful invalidating impact on the proposed methodology. The authors concept can be useful for resonance recognition in light lifts, even given marginally under-valued amplitudes. However, when considering harmonic components of heavy object lifts, one can notice a clear dependency of the components moving towards lower frequencies and an increase in the value of their amplitudes. This strongly indicates the necessity to analyse coupled systems within heavy lifts regime.

The assumed frequency of the excitation was set equal to  $\omega \approx 0.897 \text{ rad s}^{-1}$  ( $T = 7$  s), which is for medium-slow waves.

The presented simulation results depict the payload pendulation for the consecutive masses for some specific length of cable ( $l_0 \approx 48$  m), causing a parametric resonance to occur in the system. The resonating length is specified based on the excitation frequency. Naturally, the observable parametric resonance will be raised for different cable lengths. However, the examined phenomena and the qualitative results will remain valid. The authors found it valuable to present some additional simulation results prepared for different sets of the system parameters in terms of understanding the proposed methodology.

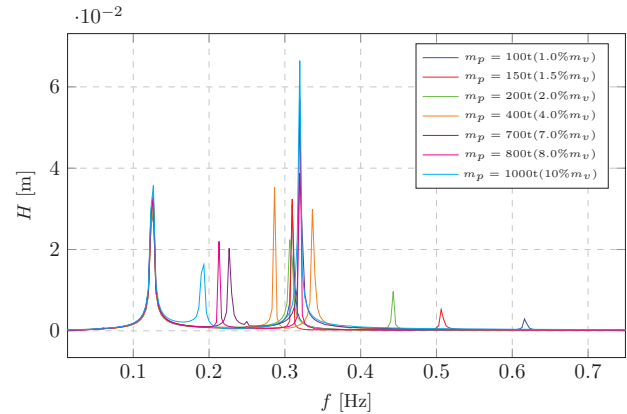
In order to support the encountered coupling limit between the systems, the authors performed numerical simulations providing a further confirmation for the claimed thesis. The presented results were prepared for a set of different parameters. The frequency of the vessel excitation was set equal to  $T = 8$  s and the length of cable was changed to  $l_0 \approx 64$  m. Depicted waveforms (Fig. 4) show the same system properties as the results presented in Fig. 2. It can be clearly observed that for the first three consecutive masses (light lift regime), the payload response remains unchanged in terms of quality of the phenomenon while after passing the threshold values, the waveforms expose a visibly different character and amplitude value of payload dynamics.



**Fig. 4.** Payload pendulation – comparative results for different payload weights ( $T = 8$  s,  $l_0 = 63.6$  m)

A similar trend of the vessel shifting frequencies when lifting heavy objects observed previously in Fig. 3, might also be captured in the spectral analysis of a vessel heave motion presented in Fig. 5. The spectral analysis for the rolling vessel motion reveals the same tendency, however, the level of the amplitudes is of a negligible magnitude and hence it was decided not to be included in the presented results.

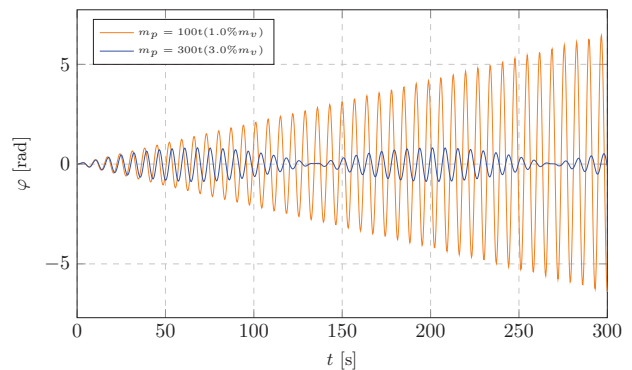
The next set of parameters used for the evaluation was prepared and presented for another interesting phenomenon appearing in the system dynamics, being payload oscillation near main resonant vibrations. As can be noticed, regardless of the type of occurring phenomenon, the excitation frequency or the cable length, the established threshold value determining the limit of coupled dynamics considerations, remains unchanged. The simulation results for the excitation period equals  $T = 7$  s and length of cable set to  $l_0 \approx 12$  m are depicted in Fig. 6. The main resonance vibrations are reached for the payload mass of  $m_p = 1\% m_v$ , which is to be considered as a lightweight object.



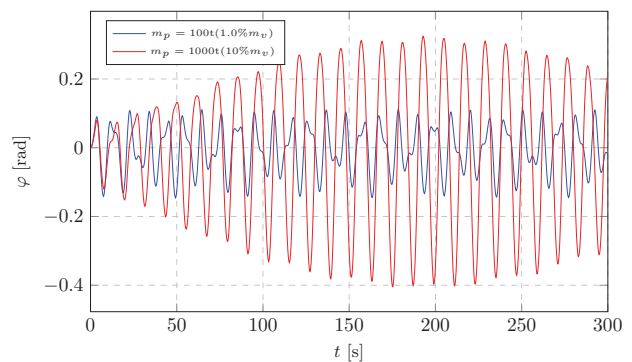
**Fig. 5.** Vessel heave spectrum – comparative results for different payload weights ( $T = 8$  s,  $l_0 = 63.6$  m)

The results obtained after passing the threshold value, for the payload mass of  $m_p = 3\% m_v$  expose a totally different nature of the payload response reflected in quality and quantity of the pendulation.

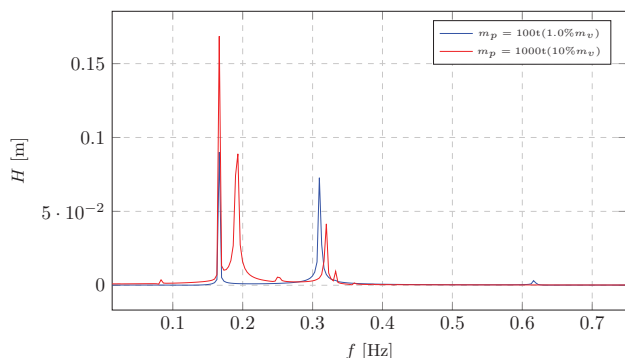
A direct comparative analysis presented in Figs. 7 and 9, where the payload responses were compared in pairs of light and heavyweight lifted objects. Figure 7, depicts a comparison



**Fig. 6.** Payload pendulation – comparative results for different payload weights ( $T = 7$  s,  $l_0 = 11.7$  m)

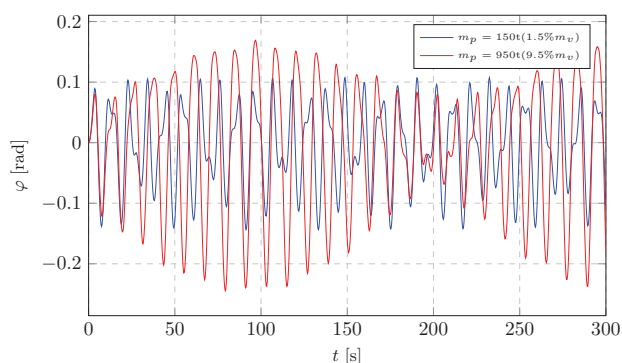


**Fig. 7.** Payload pendulation – direct comparative results for light and heavy payload weights ( $T = 6$  s,  $l_0 = 25.9$  m)



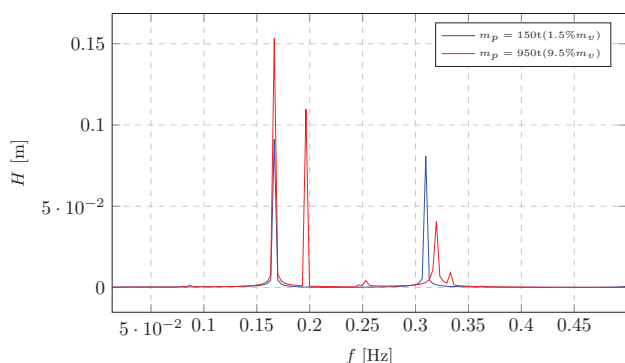
**Fig. 8.** Vessel heave spectrum – comparative results for different payload weights ( $T = 6$  s,  $l_0 = 25.9$  m)

between 1% and 10% of the payload mass to vessel displacement ratio. It can be observed that the oscillations differ for each of the mass considered in terms of quality and quantity of the results. The same properties might be seen in Fig. 9, where the floating unit displacement was examined for 1.5% and 9.5%.



**Fig. 9.** Payload pendulation – direct comparative results for light and heavy payload weights ( $T = 6$  s,  $l_0 = 25.9$  m)

Figures 8 and 10 expose the changes that occur for ship dynamics depending on the considered lifting regime. The spectra show the same nature of frequencies shift for heavy lifts to-



**Fig. 10.** Vessel heave spectrum – comparative results for different payload weights ( $T = 6$  s,  $l_0 = 25.9$  m)

wards lower values and their increase in terms of the main component amplitude level as mentioned and observed in Figs. 3, 5, 8 or 10.

## 5. CONCLUSIONS

Payload mass to ship displacement ratios have been investigated for light and heavyweight lifted objects. The expected discrepancy in quantitative results was observed immediately past the threshold value, while qualitative divergence started to appear at around 3–4%, which confirms the presented model gives satisfactory confirmation of the referenced assumption. The research carried out for similar problems highlights the lack of availability of analytical tools for reliable payload response analysis. One might find sophisticated and complex numerical environments or overly simple dynamic models which are not able to represent the comprehensive payload dynamics beyond the application of the light lifts assumption. The proposed model was used to achieve the best possible efficiency for the problems within light and heavy lifts in the air.

It can be concluded that the demonstrated approach is more widely applicable than analysis of the payload dynamics independently of a vessel. The proposed concept eliminates RAOs as a method of vessel movement representation, as this methodology is only justifiable if the light lifts assumption is fulfilled. For heavy lifts, uncoupled models cannot be utilised as high discrepancies are observed between the presented methodology and models neglecting coupling. Based on the analysis carried out, it can be stated that the model proposed by the authors is more universal and comprehensive, and this is what constitutes its main advantage.

## REFERENCES

- [1] W.G. Acero, L. Li, Z. Gao, and T. Moan, "Methodology for assessment of the operational limits and operability of marine operations," *Ocean Eng.*, vol. 125, pp. 308–327, 2016, doi: [10.1016/j.oceaneng.2016.08.015](https://doi.org/10.1016/j.oceaneng.2016.08.015).
- [2] W. Meng, L.H. Sheng, M. Qing, and B.G. Rong, "Intelligent control algorithm for ship dynamic positioning," *Arch. Control Sci.*, vol. 24, 2014, doi: [10.2478/acsc-2014-0026](https://doi.org/10.2478/acsc-2014-0026).
- [3] L. Li, Z. Gao, T. Moan, and H. Ormberg, "Analysis of lifting operation of a monopile for an offshore wind turbine considering vessel shielding effects," *Marine Struct.*, vol. 39, pp. 287–314, 2014, doi: [10.1016/j.marstruc.2014.07.009](https://doi.org/10.1016/j.marstruc.2014.07.009).
- [4] H. Zhu, L. Li, and M. Ong, "Study of lifting operation of a tripod foundation for offshore wind turbine," in *IOP Conf. Ser.: Mater. Sci. Eng.*, vol. 276, no. 1, 2017, doi: [10.1088/1757-899X/276/1/012012](https://doi.org/10.1088/1757-899X/276/1/012012).
- [5] H.-S. Kang, C.H.-H. Tang, L.K. Quen, A. Steven, and X. Yu, "Prediction on parametric resonance of offshore crane cable for lowering subsea structures," in *2016 IEEE International Conference on Underwater System Technology: Theory and Applications (USYS)*. IEEE, 2016, pp. 165–170, doi: [10.1109/USYS.2016.7893905](https://doi.org/10.1109/USYS.2016.7893905).
- [6] H.-S. Kang, C.H.-H. Tang, L.K. Quen, A. Steven, and X. Yu, "Parametric resonance avoidance of offshore crane cable in subsea lowering operation through a heuristic planner," *Indian J. Geo-Marine Sci.*, 2017.

- [7] V. Čorić, I. Ćatipović, and V. Slapničar, "Floating crane response in sea waves," *Brodogradnja: Teorija i praksa brodogradnje i pomorske tehnike*, vol. 65, no. 2, pp. 111–120, 2014.
- [8] N. Sun, Y. Wu, H. Chen, and Y. Fang, "An energy-optimal solution for transportation control of cranes with double pendulum dynamics: Design and experiments," *Mech. Syst. Signal Process.*, vol. 102, pp. 87–101, 2018, doi: [10.1016/j.ymssp.2017.09.027](https://doi.org/10.1016/j.ymssp.2017.09.027).
- [9] X. Peng, Z. Geng *et al.*, "Anti-swing control for 2-d under-actuated cranes with load hoisting/lowering: A coupling-based approach," *ISA Trans.*, vol. 95, pp. 372–378, 2019, doi: [10.1016/j.isatra.2019.04.033](https://doi.org/10.1016/j.isatra.2019.04.033).
- [10] Y.-G. Sun, H.-Y. Qiang, J. Xu, and D.-S. Dong, "The nonlinear dyn., and anti-sway tracking control for offshore container crane on a mobile harbor," *J. Marine Sci. Technol.*, vol. 25, no. 6, p. 5, 2017, doi: [10.6119/JMST-017-1226-05](https://doi.org/10.6119/JMST-017-1226-05).
- [11] Q.H. Ngo, N.P. Nguyen, C.N. Nguyen, T.H. Tran, and Q.P. Ha, "Fuzzy sliding mode control of an offshore container crane," *Ocean Eng.*, vol. 140, pp. 125–134, 2017, doi: [10.1016/j.oceaneng.2017.05.019](https://doi.org/10.1016/j.oceaneng.2017.05.019).
- [12] X. Xu and M. Wiercigroch, "Approximate analytical solutions for oscillatory and rotational motion of a parametric pendulum," *Nonlinear Dyn.*, vol. 47, no. 1-3, pp. 311–320, 2007, doi: [10.1007/s11071-006-9074-4](https://doi.org/10.1007/s11071-006-9074-4).
- [13] D. Yurchenko and P. Alevras, "Stability, control and reliability of a ship crane payload motion," *Probab. Eng. Mech.*, vol. 38, pp. 173–179, 2014, doi: [10.1016/j.pro bengmech.2014.10.003](https://doi.org/10.1016/j.pro bengmech.2014.10.003).
- [14] X. Zhao and J. Huang, "Distributed-mass payload dynamics and control of dual cranes undergoing planar motions," *Mech. Syst. Signal Process.*, vol. 126, pp. 636–648, 2019, doi: [10.1016/j.ymssp.2019.02.032](https://doi.org/10.1016/j.ymssp.2019.02.032).
- [15] Z. Ren, A.S. Verma, B. Ataei, K.H. Halse, and H.P. Hildre, "Model-free anti-swing control of complex-shaped payload with offshore floating cranes and a large number of lift wires," *Ocean Eng.*, vol. 228, 2021, doi: [10.1016/j.oceaneng.2021.108868](https://doi.org/10.1016/j.oceaneng.2021.108868).
- [16] N.-K. Ku, J.-H. Cha, M.-I. Roh, and K.-Y. Lee, "A tagline proportional-derivative control method for the anti-swing motion of a heavy load suspended by a floating crane in waves," *Proc. Inst. Mech. Eng., Part M: J. Eng. Marit. Environ.*, vol. 227, no. 4, pp. 357–366, 2013, doi: [10.1177/1475090212445546](https://doi.org/10.1177/1475090212445546).
- [17] S. Robak and R. Raczkowski, "Substations for offshore wind farms: A review from the perspective of the needs of the polish wind energy sector," *Bull. Pol. Acad. Sci. Tech. Sci.*, vol. 66, no. 4, 2018, doi: [10.24425/124268](https://doi.org/10.24425/124268).
- [18] "Recommended practice modelling and analysis of marine operations n103," *DET NORSKE VERITAS GL*, pp. Sec. 9.2–9.3, 2017.
- [19] "Recommended practice c205 environmental conditions and environmental loads," *DET NORSKE VERITAS GL*, p. Sec. 3.3.2, 2010.
- [20] *Fathom Group Ltd. Engineering Procedure*, 2018.
- [21] P. Boccotti, *Wave mechanics and wave loads on marine structures*. Butterworth-Heinemann, 2014.
- [22] B. Chilinski, A. Mackojc, R. Zalewski, and K. Mackojc, "Proposal of the 3-dof model as an approach to modelling offshore lifting dynamics," *Ocean Eng.*, vol. 203, pp. 287–314, 2020, doi: [10.1016/j.oceaneng.2020.107235](https://doi.org/10.1016/j.oceaneng.2020.107235).

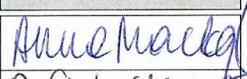
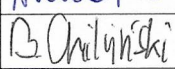


## AUTHORSHIP STATEMENT

As the authors of scientific article: Mackojć Anna, Chiliński Bogumił, *Preliminary modelling methodology of a coupled payload-vessel system for offshore lifts of light and heavy-weight objects*, Bulletin of the Polish Academy of Sciences, Technical Sciences, 2021, vol. 70, pp.9. DOI:10.24425/bpasts.2021.139003 published in 2022,

we state

the participation and contribution to development and presentation of the work in the form of a scientific publication is as follows:

Name and surname, academic degree	Participation in work	Signature
Anna Mackojć, MSc.	60%	
Bogumił Chiliński, PhD.	40%	

Warszawa, March 07, 2023

mgr inż. Anna Mackojć  
Politechnika Warszawska  
Wydział Samochodów i Maszyn Roboczych  
Instytut Podstaw Budowy Maszyn  
ul. Narbutta 84  
02-524 Warszawa

## AUTHORSHIP STATEMENT

I declare that in the work "Mackojć Anna, Chiliński Bogumił, *Preliminary modelling methodology of a coupled payload-vessel system for offshore lifts of light and heavyweight objects*, Bulletin of the Polish Academy of Sciences, Technical Sciences, 2021, vol. 70, pp.9. DOI:10.24425/bpasts.2021.139003" my participation in the article development consisted in developing the idea of the research, carrying out a comprehensive literature review, theoretical analysis of the presented problem, determining the analytical model and its numerical solution, developing research methodology, designing numerical simulation scenarios, preparing the analysed case studies, performing simulations, preparing the software tool, analysing and interpreting the results, formulating conclusions, writing (original draft), reviewing, editing and formatting the article text, preparing the final version before and after the review and the final editorial form of the article.

  
Signature

Warszawa, March 07, 2023

dr inż. Bogumił Chiliński  
Politechnika Warszawska  
Wydział Samochodów i Maszyn Roboczych  
Instytut Podstaw Budowy Maszyn  
ul. Narbutta 84  
02-524 Warszawa

## AUTHORSHIP STATEMENT

I declare that in the work "Mackojé Anna, Chiliński Bogumił, *Preliminary modelling methodology of a coupled payload-vessel system for offshore lifts of light and heavyweight objects*, Bulletin of the Polish Academy of Sciences, Technical Sciences, 2021, vol. 70, pp.9. DOI:10.24425/bpasts.2021.139003" my participation in the article development consisted in consultations of the scope and content, methodology verification and approval of the proposed approach to the problem being solved, participation in simulation research, interpretation of research results, preparing the software tool, participation in corrections in accordance with the reviewers' guidelines, writing (original draft), supervision.

  
Signature





# Analytical solution of parametrically induced payload nonlinear pendulation in offshore lifting

Bogumil Chilinski<sup>a,\*</sup>, Anna Mackojc<sup>a,\*</sup>, Krzysztof Mackojc<sup>b</sup>

<sup>a</sup> Institute of Machine Design Fundamentals, Warsaw University of Technology, Poland

<sup>b</sup> Fathom Group Ltd., 18 North Silver Street, Aberdeen, AB10 1JU, Scotland, United Kingdom of Great Britain and Northern Ireland

## ARTICLE INFO

### Keywords:

Offshore lifting analytical modelling  
Parametric payload pendulation  
Payload pendulation analytical solution  
Nonlinear dynamic system solution  
Multiple-scale perturbation method

## ABSTRACT

This paper presents a concept of analytical modelling methodology of a parametrically induced payload pendulation. A nonlinear analytical approximated solution was found for the considered 3-DOF model by simplifying to an elliptically excited Mathieu oscillator. The dynamic responses of the parametric pendulum being excited by bidirectional regular waves applied as kinematic functions at the crane tip were studied by means of the perturbation method.

In order to investigate the model's dynamic properties, an analytical first order solution was formulated through the utilisation of multiple-scale analysis. The accuracy of the solution derived was validated for two scenarios — payload oscillations outside the resonant region and on the resonance curve. The approximate analytical solution was examined for different sets of the system excitation curve parameters.

The authors conducted numerical analyses (direct integration of a nonlinear governing equation) in order to give a satisfactory confirmation of the proposed methodology and evaluate the robustness of the obtained solution.

Using the first order approximation, the results are found to be more conservative comparing to the simulations however, for all of the presented cases, the solution achieves a very good correspondence with the numerical results. The studies were summarised with an examination of the stability assessment of the lifted object.

## 1. Introduction

When discussing lifting operations undertaken offshore, the surrounding environment is one of the biggest challenges to deal with. Significant limitations for the lifting process are related to dynamic properties of the vessel-payload system (sea-keeping properties) and the sea states. In operational sea conditions, the combined horizontal and vertical oscillatory motions of a crane tip induce a specific type of excitation resulting in vibrations of the suspended payload. A movement appearing due to heaving motion itself stimulates a parametric excitation which, if the value of the excitation frequency is unfavourable may lead to the instability called parametric resonance (Fossen and Nijmeijer, 2012). An occurrence of this phenomenon during offshore lifting is one of the hazardous factors when considering oscillating system dynamics. To ensure safety during lifting operations it is crucial to eliminate possible risks at the planning stage, thus development of an effective analytical model determining the possible relations between the system combined excitation and its response, enabling in-depth studies of the possible couplings, may help to estimate the allowable

working windows for marine operations. This constitutes the need for a design process providing sufficient results. Simple analytical models serve best for these purposes, especially for the preliminary stage of computations.

Some publications addressing the problem of offshore lifting operations can be found, however in the vast majority they address analytical analyses where the system excitation is proposed as a heaving motion exclusively resulting in considerations of a Mathieu type nonlinear equation (Kovacic et al., 2018). Moreover, modelling of the payload itself is simplified to either a single degree of freedom system described in three-dimensional space (spherical pendulum) or in two-dimensional planar motion (mathematical pendulum). The authors of Ghigliazza and Holmes (2002) and Yurchenko and Alevras (2014) investigated the dynamics of parametrically induced spherical pendulum vibrations. In both, they considered a spherical pendulum with a moving support analysing its dynamics based on governing equations derived from the system energy formulation. An analytical and numerical study was carried out in Náprstek and Fischer (2009),

\* Corresponding author.

E-mail addresses: [bogumil.chilinski@pw.edu.pl](mailto:bogumil.chilinski@pw.edu.pl) (B. Chilinski), [anna.mackojc@pw.edu.pl](mailto:anna.mackojc@pw.edu.pl) (A. Mackojc), [k.mackojc@fathom-group.com](mailto:k.mackojc@fathom-group.com) (K. Mackojc).

<https://doi.org/10.1016/j.oceaneng.2022.111835>

Received 5 October 2021; Received in revised form 20 June 2022; Accepted 22 June 2022

Available online 12 July 2022

0029-8018/© 2022 The Authors. Published by Elsevier Ltd. This is an open access article under the CC BY license (<http://creativecommons.org/licenses/by/4.0/>).

where a semi-trivial solution of a spherical pendulum damper dynamics and its stability is analysed under horizontal excitation. In addition, the authors of Yurchenko and Alevras (2014) presented a S-DOF model implementing the Taylor series expansion and performing the analysis in Cartesian coordinates, which may not be intuitive for interpretation purposes of pendulum motion. The dynamics for oscillatory and rotational motion of a parametric pendulum were studied by means of analytical methods and approximate analytical solutions in Xu and Wiercigroch (2007), Lenci and Rega (2008) and Lenci et al. (2008). Numerical results for the S-DOF system under a deterministic excitation are reported in Ellermann et al. (2002), however the main focus was on nonlinear dynamic responses of crane vessels to regular waves in order to identify the limits of the operating window of floating cranes during offshore operations. The authors of Kuře et al. (2019) showed a problem of vibrations damping by appropriate changes in a pivot position in vertical direction. The model of a suspended payload was simplified to a nonlinear mathematical pendulum. A wider study of a parametric pendula damping identification is provided in Horton et al. (2008) and Sofroniou and Bishop (2014).

In the article (Čorić et al., 2014), the authors presented a dynamic model of a floating crane vessel with a hanging load. The model was defined as a linearised coupled double pendulum problem, as the pendulation of the suspended mass was limited by the assumption of small displacements. A nonlinear vibration considerations in terms of studying stability of equilibria for a double pendulum system is found in Kholostova (2009).

Other research papers regarding dynamic behaviour of pendulum-like systems under nearly parametric excitation result in considerations of a model described in Horton et al. (2011) and Sah and Mann (2012). The studies present the effects of an excitation in the form of a movement along a small ellipse, perturbing the classical parametric pendulum. Approximate rotational solutions of the pendulum under combined excitation was presented in Pavlovskaja et al. (2012). The analytical solutions were derived using asymptotic analysis for the pendulum excited elliptically and along a tilted axis. The accuracy of the approximations was examined for different values of the parameters controlling the shape of the excitation ellipse.

In Kang et al. (2016, 2017), the authors studied the dynamic behaviour of an offshore crane cable based on Mathieu equation and its unstable states referred to as a parametric resonance vibration. The analysis was conducted for long cables used in subsea lowering operations, which significantly differentiate the dynamics of the object from the one handling in air due to the damping properties of water.

The presented state of the art, despite the extensive analyses, does not offer a comprehensive approach, where the model and its investigating methodology allows for an intuitive analysis with regards to environmental factors. Besides a purely mathematical modelling, the physical context and its interpretation of the lifted load dynamic behaviour has not been yet still well-recognised. The authors motivation is to provide a qualitative information as opposed to purely numerical research in this area. The qualitative contribution is seen in a methodology that despite decoupled analysis, takes into account hydrodynamic interaction and ship seakeeping properties based on the RAOs functions. What is more, the analytical approach provides an explicit function determining the payload dynamic behaviour. That allows the analysis of the parameters constituting the vibrations of the object in terms of their selection in order to 'control' the payload response. This offers the opportunity for a better planning and understanding of lifting operations and avoidance of dangerous resonance phenomena as the undesirable parametric vibrations. It is also believed that the proposed algorithm might be preferable in terms of accessibility and computational efficiency contrary to commonly used integrating schemes being mostly used when analysing dynamics.

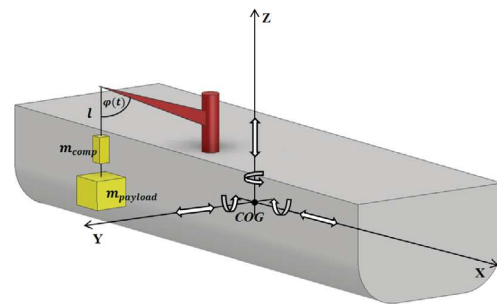


Fig. 1. A 6-DOF vessel with the 3-DOF lifting system and its parameters.

## 2. Objectives and overview

Lifting operation design consists of the modelling of many problems related to various phenomena such as pendulation, hydrodynamic interaction or impact crossing the splash zone. Mathematical description of the case and further analytical investigation enables to reveal the nature of the phenomena related to the lifting process. Based on the results, a quantitative description of the system dynamic features might be provided. The authors expect mathematical formulas as a final effect of the modelling process.

An analytical solution of the simple 3-DOF model enables a comprehensive study of the dynamic behaviour of the payload. Intuitive analysis or numerical investigation might not be as precise as the utilisation of closed form solutions for the case of the lifted object motion, since the proposed analytical approach allows for deeper investigation to obtain mathematical dependencies describing particular physical effects occurring in the system. This creates the possibility to determine laws, which govern the phenomena related to payload dynamics, especially those which are connected with the operational instability of the system.

Further investigation needs to adopt assumptions for the modelling phase and state a methodology of the analysis. First of all, the authors assumed the vessel's and the payload's vibrations to be uncoupled as stipulated by the standards devoted to offshore operations (DNV, 2017). Moreover, a planar motion was considered being parallel to the plane of the vessel rotation. The displacements of the suspension point of the pendulum are given by RAOs functions. The authors considered small vibrations which caused simplified form of the nonlinear terms. Third order approximation was utilised in order to model the nonlinear behaviour.

The proposed analytical approach is efficient where closed mathematical formulas describing the physical phenomena and mutual relations occurring in the vessel-payload system are needed. This can be used in the process of designing the payload control system, for preliminary computations in the lifting system design process, for in-depth investigation of the real object behaviour and offshore operation design.

## 3. Proposed analytical model for offshore light lifts

The dynamics of a 6-DOF vessel modelled as a rigid body (Fig. 1) excited by forces caused by hydrodynamic interaction with the hull can be replaced by response amplitude operators and phases (referred to as RAOs) in order to obtain the excitation functions (Chilinski et al., 2020).

Given the extensive simplifications in the approaches mentioned in Section 1, it is suggested to consider a model combining heave and pendulum response simultaneously. The 3-DOF model utilised for analytical modelling of the lifting system (Fig. 2), based on the processed RAOs functions, is subjected to kinematic excitation functions (regular

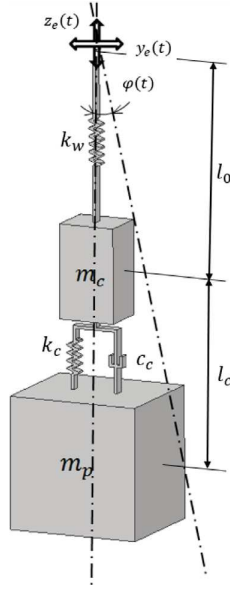


Fig. 2. The analysed 3-DOF dynamic model for offshore lifted objects (Chilinski et al., 2020).

waves applied at the remote point representing a position of the crane tip) resulting in elliptical planar motion, where:

$y_e(t) = A_y \cos(\omega t + \Phi_y)$  — lateral displacement at crane tip obtained from RAOs (a regular wave excitation),

$z_e(t) = A_z \cos(\omega t + \Phi_z)$  — vertical displacement at crane tip obtained from RAOs (a regular wave excitation),

$A_y$  — amplitude of the lateral excitation,

$A_z$  — amplitude of the vertical excitation,

$\Phi_y$  — phase angle of the lateral motion,

$\Phi_z$  — phase angle of the vertical motion,

$m_p$  — mass of payload,

$m_c$  — mass of compensator,

$k_w$  — wire stiffness,

$k_c$  — stiffness of heave compensator,

$c_c$  — viscous damping of heave compensator,

$l_0$  — length of the lifting cable,

$l_c$  — length of the attached compensating element,

$g$  — standard acceleration of gravity  $9.81 \text{ m s}^{-2}$ .

In order to obtain governing equations, the methods of Lagrangian mechanics were adopted. It was possible to determine kinetic and potential energies of the subsystems under consideration in the analytical manner (Chilinski et al., 2020). Based on the obtained Lagrangian the equations of motion were found. Hence the considered payload system might be modelled by the following system of matrix equations (1):

$$M \cdot \ddot{X} + K(t) \cdot X + F(X, t) = 0 \quad (1)$$

where:  $M$  — inertia matrix of payload,  $K(t)$  — time-dependent stiffness matrix of payload,  $F(X, t)$  — nonlinear terms and excitation vector,  $X = [\varphi \ h \ h_c]^T$  — vector of the system degrees of freedom. The linear displacement of the compensating element and the payload in vertical direction are both calculated with respect to the object suspension point.

The inertia and stiffness matrices are given as follows:

$$M = \begin{bmatrix} I_0 & 0 & 0 \\ 0 & m_p & 0 \\ 0 & 0 & m_c \end{bmatrix} \quad (2)$$

$$K = \begin{bmatrix} S_0(g - \ddot{z}_e) & m_p \ddot{y}_e & m_c \ddot{y}_e \\ m_p \ddot{y}_e & k_c & -k_c \\ m_c \ddot{y}_e & -k_c & k_c + k_w \end{bmatrix} \quad (3)$$

The simplifying substitutions were introduced in order to achieve a more readable form of the  $M$  and  $K(t)$  matrices. They are as follows:

$$I_0 = m_c r_2^2 + m_p r_1^2 \quad (4)$$

$$S_0 = m_p r_1 + m_c r_2 \quad (5)$$

where:  $I_0$  — second moment of area,  $S_0$  — first moment of area,  $r_2 = l_0 + u_{c0}$ ,  $l_w = l_0 + l_c$ ,  $u_0$  — payload equilibrium position,  $u_{c0}$  — compensator equilibrium position.

Nonlinear components were grouped, gathered and rearranged to the form of a vectors sum. Each vector represents a different type of either nonlinearity or external excitation. Analysing the particular vectors, some of them can be attributed to some physical phenomena due to the occurrence of explicit dependencies. The relationships might be seen in  $F_{NL}$  vector showing nonlinearities,  $F_G$  vector expressing Coriolis effect and gyroscopic forces or in  $F_E$  vector that exhibits an influence of the external factors and the internal parameters/properties of the system. The  $F_{\ddot{\varphi}}$  and  $F_{\ddot{\varphi}}$  represent vectors of nonlinear components regarding the payload accelerations and displacements. All of the components of  $F(X, t)$  vector are presented in the formulas (6)–(10):

$$F_{NL} = \begin{bmatrix} -\frac{S_0(g - \ddot{z}_e)\varphi^3}{6} - \frac{(m_c(r_1 + h_c) + m_p(r_2 + h))\varphi^2 \ddot{y}_e}{2} \\ \frac{m_p(g - \ddot{z}_e)\varphi^2}{2} \\ \frac{m_c(g - \ddot{z}_e)\varphi^2}{2} \end{bmatrix} \quad (6)$$

$$F_{\ddot{\varphi}} = \begin{bmatrix} (m_c(2r_1 h_c + h_c^2) + m_p(2r_2 h + h^2)) \ddot{\varphi} \\ 0 \\ 0 \end{bmatrix} \quad (7)$$

$$F_G = \begin{bmatrix} 2(m_c(r_1 + h_c) \dot{h}_c + m_p(r_2 + h) \dot{h}) \dot{\varphi} \\ m_p(-r_2 - h) \dot{\varphi}^2 \\ m_c(-r_1 - h_c) \dot{\varphi}^2 \end{bmatrix} \quad (8)$$

$$F_{\ddot{\varphi}} = \begin{bmatrix} (m_c(g - \ddot{z}_e) h_c + m_p(g - \ddot{z}_e) h) \ddot{\varphi} \\ 0 \\ 0 \end{bmatrix} \quad (9)$$

$$F_E = \begin{bmatrix} (m_c r_1 + m_p r_2) \ddot{y}_e \\ k_c u_0 - k_c u_{c0} + m_p(-g + \ddot{z}_e) \\ -k_c u_0 + k_c u_{c0} + k_w u_{c0} + m_c(-g + \ddot{z}_e) \end{bmatrix} \quad (10)$$

All the  $\varphi$ ,  $h$  and  $h_c$  symbols included within the vectors correspond to the following degrees of freedom of the considered model:

$\varphi$  — sway angle response,

$h$  — linear displacement of payload,

$h_c$  — linear displacement of compensating element.

The other symbols appearing in the vectors were explained in the descriptions for Fig. 2.

The process of diagonalisation of the system separated linear part  $M^{-1} \cdot K$  of the equations of motion and the system eigenvalues and

eigenmodes can be determined. The diagonalised matrix and the assumed parameters relations are presented in the following:

$$M^{-1}K = \begin{bmatrix} \frac{S_0 g}{I_0} & 0 & 0 \\ 0 & \frac{k_c}{m_p} & -\frac{k_c}{m_p} \\ 0 & -\frac{k_c}{m_c} & \frac{k_c + k_w}{m_c} \end{bmatrix} \quad (11)$$

The system eigenvalues and eigenmodes were determined assuming some dependencies regarding the model's masses and stiffnesses relation. The following formulas presents the assumed relationships:

$$\kappa = \frac{k_w}{k_c} \quad \mu = \frac{m_c}{m_p} \quad (12)$$

Taking into account equations (12), the eigenvalue matrix might be then expressed as follows:

$$\Omega^2 = \begin{bmatrix} \frac{S_0 g}{I_0} & 0 & 0 \\ 0 & \frac{k_c \kappa}{2m_p \mu} - \frac{k_c \lambda}{2m_p \mu} + \frac{k_c}{2m_p} + \frac{k_c}{2m_p \mu} & 0 \\ 0 & 0 & \frac{k_c \kappa}{2m_p \mu} + \frac{k_c \lambda}{2m_p \mu} + \frac{k_c}{2m_p} + \frac{k_c}{2m_p \mu} \end{bmatrix} \quad (13)$$

where the  $\lambda$  expression represents the following relation:

$$\lambda = \sqrt{1 + \kappa^2 + \mu^2 + 2\kappa + 2\mu - 2\kappa\mu} \quad (14)$$

The eigenmode matrix will take the following form (15):

$$P = \begin{bmatrix} 1 & 0 & 0 \\ 0 & \frac{\kappa}{2} + \frac{\lambda}{2} - \frac{\mu}{2} + \frac{1}{2} & \frac{\kappa}{2} - \frac{\lambda}{2} - \frac{\mu}{2} + \frac{1}{2} \\ 0 & 1 & 1 \end{bmatrix} \quad (15)$$

Having computed the matrix of eigenvectors, the modal decomposition can be applied in order to uncouple the linear part of the governing equations. The fundamental matrix of this mapping is given by the linearised system eigenmodes. Due to this, the following relationship describes a transformation law allowing to transform the generalised coordinates to a modal form:

$$Y = P^{-1} \cdot X \quad (16)$$

where:

$Y$  — vector of modal coordinates.

Utilisation of the transformation law (16) enables rearrangement of the governing equation given by the formula (1). The proposed approach results in the form of the equation allowing for the application of some methods for solving weak nonlinear equation problems. In the case under consideration, a perturbation method was applied where the matrix equation is presented as a superposition of the linear and nonlinear part:

$$M \cdot \ddot{Y} + K(t) \cdot P \cdot Y + F(P \cdot Y, t) = 0 \quad (17)$$

The next step is to separate the nonlinear and parametric components of Eq. (17). The equation of motion for the case under consideration is then as follows:

$$M \cdot \ddot{Y} + (\hat{K} + \Delta K(t)) \cdot P \cdot Y + F(P \cdot Y, t) = 0 \quad (18)$$

where:

$\hat{K}$  — linear matrix of constant stiffness coefficients,

$\Delta K(t)$  — time-dependent part of the stiffness matrix.

Further calculations lead to the following form of the governing equation:

$$M \cdot \ddot{Y} + \hat{K} \cdot P \cdot Y + \varepsilon F_\varepsilon(P \cdot Y, t) = 0 \quad (19)$$

The expression  $F_\varepsilon(P \cdot Y, t)$  represents all the nonlinear and parametric terms. Such an approach allows to introduce a recursive solution in the form of series of the small parameter  $\varepsilon$ . The explicit formula of this component is presented in (20):

$$\varepsilon F_\varepsilon(P \cdot Y, t) = \Delta K(t) \cdot P \cdot Y + F(P \cdot Y, t) \quad (20)$$

Finally, an appropriate utilisation of the matrix  $P$  enables to decompose the investigated problem to a linearly uncoupled form. The product of inverted modes matrix  $P^{-1}$  and the vector of the equation of motion have to be applied in order to obtain the desired form:

$$P^{-1} \cdot (M \cdot \ddot{Y} + \hat{K} \cdot P \cdot Y + \varepsilon F_\varepsilon(P \cdot Y, t)) = 0 \quad (21)$$

Further computations result in the final form of the system equations of motion:

$$\ddot{Y} + \Omega^2 \cdot Y + \varepsilon P^{-1} F_\varepsilon(P \cdot Y, t) = 0 \quad (22)$$

The obtained form of linearly decoupled system allows the analysis of equations separately. It is possible to eliminate some formulas from the investigation, if the selected initial conditions result in lack of solution for a particular degree of freedom.

#### 4. Analytical solution - multiple-scale analysis based approach

The system of equations (22) can be solved with a method presented in Hunter (2004) and Nayfeh and Balachandran (2008). In order to utilise it, the following predicted form of the solution has to be applied:

$$Y = Y_0(t_0(t), t_1(t)) + \varepsilon Y_1(t_0(t), t_1(t)) + O(\varepsilon^2) \quad (23)$$

where:

$Y_0$  — zeroth order approximation of the solution  $Y$ ,

$Y_1$  — first order approximation of the solution  $Y$ ,

$O(\varepsilon^2)$  — higher order terms of the considered solution, which can be omitted in the analysis.

In order to represent time dependency on multiple time scales, dimensionless times  $t_0, t_1, \dots$  were introduced. This approach allows to represent differences in time history rates of the phenomena occurring in the system.

An analytical solution might be obtained by a substitution of the relationship (23) to the governing equation (22). It results in a new form of Eq. (22), which becomes a power series of the small parameter  $\varepsilon$ . The zeroth approximation is the part of the governing equation representing the linear and time-independent system properties. The formula of the zeroth approximation is described by the following:

$$\ddot{Y}_0 + \Omega^2 \cdot Y_0 = 0 \quad (24)$$

The Eq. (24) can be solved applying standard procedure for linear second order ODE's. The function that satisfies the equation has a form of a combination of sine and cosine components of the natural frequencies and the vibration modes. After this, the explicit form of the  $Y_0$  exists and can be used as an input for higher approximations:

$$\ddot{Y}_1 + \Omega^2 \cdot Y_1 + P^{-1} F_\varepsilon(P \cdot Y_0, t) = 0 \quad (25)$$

The determined system of governing equations expressed in the modal coordinates allows to obtain the approximate solution. For this type of problems, a perturbation method can be used efficiently. The obtained solution is mainly composed of the elements which come from the linear part of the ODE's (formula (24)). Additional small components (proportional to small parameter) are caused by a cubic nonlinearity and parametric effects. These harmonic functions correspond with triple  $(3\omega_p, 3\Omega)$  and combined frequencies  $(\omega_p - \Omega, \omega_p + \Omega)$ , where  $\omega_p$  determines the natural frequency of payload.

A solution of the equation of motion (26) was derived based on the method of multiple scales of time.

$$\ddot{Y}(t) + \omega^2 Y(t) + \varepsilon \omega^2 Y^3(t) + F_e(Y(t), t) = 0 \quad (26)$$

The authors assumed the first-order two-scale expansion  $t_0(t), t_1(t)$  adopted to the form of predicted solution presented in (27):

$$Y = Y_{00}(t_0(t), t_1(t)) + \varepsilon Y_{01}(t_0(t), t_1(t)) + O(\varepsilon^2) \quad (27)$$

The adopted assumption is a resultant of the vector  $Y$  that is determined as  $Y = [Y_\varphi \ Y_h \ Y_{h_c}]^T$ . The authors assumed the following dependencies:  $Y_\varphi = Y_{00}$ ,  $Y_h = Y_{10}$  and  $Y_{h_c} = Y_{20}$ , where the first digit in the  $Y$  subscript stands for the consecutive generalised coordinates and the second digit is a representation of the order of the equation considered.

In order to give a reliable insight on the dynamics of the parametrically induced payload pendulation, the considered 3-DOF model has been simplified to the model close to Mathieu oscillator based on the model's similar behaviour presented in Chilinski et al. (2020). The dynamic responses of the parametric pendulum being excited by an elliptical crane tip motion resulting from the excitation of regular wave were studied by means of perturbation methods. To understand the model's fundamental resonance properties, an undamped parametric analytical solution was formulated. The presented study forms a basis to propose an automatic control system able to follow the intended motion.

The payload pendulatory motion is determined by the generalised coordinate  $\varphi(t)$  and hence the equation of motion might be presented as follows:

$$\begin{aligned} & -A_y \omega^2 \varepsilon \cos(\Phi_y + \omega t) \\ & - \frac{A_z \omega^2 \varepsilon \varphi^3 \cos(\Phi_z + \omega t)}{6} \\ & + A_z \omega^2 \varepsilon \varphi \cos(\Phi_z + \omega t) - \frac{\omega^2 (\delta \varepsilon + 1) \varphi^3}{24} \\ & + \frac{\omega^2 (\delta \varepsilon + 1) \varphi}{4} + \ddot{\varphi} = 0 \end{aligned} \quad (28)$$

Therefore, taking into account the previous assumptions and the methodology implemented, the equation of motion of the system is presented as the following formula (29):

$$-\frac{\omega^2 (\delta \varepsilon + 1) \varphi^3}{24} + \frac{\omega^2 (\delta \varepsilon + 1) \varphi}{4} + \ddot{\varphi} + \frac{\varphi^3 \ddot{z}_e}{6l_w} - \frac{\varphi \ddot{z}_e}{l_w} + \frac{\ddot{y}_e}{l_w} = 0 \quad (29)$$

The equation given in (30) represents the governing equation (29) in which, specified exciting functions were introduced. The small parameter  $\varepsilon$  was determined as a term  $\frac{1}{l_w}$  and the excitation adopted as defined in Section 3. The  $\delta$  coefficient is included to the equation in order to study how stable and unstable regions (the tongues) within the Ince-Strutt diagram evolve under its variation, affecting dynamic properties of the considered system.

$$\begin{aligned} & -A_y \omega^2 \varepsilon \cos(\Phi_y + \omega t) \\ & - \frac{A_z \omega^2 \varepsilon \varphi^3 \cos(\Phi_z + \omega t)}{6} \\ & + A_z \omega^2 \varepsilon \varphi \cos(\Phi_z + \omega t) - \frac{\omega^2 (\delta \varepsilon + 1) \varphi^3}{24} \\ & + \frac{\omega^2 (\delta \varepsilon + 1) \varphi}{4} + \ddot{\varphi} = 0 \end{aligned} \quad (30)$$

The ordering and separation of Eq. (30) in terms of the power of a small parameter  $\varepsilon$  leads to obtaining of a recursive sequence of linear equations of motion leading to the solution of the nonlinear equation. The zeroth-order approximate linear equation is given in (31) where the dependency  $\varphi_0(t_0, t_1) = Y_{00}(t_0, t_1)$  was assumed for the zeroth-order solution of the time variable:

$$\frac{\omega^2 Y_{00}(t_0, t_1)}{4} + \frac{d^2}{dt_0(t)^2} Y_{00}(t_0(t), t_1(t)) = 0 \quad (31)$$

Since  $t_0$  and  $t_1$  are treated as independent, the differential equation becomes a partial differential equation for a function  $Y_{00}(t_0, t_1)$  of two variables  $t_0$  and  $t_1$ . Therefore the general solution may be obtained from the general solution of the corresponding ordinary differential equation by the assumptions of the arbitrary constants becoming the arbitrary functions of  $t_1$ . Thus solving the considered equation for the unformulated initial conditions, it can be assumed that the predicted solution for the zeroth-order approximation  $Y_{00}(t_0, t_1)$  has the following form:

$$Y_{00}(t_0, t_1) = C_1(t_1) \sin\left(\frac{\omega t_0}{2}\right) + C_2(t_1) \cos\left(\frac{\omega t_0}{2}\right) \quad (32)$$

where:

$C_1(t_1), C_2(t_1)$  — constant while considering  $t_0$  changes (may vary over  $t_1$ ).

In order to determine the functions  $C_1(t_1), C_2(t_1)$  and hence  $Y_{00}(t_0, t_1)$ , the first-order approximate equation has to be considered:

$$\begin{aligned} & -A_y \omega^2 \cos(\Phi_y + \omega t_0) \\ & - \frac{A_z \omega^2 Y_{00}^3(t_0, t_1) \cos(\Phi_z + \omega t_0)}{6} \\ & + A_z \omega^2 Y_{00}(t_0, t_1) \cos(\Phi_z + \omega t_0) \\ & + \frac{\delta \omega^2 Y_{00}(t_0, t_1)}{4} \\ & - \frac{l_w \omega^2 Y_{00}^3(t_0, t_1)}{24} + \frac{\omega^2 Y_{01}(t_0, t_1)}{4} \\ & + \frac{d^2}{dt_0(t)^2} Y_{01}(t_0(t), t_1(t)) \\ & + 2 \frac{d^2}{dt_1(t) dt_0(t)} Y_{00}(t_0(t), t_1(t)) = 0 \end{aligned} \quad (33)$$

Substituting of the predicted solution form given in (27) leads to first-order equation containing the terms being proportional to  $\sin\left(\frac{\omega t_0}{2}\right)$  and  $\cos\left(\frac{\omega t_0}{2}\right)$ . It results in introducing the secular terms to the particular solution of  $Y_{01}(t_0, t_1)$ . Thus, the condition allowing for a removal of the secular terms has to be fulfilled by vanishing the coefficients of  $\sin\left(\frac{\omega t_0}{2}\right)$  and  $\cos\left(\frac{\omega t_0}{2}\right)$ . Removal of these coefficients yields the condition for the determination of  $C_1(t_1)$  and  $C_2(t_1)$  function:

$$\begin{aligned} & -\left(\frac{A_z \omega \cos(\Phi_z)}{2} - \frac{\delta \omega}{4}\right) C_2(t_1) \\ & + \frac{A_z \omega C_1(t_1) \sin(\Phi_z)}{2} + \frac{d}{dt_1} C_1(t_1) = 0 \\ & -\left(\frac{A_z \omega \cos(\Phi_z)}{2} + \frac{\delta \omega}{4}\right) C_1(t_1) + \\ & - \frac{A_z \omega C_2(t_1) \sin(\Phi_z)}{2} + \frac{d}{dt_1} C_2(t_1) = 0 \end{aligned} \quad (34)$$

The solutions of the system of equations (34) are as follows:

$$C_1(t_1) = C_1 e^{-\frac{\omega \sqrt{2A_z - \delta} \sqrt{2A_z + \delta} t_1}{4}} + C_2 e^{\frac{\omega \sqrt{2A_z - \delta} \sqrt{2A_z + \delta} t_1}{4}} \quad (35)$$

$$\begin{aligned} C_2(t_1) = & -\frac{C_1 \cdot (2A_z \cos(\Phi_z) + \delta) e^{-\frac{\omega \sqrt{2A_z - \delta} \sqrt{2A_z + \delta} t_1}{4}}}{2A_z \sin(\Phi_z) + \sqrt{2A_z - \delta} \sqrt{2A_z + \delta}} \\ & + \frac{C_2 \cdot (2A_z \cos(\Phi_z) + \delta) e^{\frac{\omega \sqrt{2A_z - \delta} \sqrt{2A_z + \delta} t_1}{4}}}{2A_z \sin(\Phi_z) - \sqrt{2A_z - \delta} \sqrt{2A_z + \delta}} \end{aligned} \quad (36)$$

where  $C_1$  and  $C_2$  are constants of integration. To obtain  $Y_{00}(t_0, t_1)$ , substitution of Eqs. (35) and (36) was done into Eq. (32) and the following time scales were introduced  $t_0(t) = t, t_1(t) = \varepsilon t$ . Therefore,



the simplified formula for the  $Y_{00}(t)$  can be presented as follows:

$$Y_{00}(t) = \left( C_1 e^{-\frac{\omega t \epsilon \sqrt{4A_z^2 - \delta^2}}{4}} + C_2 e^{\frac{\omega t \epsilon \sqrt{4A_z^2 - \delta^2}}{4}} \right) \cos\left(\frac{\omega t}{2}\right) + \left( \frac{C_1 (2A_z \cos(\Phi_z) + \delta) e^{-\frac{\omega t \epsilon \sqrt{4A_z^2 - \delta^2}}{4}}}{2A_z \sin(\Phi_z) - \sqrt{4A_z^2 - \delta^2}} + \frac{C_2 (2A_z \cos(\Phi_z) + \delta) e^{\frac{\omega t \epsilon \sqrt{4A_z^2 - \delta^2}}{4}}}{2A_z \sin(\Phi_z) + \sqrt{4A_z^2 - \delta^2}} \right) \sin\left(\frac{\omega t}{2}\right) \quad (37)$$

First-order approximation of a particular solution for the excited vibrations given in the general form of  $Y(t_0, t_1) = Y_{00} + \epsilon Y_{01}$ , takes the form presented in (38). The consecutive approximations can be obtained by repeating the procedure described.

$$Y(t_0, t_1) = -\frac{4A_y \epsilon \cos(\Phi_y + \omega t_0)}{3} - \frac{A_z \epsilon C_1^3(t_1) \sin\left(\Phi_z + \frac{3\omega t_0}{2}\right)}{32} + \frac{A_z \epsilon C_1^3(t_1) \sin\left(\Phi_z + \frac{5\omega t_0}{2}\right)}{288} - \frac{A_z \epsilon C_1^2(t_1) C_2(t_1) \cos\left(\Phi_z + \frac{3\omega t_0}{2}\right)}{32} + \frac{A_z \epsilon C_1^2(t_1) C_2(t_1) \cos\left(\Phi_z + \frac{5\omega t_0}{2}\right)}{96} - \frac{A_z \epsilon C_1(t_1) C_2^2(t_1) \sin\left(\Phi_z + \frac{3\omega t_0}{2}\right)}{32} - \frac{A_z \epsilon C_1(t_1) C_2^2(t_1) \sin\left(\Phi_z + \frac{5\omega t_0}{2}\right)}{96} + \frac{A_z \epsilon C_1(t_1) \sin\left(\Phi_z + \frac{3\omega t_0}{2}\right)}{4} - \frac{A_z \epsilon C_2^3(t_1) \cos\left(\Phi_z + \frac{3\omega t_0}{2}\right)}{32} - \frac{A_z \epsilon C_2^3(t_1) \cos\left(\Phi_z + \frac{5\omega t_0}{2}\right)}{288} + \frac{A_z \epsilon C_2(t_1) \cos\left(\Phi_z + \frac{3\omega t_0}{2}\right)}{4} + \frac{l_w \epsilon C_1^3(t_1) \sin\left(\frac{3\omega t_0}{2}\right)}{192} + \frac{l_w \epsilon C_1^2(t_1) C_2(t_1) \cos\left(\frac{3\omega t_0}{2}\right)}{64} - \frac{l_w \epsilon C_1(t_1) C_2^2(t_1) \sin\left(\frac{3\omega t_0}{2}\right)}{64} - \frac{l_w \epsilon C_2^3(t_1) \cos\left(\frac{3\omega t_0}{2}\right)}{192} + \epsilon C_1(t_1) \sin\left(\frac{\omega t_0}{2}\right) + \epsilon C_2(t_1) \cos\left(\frac{\omega t_0}{2}\right) + C_1(t_1) \sin\left(\frac{\omega t_0}{2}\right) + C_2(t_1) \cos\left(\frac{\omega t_0}{2}\right) \quad (38)$$

The formulas for the constants  $C_1(t_1)$  and  $C_2(t_1)$  are given as presented in (35) and (36). The numerical function of the first-order term of approximate solution  $Y(t)$  and the design parameters used are provided in Appendix.

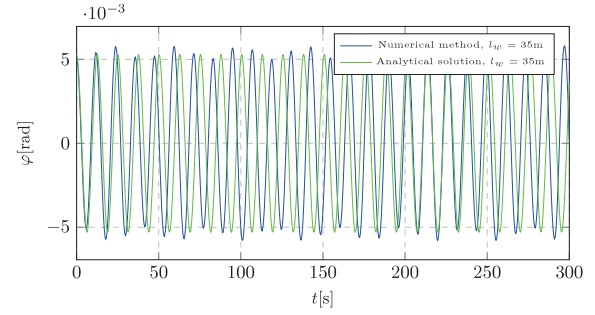


Fig. 3. Payload pendulation comparative results for a numerical and analytical solution (elliptical excitation at the pivot point for  $A_y = 0$  m,  $A_z = 1$  m, cable length = 35 m).

The analysis presented describes a method for finding an analytical approximate solution for nonlinear dynamics of a payload forced pendulation. As might be expected, the discrepancies with numerical results in the derived formula are less significant as more terms from the predicted solution (27) are considered, however taking into a consideration the value of a small parameter recognised as  $\epsilon = \frac{1}{l_w}$ , it can be concluded that a much better results convergence will not be achieved in terms of quantitative results with the consecutive approximations.

## 5. Numerical verification and analysis

The authors conducted numerical analyses in order to give a satisfactory confirmation of the proposed methodology. In this section the results obtained on the basis of a direct integration of the nonlinear governing equation, are provided for comparative purposes and for an assessment of the discrepancy between the predicted analytical approximations and the numerical results. All of the analytical results are provided based on the first approximate solution (38) presented in Section 4. The results are obtained for the excitation by one directional regular wave (vessel excitation) resulting in a bidirectional elliptical movement of the crane tip. The proposed methodology is validated for two scenarios — payload oscillations outside the resonant region and on the resonance curve. The accuracy of the approximate solutions was examined for different sets of the system parameters.

Fig. 3 illustrates the time trace in the form of comparison between numerical and analytical results for vertically excited pendulum. Simulations were run for an idealised regular wave scenario, which utilising RAOs was transformed to boom tip motion. The payload sway response were studied for a cable length being in the operational range 35 m and for  $T = 7$  s wave period (medium-slow waves). The semi-axis of the exciting ellipse were set equal to  $A_y = 0$  m and  $A_z = 1$  m. As can be observed, the two solutions are almost of the same character. Only slight differences might be seen on the amplitude values and phase.

As can be seen in all of the time histories of payload motion (Figs. 3, 5, 7), some inaccuracies appear between the phases of the compared responses. These are the result of an assumption made in order to simplify the procedure of determination of the analytical solution based on the multiple-scale method adopted. Applying the assumption in solving scheme allowed for a significant reduction in time needed to obtain a fully nonlinear analytical solution. The adopted simplification assumes a mean (constant) value of the omega ( $\omega$ ) for the nonlinear first-order solution, while in fact the vibration frequency of the nonlinear system is a fluctuating value. This assumption leads to a significant increase of time efficiency in terms of seeking the solution at the expense of small, local phase discrepancies. It is worth noting that at this stage, a consideration of successive approximations to the solution will not result in a significant improvement in the qualitative results, and the quantitative changes will be only slight so the authors assessed the time costs incurred in finding and implementing the exact

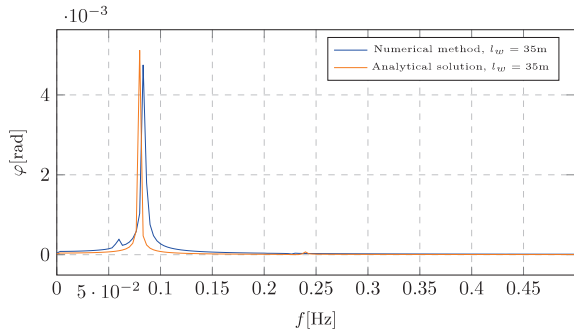


Fig. 4. Payload pendulation spectrum for a numerical and analytical solution (elliptical excitation at the pivot point for  $A_y = 0$  m,  $A_z = 1$  m, cable length = 35 m).

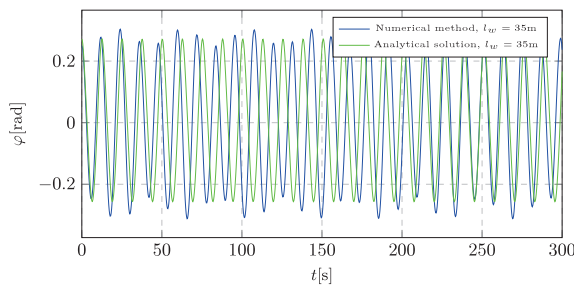


Fig. 5. Payload pendulation comparative results for a numerical and analytical solution (elliptical excitation at the pivot point for  $A_y = 0.1$  m,  $A_z = 1$  m, cable length = 35 m).

frequency value, to be greater than the improvement of the obtained results in terms of the quality of the model response. In order to get more detailed insight into the system behaviour in terms of phase shifts, the authors performed spectral analysis depicted in Fig. 4. The results presented confirm a very good correspondence between the analytical approximation and the numerically integrated responses, in spite of the local phase discrepancy observed in the time traces.

Figs. 5, 6, 7 and 8 demonstrate the solutions evaluated in time domain for a crane tip elliptical excitation. The results were prepared so that the elliptical excitation was formulated differently for each of the two presented sets of the solutions. The two exciting ellipses were diversified by a ratio of the semi-axes, resulting in two different exciting curves. One having the exciting amplitudes set to semi-axis ratio equals  $e = \frac{A_z}{A_y} = \frac{1}{0.1} = 10$  and the other one  $e = \frac{A_z}{A_y} = \frac{1.5}{0.5} = 3$ .

It is worth noting that the presented two sets differ from the previous analysis by adding a lateral excitation  $A_y$  that affects the results achieved. The direct comparison can be made between Figs. 3 and 5. As can be seen, additional lateral motion of a crane tip causes higher values of sway response amplitudes.

More interesting dynamic properties might be observed based on the comparative analysis of spectral results. One might notice that the added lateral excitation resulting in an elliptical movement of the pivot point leads to greater accuracy in terms of main component value observed in the frequency domain. What is more, the analytical approximation shows two additional higher frequency components of negligible amplitudes, being a multiple of the main component.

Figs. 7 and 8 depict the repeating regularity in the context of the appearance of higher components for a larger value of the lateral excitation. It is especially visible in the spectral analysis (Fig. 8), where not only the analytically predicted solution shows the additional higher harmonic components but also the numerically simulated responses start to reveal the same trend.

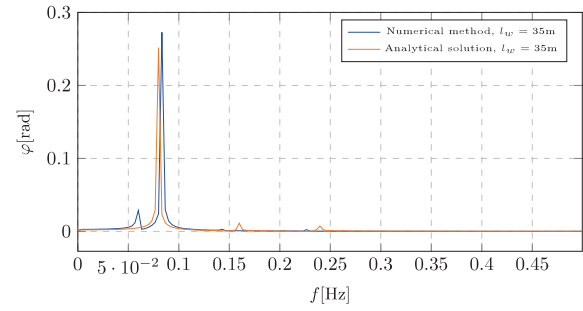


Fig. 6. Payload pendulation spectrum for a numerical and analytical solution (elliptical excitation at the pivot point for  $A_y = 0.1$  m,  $A_z = 1$  m, cable length = 35 m).

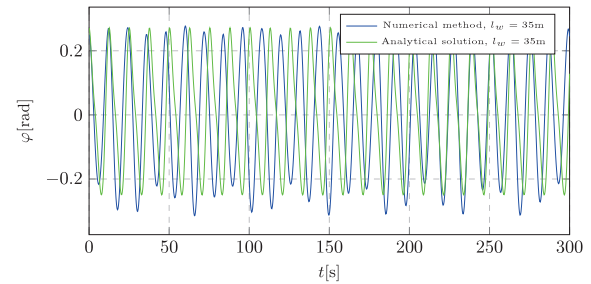


Fig. 7. Payload pendulation comparative results for a numerical and analytical solution (elliptical excitation at the pivot point for  $A_y = 0.5$  m,  $A_z = 1.5$  m, cable length = 35 m).

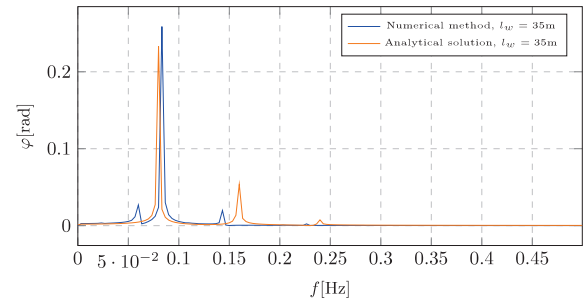


Fig. 8. Payload pendulation spectrum for a numerical and analytical solution (elliptical excitation at the pivot point for  $A_y = 0.5$  m,  $A_z = 1.5$  m, cable length = 35 m).

Their later appearance in the results of an integration process of the solution evaluation may be the result of numerical damping implemented in the integration scheme. This proves the correctness of the analytically predicted and approximated solution beyond the resonance regime and indicates that due to the lack of numerical damping, it provides more conservative results, however, for all the presented simulations the approximate solution achieves a good correspondence with the numerical one.

The second scenario used for validation purposes is an investigation of the model performance at the resonance curve. Figs. 9 and 10 present, similarly as in case of non-resonant analysis, the oscillations induced by vertical motion of the pivot point. The solutions were prepared for a resonant cable length (about 48.7 m). The rest of the system parameters remained unchanged. As can be seen, the responses evaluated on the resonance curve lead towards conclusion on a good solutions compatibility. This is proven by either the time histories or spectral analyses. Only slight difference between the solutions is locally revealed in a little bit higher dynamics of the analytical approximation.

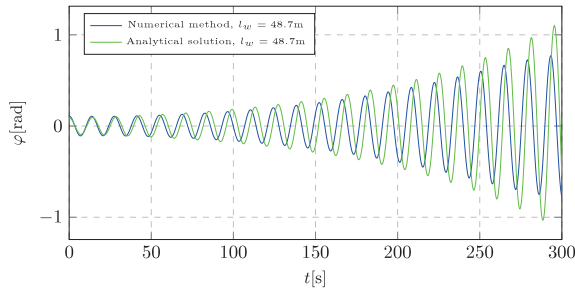


Fig. 9. Payload pendulation comparative results for a numerical and analytical solution (elliptical excitation at pivot point for  $A_y = 0\text{ m}$ ,  $A_z = 1\text{ m}$ , resonant cable length).

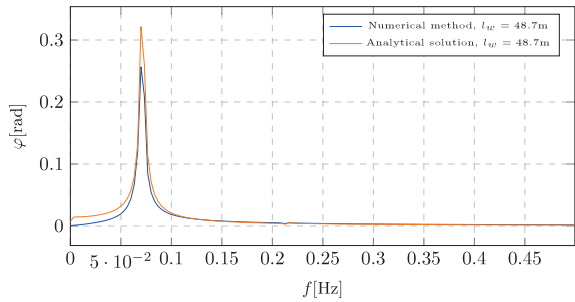


Fig. 10. Spectral analysis for a numerical and analytical solution (elliptical excitation at pivot point for  $A_y = 0\text{ m}$ ,  $A_z = 1\text{ m}$ , resonant cable length).

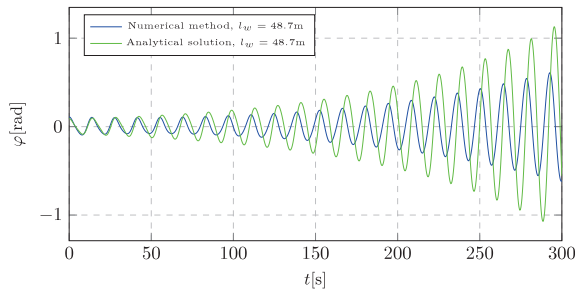


Fig. 11. Payload pendulation comparative results for a numerical and analytical solution (elliptical excitation at pivot point for  $A_y = 0.5\text{ m}$ ,  $A_z = 1\text{ m}$ , resonant cable length).

This is the result of the assumption made (a constant mean frequency value), resulting in a local loss of a faithful mapping of the nonlinear character of the approximate waveform.

On the same basis of previous sets of parameters and excitations forms, the authors prepared correspondingly the next two sets of comparisons. Figs. 11 and 12 reveal not only a slight difference in quantitative results comparing to the results obtained without the lateral crane tip motion (Figs. 9, 10) but also a clear qualitative difference in the results can be noticed. The waveform character is mainly changed in the initial phase of the payload motion where some slope of the responses can be noticed. Notwithstanding this difference in system response, it can still be concluded that the approximate analytical solution faithfully maps the nature of the numerical one.

Figs. 13 and 14 confirm the correctness of mapping the nonlinear numerical model result, however, they reveal the relationship showing that the greater the amplitude of the lateral and vertical movements, the greater the divergences between the results for the applied approximation order of the analytical solution.

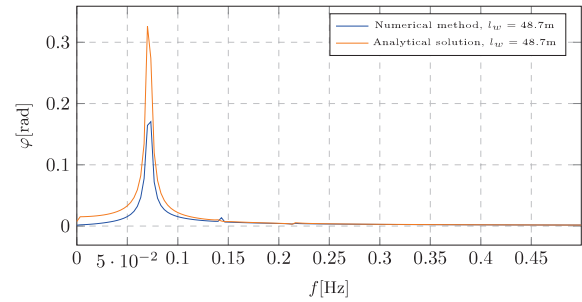


Fig. 12. Spectral analysis for a numerical and analytical solution (elliptical excitation at pivot point for  $A_y = 0.5\text{ m}$ ,  $A_z = 1\text{ m}$ , resonant cable length).

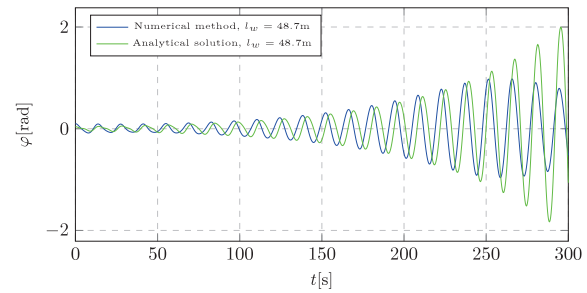


Fig. 13. Payload pendulation comparative results for a numerical and analytical solution (elliptical excitation at pivot point for  $A_y = 0.5\text{ m}$ ,  $A_z = 1.5\text{ m}$ , resonant cable length).

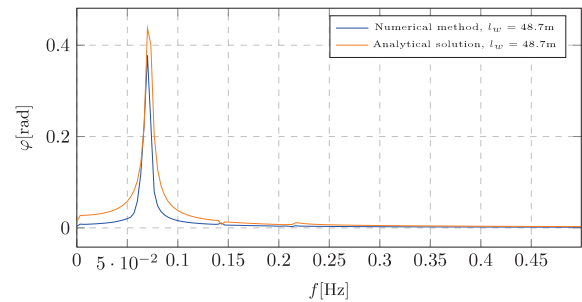


Fig. 14. Spectral analysis for a numerical and analytical solution (elliptical excitation at pivot point for  $A_y = 0.5\text{ m}$ ,  $A_z = 1.5\text{ m}$ , resonant cable length).

The comprehensiveness of the proposed method of seeking the approximate analytical solution might be proven in a comparative analysis of numerically integrated results vs. analytically derived solutions. The evidence on the approximated results accuracy and its potential use in operation planning is presented in Figs. 15 and 16 where one can study the results of the lifted object dynamic behaviour presented as a direct confrontation of the magnitudes reached by the analysed models in a wide range of lifting cable lengths. The comparison was performed for numerous scenarios of two different excitation frequencies  $T = 7\text{ s}$  and  $T = 8\text{ s}$  and some of the results obtained are reported in Tables 1 and 2. The results cover a range of two resonant states and a wide span of cable lengths in the out-of-resonance zone.

As one might have noticed, the analytical solution provides more conservative responses resulting in slightly higher amplitude values. However, the discrepancy between the magnitude values is that small it can be considered negligible. Based on this feature of the proposed approach, the solution might be used to evaluate whether the payload dynamics remains stable, unstable or is on a stability limit during



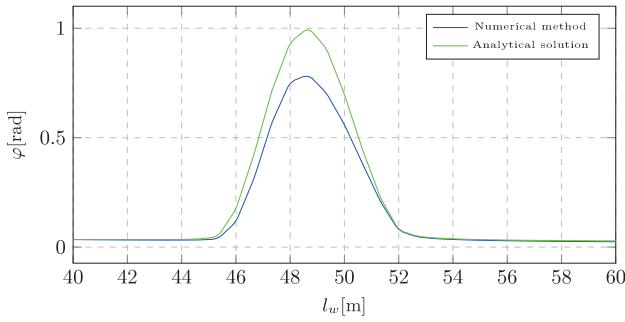


Fig. 15. Results of a comparative analysis between the analytical and numerical solution  $T = 7$  s.

Table 1

Results of a comparative analysis between the solutions for some individual cable lengths  $T = 7$  s.

$l_w$ [m]	$\varphi_N$ [rad]	$\varphi_A$ [rad]	$\Delta$
40.0	0.034304	0.034762	0.013338
42.0	0.032611	0.033898	0.039487
44.0	0.032023	0.035141	0.097378
46.0	0.114526	0.173209	0.512407
48.0	0.754781	0.934904	0.238643
50.0	0.559561	0.697607	0.246705
52.0	0.075130	0.077470	0.031142
54.0	0.034651	0.037803	0.090977
56.0	0.028955	0.032293	0.115259
58.0	0.026170	0.029623	0.131960
60.0	0.024310	0.028240	0.161669

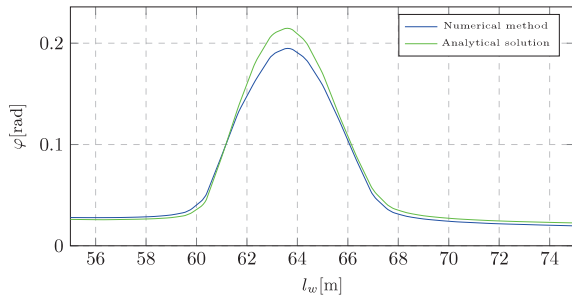


Fig. 16. Results of a comparative analysis between the analytical and numerical solution  $T = 8$  s.

planning process of a lifting operation. Detailed comparative results are presented in Table 1 for a wave period  $T = 7$  s.

Even more accurate mapping can be observed for a longer wave period  $T = 8$  s resulting in longer cable lengths and thus lower payload amplitude values. The detailed comparative results are reported in Fig. 16 and in Table 2.

Apart from a very good convergence obtained during direct comparison of the simulation results for both solutions in time and frequency domains, one should also mention the significant advantage coming from a utilisation of an analytical solution when a series of simulations are performed. The evaluation of results based on the analytical method consists of the numeration of the symbolic form solution for subsequent simulations, eg. when assuming the variability of the analysed parameters. This makes the process of obtaining a single numerized result much faster than when dealing with integrating schemes, where a new, single numerical solution is created during each simulation. The CoCalc computing cloud was utilised for the numerical investigation. The set up of the environment was as follows: - Intel's Xeon processor (4 cores - 2.8 GHz per core), 32 GB RAM. There was no support of

Table 2

Results of a comparative analysis between the solutions for some individual cable lengths  $T = 8$  s.

$l_w$ [m]	$\varphi_N$ [rad]	$\varphi_A$ [rad]	$\Delta$
55.0	0.027944	0.026108	-0.065697
57.0	0.027944	0.026005	-0.069377
59.0	0.030353	0.027748	-0.085847
61.0	0.089145	0.087608	-0.017249
63.0	0.189172	0.209292	0.106357
65.0	0.158835	0.170381	0.072692
67.0	0.049193	0.054613	0.110180
69.0	0.026453	0.029598	0.118920
71.0	0.022860	0.025657	0.122361
73.0	0.021046	0.023773	0.129557
75.0	0.019703	0.022607	0.147368

Table 3

Comparative results of computing times for the analysed algorithms.

$l_w$ [m]	Computing time [s]	Analytical solution
	Numerical method	
40.0	0.843940	0.008568
44.0	0.879129	0.008747
48.0	0.826232	0.008472
52.0	0.894133	0.011800
56.0	0.897533	0.008663
60.0	1.082685	0.008101

GPU card. Approximately 1000 simulations were performed in order to get averaged results. Examples of simulation times for solutions of both methods are presented in Table 3.

However, it should be remembered that the determination process of an analytical solution is a time-consuming and complicated process with a significant entry point for an inexperienced user.

### 5.1. Comparison of linearised and nonlinear solution

In order to emphasise an importance of choosing and utilising the appropriate model and its solution, the authors prepared a comparative analysis. The study was performed in order to investigate whether the complex nonlinear solution could be replaced with simpler linearised one, drastically reducing the formulation complexity. Fig. 17 demonstrates the trajectories of both solutions for the discussed model performed for out-of-resonance cable length ( $l_w = 35$  m,  $T = 7$  s).

Based on the previous simulation results and including the results presented in Fig. 17 it can be stated that the linearisation of the model allows for a reliable prediction of a resonance occurrence. It is also clearly noticeable that for non-resonant states only the nonlinear models capture the real character of the payload's dynamic behaviour. Based on the results provided, the linear model can be successfully utilised in order to evaluate the regions of resonance occurrence (lifting cable lengths determination for given amplitudes and frequencies of excitation). However, it is too much of a simplification that could lead to significant errors in the evaluation of the dynamics of the lifted object when planning the operation. This particular difference can be seen clearly by the divergences in the two blue payload trajectories. As might be expected, the error in the results of the comparative solutions decreases as more nonlinear terms are added to the equation of motion.

## 6. Conclusions

Concluding the paper, the aim of introducing a simplified but comprehensive nonlinear model for an excited hanging object was achieved. In this work, an analytical approximation of the governing equation was derived applying the perturbation method allowing the equation of motion to be represented by a superposition of linear and

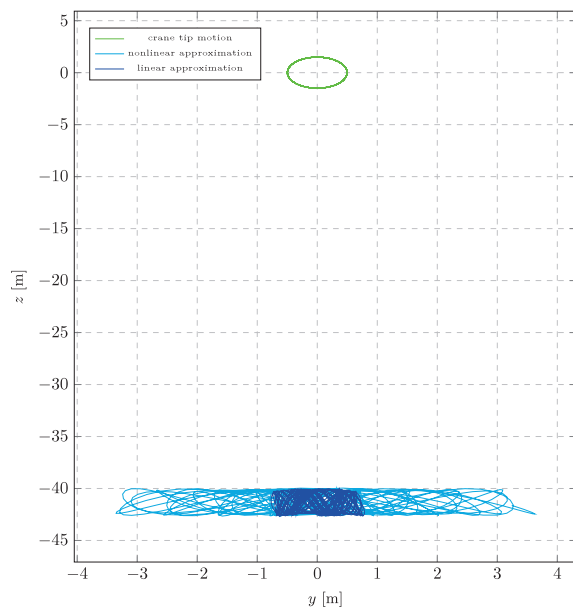


Fig. 17. Payload trajectories for a linear and nonlinear approximated analytical solutions. (For interpretation of the references to colour in this figure legend, the reader is referred to the web version of this article.)

nonlinear components. Utilisation of the linear part allows for convenient computations of eigenvalues and eigenmodes for the considered system.

The proposed analytical model allows description of the lifting dynamics in a more interpretable form by exposing the influence factors in the analysis formulas. This enables better targeting at the design stage and might provide interesting insights into control system design. Moreover, having the analytical model and its closed solution form for the equation of motion, aids the analysis process by supporting the numerical processing requirement as well as provides a tool for generalisation and perhaps standardisation of the early stage lifting process design tool.

Furthermore, a unique representation of the equations of motion in the form of vectors representing different but ordered types of mathematical terms indicates the nature of occurring phenomena and assign them a physical context. This may allow for a better understanding of governing laws especially in terms of the contributors disturbing stability of the lifted objects. It should be noted that the analysis of the governing equations shows a lack of coupling between heave motion and payload pendulation, even in the field of nonlinear vibrations. This allows the use of separate models for both of these movements. None of the previously encountered research papers did exhibit an evident reason behind this assumption.

The analysis indicates that the analytical approximation provides a good estimate for a nonlinear model nevertheless the results provided for the linearised model reveal difficulties in mapping accurately the system dynamics within all of the dynamic states. The linearisation can be successfully utilised to evaluate the regions of resonance occurrence, however, it is too much of a simplification that could lead to significant errors in the evaluation of the dynamics of the hanged object when planning the operation.

Application of a perturbative method with regards to seeking the analytical formulation of the solution is related to some disadvantages. Due to the nature of the analysis, the process requires an identification and removal of secular terms. Consequently, it causes the terms associated with the lateral excitation to be omitted which introduces inaccuracy of the obtained results. Therefore, the awareness of choosing

a suitable method of investigating the analytical solution needs to be highlighted.

Despite the condition of a requirement of a good knowledge of nonlinear vibration's theory, the authors found the biggest advantages in the following methodology's features:

- the analytical approach provides an explicit function determining the payload dynamic behaviour. That allows the analysis of the parameters constituting the vibrations of the object in terms of their selection in order to 'control' the payload response. Industrially, the methodology offers an efficient recognition of a potentially problematic scenario at early conceptual stages. Additionally, it can constitute an additional step in a verification of numerical results. Ultimately, in simpler cases, it can replace the numerical approaches completely.
- the presented algorithm is also preferable in terms of performing a significant number of simulations. The evaluation of a single result is much faster (Table 3) due to the numeration of the already existing symbolic function of time. The process of numeration requires much less time investment and computational resource in order to execute in a contrary to commonly used integrating schemes in which a new, single numerical solution is created during each simulation. It also gives an advantage when simulating scenarios assuming the variability of the analysed parameters.
- in order to access the stability regions (in terms of planning the system operation), the presented methodology does not require a full analysis of the considered system dynamics. The information provided by the conditions for a removal of the secular terms (the constants  $C_1(t_1)$  and  $C_2(t_1)$ ) allows for a determination of stable and unstable zones.

An assumption made in order to simplify the procedure of determination of an analytical solution based on the adopted multiple-scale method, introduced a slight discrepancy in a vibration frequency value. The adopted simplification assumes mean (constant) value of  $\omega$  for the nonlinear first term approximation, however it leads also to a significant increase of time efficiency in terms of seeking the solution at the expense of small, local phase discrepancies. It is worth noting that a consideration of successive approximations to the solution will not result in a significant improvement in the quality of results, and the quantitative changes will only be slight. The results presented confirm already a very good correspondence between the analytical approximation and the numerically integrated response. The differences in amplitude values are the results of secular terms removal process but it can be reduced and the convergence improved by manipulation of initial conditions. However, despite the linearisation in the neighbourhood of 0 point, which is rather a significant simplification, the dynamics of the phenomenon is still faithfully reproduced ensuring a good convergence of the results.

#### CRediT authorship contribution statement

**Bogumil Chilinski:** Conceptualization, Methodology, Software, Validation, Formal analysis, Writing – original draft, Supervision, Investigation. **Anna Mackojc:** Conceptualization, Methodology, Validation, Formal analysis, Investigation, Project administration, Data curation, Writing – original draft, Writing – review & editing, Visualization, Project administration. **Krzysztof Mackojc:** Writing – review & editing.

#### Declaration of competing interest

The authors declare that they have no known competing financial interests or personal relationships that could have appeared to influence the work reported in this paper.

## Data availability

Data will be made available on request.

## Appendix

Numerical First-order Term Approximation (see Table A.1)

$$\begin{aligned}
 Y(t) = & 0.047e^{\frac{\sqrt{5}\pi t}{672}} \sin\left(\frac{\pi t}{7}\right) + 1.4 \cdot 10^{-7} e^{\frac{\sqrt{5}\pi t}{672}} \sin\left(\frac{3\pi t}{7}\right) \\
 & - 0.00036e^{\frac{\sqrt{5}\pi t}{672}} \sin\left(\frac{5\pi t}{7} + 0.315\right) \\
 & + 2.4 \cdot 10^{-8} e^{\frac{\sqrt{5}\pi t}{672}} \sin\left(\frac{5\pi t}{7} + 0.315\right) \\
 & + 0.031e^{\frac{\sqrt{5}\pi t}{672}} \cos\left(\frac{\pi t}{7}\right) + 1.8 \cdot 10^{-7} e^{\frac{\sqrt{5}\pi t}{672}} \cos\left(\frac{3\pi t}{7}\right) \\
 & - 0.00023e^{\frac{\sqrt{5}\pi t}{672}} \cos\left(\frac{3\pi t}{7} + 0.315\right) + 2.9 \\
 & \cdot 10^{-8} e^{\frac{\sqrt{5}\pi t}{672}} \cos\left(\frac{5\pi t}{7} + 0.315\right) - 9.6 \\
 & \cdot 10^{-7} e^{\frac{\sqrt{5}\pi t}{336}} \sin\left(\frac{4\pi t}{7} - 2.396\right) - 1.0 \\
 & \cdot 10^{-5} e^{\frac{\sqrt{5}\pi t}{336}} \cos\left(\frac{2\pi t}{7} - 2.396\right) + 4.2 \\
 & \cdot 10^{-7} e^{\frac{\sqrt{5}\pi t}{336}} \cos\left(\frac{4\pi t}{7} - 2.396\right) + 1.4 \\
 & \cdot 10^{-5} e^{\frac{\sqrt{5}\pi t}{336}} + 1.8 \cdot 10^{-8} e^{\frac{\sqrt{5}\pi t}{224}} \sin\left(\frac{3\pi t}{7}\right) \\
 & + 1.4 \cdot 10^{-7} e^{\frac{\sqrt{5}\pi t}{224}} \sin\left(\frac{3\pi t}{7} + 0.315\right) \\
 & + 2.9 \cdot 10^{-9} e^{\frac{\sqrt{5}\pi t}{224}} \sin\left(\frac{5\pi t}{7} + 0.315\right) \\
 & - 1.1 \cdot 10^{-7} e^{\frac{\sqrt{5}\pi t}{224}} \cos\left(\frac{3\pi t}{7}\right) + 8.8 \\
 & \cdot 10^{-8} e^{\frac{\sqrt{5}\pi t}{224}} \cos\left(\frac{3\pi t}{7} + 0.315\right) - 1.8 \\
 & \cdot 10^{-8} e^{\frac{\sqrt{5}\pi t}{224}} \cos\left(\frac{5\pi t}{7} + 0.315\right) + 4.6 \\
 & \cdot 10^{-7} \sin\left(\frac{4\pi t}{7} - 2.396\right) + 0.014 \cos\left(\frac{2\pi t}{7} - 2.396\right) \\
 & - 1.4 \cdot 10^{-6} \cos\left(\frac{4\pi t}{7} - 2.396\right) - 2.0 \\
 & \cdot 10^{-5} + 2.6 \cdot 10^{-8} e^{-\frac{\sqrt{5}\pi t}{224}} \sin\left(\frac{3\pi t}{7}\right) \\
 & - 5.4 \cdot 10^{-8} e^{-\frac{\sqrt{5}\pi t}{224}} \sin\left(\frac{3\pi t}{7} + 0.315\right) \\
 & + 4.4 \cdot 10^{-9} e^{-\frac{\sqrt{5}\pi t}{224}} \sin\left(\frac{5\pi t}{7} + 0.315\right) \\
 & - 2.6 \cdot 10^{-8} e^{-\frac{\sqrt{5}\pi t}{224}} \cos\left(\frac{3\pi t}{7}\right) + 1.4 \\
 & \cdot 10^{-8} e^{-\frac{\sqrt{5}\pi t}{224}} \cos\left(\frac{3\pi t}{7} + 0.315\right) - 4.4 \\
 & \cdot 10^{-9} e^{-\frac{\sqrt{5}\pi t}{224}} \cos\left(\frac{5\pi t}{7} + 0.315\right) \\
 & + 2.6 \cdot 10^{-7} e^{-\frac{\sqrt{5}\pi t}{336}} \sin\left(\frac{4\pi t}{7} - 2.396\right) \\
 & - 5.1 \cdot 10^{-6} e^{-\frac{\sqrt{5}\pi t}{336}} \cos\left(\frac{2\pi t}{7} - 2.396\right) + 4.4 \\
 & \cdot 10^{-7} e^{-\frac{\sqrt{5}\pi t}{336}} \cos\left(\frac{4\pi t}{7} - 2.396\right) + 2.3 \\
 & \cdot 10^{-6} e^{-\frac{\sqrt{5}\pi t}{336}} - 0.038e^{-\frac{\sqrt{5}\pi t}{672}} \sin\left(\frac{\pi t}{7}\right) \\
 & - 1.6 \cdot 10^{-7} e^{-\frac{\sqrt{5}\pi t}{672}} \sin\left(\frac{3\pi t}{7}\right) \\
 & + 0.00029e^{-\frac{\sqrt{5}\pi t}{672}} \sin\left(\frac{3\pi t}{7} + 0.315\right)
 \end{aligned}$$

Table A.1

Design parameters used in simulations.

	Parameter	Corresponding value
Swaying motion	$y_e$	$A_y \cos(\omega t - 2.396)$
Heaving motion	$z_e$	$A_z \cos(\omega t + 0.315)$
Lateral amplitude	$A_y$	0 m to 0.5 m
Vertical amplitude	$A_z$	1 m to 1.5 m
Lifting set length	$l_w$	35 m to 75 m
Epsilon	$\varepsilon$	$\frac{1}{l_w}$
Delta coefficient	$\delta$	$\frac{4g}{l_w \omega^2 \varepsilon} - \frac{1}{\varepsilon}$
Exciting frequency	$\omega$	$\frac{1}{T}$ rad s <sup>-1</sup>
Wave period	$T$	7 s to 8 s
Payload mass	$m_p$	100 t
Compensator mass	$m_c$	10 t
Crane stiffness	$k_{cs}$	5000 kN m <sup>-1</sup>
Equivalent stiffness	$k_{eq}$	3980 kN m <sup>-1</sup>
Young modulus	$E$	92 GPa
Cable diameter	$d_w$	0.10 m

$$\begin{aligned}
 & - 2.6 \cdot 10^{-8} e^{-\frac{\sqrt{5}\pi t}{672}} \sin\left(\frac{5\pi t}{7} + 0.315\right) \\
 & + 0.01e^{-\frac{\sqrt{5}\pi t}{672}} \cos\left(\frac{\pi t}{7}\right) - 8.3 \\
 & \cdot 10^{-9} e^{-\frac{\sqrt{5}\pi t}{672}} \cos\left(\frac{3\pi t}{7}\right) - 7.8 \\
 & \cdot 10^{-5} e^{-\frac{\sqrt{5}\pi t}{672}} \cos\left(\frac{3\pi t}{7} + 0.315\right) - 1.4 \\
 & \cdot 10^{-9} e^{-\frac{\sqrt{5}\pi t}{672}} \cos\left(\frac{5\pi t}{7} + 0.315\right)
 \end{aligned}$$

## References

- Chilinski, B., Mackojc, A., Zalewski, R., Mackojc, K., 2020. Proposal of the 3-DOF model as an approach to modelling offshore lifting dynamics. *Ocean Eng.* 203, 287–314.
- Čorić, V., Čatipović, I., Slapničar, V., 2014. Floating crane response in sea waves. *Brodogr.: Teor. Praksa Brodogr. Pomor. Teh.* 65 (2), 111–120.
2017. Recommended Practice N103 Modelling and Analysis of Marine Operations. DET NORSKE VERITAS GL, Sec.9.2 – 9.3.
- Ellermann, K., Kreuzer, E., Markiewicz, M., 2002. Nonlinear dynamics of floating cranes. *Nonlinear Dynam.* 27 (2), 107–183.
- Fossen, T., Nijmeijer, H., 2012. *Parametric Resonance in Dynamical Systems*. Springer Science & Business Media.
- Ghigliazza, R., Holmes, P., 2002. On the dynamics of cranes, or spherical pendula with moving supports. *Int. J. Non-Linear Mech.* 37 (7), 1211–1221.
- Horton, B., Sieber, J., Thompson, J., Wiercigroch, M., 2011. Dynamics of the nearly parametric pendulum. *Int. J. Non-Linear Mech.* 46 (2), 436–442.
- Horton, B., Wiercigroch, M., Xu, X., 2008. Transient tumbling chaos and damping identification for parametric pendulum. *Philos. Trans. R. Soc. Lond. Ser. A Math. Phys. Eng. Sci.* 366 (1866), 767–784.
- Hunter, J.K., 2004. *Asymptotic Analysis and Singular Perturbation Theory*. Department of Mathematics, University of California at Davis, pp. 1–3.
- Kang, H.-S., Tang, C.H.-H., Quen, L.K., Steven, A., Yu, X., 2016. Prediction on parametric resonance of offshore crane cable for lowering subsea structures. In: 2016 IEEE International Conference on Underwater System Technology: Theory and Applications (USYS). IEEE, pp. 165–170.
- Kang, H.-S., Tang, C.H.-H., Quen, L.K., Steven, A., Yu, X., 2017. Parametric resonance avoidance of offshore crane cable in subsea lowering operation through A\* heuristic planner.
- Kholostova, O., 2009. On the motions of a double pendulum with vibrating suspension point. *Mech. Solids* 44 (2), 184–197.
- Kovacic, I., Rand, R., Mohamed Sah, S., 2018. Mathieu's equation and its generalizations: overview of stability charts and their features. *Appl. Mech. Rev.* 70 (2).
- Kuře, M., Bušek, J., Vyhřídál, T., Niculescu, S.-I., 2019. Damping oscillation of suspended payload by up and down motion of the pivot base-time delay algorithms for UAV applications. *IFAC-PapersOnLine* 52 (18), 121–126.
- Lenci, S., Pavlovskaja, E., Rega, G., Wiercigroch, M., 2008. Rotating solutions and stability of parametric pendulum by perturbation method. *J. Sound Vib.* 310 (1–2), 243–259.
- Lenci, S., Rega, G., 2008. Competing dynamic solutions in a parametrically excited pendulum: attractor robustness and basin integrity. *J. Comput. Nonlinear Dyn.* 3 (4).

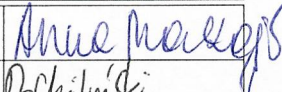
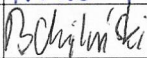
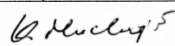
- Náprstek, J., Fischer, C., 2009. Auto-parametric semi-trivial and post-critical response of a spherical pendulum damper. *Comput. Struct.* 87 (19–20), 1204–1215.
- Nayfeh, A.H., Balachandran, B., 2008. *Applied Nonlinear Dynamics: Analytical, Computational, and Experimental Methods*. John Wiley & Sons.
- Pavlovskaja, E., Horton, B., Wiercigroch, M., Lenci, S., Rega, G., 2012. Approximate rotational solutions of pendulum under combined vertical and horizontal excitation. *Int. J. Bifurcation Chaos* 22 (05), 1250100.
- Sah, S.M., Mann, B., 2012. Transition curves in a parametrically excited pendulum with a force of elliptic type. *Proc. R. Soc. Lond. Ser. A Math. Phys. Eng. Sci.* 468 (2148), 3995–4007.
- Sofroniou, A., Bishop, S., 2014. Dynamics of a parametrically excited system with two forcing terms. *Mathematics* 2 (3), 172–195.
- Xu, X., Wiercigroch, M., 2007. Approximate analytical solutions for oscillatory and rotational motion of a parametric pendulum. *Nonlinear Dynam.* 47 (1–3), 311–320.
- Yurchenko, D., Alevras, P., 2014. Stability, control and reliability of a ship crane payload motion. *Prob. Eng. Mech.* 38, 173–179.

## AUTHORSHIP STATEMENT

As the authors of scientific article: Chiliński Bogumił, Mackojć Anna, Mackojć Krzysztof, *Analytical solution of parametrically induced payload nonlinear pendulation in offshore lifting*, Ocean Engineering, 2022, vol. 259, pp.111835. DOI:10.1016/j.oceaneng.2022.111835 published in 2022,

we state

the participation and contribution to development and presentation of the work in the form of a scientific publication is as follows:

Name and surname, academic degree	Participation in work	Signature
Anna Mackojć, MSc	50%	
Bogumił Chiliński, PhD	45%	
Krzysztof Mackojć, MSc	5%	



Warszawa, March 07, 2023

mgr inż. Anna Mackojć  
Politechnika Warszawska  
Wydział Samochodów i Maszyn Roboczych  
Instytut Podstaw Budowy Maszyn  
ul. Narbutta 84  
02-524 Warszawa

## AUTHORSHIP STATEMENT

I declare that in the work "Chiliński Bogumił, Mackojć Anna, Mackojć Krzysztof, *Analytical solution of parametrically induced payload nonlinear pendulation in offshore lifting*, Ocean Engineering, 2022, vol. 259, pp.111835. DOI:10.1016/j.oceaneng.2022.111835" my participation in the article development consisted in developing the idea of analytical and numerical research, carrying out a comprehensive literature review, theoretical analysis of the presented problem, developing a novel research methodology, determining the model and its analytical approximate solution, preparing the analysed case studies, investigating the system unstable dynamic behaviour scenarios, performing simulations, preparing the analytical and numerical software tool, model validation, analysing and interpreting the results, statistical research, formulating conclusions, writing (original draft), reviewing, editing and formatting the article text, preparing the final version before and after the review and the final editorial form of the article.

  
Signature

Warszawa, March 07, 2023

dr inż. Bogumił Chiliński  
Politechnika Warszawska  
Wydział Samochodów i Maszyn Roboczych  
Instytut Podstaw Budowy Maszyn  
ul. Narbutta 84  
02-524 Warszawa

## AUTHORSHIP STATEMENT

I declare that in the work "Chiliński Bogumił, Mackojć Anna, Mackojć Krzysztof *Analytical solution of parametrically induced payload nonlinear pendulation in offshore lifting*, Ocean Engineering, 2022, vol. 259, pp.111835. DOI:10.1016/j.oceaneng.2022.111835" my participation in the article development consisted in consultations of the scope and content, giving advice in the field of nonlinear vibration theory and analysis, suggestions and verification of a novel research methodology and approval of the proposed approach to considered problem, determining the model analytical solution, creating the analytical and numerical software tool, participation in corrections in accordance with the reviewers' guidelines, writing (original draft), supervision.

  
Signature

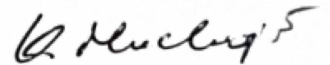
Warszawa, March 07, 2023

mgr inż. Krzysztof Mackojć  
Fathom Group Ltd.  
18 North Silver Street  
Aberdeen, AB10 1JU, Scotland  
United Kingdom of Great Britain and Northern Ireland

## AUTHORSHIP STATEMENT

I declare that in the work "Chiliński Bogumił, Mackojć Anna, Mackojć Krzysztof, *Analytical solution of parametrically induced payload nonlinear pendulation in offshore lifting*, Ocean Engineering, 2022, vol. 259, pp.111835. DOI:10.1016/j.oceaneng.2022.111835" my participation in the article development was limited to an assessment of the usability of the model in the context of applicability for engineering purposes and reviewing process.

Signature





# Preliminary research of a symmetrical controllable granular damper prototype

Anna MACKOJC<sup>✉\*</sup>, Bogumil CHILINSKI<sup>✉</sup>, and Robert ZALEWSKI<sup>✉</sup>

Institute of Machine Design Fundamentals, Warsaw University of Technology, Poland

**Abstract.** This paper concerns the problem of empirical investigation and mathematical modelling of a novel controllable damper using Vacuum Packed Particles. Vacuum Packed Particles tend to be placed among the group of so-called ‘smart structures’. The macroscopic mechanical features of such structures can be controlled by the partial vacuum parameter. The authors consider an application of Bouc-Wen model in order to represent the dynamic behaviour of the investigated device. The verification of the model response with experimental data is discussed. The Bouc-Wen model parameters identification is described.

**Key words:** granular materials; Vacuum Packed Particles; Bouc-Wen model; hysteresis loop; experimental results; model identification.

## 1. INTRODUCTION

Mechanical vibration is a common phenomenon occurring in many branches of engineering. Depending on needs, they are either a purposely generated factor necessary to implement specific technological processes or an undesirable phenomenon accompanying the operations of machines and their components. In order to reduce and control the process of vibrations, dampers are commonly used in a wide range of engineering fields.

One might distinguish general types of dampers. The interesting examples are those based on variable and controllable physical properties of magnetorheological (MR) or electrorheological (ER) fluids [1]. They belong to the group of smart materials that have been an object of an industrial and scientific interest over the years. Working principle of MR damper is based on a reaction of a mixture of oil and magnetic particles on an external magnetic field. This phenomenon ensures an external factor, which allows to control damper characteristics. It provides an interesting mechanism for the damper dynamics control [2–4] that allows us to introduce a significant adjustment of the damper response [5, 6].

Another group of controllable dampers are electrorheological fluid (ERF) dampers. The idea of this kind of devices is based on the interaction between ferromagnetic particles and an external electric field. Interesting control strategies can be applied with a utilization of ERF dampers [7]. The evidence suggest that it is possible to use it in order to control engineering structures dynamics.

Contrary to the aforementioned MR and ER fluids, a new type of smart material referred as Vacuum Packed Particles (VPP) is not yet fully recognized [8, 9]. The mechanical charac-

teristics of VPPs such as shape, stiffness or damping are easy to change and control. The term “granular material under the vacuum conditions” refers to a structure made of plastomer grains. The loose grains are enclosed in a hermetic and flexible envelope. The air is being pumped out of the hermetic container generating an underpressure causing the controllable and reversible changes in the mechanical properties of the system [10]. VPP allow to introduce innovative vibrations attenuation and control strategies thanks to their lower cost in comparison with usually utilised MR or ER materials. Many potential applications of VPP can be found as it might be applied to the elements of any shape to control their vibrations.

There are some theoretical and empirical considerations about the static response of the granular specimen on external load [11, 12]. Literature offers many examples, where VPP are used as a flexible element available to fit its outline to the specific shape of a cooperating element [13]. It is a base for numerous types of “smart” grippers, which enable us to grab and move elements with non-regular surface [14]. Moreover, this “material” can be utilized as an active element of adjustable dampers, which are competitive to MR or ERF dampers [9, 15, 16]. The biggest advantage of those structures is a relatively low manufacturing and operating cost. Concepts of tuneable elements utilising VPPs are described in some works and show efficient control strategies [11]. Regarding shaping and control of the dynamics with smart materials, the authors of [17] studied on a new type of smart structure, which is a so-called sponge particle structure (SPS). The authors proposed a method for controlling the dynamics of a slender beam filled with SPS by shaping its frequency structure by redistribution of the investigated system mass.

Many practical applications of VPP-based devices might be incorporated into medicine. A direct example of the practical utilisation of the granular damper features is a vacuum mattress – a medical device used for immobilization of patients, especially in the case of vertebra, pelvis or limb trauma [18].

\*e-mail: anna.mackojc@pw.edu.pl

Manuscript submitted 2021-02-26, revised 2021-12-15, initially accepted for publication 2022-03-04, published in June 2022.

## 2. OBJECTIVES

The aim of this paper is to preliminarily investigate a prototype of a symmetrical controllable granular damper in the numerical and empirical manner. Analysis of the concept, design of prototype and preliminary experiments are the main goals of this study. Moreover, the assumed mathematical model is proposed in order to enable further theoretical analysis and identification/validation.

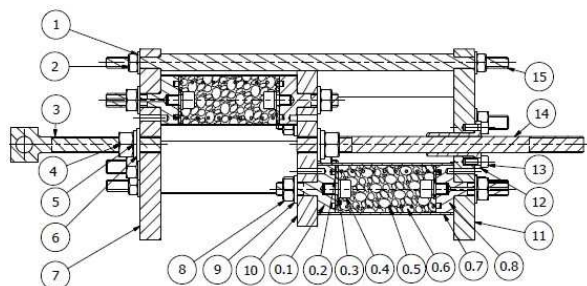
The biggest disadvantage of the existing VPP dampers designs is non-symmetrical stiffness and viscous characteristics. Such a phenomenon is caused by observed differences in loading axial forces values related to compression and elongation of the cylinder samples made of VPP [19]. Moreover, during the elongation process of the structure, the envelope plays a significant role and makes the entire structure stiffer [20]. In the case of compression, stiffness of the hermetic sleeve is several times lower (due to surface buckling) and does not affect the system under consideration. It results in a completely different resistant force for negative and positive values of damper clamps relative displacement.

In this paper an innovative construction of the VPP damper with symmetrical damping characteristics is proposed and discussed in details. The novel system with doubled VPP component on the both sides of the device is proposed. Simultaneously, one elastic element is compressed when the other is tensioned. This implies the resultant force to be always the same and having a form of a sum of tensioning and compressing components.

## 3. DAMPER PROTOTYPE

### 3.1. Prototype description

The proposed concept of a damper with symmetrical characteristics was configured as a set of granular structures. The prototype is composed of: several granular elastic elements, three plates supporting the connectors, pushing rod and thin columns which ensure the distance between outer plates and allow a proper motion of the middle plate. The last part is a slider connected with a side disk by the granular connectors. An inner plate can move to the left or right side along the columns. free connectors limit the slider motion. The described solution is presented in Fig. 1.



**Fig. 1.** Design of the granular damper prototype – cross-section view (1 – guiding rod; 2 – fixing nut; 3 – handle; 4 – nut; 5, 6 – pads; 7 – lower disc; 8 – fastening nut; 9 – cylinder nut; 10 – middle movable plate; 11 – upper plate; 13 – slider fastening nut; 14 – guiding rod; 15 – fixing nut; 0.1–0.8 – elements of the inner VPP cylinder)

The proposed prototype has a symmetric characteristics. It is assured by an appropriate connection between the side plates. When one side is compressed then the elements on the other will be tensioned. The damper operates in the negative and positive direction at the same time as the two opposite sides are actuated simultaneously. This simple solution ensures the desired behaviour eliminating the response discrepancy in tension and compression.

### 3.2. Possible applications

The former experimental results indicate the feasibility of applying VPP to control vibrations of mechanical elements. In order to damp oscillating motions of mechanical components, the granular damper prototype needs to be implemented so that the vibrating part is enclosed in a flexible envelope filled with granulated polymers or any other non-polymer granules, where the applied underpressure increases or decreases the compression of the granules, causing the system to become more or less rigid. This, in turn, increases or decreases the energy dissipation, which provides the damping control mechanism of the system vibrations. It can be stated that the properties mentioned provide the possibility to design efficient devices with an application to machine elements such as beams, rods, plates, robotic arms etc. in order to attenuate their vibrations.

When the air is pumped out of the sleeve, the generated underpressure causes the grains to compact so that the structure becomes more rigid and its internal damping, caused by the friction among the grains, increases. In this manner, one can easily and effectively control the shape, stiffness, and damping characteristics of the mechanical element.

Previous consideration indicates that mechanical properties of a granular damper are strictly connected with working principle of this device [9]. It introduces some utilization barriers for dampers based on VPP. Generally, it can be stated that granular dampers are better for slowly vibrating designs due to high friction force and possible heat production. Moreover, asymmetric hysteresis loop is a considerable limitation, which makes the application difficult [15]. However, concept presented in this work allows to omit those operational issues and enable the solution to satisfy requirements of engineering designs, especially in civil engineering structures.

Operational time of VPP-based designs is one of the most crucial problems. It is strictly connected with a wear and high friction inside the VPP structure [21]. Therefore, a wear of the damper may be neglected in short-term applications, damping buildings or bridges during an earthquake what brings some potential application also in civil engineering. Shape Memory Alloys often need to be replaced soon after the earthquake episode. However, they increase the safety level in case of an emergency [22]. Applying harder grains would address this problem but this in turn significantly changes the damper properties. Depending on working conditions filling of the VPP damper should be selected appropriately.

## 4. EXPERIMENTS

The purpose of the experimental research described in this article was to investigate the influence of changes in underpressure

value on the mechanical properties of the grain material by assessing the density of energy dissipated during one cycle.

Tests of the symmetrical granular damper prototype having the dimensions of the global cylindrical shape including 250 mm diameter and 400 mm length were carried out for a specific type of granular material. The polystyrene (PS) grains serve as a filling of the elastic connectors of damper prototype. The single grain has mechanical properties as specified in Table 1.

**Table 1**

Physical properties of the granulates used in experimental investigation

Polystyrene properties		Polystyrene properties	
Young modulus [GPa]	3.2	Tensile strength [MPa]	55
Shear modulus [GPa]	1.2	Break elongation [%]	3
Bulk modulus [GPa]	3.4	Dimensions [mm]	3
Poisson's ratio [–]	0.33	Density [g/cm <sup>3</sup> ]	1

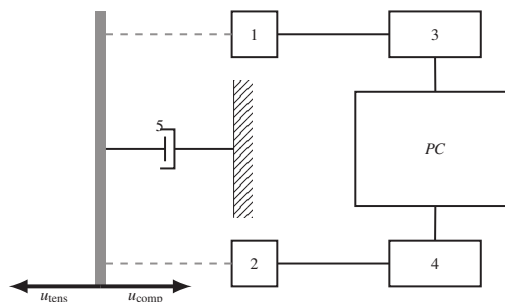
The experimental studies were carried out on the SHIMADZU EZ-LX testing machine equipped with a force load cell of a maximum 5000 N depicted in Fig. 2. The prototype of the symmetrical damper was mounted in clamps – one being fixed and the other movable, through which sine kinematic excitation was applied. The tests were carried out for underpressure value being in range of 0 MPa to 0.09 MPa. During the experiments, specified displacement and velocity of the exciter were applied, while a force and the actual displacement and velocity of the clamp were measured in time. Results in the form of a hysteresis loops for the granular material type tested at various underpressures are presented and discussed further in the article.



**Fig. 2.** Test stand

The measuring system utilised during the tests is presented on the scheme in Fig. 3. The measuring system is composed of two simultaneously operating sensors depicted as 1 and 2 in Fig. 3. First device measures the displacement of the specimen moving clamp. Force measurement are performed using

the piezoelectric force sensor being able to register the force in a range of 10 N to 5000 N. Both detectors were plugged to DAQ devices presented as 3 and 4. These are analog-digital converters with sampling frequency of 1024 Hz connected to a computer (PC) for data acquisition.



**Fig. 3.** Scheme of the measuring system used. 1 – displacement sensor, 2 – force sensor, 3, 4 – DAQ devices, 5 – investigated damper,  $u_{tens}$  – facing of tensioning of a specimen,  $u_{comp}$  – facing of compressing of a specimen

The experimental results are provided in Figs. 5–6. For the identification purposes, only one loop for arbitrary values of the underpressure was analysed. The reference cycle was obtained by averaging of five periods of the recorded signals. During this process, a standard deviation was estimated for the results obtained. All of the errors are presented in Table 2, where MAX is a maximum value of the analysed parameter,  $\Delta$  stands for deviation of the analysed parameter,  $|\Delta|$  represents an absolute error and the last column is a total error of the tests performed.

**Table 2**

Measurement errors for the data acquisition system parameters

	MAX	$\Delta$	$ \Delta $	Total error
$F$ [N]	800	30	4	30.3
$x$ [mm]	44 (40 initial)	0.02	0.22	0.22

The results are presented in a form of force diagrams as a function of displacement  $F(x)$  and velocity  $F(\dot{x})$ , grouped so that the effect of the applied underpressure can be observed in both types of hysteretic characteristics ( $F(x)$ ,  $F(\dot{x})$ ) of the analysed symmetrical granular damper for various combinations of granules.

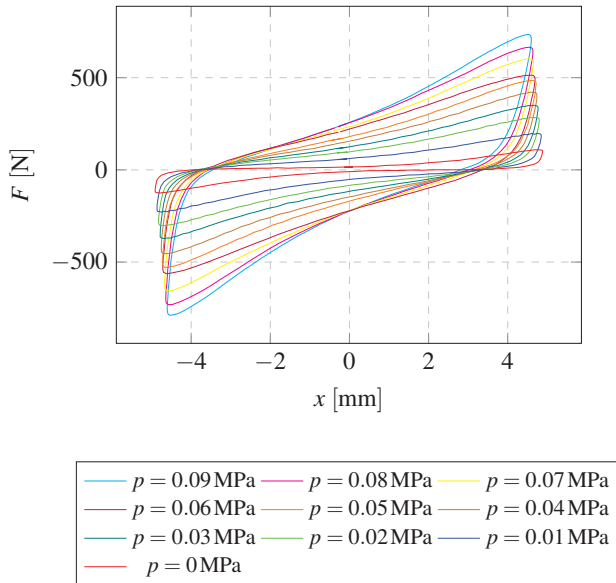
#### 4.1. VPP damper filled with PS granules

In experimental studies the authors used the polystyrene granules shown in Fig. 4. Polystyrene is a granulate characterised with various visco-elastic properties which reflects in a much higher Young modulus, compressive strength and coefficient of friction comparing to other types of materials. In addition, one might observe that the granules have uniform dimensions and shapes, which results in a significant influence of the clusters occurring inside the sealed housing of the VPP damper.

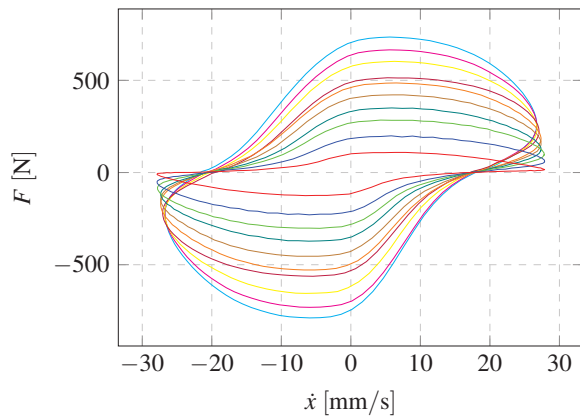
Figures 5 and 6 depict the experimental results. The tests were carried out to cover various values of underpressure.



**Fig. 4.** VPP damper filled with polystyrene



**Fig. 5.** Hysteresis loops registered for a variety of underpressure values for PS type of material (displacements)



**Fig. 6.** Hysteresis loops registered for a variety of underpressure values for PS type of material (velocities)

Based on data presented in Figs. 5 and 6 it can be stated that polystyrene granules allowed us to obtain quite high values of damping forces. However, the utilisation of this material might cause some potential operational problems as some powdered polystyrene material was found inside the damper after many

compression cycles. This is a result of crushing the polystyrene granule which in further exploitation may lead to a reduction in the value of damping force as a function of the load cycles number carried out. In Fig. 4 one might notice some accumulation of the granular material in the central part of the damper. This phenomenon causes not only a reduction of damping force but an occurrence of the so-called dead zone at the damper operational range being a result of empty spaces between the two damper bases besides the granular material. These two phenomena affect the damper dissipative capability unfavourably and cause problems with sealing and durability of the matrix.

## 5. PROPOSITION OF BOUC-WEN MODEL UTILIZATION

Modelling of metamaterials as VPP is a complex mechanical and mathematical problem. It is necessary to deal with a structure, which is composed of a large number of particles that then need to be simplified to enable engineering calculations. The Finite Elements Analysis or Discrete Elements Method are then commonly utilized. It is an explanation why phenomenological models could be interesting and useful [23].

Non-linear Bouc-Wen model of a damper was proposed in this paper. It is a single degree of freedom system with a linear damping coefficient and non-linear elastic force [24]. The model under consideration is characterized by two main elements: restoring action and hysteresis loop. It models elastic and hysteretic component by two different factors of the restoring force, which are fixed for the assumed system parameters. In this work, an extra dependency between VPP parameters was introduced which makes the proposed model sensitive to underpressure and grains physical parameters.

The mathematical model of the damper under consideration is as follows:

$$m\ddot{x}(t) + c\dot{x}(t) + F(x(t), t) = f(t), \quad (1)$$

where:  $t$  – time,  $x(t)$  – displacement,  $m$  – oscillating mass,  $c$  – damping coefficient,  $F(x(t), t)$  – nonlinear elastic force,  $f(t)$  – resultant external force.

According to Bouc-Wen model, a decomposition of the restoring force  $F(t)$  can be done. Two parts components are distinguished, an elastic  $F^{el}(t)$  and a hysteretic  $F^h(t)$  force described as per the following formulas:

$$F(x(t), t) = F^{el}(t) + F^h(t), \quad (2)$$

$$F^{el}(t) = ak_i x(t), \quad F^h(t) = (1 - a)k_i z(t), \quad (3)$$

where:  $z(t)$  – non-observable hysteretic parameter,  $a$  – ratio of post-yield  $k_f$  to pre-yield  $k_i$  stiffness,  $k_i$  – ratio of the yield force to the yield displacement.

The hysteretic displacement  $z(t)$  is compliant with the following non-linear differential equation having a zero initial condition ( $z(0) = 0$ ):

$$\dot{z}(t) = \dot{x}(t) \{A - [\beta \text{sign}(z(t))\dot{x}(t) + \gamma]|z(t)|^n\}, \quad (4)$$

where:  $A$ ,  $\beta$ ,  $\gamma$ ,  $n$  – dimensionless quantities controlling a behaviour of the considered model.



It was assumed that the influence of pressure and grains arrangement on the system dynamics can be described by an elastic component  $F^{el}(t) = F(x(t), t)$  only. The numerical simulations can be performed based on the proposed model. Preliminary analysis shown that the model is sensitive to underpressure and operation time parameters [20]. Moreover, the proposed methodology of modelling can be efficient as it was presented in different studies [25]. Because of relative simplicity of the proposed model, it is proved that it can be successfully applied for a numerical and empirical data comparison. As a result of this process, the system equivalent parameters can be identified.

## 6. NUMERICAL VERIFICATION

The dynamic model of the granular damper prototype considered within the article is determined by a second order ordinary differential equation (1). The transformation of the formula to the first order form enables its implementation to the numerical solver utilising some integrating method. The results of the integration provide a basic information about the system dynamic behaviour. The ordinary differential equation was solved using the Isoda from the FORTRAN library odepack.

Based on that, numerical simulations of the investigated model prototype were carried out. The results of the numerical research are provided and discussed further within this section.

Results of the simulations carried out are depicted in Figs. 7 and 8. It is evident that a non-linear part of Bouc-Wen model

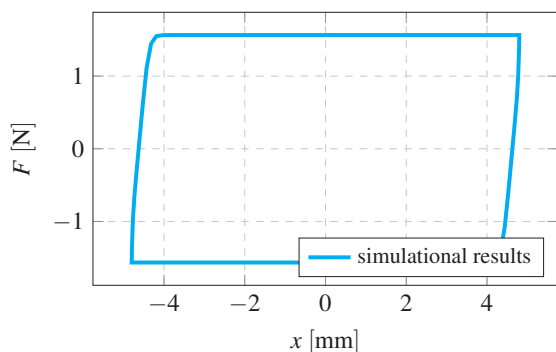
enables the non-elastic properties of the considered material. From the modelling point of view, the proposed approach is especially useful for high values of  $n$  and  $\beta$  parameters - obtained results are close to behaviour of materials with a constant yield limit (bilinear characteristic). In order to estimate applied model parameters the following methodology further described in this subsection was used. For empirical results stiffness of the entire system was assumed. Based on that parameter, series of simulations were carried out with displacements and velocities based on the experimental data. For the computed values, a relative RMS (Root Mean Square) error was calculated with a utilisation of formula (5).

$$RMS = \sqrt{\frac{\sum_{i=1}^N F_{emp}(x_i)^2 - F_{B-W}(x_i)^2}{\sum_{i=1}^N F_{emp}(x_i)^2}}, \quad (5)$$

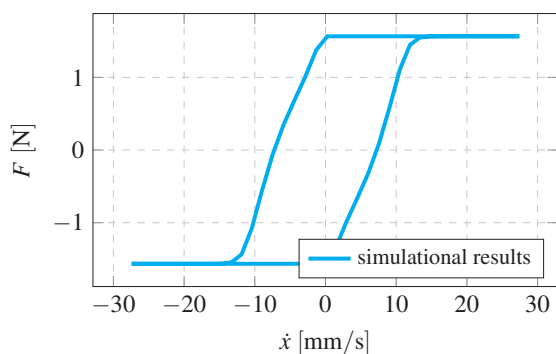
where:  $x_i$  – damper linear deformation for  $i$  step,  $N$  – number of probes,  $F_{emp}(x)$  – force value obtained during experiment,  $F_{B-W}(x)$  – computational force value.

The best results are presented in Figs. 9–16.

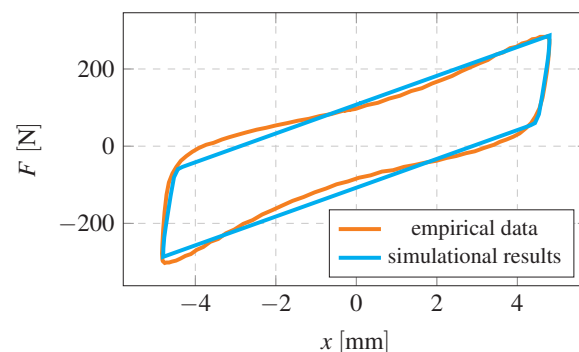
The conducted simulations outcome depicted in Figs. 9 and 10 show that for the assumed parameters of Bouc-Wen model, the obtained results are close to the empirical data. Some discrepancies are connected with the additional non-linear or dynamic effects, which cannot be taken into account in the proposed approach. Still, the computed values model the prototype in an acceptable way. The total RMS error was smaller than 0.01.



**Fig. 7.** Hysteresis loop for a B-W model parameters values  $a = 0.35$ ,  $A = 6$ ,  $\beta = 3.5$ ,  $\gamma = -2.5$ ,  $n = 4$



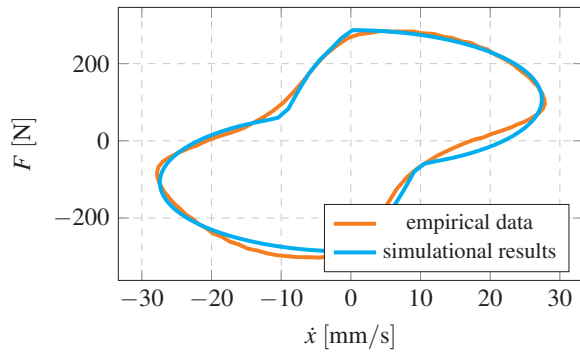
**Fig. 8.** Hysteresis loop for a B-W model parameters values  $a = 0.35$ ,  $A = 6$ ,  $\beta = 3.5$ ,  $\gamma = -2.5$ ,  $n = 4$



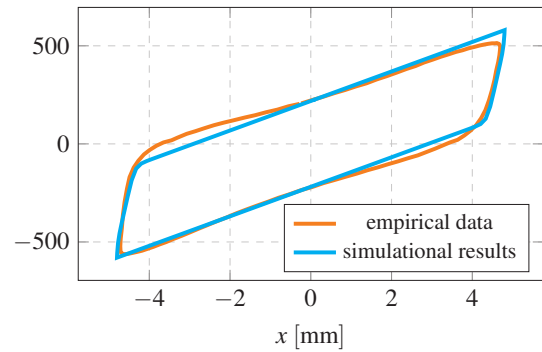
**Fig. 9.** Experimental hysteresis loop for  $p = 0.02$  MPa; B-W model identified for the following parameters:  $a = 0.36$ ,  $A = 9$ ,  $\beta = 4$ ,  $\gamma = -3$ ,  $n = 5$

Results presented in Figs. 11 and 12 correspond to the effects of the previous simulations. Some discrepancies from the experiment are still visible but generally acceptable as the total RMS error was smaller than 0.006. It is evident that for the subsequent underpressure, the corresponding force extreme values are higher and that the proposed method model its behaviour accurately despite slight divergence.

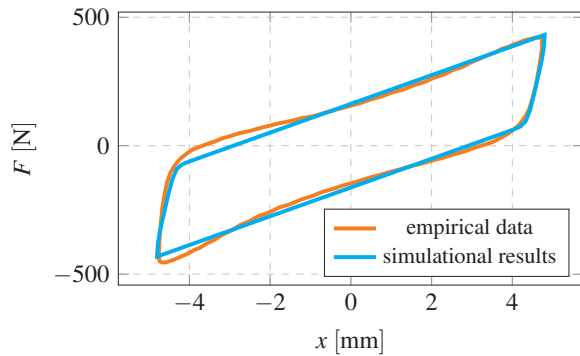
The results of simulations for underpressure equals  $p = 0.06$  MPa (Figs. 13 and 14) indicate subsequent increasing of



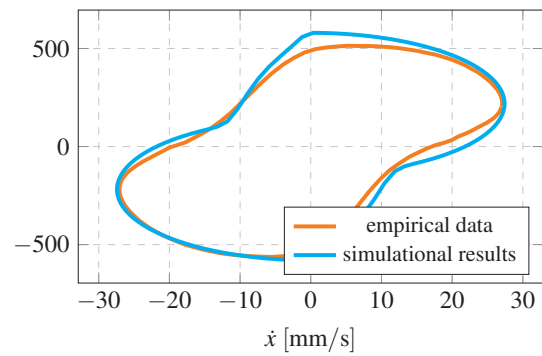
**Fig. 10.** Experimental hysteresis loop for  $p = 0.02$  MPa; B-W model identified for the following parameters:  $a = 0.36, A = 9, \beta = 4, \gamma = -3, n = 5$



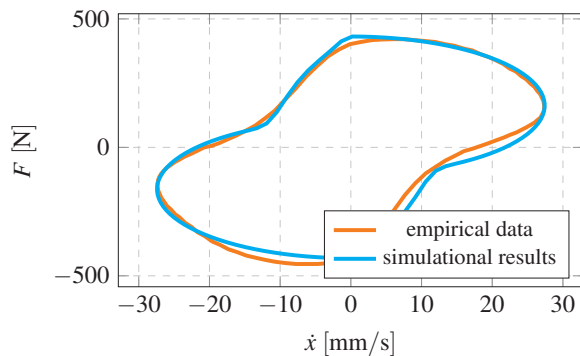
**Fig. 13.** Experimental hysteresis loop for  $p = 0.06$  MPa; B-W model identified for the following parameters:  $a = 0.35, A = 6, \beta = 3, \gamma = -2, n = 4$



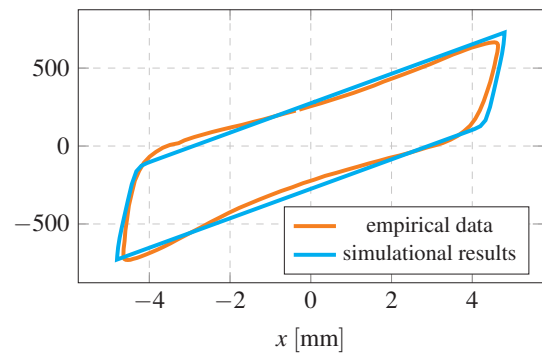
**Fig. 11.** Experimental hysteresis loop for  $p = 0.04$  MPa; B-W model identified for the following parameters:  $a = 0.35, A = 6, \beta = 3, \gamma = -2, n = 4$



**Fig. 14.** Experimental hysteresis loop for  $p = 0.06$  MPa; B-W model identified for the following parameters:  $a = 0.35, A = 6, \beta = 3, \gamma = -2, n = 4$



**Fig. 12.** Experimental hysteresis loop for  $p = 0.04$  MPa; B-W model identified for the following parameters:  $a = 0.35, A = 6, \beta = 3, \gamma = -2, n = 4$

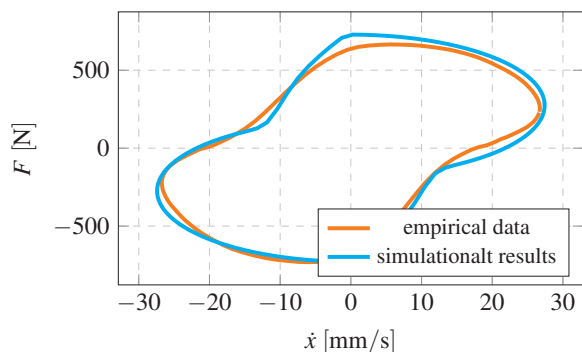


**Fig. 15.** Experimental hysteresis loop for  $p = 0.08$  MPa; B-W model identified for the following parameters:  $a = 0.35, A = 6, \beta = 2, \gamma = -1, n = 4$

the force value. For this case the total RMS error was smaller than 0.0085. Numerous simulations were performed in order to achieve the best system parameters.

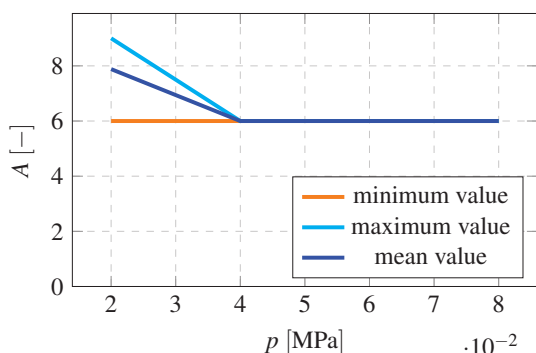
For the last case, the results of identification are presented in Figs. 15 and 16. The obtained values are similar to the previous simulations and reflect the prototype dynamic behaviour. For this case the total RMS error was smaller than 0.01.

In Figs. 17–20 the variations of the identified Bouc-Wen model parameters in the partial vacuum function are depicted. It should be stated that at the recent stage of the VPP damper research it is hard to define universal trends related to the model coefficients characteristics. Although basing on data presented in Figs. 17 and 20,  $A$  and  $n$  parameters values seem to stabilize for higher values of underpressure while similar dependencies

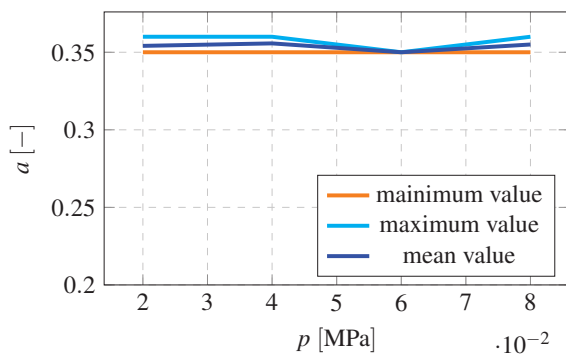


**Fig. 16.** Experimental hysteresis loop for  $p = 0.08$  MPa; B-W model identified for the following parameters:  $a = 0.34$ ,  $A = 6$ ,  $\beta = 2$ ,  $\gamma = -1$ ,  $n = 4$

for  $a$  and  $\beta$  parameters are not observed. To establish universal dependencies for the B-W model coefficients in the underpressure function, more complex experiments should be carried out. The parameters sets were determined by a systematic search algorithm and for each of the tested underpressures, some specified RMS threshold value was set. As can be seen in Figs. 17, 18, 19 and 20, the range of values of each parameter appears very narrow or even becomes constant. The presented values

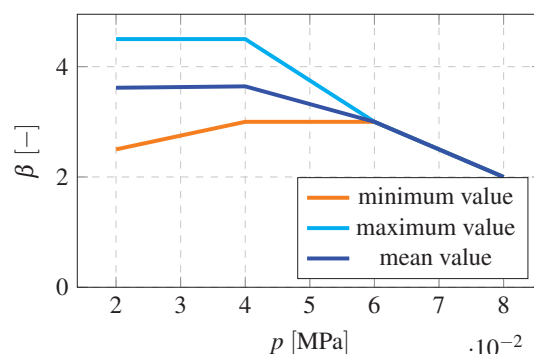


**Fig. 17.** Influence of underpressure on  $A$  parameter – the smallest RMS errors

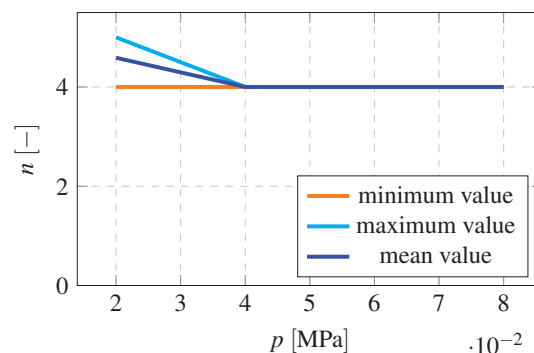


**Fig. 18.** Influence of underpressure on  $a$  parameter – the smallest RMS errors

represent the smallest RMS error that could have been achieved for each of the underpressure considered separately. Unfortunately, other sets of parameters produced, significantly worse mapping of the experimental hysteresis loops, and thus the error value exceeding the established RMS threshold for numerical simulations. For the future research the authors are going to implement more sophisticated identification procedure, based on heuristic algorithms (as Evolutionary Algorithms or Simulated Annealing). Modifying the initial form of Bouc-Wen model by introducing into it the non-linear functions of the underpressure will enable the engineers and researchers to carry out fast and reliable numerical simulations for novel controllable linear dampers.



**Fig. 19.** Influence of underpressure on  $\beta$  parameter – the smallest RMS errors



**Fig. 20.** Influence of underpressure on  $n$  parameter – the smallest RMS errors

The simulations carried out allow to state the correctness of the proposed methodology. Bouc-Wen model which was utilized for the simulational purposes returns corresponding values as empirical data. The appropriate model parameters ensure the convergence of the numerical solution. Unfortunately, they depend on the control parameter in the form of the underpressure inside the structure. However, the minimal and maximal value equivalent parameters are similar. It allows to estimate optimal value of the model parameters as the mean value as presented in Figs. 18–20.



## 7. SUMMARY

The control of vibrations with an absorber made of granular material has been modelled, numerically simulated and experimentally verified. Pumping air out of or into the envelope increases or decreases the compression of the granules, causing the system to become more or less deformable. This, in turn, increases or decreases the dissipation energy, which provides the damping control mechanism of the system vibrations. The changes to the dissipative characteristics of the damper caused by the rearrangement and compacting of the granules were described by a Bouc-Wen model. A numerical algorithm for the problem was presented along with the simulations results with special attention to the changes in oscillations as the grain rearrangement progresses. Then, the executed predictions were compared to the experimental results and proven good convergence with a discrepancy measured by RMS within a generally acceptable range.

The main observations gained are presented below:

1. Underpressure allows us for significant, macroscopic changes in the mechanical properties of the examined structure.
  2. An increase in underpressure value causes a significant increase in the damper stiffness and increases the damping properties.
  3. A utilisation of hard granulates as polystyrene allows us to obtain higher forces, but leads to a number of negative effects – mainly increased wear of the granular core by crushing, abrasion and aggregation.
  4. Dissipative characteristics and hysteresis loop are non-linear.
  5. According to theoretical assumptions, it is possible to obtain a symmetry of forces during tensioning and compressing the damper. This was proven in practice but some inaccuracies may be encountered: leaks, inaccurate assembling in the neutral position and uneven distribution of granular material in the individual VPP damper. Those should be managed at the engineering and procedural level.
  6. Proposed novel concept is characterised by symmetrical mechanical features. This distinguishes the presented design from the existing solutions, which are exclusively of an asymmetrical character.
  7. A Bouc-Wen model of the proposed design has almost constant parameters corresponding with the hysteresis loop. That makes the identification process much easier comparing to procedures presented in the referred papers. The authors checked the response of the model for the selected values of nonlinear parameters and observed that the convergence of simulations and empirical results is satisfactory.
- It is concluded that a granular material damper may be an easy to implement and cost effective way to dampen vibrations in mechanical systems.

## REFERENCES

- [1] C. Graczykowski and P. Pawłowski, "Exact physical model of magnetorheological damper," *Appl. Math. Modell.*, vol. 47, pp. 400–424, 2017, doi: 10.1016/j.apm.2017.02.035.
- [2] M. Makowski and L. Knap, "Reduction of wheel force variations with magnetorheological devices," *J. Vib. Control*, vol. 20, no. 10, pp. 1552–1564, 2014, doi: 10.1177/1077546312472916.
- [3] P. Martynowicz, "Study of vibration control using laboratory test rig of wind turbine tower-nacelle system with mr damper based tuned vibration absorber," *Bull. Pol. Acad. Sci. Tech. Sci.*, vol. 64, no. 2, pp. 347–359, 2016, doi: 10.1515/bpasts-2016-0040.
- [4] T. Butz and O. v. Stryk, "Modelling and simulation of electro- and magnetorheological fluid dampers," *ZAMM – J. Appl. Math. Mech.*, vol. 82, no. 1, pp. 3–20, 2002, doi: 10.1002/1521-4001(200201)82:1<3::AID-ZAMM3>3.0.CO;2-O.
- [5] J. Wang and G. Meng, "Magnetorheological fluid devices: Principles, characteristics and applications in mechanical engineering," *Proc. Inst. Mech. Eng., Part L: J. Mater.: Des. Appl.*, vol. 215, no. 3, pp. 165–174, 2001, doi: 10.1243/1464420011545012.
- [6] G. Yang, B.F. Spencer Jr, H.-J. Jung, and J.D. Carlson, "Dynamic modeling of large-scale magnetorheological damper systems for civil engineering applications," *J. Eng. Mech.*, vol. 130, no. 9, pp. 1107–1114, 2004, doi: 10.1061/(ASCE)0733-9399(2004)130:9(1107).
- [7] C.A. Vivas-Lopez, D. Hernández-Alcantara, R. Morales-Menendez, R.A. Ramírez-Mendoza, and H. Ahuett-Garza, "Method for modeling electrorheological dampers using its dynamic characteristics," *Math. Probl. Eng.*, 2015, doi: 10.1155/2015/905731.
- [8] M. Cates, J. Wittmer, J.-P. Bouchaud, and P. Claudin, "Jamming, force chains, and fragile matter," *Phys. Rev. Lett.*, vol. 81, no. 9, p. 1841, 1998, doi: 10.1103/PhysRevLett.81.1841.
- [9] R. Zalewski and P. Chodkiewicz, "Semi-active linear vacuum packed particles damper," *J. Theor. Appl. Mech.*, vol. 54, no. 1, pp. 311–316, 2016, doi: 10.15632/jtam-pl.54.1.311.
- [10] A. Jiang, T. Aste, P. Dasgupta, K. Althoefer, and T. Nanyakkara, "Granular jamming with hydraulic control," *Am. Soc. Mech. Eng.*, vol. 55935, 2013, doi: 10.1115/DETC2013-12213.
- [11] J.M. Bajkowski, B. Dyniewicz, and C.I. Bajer, "Semi-active damping strategy for beams system with pneumatically controlled granular structure," *Mech. Syst. Sig. Process.*, vol. 70–71, pp. 387–396, 2016, doi: 10.1016/j.ymssp.2015.09.026.
- [12] R. Zalewski and T. Szmidi, "Application of special granular structures for semi-active damping of lateral beam vibrations," *Eng. Struct.*, vol. 65, pp. 13–20, 2014, doi: 10.1016/j.eng struct.2014.01.035.
- [13] A.J. Loeve, O.S. van de Ven, J.G. Vogel, P. Breedveld, and J. Dankelman, "Vacuum packed particles as flexible endoscope guides with controllable rigidity," *Granular Matter*, vol. 12, no. 6, pp. 543–554, 2010, doi: 10.1007/s10035-010-0193-8.
- [14] E. Brown *et al.*, "Universal robotic gripper based on the jamming of granular material," *PNAS*, vol. 107, no. 44, pp. 18 809–18 814, 2010, doi: 10.1073/pnas.1003250107.
- [15] R. Zalewski, P. Chodkiewicz, and M. Shillor, "Vibrations of a mass-spring system using a granular-material damper," *v*, vol. 40, no. 17, pp. 8033–8047, 2016, doi: 10.1016/j.apm.2016.03.053.
- [16] D. Rodak and R. Zalewski, "Innovative controllable torsional damper based on vacuum packed particles," *Materials*, vol. 13, no. 19, p. 4356, 2020, doi: 10.3390/ma13194356.
- [17] M. Żurawski, B. Chiliński, and R. Zalewski, "A novel method for changing the dynamics of slender elements using sponge particles structures," *Materials*, vol. 13, no. 21, p. 4874, 2020, doi: 10.3390/ma13214874.

## Preliminary research of a symmetrical controllable granular damper prototype

- [18] M.D. Luscombe and J.L. Williams, "Comparison of a long spinal board and vacuum mattress for spinal immobilisation," *Emergency Med. J.*, vol. 20, no. 5, pp. 476–478, 2003, doi: 10.1136/emj.20.5.476.
- [19] P. Bartkowski and R. Zalewski, "A concept of smart multiaxial impact damper made of vacuum packed particles," *MATEC Web of Conferences*, vol. 157, p. 05001, 2018, doi: 10.1051/matec-conf/201815705001.
- [20] P. Bartkowski, R. Zalewski, and P. Chodkiewicz, "Parameter identification of bouc-wen model for vacuum packed particles based on genetic algorithm," *Arch. Civ. Mech. Eng.*, vol. 19, no. 2, pp. 322–333, 2019, doi: 10.1016/j.acme.2018.11.002.
- [21] R. Zalewski and M. Pyrz, "Experimental study and modeling of polymer granular structures submitted to internal underpressure," *Mech. Mater.*, vol. 57, pp. 75–85, 2013, doi: 10.1016/j.mechmat.2012.11.002.
- [22] A. Zbiciak and K. Wasilewski, "Constitutive modelling and numerical implementation of sma material with internal loops," *Arch. Civ. Eng.*, vol. 64, no. 4/I, 2018, doi: 10.2478/ace-2018-0053.
- [23] M. Sánchez, G. Rosenthal, and L.A. Pagnaloni, "Universal response of optimal granular damping devices," *J. Sound Vib.*, vol. 331, no. 20, pp. 4389–4394, 2012, doi: 10.1016/j.jsv.2012.05.001.
- [24] R. Bouc, "Forced vibration of mechanical systems with hysteresis," *Proceedings of Fourth Conference on Non-Linear Oscillation*, Prague, 5–9 September 1967.
- [25] M. Ismail, F. Ikhouane, and J. Rodellar, "The hysteresis bouc-wen model, a survey," *Arch. Comput. Methods Eng.*, vol. 16, no. 2, pp. 161–188, 2009, doi: 10.1007/s11831-009-9031-8.

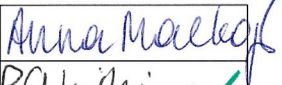
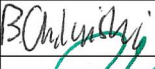

Warszawa, March 8, 2023

## AUTHORSHIP STATEMENT

As the authors of scientific article: Mackojć Anna, Chiliński Bogumił, Zalewski Robert, *Preliminary research of a symmetrical controllable granular damper prototype*, Bulletin of the Polish Academy of Sciences, Technical Sciences, 2022, vol. 70, no. 3, pp.1-9, Article number:e141002. DOI:10.24425/bpasts.2022.141002 published in 2022,

we state

the participation and contribution to development and presentation of the work in the form of a scientific publication is as follows:

Name and surname, academic degree	Participation in work	Signature
Anna Mackojć, MSc	45%	
Bogumił Chiliński, PhD	35%	
Robert Zalewski, Prof. PhD. DSc.	20%	

Warszawa, March 09, 2023

mgr inż. Anna Mackojć  
Politechnika Warszawska  
Wydział Samochodów i Maszyn Roboczych  
Instytut Podstaw Budowy Maszyn  
ul. Narbutta 84  
02-524 Warszawa

## AUTHORSHIP STATEMENT

I declare that in the work "Mackojć Anna, Chiliński Bogumił, Zalewski Robert, *Preliminary research of a symmetrical controllable granular damper prototype*, Bulletin of the Polish Academy of Sciences, Technical Sciences, 2022, vol. 70, no. 3, pp.1-9, Article number:e141002. DOI:10.24425/bpasts.2022.141002" my participation in the article development consisted in theoretical analysis of the presented problem, adaptation of the mathematical model used for numerical research (Bouc-Wen model), developing research methodology, investigation on numerical simulation scenarios, performing numerical simulations, preparing the software tool, processing of experimental results, model validation and statistical research, analysing and interpreting the results, formulating conclusions, editing and formatting the article text, preparing the final version before and after the review and the final editorial form of the article.

  
Signature



Warszawa, March 09, 2023

dr inż. Bogumił Chiliński  
Politechnika Warszawska  
Wydział Samochodów i Maszyn Roboczych  
Instytut Podstaw Budowy Maszyn  
ul. Narbutta 84  
02-524 Warszawa

## AUTHORSHIP STATEMENT

I declare that in the work "Mackojć Anna, Chiliński Bogumił, Zalewski Robert, *Preliminary research of a symmetrical controllable granular damper prototype*, Bulletin of the Polish Academy of Sciences, Technical Sciences, 2022, vol. 70, no. 3, pp.1-9, Article number:e141002. DOI:10.24425/bpasts.2022.141002" my participation in the article development consisted in adaptation of the mathematical model used for numerical research (Bouc-Wen model), developing research methodology, investigation on numerical simulation scenarios, preparing the software tool, participation in simulation research and model validation, processing of experimental results, interpretation of research results, participation in corrections in accordance with the reviewers' guidelines, consultations of the scope and content of the article's text.



Signature

Warszawa, March 09, 2023

prof. dr hab. inż. Robert Zalewski  
Politechnika Warszawska  
Wydział Samochodów i Maszyn Roboczych  
Instytut Podstaw Budowy Maszyn  
ul. Narbutta 84  
02-524 Warszawa

## AUTHORSHIP STATEMENT

I declare that in the work "Mackojć Anna, Chiliński Bogumił, Zalewski Robert, *Preliminary research of a symmetrical controllable granular damper prototype*, Bulletin of the Polish Academy of Sciences, Technical Sciences, 2022, vol. 70, no. 3, pp.1-9, Article number:e141002. DOI:10.24425/bpasts.2022.141002" my participation in the article development consisted in conceptualization of Vacuum Packed Particles (VPP) damper, carrying out a comprehensive literature review, preparing the damper test stand and conducting experimental research, preparation of experimental results, consultations of scope and content of the article's text, methodology verification and approval, supervision.



Signature

# Proposal of the Coupled Thermomechanical Model of a Crank Mechanism

Bogumil CHILINSKI<sup>1</sup> and Anna MACKOJC

*Institute of Machine Design Fundamentals, Warsaw University of Technology, Poland*

**Abstract.** The aim of the paper is to propose analytical coupled thermomechanical model of the crankshaft system, which includes the mutual interaction between thermodynamic and mechanical phenomena occurring in engines. The most relevant dynamic effects observable in the crank system are connected with its kinematics. When the mechanism operates there are also additional effects corresponding with stress, strain and thermal fields. Elastic properties of the system parts and changeable stiffness of the fuel-air mixture cause different dynamics of the entire device. The authors assumed that rigid motion of the crank mechanism, parts deformation and thermodynamic effects and their mutual dependencies will be included in the modelling process. Elasticity of the crankshaft system components is the reason for the difference between a rigid 'ideal' motion and the real movement of crankshaft elements. In most cases, it is enough to assume linear elastic material features based on the relatively high stiffness of the system preventing big deformations. This ensures small displacements and the correctness of the applied model. The performed investigations have shown an influence of the crank system flexibility on the overall device response. Moreover, the parameters that change due to thermodynamic and mechanical properties of the working medium were taken into account. The authors have applied simple engine cycles (Otto, Diesel or combined model) for determining engine load including the connection between mechanical and thermodynamic state variables. This caused another decrease of the total system stiffness. Further numerical testing proved a visible effect of the applied approach in the global system response. The main discrepancies are observable in natural frequencies and vibration modes. It can also be stated that the utilization of different engine cycles results in different engine features. The paper is concluded with an analysis of the existing systems and mutual reactions from the assumed phenomena. The authors have shown the necessity to take a transdisciplinary approach into account in order to model complex systems..

**Keywords.** Crank mechanism, dynamic model, engine vibration, coupled thermomechanical model, analytical modelling, Python and SymPy application

## Introduction

Current trends in high efficiency engines and their low fuel consumption raise the need for the development of new concepts, application of extraordinary solutions and improvement of existing designs. This drives the demand for more sophisticated tools.

---

<sup>1</sup> Corresponding Author, Mail: bogumil.chilinski@pw.edu.pl.



Models previously used become inaccurate and require a process of recreation that takes into account more physical phenomena in order to enable them to be closer to reality. In order to meet these requirements, a transdisciplinary approach in the modelling process [3, 8] shall be considered. Scientific papers regarding a merge of different scientific or industrial disciplines indicate the proposed new approach of investigation might relevantly enhance solving problems in design process methodology [11]. Moreover, they present the transdisciplinary modelling as an extensive discipline that might enable obtaining much more comprehensive results comparing with conventional approach. Furthermore, in the world-wide literature one might encounter scientific articles presenting the transdisciplinary engineering as unspecified in terms of having a precise or unique definition what allows to consider the paper's topic as transdisciplinary [10].

Operational problems of engines are connected mostly with dynamic phenomena occurring during operation. In most cases, they are caused by elastic and inertial properties of the engine components. The combination of both results in engine part vibrations affecting the system operability [6, 14]. Moreover, a thermodynamic gas force which is the reason for limiting cycle existence impacts the system dynamics relevantly. In-depth analysis of the behaviour of system dynamics and a transdisciplinary approach can enable improved engine performance and its operational parameters.

Due to the complexity of the engine design, the designing process is based on a step-by-step improvement process, which leads to the final form of the particular motor. Designers are reluctant to introduce significant enhancements as that could lead to the unpredictable changes in dynamics of the motor. The satisfactory results of current engine designs are an effect of the confirmed industrial practice. However, due to power unit accessories design, more frequent process difficulties raise the need of new computational methods or models. Moreover, the required models should be accurate and fast. One of the projects related to engine equipment design was aimed on some efficient tools to be utilised in computations of Torsional Vibration Dampers [6]. The tools were required to be compatible with industrial specification and take into account manufacturing process of the object. The investigation carried out shows the necessity of transdisciplinary overcoming of limitations to ensure interchange of the older and current version of the part and dynamic conditions which lead to proper mechanical properties of the engine. For this purpose, a comprehensive engine model is necessary in order to allow precise system design process.

The main advantage of a transdisciplinary modelling are simultaneous considerations of mechanical and thermodynamic state variables. This allows for a complex analysis of the mutual influence of the system parameters on generated engine power. A typical approach assumes only the consideration of the mechanism geometry and dynamically independent changes of the rotational speed [1, 2]. Practical cases show there is an influence of the component vibrations on engine dynamics and operational parameters [7, 13]. These are mainly caused by additional stiffness of a fuel-air mixture or the crank system parts. This creates the need for a more detailed investigation of the engine complex model.

The engines main features are connected with the elastic properties of its components. Typically, they are not taken into account which limits the system vibrations [9, 12]. What is more, a crankshaft angle of rotation depends on the instantaneous state of the system. Even for a rigid crank and rod, the elasticity of the fuel-air mixture allows for small changes of the crank from its nominal position.

Inclusion of the thermodynamic effect provides the nonlinear relationship of the gas force and state variables.

## **1. Objectives and overview**

The aim of the paper is to propose the analytical coupled thermomechanical model of a crank mechanism, which considers mutual interactions between thermodynamic and mechanical phenomena occurring in engines. The proposed coupled model emphasises the importance of a transdisciplinary approach in modelling of complex systems. The authors proposed a mathematical model of the crank-piston mechanism in order to enable theoretical analysis and the concept identification. The model analysis is intended to determine the kinematics and dynamics of the crank system and to analyse the impact of the selected system parameters on the total system dynamic response.

Because of a preliminary nature of the investigation carried out, it considers only the analytical and the numerical investigation on the object. The authors states that it is necessary to recognise particular model features before Finite Element Analysis and further experimental investigation. Moreover, it was decided to take into account only the simplest models of the considered phenomena. This was motivated by the papers aim to propose a model with the ability to represent the coupling and the mutual relationships between the state variables.

Based on the paper's aim and scope, the authors must apply some simplifying assumptions corresponding with the problem under investigation. The most relevant simplification is connected with the paper character. The aim of the study is to state a coupled thermomechanical model as previously mentioned. In order to achieve a model coupling, maximum simplifications of the particular phenomena are assumed.

Due to the aforementioned objectives, the following assumptions were adopted:

- the Otto cycle as a description of the engine working principle,
- a nonlinear kinematics of the crank mechanism,
- a dynamic value of crankshaft angle caused by the equilibrium of acting and resistance moments,
- numerical simulations based on the derived nonlinear governing equations,
- linear elasticity of the crank system reduced to the piston rod.

Based on the paper's introduction and objectives, it was stated that the realisation of the aim will need the following steps:

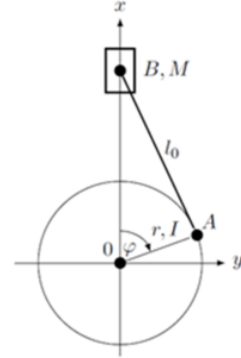
- modelling of a crank mechanism based on the selected assumptions,
- numerical simulations devoted to sensitivity analysis,
- the model identification based on the experimental data,
- the model aided investigation for recognition of the crucial discrepancies with currently utilised models.

Proper modelling of the mechanism and numerical simulations seems to be crucial for the presented work. The proposed assumptions make it possible to achieve preliminary results.

## 2. Crank mechanism model

Determination of dynamic loads of the considered model of crank mechanism and hence the other basic engine parts, primarily a block and a cylinder head, are related to the determination of the kinematics of this system.

The diagram of the crank mechanism model is shown in figure 1, which also represents the following engine parts: O - crankshaft, A - crank pin, I - crank moment of inertia, B - piston pin, M - piston mass. Additionally, the following symbols describing the model configuration were introduced:  $r$  - the crank length (distance between the crankshaft and crank pin axes),  $l_0$  - the connecting rod length (distance between the crank pin and piston pin axes),  $\varphi$  - crank rotation angle. The piston displacement and velocity for any crank rotation angle  $\varphi$  can be determined on the basis of mechanism configuration presented in figure 1. Determination formulas given for the piston displacement and velocity are presented respectively in equation (1) and (2).



**Figure 1.** The scheme of the crank mechanism model Short description of figure.

$$x = r \cos(\varphi) + \sqrt{-r^2 \sin^2(\varphi) + (l_0 + u)^2} \quad (1)$$

$$\dot{x} = -r \sin(\varphi) \dot{\varphi} + \frac{-r^2 \sin(\varphi) \cos(\varphi) \dot{\varphi} + (l_0 + u) \dot{u}}{\sqrt{-r^2 \sin^2(\varphi) + (l_0 + u)^2}} \quad (2)$$

Kinematic analysis of mechanisms is used to study motion and is an integral element of investigating the causes of existing motions that dynamics deals with. The dynamic analysis takes into account external forces, inertia forces, gravity forces and the force moments acting on the elements of the mechanism.

The kinetic energy was determined as the sum of the energy of the system mass of connecting rod  $l_0$  and inertia moment of the crank  $r$ . The potential energy in the discussed system results from the elastic properties of the connecting rod  $l_0$ .

Hence, the Lagrangian (3) represents the total energy of the system under consideration presented in figure 1. The equation describing  $L$  is given in (3):

$$L = \frac{1}{2} I \dot{\varphi}^2 + \frac{1}{2} M \dot{x}^2 - \frac{k \left( r \cos(\varphi) + \sqrt{-r^2 \sin^2(\varphi) + (l_0 + u)^2} - l_0 \right)^2}{2} \quad (3)$$

Nonholonomic model forces acting on the particular crank are caused by the other parts of a crankshaft, the entire powertrain or gas forces, which are the reason for stable operation of the engine. Thermodynamic force is the result of phenomenon connected with the particular stroke and instantaneous volume of the cylinder during operation. Depending on the assumed cycle, there is another thermodynamic transformation for

the particular working stage. It states the relationship between the current value of the piston volume and the working pressure. After complex rearrangement of the formulas it is possible to determine an equation which relates the piston motion and the system pressure.

The considered engine load - Otto cycle is presented in figure 2 and has the following form:

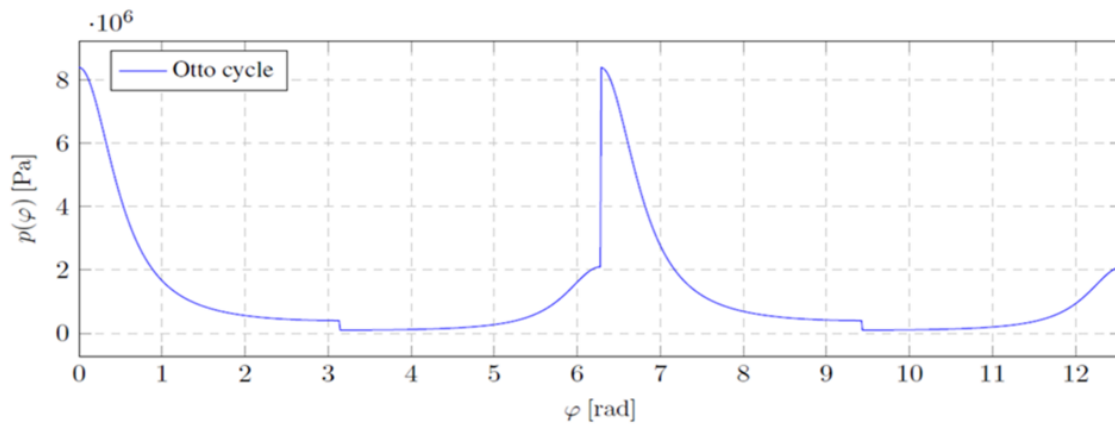


Figure 2. Otto cycle.

The assumed engine cycle describes particular stages of the engine operation. It assumes an infinite fast combustion and a process of temperature increasing. Moreover, it was adopted that compression and working cycle do not consider heat transfer (governed by an adiabatic transformation). Intake and exhaust strokes are given by an isobaric transformation with the atmospheric pressure.

### 3. Description of the engine under investigation

The considerations concern the TwinAir engine, which is a straight-twin type of an engine designed by Fiat Powertrain Technologies. The engine has hydraulically actuated variable valve timing and lift technology. It is offered in naturally aspirated and turbocharged variants. The TwinAir is popular for its reduced size, weight, fuel consumption and CO<sub>2</sub> emissions.

The considerations concern the Fiat TwinAir engine since the author participated in the industrial research projects aimed at the process of redesigning a diesel engine vibration absorber [4], [5]. The engine body, head and crankshaft were provided in order to examine torsional vibration dampers on a built test stand. Having the engine geometrical parameters and mechanical properties enabled numerical analyses simulating real processes of combustion considering thermodynamic parameters of the Fiat TwinAir combustion chamber. On this basis the engine load was obtained by numerical computations.

The engine is characterized by the geometrical parameters and mechanical properties presented respectively in table 1 and 2.

**Table 1.** Fiat TwinAir - geometrical parameters.

TwinAir engine geometrical parameters	
Geometrical parameter	Naturally aspirated
Displacement	1.0l (964cm <sup>3</sup> )
Cylinder bore	83.5mm (3.29in)
Piston stroke	88mm (3.5in)

**Table 2.** Fiat TwinAir - mechanical properties.

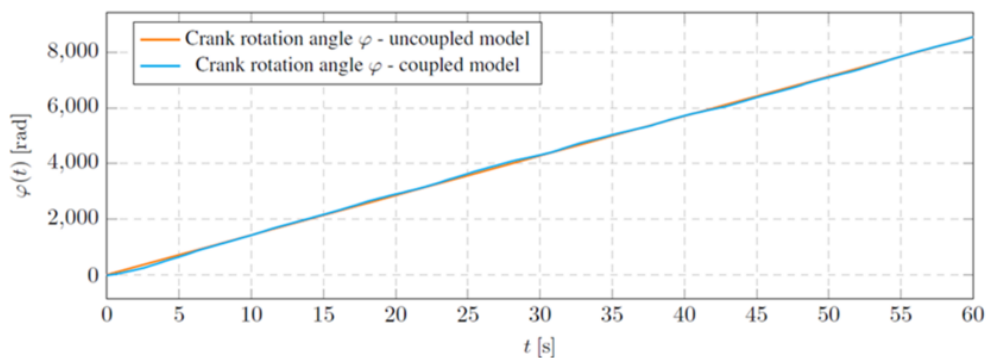
TwinAir engine mechanical properties	
Mechanical properties	Naturally aspirated
Power output	60PS (44kW)
Torque output	88Nm at 3500min <sup>-1</sup>
Compression ratio	11.2:1

The information in tables 1 and 2 show that the object under investigation is a small engine with high operational properties. It indicates different dynamics of the device than for the older industrial solutions. Practical observations present the demand of the additional equipment to control the object dynamics and the most efficient tools for the design calculations. That causes a need for more detailed modelling of the engine, especially in the field of a transdisciplinary engineering.

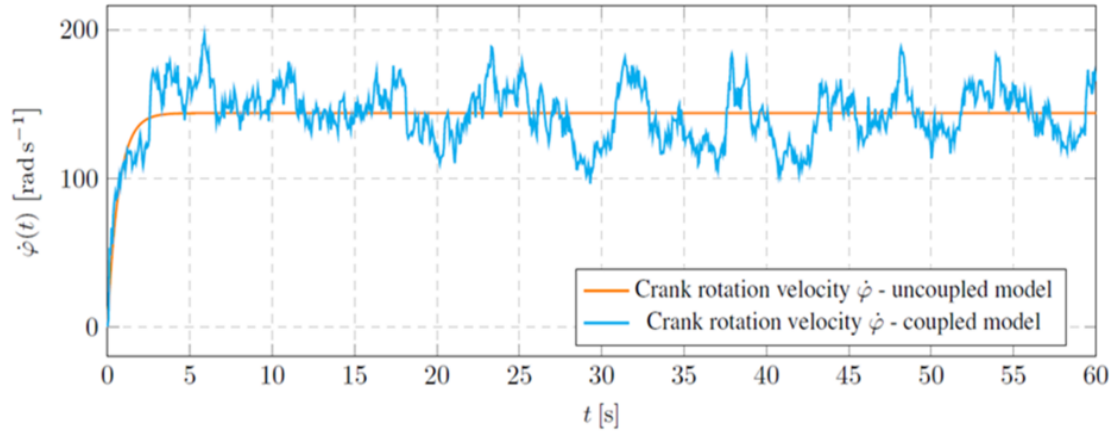
#### 4. Numerical simulations

In order to study the proposed dynamic coupled model, the authors performed some numerical simulations allowing for reliable evaluation of the modelling based on a transdisciplinary approach.

The plot depicted in figure 3 presents a crank displacement being influenced by the system's flexible properties. The linear curve was introduced for comparative purposes and shows the dynamic response of the uncoupled system where its rigidity was not included in the considerations. It can be stated that despite the small impact on dynamics in quantitative terms, qualitative changes in the dynamic response of the system can be captured. By analysing the oscillatory nature of the crank displacement, it can be concluded that the system equivalent stiffness is affected not only by the elastic properties of the gas force, having relatively less impact on the system dynamics, but mostly by the crank system stiffness taken into consideration. This indicates the importance of considerations of mutual relations between the thermodynamic and mechanical system properties as the latter are often omitted in the engine modelling process.

**Figure 3.** Crank rotation angle.

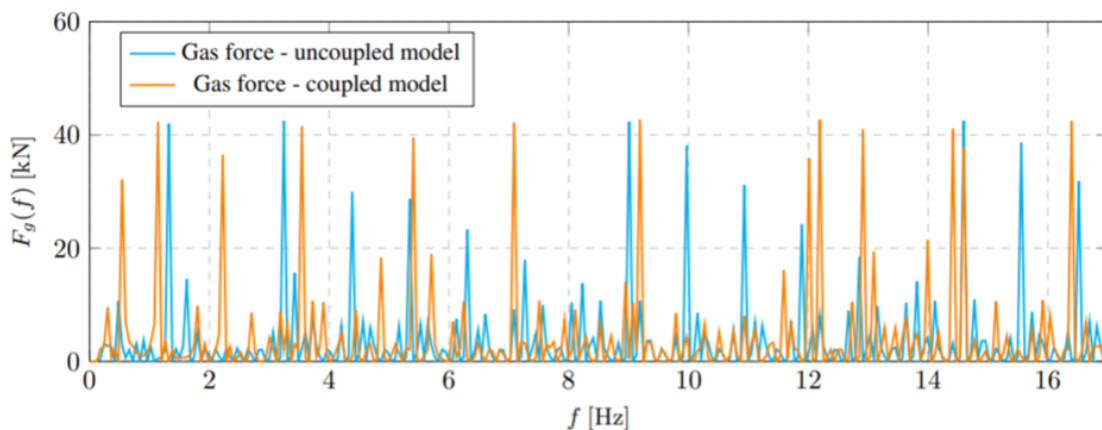
More significant qualitative and quantitative changes can be seen on the crank rotational speed plot presented in figure 4. The rotational speed oscillation is stable but not periodic. The results of simulations reveal a stochastic character of the engine dynamics. The phenomenon is compatible with empirical observations, which are uncorrelated and have random properties.



**Figure 4.** Crank angular velocity.

It can be stated that the obtained numerical simulations depict significant difference between an uncoupled mechanical approach and transdisciplinary modelling. The evaluated values have similar integral properties as a mean value or an average slope and very different dynamic features as a signal velocity or Root Mean Square (RMS) value.

Figure 5 depicts plots of gas forces considered in a modelling process of the engine dynamics. Gas forces computed based on the coupled (thermodynamic) and uncoupled (kinematic) model are presented and discussed as they reveal strong qualitative differences resulting in a different system dynamic response. The blue waveform represents a case of a kinematic-based engine load (due to displacements based on the uncoupled model) while the orange one stands for a fully dynamic gas force implementation (computed with the coupled model). Based on a comparative analysis, a repetitive, cyclic load in case of kinematically simulated gas force can be easily observed, while the changes of a dynamic engine load is a unique process related to the combustion process of the air-fuel mixture, which is never repeatable.



**Figure 5.** Gas force - comparative results.

Non-periodical characters of transdisciplinary modelling results indicate the essential difference between the two types of numerical models' simulations. That leads to conclude the proposed model better represents an irregular character engine operation. Moreover, it can be stated that a random character of the subsequent working cycles can also be caused by the irregularity of the system velocity, not only by a stochastic process of combustion.

## **5. Conclusions**

It can be concluded that the application of transdisciplinary engineering enables qualitatively new results which differ significantly from the results of a typical kinematic analysis of a combustion process in a reciprocating engine. On one hand, simulations which were carried out have similar general properties to the simpler models, especially in the area of the integral properties as a mean value or an average power. On the other hand, they are characterised by very different system dynamics, which reflects in a relatively high irregularity of the instantaneous value of the angular velocity. Comparatively to commonly utilised models, the performed analysis of the proposed uncoupled model delivers results which are closer to real engine dynamic behaviour.

The industrial research project creates a need of simple computational model of the engine for design processes of the Torsional Vibration Damper being Dynamic Vibration Absorber. Considering an operational principle of this kind of damper, the designed device has to be tuned to the power unit properties. Despite the model of simple double degree of freedom rotor was enough for this purpose, a determination of the excitation (caused by thermodynamic cycle) had to be supported by more sophisticated model. Articles and reports regarding the investigation present efficiency of sophisticated models in case of solving industrial problems [6, 14]. Transdisciplinary modelling of the engine operation enables to obtain relevantly better results as shown in the paper. Such an approach is necessary in order to select proper parameters of the designed device especially in case of the simultaneous fulfilling operational (expected engine dynamics) and functional conditions (desired inertial and geometrical parameters).

The carried out investigation presented in the subsequent sections of the paper allows for the formulation of the following conclusions:

1. As modern spark ignition engines become lighter, more efficient and more loaded than commonly used units, it results in different dynamics of the entire powertrain and also creates the demand for a more accurate model for the purposes of engine design, equipment selection and powertrain control. The transdisciplinary engineering approach enables the preparation of a tool that meets the above requirements.
2. The model proposed by the authors takes into account more details of crank system stiffness, gas force elasticity, viscous and inertial properties and enables the investigation of their mutual relationships. It results in a complex but solvable problem. The obtained result expands on models known in literature but keeps all the properties of simpler models.



3. The results of the performed investigation present complex dynamics of the engine outputs as an angular displacement or velocity. It is strictly connected with nonlinear features of the proposed coupled model. The authors assumed that excitation in the form of a gas force generated in the combustion process depends not only on time but also on state variables. It results in a nonlinear system with extremely different dynamic properties. From the vibrational point of view, it is a self-excited system characterised by the limit cycle which is the same operational velocity of the engine.

The proposed approach can be used to offer results qualitatively compatible with existing engines but there are some areas where even better results can be obtained. Some weakness of the presented method is the simplified model of the gas force. This will lead to some discrepancies when comparing to experimental data but still external outputs of the engine model are close to reality which brings the conclusion that even the proposed simplified methodology can be used successfully.

This transdisciplinary modelling approach might contribute in process of engines design being upgraded in terms of technical level what constitutes the added value resulting from a merge of two disciplines thermodynamics and mechanics of machines.

## References

- [1] B. Bellakhdhar, A. Dogui and J.-L. Ligier, A simplified coupled crankshaft–engine block model, *Comptes Rendus Mecanique*, 2013, Vol. 341, pp. 743–754.
- [2] E. Brusa, C. Delprete and G. Genta, Torsional vibration of crankshafts: effects of non-constant moments of inertia, *Journal of sound and vibration*, 1997, Vol. 205, pp. 135–150.
- [3] J.V. Chelsom, Concurrent engineering case studies: Lessons from Ford Motor Company Experience. In: C.S. Syan, U. Menon (eds.) *Concurrent Engineering*. Springer, Dordrecht, 1994, pp. 25–48.
- [4] Grant No. NN5095 74639 - *Modelling and design of the torsional vibration dampers of drive systems* (2012-2015).
- [5] Chilinski, B. Grant No. PBS1/B6/11/2012 - *High-strength torsional vibration dampers of the crankshafts* (2012-2015).
- [6] B. Chilinski and M. Zawisza, Analysis of bending and angular vibration of the crankshaft with a torsional vibrations damper, *Journal of Vibroengineering*, 2016, 18, 5353–5363.
- [7] M. Desbazeille, R. Randall, F. Guillet, M. El Badaoui and C. Hoisnard, Model-based diagnosis of large diesel engines based on angular speed variations of the crankshaft, *Mechanical Systems and Signal Processing*, 2010, Vol. 24, pp. 1529–1541.
- [8] G. Iosif, I. Iordache, V. Stoica, A.M. Luchian, E. Costea, G. Suciuc and V. Suciuc, Achieving a More Electric Aircraft: a comparative study between the concurrent and traditional engineering models, *INCAS Bulletin*, 2018, Vol. 10, pp. 221–228.
- [9] H. Karabulut, Dynamic model of a two-cylinder four-stroke internal combustion engine and vibration treatment, *International Journal of Engine Research*, 2012, Vol. 13, pp. 616–627.
- [10] S. Lattanzio, E. Carey, A. Hultin, R. Imani Asrai, M. McManus, N. Mogles, G. Parry and L.B. Newnes, Transdisciplinarity within the Academic Engineering Literature, *International Journal of Agile Systems and Management*, 2020, Vol. 13, No. 2, pp. 213–232.
- [11] J. Pokojski, Integration of Knowledge Based Approach and Multi-Criteria Optimization in Multi-Disciplinary Machine Design, *Advances in Transdisciplinary Engineering*, Vol. 2, 2015, pp. 683 – 692.
- [12] Q.H. Qin and C.X. Mao, Coupled torsional-flexural vibration of shaft systems in mechanical engineering—I. Finite element model, *Computers & Structures*, 1996, Vol. 58, pp. 835–843.
- [13] J.K. Sinha, F. Gu, L. Lidstone and A.D. Ball, Detecting the crankshaft torsional vibration of diesel engines for combustion related diagnosis, *Journal of Sound and Vibration*, 2009, Vol. 321, pp. 1171–1185.

- [14] B. C. Zbigniew Dabrowski, Identification of a model of the crankshaft with a damper of torsional vibrations. *Journal of Sound and Vibration*, 2017, Vol. 19, pp. 539–548.

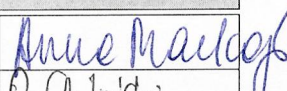
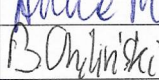
Warszawa, March 7, 2023

## AUTHORSHIP STATEMENT

As the authors of scientific article: Chiliński Bogumił, Mackojć Anna, *Proposal of the Coupled Thermomechanical Model of a Crank Mechanism*, In: Transdisciplinary Engineering for Complex Socio-technical Systems – Real-life Applications / Pokojński Jerzy [et al.] (eds.), 2020, vol. 12, IOS Press, ISBN 978-1-64368-110-8. DOI:10.3233/ATDE200098 published in 2020,

we state

the participation and contribution to development and presentation of the work in the form of a scientific publication is as follows:

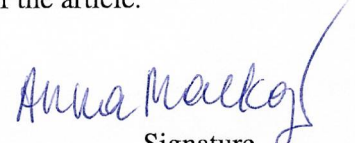
Name and surname, academic degree	Participation in work	Signature
Anna Mackojć, MSc.	50%	
Bogumił Chiliński, PhD.	50%	

Warszawa, March 07, 2023

mgr inż. Anna Mackojć  
Politechnika Warszawska  
Wydział Samochodów i Maszyn Roboczych  
Instytut Podstaw Budowy Maszyn  
ul. Narbutta 84  
02-524 Warszawa

## AUTHORSHIP STATEMENT

I declare that in the work "Chiliński Bogumił, Mackojć Anna, *Proposal of the Coupled Thermomechanical Model of a Crank Mechanism*, In: Transdisciplinary Engineering for Complex Socio-technical Systems – Real-life Applications / Pokojski Jerzy [et al.] (eds.), 2020, vol. 12, IOS Press, ISBN 978-1-64368-110-8. DOI:10.3233/ATDE200098" my participation in the article development consisted in carrying out a literature review, theoretical analysis of the presented problem, determining the analytical model and its numerical solution, developing research methodology, designing numerical simulation scenarios, performing simulations, preparing the software tool, analysing and interpreting the results, formulating conclusions, editing and formatting the article text, preparing the final editorial form of the article.

  
Signature

Warszawa, March 07, 2023

dr inż. Bogumił Chiliński  
Politechnika Warszawska  
Wydział Samochodów i Maszyn Roboczych  
Instytut Podstaw Budowy Maszyn  
ul. Narbutta 84  
02-524 Warszawa

## AUTHORSHIP STATEMENT

I declare that in the work "Chiliński Bogumił, Mackojć Anna, *Proposal of the Coupled Thermomechanical Model of a Crank Mechanism*, In: Transdisciplinary Engineering for Complex Socio-technical Systems – Real-life Applications / Pokojński Jerzy [et al.] (eds.), 2020, vol. 12, IOS Press, ISBN 978-1-64368-110-8. DOI:10.3233/ATDE200098" my participation in the article development consisted in developing research idea, consultations of the scope and content, methodology verification and approval of the proposed approach to the problem, participation in simulation research, interpretation of research results, preparing the software tool, participation in corrections in final article version.

  
Signature

## References

1. Acero, W. G., Li, L., Gao, Z. & Moan, T. Methodology for assessment of the operational limits and operability of marine operations. *Ocean Engineering* **125**, 308–327. <https://doi.org/10.1016/j.oceaneng.2016.08.015> (2016).
2. Albers, P. Motion Control in Offshore and Dredging. *Springer Dordrecht Heidelberg London New York* **11**, 208–227 (2010).
3. Balachandran, B., Li, Y. & Fang, C. A mechanical filter concept for control of nonlinear crane-load oscillations. *Journal of Sound and Vibrations* **228**, 651–682 (1999).
4. Capecchi, D & Bishop, S. Periodic and non-periodic responses of a parametrically excited pendulum. *Report* **3**, 90 (1990).
5. Chilinski, B., Mackojc, A., Zalewski, R. & Mackojc, K. Proposal of the 3-DOF model as an approach to modelling offshore lifting dynamics. *Ocean Engineering* **203**, 287–314 (2020).
6. Chilinski, B., Mackojc, A. & Mackojc, K. Analytical solution of parametrically induced payload nonlinear pendulation in offshore lifting. *Ocean Engineering* **259**, 111835 (2022).
7. Clifford, M. & Bispop, S. Approximating the escape zone for the parametrically excited pendulum. *Journal of Sound Vibration* **172**, 572–576 (1994).
8. Čorić, V., Čatipović, I. & Slapničar, V. Floating crane response in sea waves. *Brodogradnja: Teorija i praksa brodogradnje i pomorske tehnike* **65**, 111–120 (2014).
9. De Paula, A. S., Savi, M. A., Wiercigroch, M. & Pavlovskaja, E. Bifurcation control of a parametric pendulum. *International Journal of Bifurcation and Chaos* **22**, 1250111 (2012).
10. DNV, D. N. V. *DNV Official Website* <https://www.dnv.com/>. (accessed:09.08.2022).
11. DNV, D. N. V. *DNV Official Website* <https://www.dnv.com/software/products/sesam-products.html>. (accessed:09.08.2022).
12. Fałat, P. Dynamic analysis of a sea crane of an A-frame type. *PhD Dissertation [in Polish], University of Bielsko-Biała, Poland* (2004).
13. Fossen, T. & Nijmeijer, H. *Parametric resonance in dynamical systems* (Springer Science & Business Media, 2012).
14. Fragopoulos, D., Spathopoulos, M. P. & Zheng, Y. A pendulation control system for offshore liftig operations. *14th World Congress of IFAC*.
15. Ghigliazza, R. & Holmes, P. On the dynamics of cranes, or spherical pendula with moving supports. *International journal of non-linear mechanics* **37**, 1211–1221 (2002).
16. Health & HSE, S. E. *Annual offshore statistics and regulatory activity reports* <https://www.hse.gov.uk/offshore/statistics/>. (accessed: 28.07.2022).
17. Hook, F. A. R. *Fathom Group Official Website* <https://fathom-group.com/equipment/accropode-release-hooks-2/>. (accessed:02.10.2022).



18. Horton, B, Sieber, J, Thompson, J. & Wiercigroch, M. Dynamics of the nearly parametric pendulum. *International journal of non-linear mechanics* **46**, 436–442 (2011).
19. Horton, B., Wiercigroch, M. & Xu, X. Transient tumbling chaos and damping identification for parametric pendulum. *Philosophical Transactions of the Royal Society A: Mathematical, Physical and Engineering Sciences* **366**, 767–784 (2008).
20. Kang, H.-S., Tang, C. H.-H., Quen, L. K., Steven, A. & Yu, X. *Prediction on parametric resonance of offshore crane cable for lowering subsea structures in 2016 IEEE International Conference on Underwater System Technology: Theory and Applications (USYS)* (2016), 165–170.
21. Kang, H.-S., Tang, C. H.-H., Quen, L. K., Steven, A. & Yu, X. Parametric resonance avoidance of offshore crane cable in subsea lowering operation through A\* heuristic planner (2017).
22. Kholostova, O. On the motions of a double pendulum with vibrating suspension point. *Mechanics of solids* **44**, 184–197 (2009).
23. Koch, B., Leven, R., Pompe, B & Wilke, C. Experimental evidence for chaotic behaviour of a parametrically forced pendulum. *Physics Letters A* **96**, 219–224 (1983).
24. Kovacic, I., Rand, R. & Mohamed Sah, S. Mathieu's equation and its generalizations: overview of stability charts and their features. *Applied Mechanics Reviews* **70** (2018).
25. Ku, N.-K., Cha, J.-H., Roh, M.-I. & Lee, K.-Y. A tagline proportional–derivative control method for the anti-swing motion of a heavy load suspended by a floating crane in waves. *Proceedings of the Institution of Mechanical Engineers, Part M: Journal of Engineering for the Maritime Environment* **227**, 357–366. <https://doi.org/10.1177/1475090212445546> (2013).
26. Kuře, M., Bušek, J., Vyhlídal, T. & Niculescu, S.-I. Damping oscillation of suspended payload by up and down motion of the pivot base-time delay algorithms for UAV applications. *IFAC-PapersOnLine* **52**, 121–126 (2019).
27. Kurowski, J., Maczyński, A. & Szczotka, M. The influence of a shock absorber on dynamics of an offshore pedestal crane. *Journal of Theoretical and Applied Mechanics*, 953–966 (2012).
28. Lenci, S, Pavlovskaja, E, Rega, G & Wiercigroch, M. Rotating solutions and stability of parametric pendulum by perturbation method. *Journal of sound and vibration* **310**, 243–259 (2008).
29. Lenci, S. & Rega, G. Competing dynamic solutions in a parametrically excited pendulum: attractor robustness and basin integrity. *Journal of computational and nonlinear dynamics* **3** (2008).
30. Leven, R., Pompe, B, Wilke, C & Koch, B. Experiments on periodic and chaotic motions of a parametrically forced pendulum. *Physica D: Nonlinear Phenomena* **16**, 371–384 (1985).



31. Li, L., Gao, Z., Moan, T. & Ormberg, H. Analysis of lifting operation of a monopile for an offshore wind turbine considering vessel shielding effects. *Marine structures* **39**, 287–314 (2014).
32. Ltd, O. *Orcina Ltd Website* <https://www.orcina.com/about/history/>. (accessed:09.08.2022).
33. Mann, B. & Koplow, M. Symmetry breaking bifurcations of a parametrically excited pendulum. *Nonlinear Dynamics* **46**, 427–437 (2006).
34. Masoud, Z. A control system for the reduction of cargo pendulation of ship-mounted cranes. *PhD Dissertation, Virginia Polytechnic Institute and State University, Blacksburg, Virginia* (2000).
35. Masoud, Z., Nayfeh, A. & Mook, D. Cargo pendulation reduction of ship-mounted cranes. *Nonlinear Dynamics* **35**(3), 299–311 (2004).
36. Miles, J. On resonant rotation of a weakly damped pendulum. *Journal of sound and vibration* **280**, 401–406 (2005).
37. Náprstek, J. & Fischer, C. Auto-parametric semi-trivial and post-critical response of a spherical pendulum damper. *Computers & structures* **87**, 1204–1215 (2009).
38. Ngo, Q. & Hong, K. Sliding-mode antisway control of an offshore container crane. *IEEE/ASME Transactions on Mechatronics* **17**, 201–209 (2012).
39. Ngo, Q. H., Nguyen, N. P., Nguyen, C. N., Tran, T. H. & Ha, Q. P. Fuzzy sliding mode control of an offshore container crane. *Ocean Engineering* **140**, 125–134. <https://doi.org/10.1016/j.oceaneng.2017.05.019> (2017).
40. Of Safety, B. & BSEE, E. E. *Offshore Incident Statistics* <https://www.bsee.gov/stats-facts/offshore-incident-statistics>. (accessed: 28.07.2022).
41. Osiński, M. & Wojciech, S. Application of nonlinear optimisation methods to input shaping of the hoist driver of an offshore crane. *Nonlinear Dynamics* **17**, 369–386 (1998).
42. Pavlovskaja, E., Horton, B., Wiercigroch, M., Lenci, S. & Rega, G. Approximate rotational solutions of pendulum under combined vertical and horizontal excitation. *International Journal of Bifurcation and Chaos* **22**, 1250100 (2012).
43. Peng, X., Geng, Z., *et al.* Anti-swing control for 2-D under-actuated cranes with load hoisting/lowering: A coupling-based approach. *ISA transactions* **95**, 372–378. <https://doi.org/10.1016/j.isatra.2019.04.033> (2019).
44. Recommended Practice N103 Modelling and analysis of marine operations. *DET NORSKE VERITAS GL*, Sec.9.2–9.3 (2017).
45. Ren, Z., Verma, A. S., Ataei, B., Halse, K. H. & Hildre, H. P. Model-free anti-swing control of complex-shaped payload with offshore floating cranes and a large number of lift wires. *Ocean Engineering* **228**. <https://doi.org/10.1016/j.oceaneng.2021.108868> (2021).

46. Sah, S. M. & Mann, B. Transition curves in a parametrically excited pendulum with a force of elliptic type. *Proceedings of the Royal Society A: Mathematical, Physical and Engineering Sciences* **468**, 3995–4007 (2012).
47. Schaub, H. Rate-based ship-mounted crane payload pendulation control system. *Control Engineering Practice* **16**, 132–145 (2008).
48. Sofroniou, A. & Bishop, S. Dynamics of a parametrically excited system with two forcing terms. *Mathematics* **2**, 172–195 (2014).
49. Standard for Certification No. 2.22 Lifting Appliance. *DET NORSKE VERITAS GL*, Ch.2 Sec.2–39 (2011).
50. Sun, N., Wu, Y., Chen, H. & Fang, Y. An energy-optimal solution for transportation control of cranes with double pendulum dynamics: Design and experiments. *Mechanical Systems and Signal Processing* **102**, 87–101. <https://doi.org/10.1016/j.ymssp.2017.09.027> (2018).
51. Sun, Y., Qiang, H., Xu, J. & Dong, D. The non-linear dynamics and anti-sway tracking control for offshore container crane on a mobile harbor. *Journal of Marine Science and Technology* **25**, 656–665 (2017).
52. Sun, Y.-G., Qiang, H.-Y., Xu, J. & Dong, D.-S. The nonlinear dynamics and anti-sway tracking control for offshore container crane on a mobile harbor. *Journal of Marine Science and Technology* **25**, 5. <https://doi.org/10.6119/JMST-017-1226-05> (2017).
53. Supplier, B. P. *Barge Master: Motion Compensation Systems* <https://www.barge-master.com/products>. (accessed: 25.07.2022).
54. Supplier, C. P. *Cranemaster: Passive Heave Compensator* <https://www.ynfpublishers.com/2016/09/cranemaster-launching-worlds-largest-passive-heave-compensator>. (accessed: 25.07.2022).
55. Supplier, M. P. *Macgregor: 3D Motion Compensator* <https://www.macgregor.com/Products/products/offshore-and-subsea-load-handling/3-axis-motion-compensation-cranes/>. (accessed: 25.07.2022).
56. System, F. M. R. *Fathom Group Official Website* <https://fathom-group.com/equipment/modular-recovery-system/>. (accessed: 02.10.2022).
57. Szczotka, M. Active heave compensation in offshore equipment with a neural network based control system. *Measurement Automation and Monitoring [in Polish]* **56(6)**, 593–596 (2010).
58. Tomczyk, J. Review of automation cranes methods. *Industrial Transport and Construction Machinery HMR-TRANS Ltd. [in Polish]* **4(6)**, 22–30 (2009).
59. Tong, M., Wang, Y. & Qiu, H. Research on dynamic heave compensation on large floating crane in deep sea. *Fifth Conference on Measuring Technology and Mechatronics Automation*, 898–901 (2013).

60. Wiercigroch, M. A new concept of energy extraction from waves via parametric pendulor. *UK patent application* (2010).
61. Xu, X, Pavlovskaja, E, Wiercigroch, M., Romeo, F & Lenci, S. Dynamic interactions between parametric pendulum and electro-dynamical shaker. *ZAMM-Journal of Applied Mathematics and Mechanics/Zeitschrift für Angewandte Mathematik und Mechanik: Applied Mathematics and Mechanics* **87**, 172–186 (2007).
62. Xu, X. & Wiercigroch, M. Approximate analytical solutions for oscillatory and rotational motion of a parametric pendulum. *Nonlinear Dynamics* **47**, 311–320 (2007).
63. Xu, X., Wiercigroch, M. & Cartmell, M. Rotating orbits of a parametrically-excited pendulum. *Chaos, Solitons & Fractals* **23**, 1537–1548 (2005).
64. Yurchenko, D. & Alevras, P. Stability, control and reliability of a ship crane payload motion. *Probabilistic Engineering Mechanics* **38**, 173–179 (2014).
65. Zhu, H., Li, L & Ong, M. *Study of lifting operation of a tripod foundation for offshore wind turbine* in *IOP conference series: materials science and engineering* **276** (2017).